

**Transition metal-catalyzed oxidative cleavage of lignin and lignin
 β -O-4 model compounds**

Von der Fakultät für Mathematik, Informatik und Naturwissenschaften der RWTH Aachen
University zur Erlangung des akademischen Grades eines Doktors der Naturwissenschaften
genehmigte Dissertation

vorgelegt von

Master of Science

Jakob Mottweiler

aus Köln

Berichter: Prof. Dr. rer. nat. Carsten Bolm
Prof. Dr. rer. nat. Walter Leitner

Tag der mündlichen Prüfung: 24.11.2015

Diese Dissertation ist auf den Internetseiten der Universitätsbibliothek online verfügbar.

The work presented in this dissertation was carried out from June 2010 until April 2015 at the Institute of Organic Chemistry, RWTH Aachen University, Aachen, Germany under the supervision of Professor Dr. Carsten Bolm. Part of the experiments presented in chapter II.4 and II.5 were conducted from March until May 2012, July 2012 and April 2014 at the Instituto de Tecnología Química (UPV-CSIC), Valencia, Spain under the supervision of Professor Dr. Avelino Corma Canós.

I would like to thank Professor Dr. Carsten Bolm for giving me the opportunity to perform my thesis in his group and for the help and guidance that he has given me during the entire process.

Furthermore, I would like to thank Professor Dr. Avelino Corma Canós for making my stay in Valencia possible and being a mentor over the last three years.

I am grateful to the NRW Graduate School BrenaRo and the German Academic Exchange Service (DAAD) for predoctoral stipends and for the support by the Cluster of Excellence “Tailor Made Fuels from Biomass” (TMFB) funded by the Excellence Initiative of the German federal and state governments.

Parts of this work have already been published:

J. Buendia, J. Mottweiler, C. Bolm, *Chem. Eur. J.* **2011**, *17*, 13877–13882.

P. Picart, C. Müller, J. Mottweiler, L. Wiermans, C. Bolm, P. Domínguez de María, A. Schallmeyer, *ChemSusChem* **2014**, *7*, 3164–3171.

J. Mottweiler, M. Puche, C. Räuber, T. Schmidt, P. Concepción, A. Corma, C. Bolm, *ChemSusChem* **2015**, *8*, 2106–2113.

S. Dabral, J. Mottweiler, T. Rinesch, C. Bolm, *Green Chem.* **2015**, *17*, 4908–4912.

J. Mottweiler, T. Rinesch, C. Besson, J. Buendia, C. Bolm, *Green Chem.* **2015**, *17*, 5001–5008.

Für meine Familie

Table of content

I. Introduction and Research Objective	1
1. Introduction	1
1.1. Lignin pretreatment methods.....	2
1.2. Synthesis of lignin model compounds.....	3
1.3. Catalytic lignin cleavage	6
1.4. Hydrotalcite-like catalysts in organic synthesis	15
1.5. Research aim	17
II. Results and Discussion	18
1. Synthesis of lignin model compounds.....	18
1.1. Synthesis of diastereomerically pure 1,3-dilignol β -O-4 model compounds	18
1.2. Synthesis of other lignin model compounds.....	23
2. Oxidative cleavage of lignin model compounds with nonheme iron complexes	26
2.1. Synthesis of nonheme iron catalysts.....	26
2.2. Cleavage studies of dilignol 3aE and nonheme iron catalysts	27
3. Oxidative cleavage of lignin model compounds with FeCl ₃ -derived iron complexes	33
3.1 Synthesis and characterization of FeCl ₃ -derived iron complexes	33
3.2. Cleavage studies of dilignol 3aE with FeCl ₃ -derived iron catalysts	36
4. Oxidative cleavage of lignin model compounds with supported gold catalysts.....	47
4.1. Cleavage studies of dilignol 3aE with air calcined Au/CeO ₂	47
4.2. Cleavage studies of dilignol 3aE with reduced supported gold catalysts	48
5. Oxidative cleavage of lignin with hydrotalcite-like catalysts and V(acac) ₃ /Cu(NO ₃) ₂ ·3H ₂ O as catalyst.....	56
5.1. Cleavage studies of dilignol 3aE with hydrotalcite-like catalysts.....	56
5.2. Catalyst recycling and catalyst leaching studies.....	61
5.3. Reaction kinetics and reaction pathways.....	66
5.4. Lignin cleavage studies	76
III. Summary and Outlook.....	87

1. Summary	87
1.1. Synthesis of diastereomerically pure 1,3-dilignol β -O-4 model compounds	87
1.2. Oxidative cleavage of lignin model compounds with nonheme iron complexes	88
1.3. Oxidative cleavage of lignin model compounds with FeCl ₃ -derived iron complexes.....	88
1.4. Oxidative cleavage of lignin model compounds with supported gold catalysts.....	89
1.5. Oxidative cleavage of lignin with hydrotalcite-like catalysts.....	90
1.6. Oxidative cleavage of lignin with V(acac) ₃ /Cu(NO ₃) ₂ ·3H ₂ O.....	91
2. Outlook.....	93
2.1. Oxidative cleavage of lignin model compounds with nonheme iron complexes	93
2.2. Oxidative cleavage of lignin model compounds with FeCl ₃ -derived iron complexes.....	93
2.3. Oxidative cleavage of lignin model compounds with supported gold catalysts.....	93
2.4. Oxidative cleavage of lignin with hydrotalcite-like catalysts and V(acac) ₃ /Cu(NO ₃) ₂ ·3H ₂ O	94
IV. Experimental Section	95
1. General Information	95
1.1. General	95
1.2. NMR.....	95
1.3. Mass spectrometry.....	95
1.4. HPLC.....	95
1.5. EPR.....	95
1.6. SEC.....	96
1.7. MALDI.....	96
1.8. ICP-OES	96
1.9. XRD.....	96
1.10. Raman.....	96
2. Synthesis of model compounds	97
2.1. Synthesis of 1,3-dilignol β -O-4 model compounds.....	97
2.2. Synthesis of monolignol and β -hydroxy ketones	109
2.3. Synthesis 1-(3,4-dimethoxyphenyl)-2-(2-methoxyphenoxy)prop-2-en-1-one	114

3.	Synthesis and catalysis with iron catalysts	116
3.1.	Synthesis of FeCl ₃ -derived iron complexes.....	116
3.2.	Catalysis reaction with FeCl ₃ -derived iron complexes.....	117
3.3.	Synthesis of nonheme iron complexes	118
3.4.	Catalysis reaction with nonheme iron complexes	119
4.	Synthesis and catalysis with supported gold catalysts.....	120
4.1.	Synthesis of supported gold catalysts.....	120
5.	Synthesis and catalysis with hydrotalcite-like catalysts	123
5.1.	Spectroscopic data for the hydrotalcite-like catalysts	123
5.2.	Catalysis with hydrotalcite-like catalysts	127
5.3.	Spectroscopic data of HTc-Cu-V after reaction	131
6.	Catalysis with V(acac) ₃ and Cu(NO ₃) ₂ ·3H ₂ O.....	132
7.	Spectroscopic data of isolated products	134
8.	Spectroscopic data of lignin	137
8.1.	HSQC spectra of lignin	137
8.2.	SEC of lignin.....	142
8.3.	MALDI spectra of lignin	147
8.4.	Elemental analysis of lignin	149
9.	Rate constants <i>k</i> in kinetic experiments.....	150
9.1.	Rate constants <i>k</i> for the cleavage of 3aE with V(acac) ₃ and Cu(NO ₃) ₂ ·3H ₂ O	150
9.2.	Rate constants <i>k</i> for cleavage reactions with HTc-Cu-V.....	152
10.	HPLC calibration.....	154
10.1.	HPLC calibration for <i>erythro</i> 1-(3,4-Dimethoxyphenyl)-2-(2-methoxyphenoxy)-1,3-propanediol.....	154
10.2.	HPLC calibration for 1-(3,4-Dimethoxyphenyl)-3-hydroxy-2-(2-methoxyphenoxy)propan-1-one.....	154
10.3.	HPLC calibration for 3,4-Dimethoxybenzaldehyde	155
10.4.	HPLC calibration for 3,4-Dimethoxybenzoic acid.....	155
V.	Abbreviations	156

Table of Content

VI. References	160
VII. Acknowledgements.....	166
VIII. Curriculum vitae.....	169

I. Introduction and Research Objective

1. Introduction

Biomass is defined as organic material that was produced by photosynthesis. Annually 170 billion metric tons are generated by nature.^[1] Among the different types of biomass lignocellulose constitutes the largest fraction on earth.^[2] Lignocellulose consists of three main components, cellulose, hemicellulose and lignin.^[3] Cellulose is a linear polymer of D-glucose chains, contributing with a share of 40% to 50% in hard and soft wood biomass.^[4] Hemicellulose is another major constituent of lignocellulose (16% to 33%). Unlike cellulose, hemicellulose is a branched polymer containing a variety of different sugar units. Both cellulose and hemicellulose are regarded as renewable feedstocks for generating fuels, chemicals and energy and have been subject to extensive valorization studies within the last decades.^[1-5] This research was facilitated by the ambitious goals of both European and U.S. legislation. The European Union defined a mandatory target for all member states that 20% of its entire energy consumption should stem from renewable sources with a minimum of 10% biofuels.^[6] Along those lines the U.S. Department of Agriculture and U.S. Department of Energy strive to cover 20% of its transportation fuel and 25% of U.S. chemical needs from biomass by the year 2030.^[7] In order to achieve these goals in a profitable manner it will be necessary to also utilize lignin, the third major component of lignocellulosic biomass. Lignin is a three-dimensional amorphous polymer consisting of methoxylated phenylpropane structures. It accounts for 15% to 30% of the weight and 40% of the energy content in lignocellulose.^[8] Lignin gives plants rigidity, enables the water transport and protects the cellulose fibers from microbial attackers.^[9] The biosynthesis is believed to proceed through the three monolignols *p*-coumaryl alcohol, coniferyl alcohol and sinapyl alcohol in a radical polymerization.^[8,9] Depending on the plant type these monolignols are incorporated in different ratios. The radical polymerization mechanism leads to a plethora of linkages that connect the different monomers. Figure I.1 highlights the most commonly found interconnecting bonds within lignin.

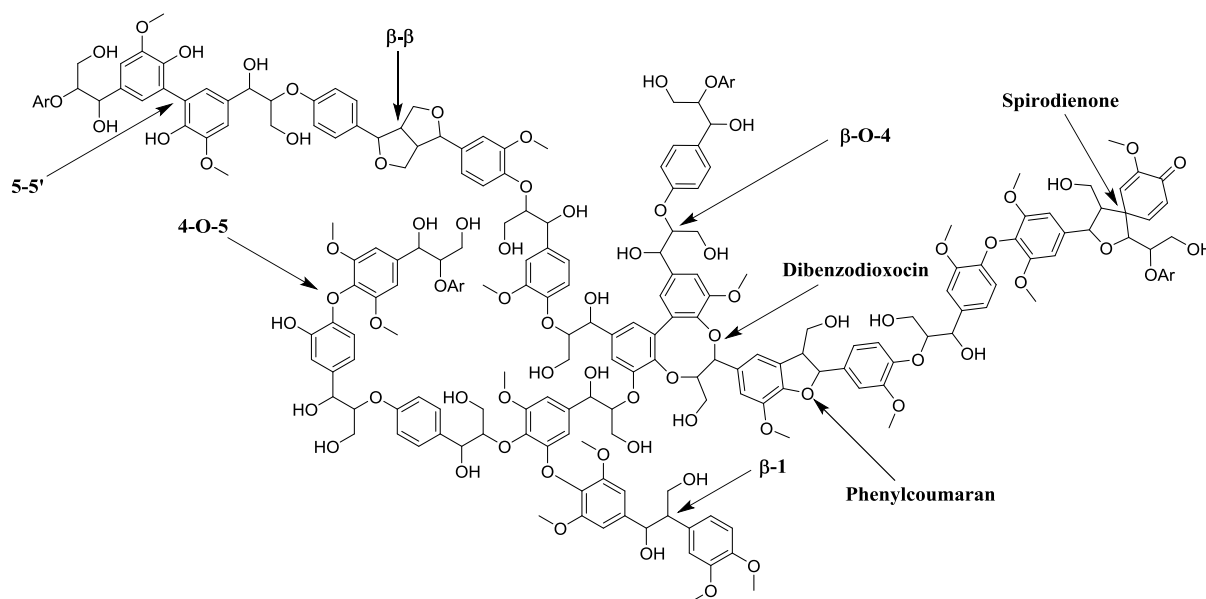


Figure I.1. Schematic representation of a lignin structure.

The β -O-4 bond accounts for 45% to 60% of the linkages, depending on the wood type.^[8,9] Other common structural motifs within lignin are the 5-5', phenylcoumaran (β -5), resinol structure (β - β), 4-O-5, β -1, dibenzodioxocin and spirodienone. The most stable of the aforementioned bonds is the 5-5' with a bond dissociation enthalpy of about $490 \text{ kJ}\cdot\text{mol}^{-1}$, making it one of the highest bond dissociation enthalpies found in nature.^[10] In comparison the β -O-4 bond dissociation enthalpies vary from $290 \text{ kJ}\cdot\text{mol}^{-1}$ to $305 \text{ kJ}\cdot\text{mol}^{-1}$. This multitude of interconnecting bonds, that varies in each plant, the high bond stabilities and its recalcitrant nature are the main reasons why lignin valorization processes are still at an initial stage. It is still mainly used as a low value energy source through incineration. In the last five years, however, the number of publications on lignin valorization has doubled.^[8c] The target in many of these lignin valorization studies was the β -O-4 linkage due to its prominence in lignin. It was also the focal point of the studies that were conducted in this dissertation.

1.1. Lignin pretreatment methods

To separate lignin from other constituents of lignocellulose, different pretreatment methods are frequently applied.^[8] These pretreatment methods influence greatly the morphology, impurities, polymer size and chemical structure within lignin. In the lignin cleavage studies described in this thesis, both organosolv lignin and kraft lignin were employed. Therefore these pretreatment techniques are briefly elaborated here.

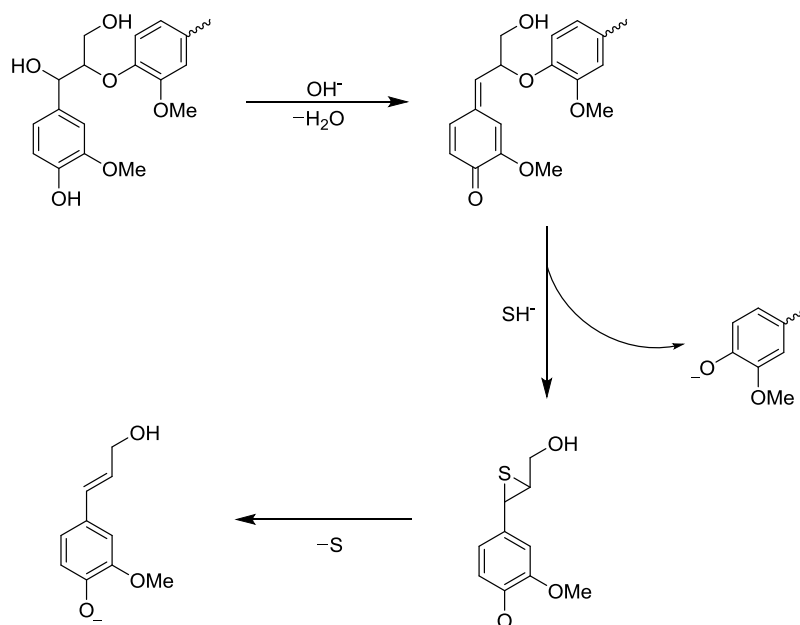
1.1.1. Organosolv Process

In the organosolv process commonly volatile alcohols such as ethanol and methanol are employed as solvent.^[8,9] A prominent example of an organosolv process is the Alcell process. In the first separation step a 1:1 mixture of water and ethanol is used. Cellulose is insoluble in this mixture, whereas lignin and hemicellulose are dissolved. After the separation of the

cellulose, lignin is precipitated through the addition of an excess of water while hemicellulose remains in solution.^[11] During the fractionation of biomass, catalysis plays a crucial role. Many of the known organosolv processes are autocatalyzed by the formation of acetic acid, which is generated through hydrolysis of acetate groups within hemicellulose. Alternatively, acids can also be added, which allows the use of milder reaction conditions.^[11]

1.1.2. Kraft Process

The most commonly used pretreatment method in pulping is the kraft lignin process.^[8a] It is conducted in an aqueous solution of NaOH and Na₂S at temperatures between 150 °C and 180 °C.^[11,12] Lignin is cleaved by sulfite anions as shown in Scheme I.1. Soluble kraft lignin is formed, which is then separated from the remaining constituents.^[13] Anthraquinone can be employed as catalyst to facilitate this process.^[12]



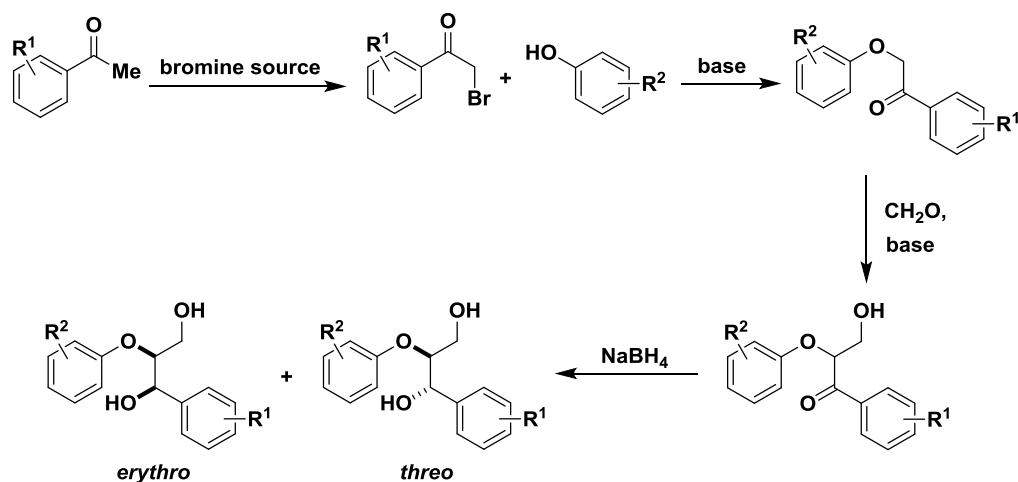
Scheme I.1. Cleavage of the β -O-4 linkage within lignin during the kraft lignin process.

1.2. Synthesis of lignin model compounds

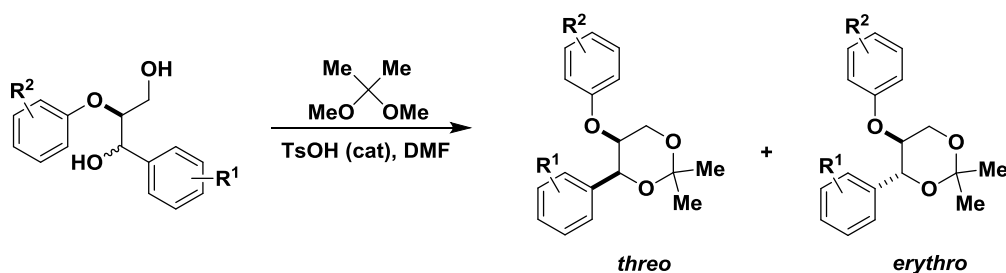
The structural complexity of lignin has led many researchers to perform their initial studies with lignin model compounds. A great variety of lignin model compounds and the references for their synthesis has been presented in the extensive review on catalytic lignin valorization by Weckhuysen and co-workers.^[8a] Here, only synthetic strategies for the synthesis of β -O-4 1,3-dilignol model compounds will be discussed.

The first protocol for the synthesis of 1,3-dilignols was published in the year 1952.^[14] Adler and co-workers employed commercially available acetophenone derivatives as starting material that were brominated in the first step, followed by nucleophilic substitution with phenol derivatives in the presence of a base (Scheme I.2).^[14,15] The corresponding keto aryl ethers were then transformed in an aldol addition to β -hydroxy ketones. In the final step these

β -hydroxy ketones were reduced with NaBH_4 to form both the *erythro* and *threo* 1,3-dilignols. These diastereomers, however, cannot be separated completely from each other by crystallization or column chromatography. To obtain the pure diastereomers further derivatization to the corresponding acetonides is necessary (Scheme I.3).^[16,17] After separating the *erythro* and *threo* acetonides by column chromatography, the diastereomerically pure 1,3-dilignols are obtained after hydrolysis.

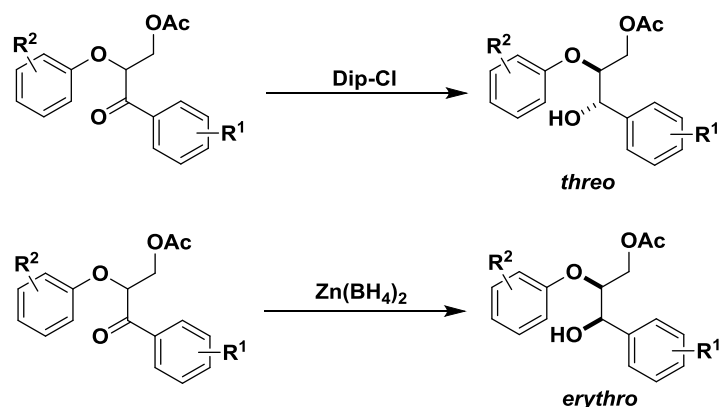


Scheme I.2. Synthetic route to 1,3-dilignols by Adler and co-workers.^[14,15]



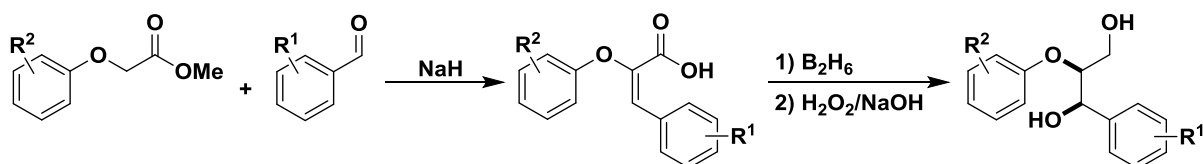
Scheme I.3. Conversion of 1,3-dilignols to the corresponding acetonides.

To avoid derivatization of 1,3-dilignols, Helm and co-workers have reported a diastereoselective reduction of the corresponding acetylated β -hydroxy ketones (Scheme I.4).^[18,19] Diisopinocampheyl chloroborane ($\text{Dip-Cl}^{\text{TM}}$) was employed for the reduction to the corresponding *threo* 1,3-dilignol and $\text{Zn}(\text{BH}_4)_2$ used for obtaining the *erythro* 1,3-dilignol.



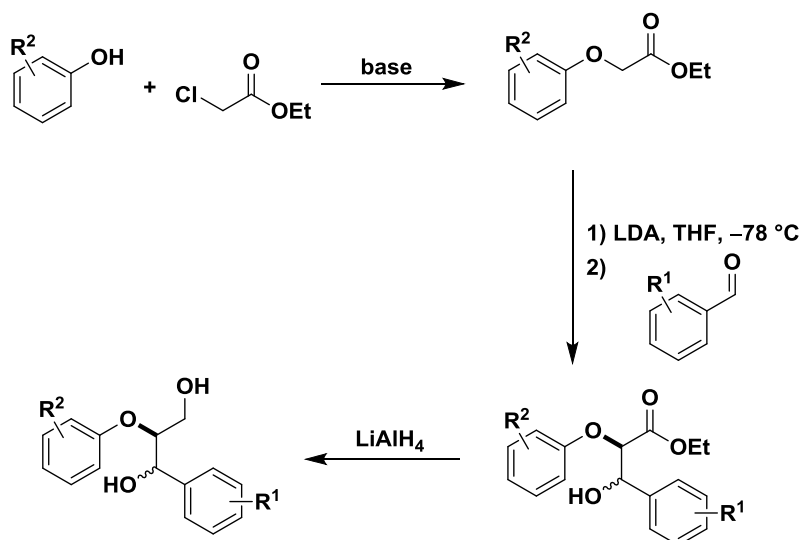
Scheme I.4. Diastereoselective reduction of β -hydroxy ketones by Helm and co-workers.^[18,19]

Lundquist and co-workers described an *erythro* selective route for the synthesis of 1,3-dilignols.^[20] Starting from a methyl aryloxy ester and a benzaldehyde derivative, an α,β -unsaturated acid was obtained after 1,2-addition, saponification and condensation in the presence of sodium hydride. The desired *erythro* 1,3-dilignol was then obtained after hydroboration and subsequent oxidation in total diastereoselectivity.



Scheme I.5. Synthesis of 1,3-dilignols under the conditions by Lundquist and co-workers.^[20]

The most commonly used route for the synthesis of 1,3-dilignols was first described by Nakatsubo *et al.* (Scheme I.6).^[21] His synthesis started off from commercially available ethyl chloroacetate and 2-methoxyphenol that were set to react in the presence of a base to form the corresponding aryloxy ester. In the next step the corresponding lithium enolate of the aryloxy ester reacted with a benzaldehyde derivative in a 1,2-addition to form a β -hydroxy ester. The formation of the *erythro* diastereomer was favored over the *threo* diastereomer which resulted in a low yield for the corresponding *threo* β -hydroxy ester.^[22,23] In the last step the β -hydroxy ester was reduced with $LiAlH_4$.



Scheme I.6. Synthesis of 1,3-dilignols after the reaction conditions of Nakatsubo *et. al.*^[21]

1.3. Catalytic lignin cleavage

Over the last century many different strategies have been employed for the cleavage of lignin with catalysis playing a crucial role in many of these processes.^[8] Due to the great diversity of this research area only catalyzed reactions are discussed below. Studies that utilized model compounds that lack key structural features of lignin (e.g., ferulic acid or veratryl alcohol) are not included because of the limited significance of these results for the depolymerization of lignin. Furthermore, acid^[24] and base^[25,26] catalyzed lignin cleavage reactions will not be elaborated on, as the focus of this dissertation was to find suitable transition metal catalysts for the cleavage of lignin.

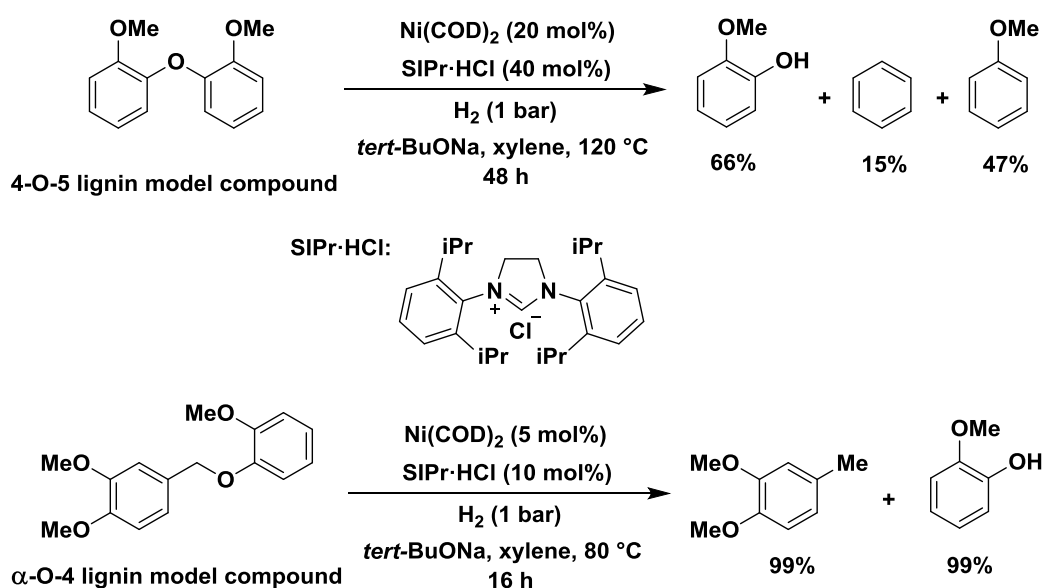
1.3.1. Heterogeneously catalyzed reductive lignin cleavage

Heterogeneous transition metal catalysts have been frequently utilized for the hydrogenation and hydrodeoxygenation of lignin.^[8a,27-29] They provide access to a plethora of phenolic, phenyl, and cyclohexyl derivatives. In general, reductive lignin cleavage leads to less functionalized products as these reaction conditions promote the removal of functional groups. Among the first catalysts screened for reductive lignin cleavage were copper-chromium oxide and Rainey nickel.^[27] Another class of catalysts that has found frequent application in recent years is supported noble metal catalysts. In their pioneering work in the 1960s, Pepper and co-workers employed Pd-C, Rh-C, Ru-C and Ru-alumina.^[28] Depending on the catalyst and the reaction conditions they obtained dihydroconiferyl alcohol, phenol, guaiacol and various guaiacol and cyclohexyl derivatives.

1.3.2. Homogeneously catalyzed reductive and redox neutral lignin cleavage

Compared to heterogeneous catalysis there are fewer examples in literature that utilize homogeneous transition metal catalysts for reductive lignin cleavage.^[30,31] Ragauskas and

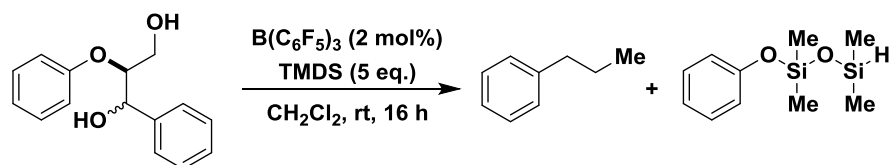
co-workers compared the reactivity of NaBH_4/I_2 , $\text{RhCl}(\text{PPh}_3)_3$, $\text{Ru}(\text{Cl})_2(\text{PPh}_3)_3$, $\text{Ru}(\text{H})(\text{Cl})(\text{PPh}_3)_3$ and Ru-polyvinylpyrrolidone nanoparticles (Ru-PVP) with previously mentioned heterogeneous catalysts such as Rainey-nickel and Pd-C for the hydrogenolysis of organosolv lignin.^[31b] In general, the homogeneous catalysts afforded higher yields, but had some stability issues at elevated temperatures and were difficult to separate from the formed products. In a study with lignin model compounds, Hartwig and co-workers reported the hydrogenolysis of aryl ethers.^[31c] As catalyst they employed $\text{Ni}(\text{COD})_2$ in presence of a *N*-heterocyclic carbene ligand (NHC) with *tert*-BuONa as base and xylene as solvent (Scheme I.7). For a 4-O-5 and α -O-4 model compound good to excellent yields for the aryl ether cleavage products were obtained. The cleavage of a 1,3-dilignol model compound (not shown) proceeded without catalyst in a *tert*-BuONa-mediated reaction affording 2-methoxyphenol as main product.



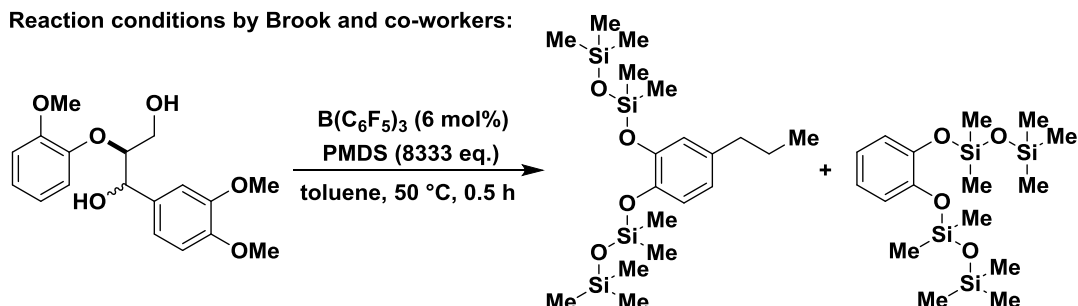
Scheme I.7. Aryl ether cleavage by Hartwig and co-workers.^[31c]

Recently, Lewis acid catalyzed reductive cleavage of lignin model compounds and lignin has been described under Piers-Rubinsztajn-type reaction conditions using either tetramethyldisiloxane (TMDS) or pentamethyldisiloxane (PMDS) as reducing agent (Scheme I.8).^[32] The cleavage of the β -O-4 linkage was demonstrated for both lignin model compounds and extracted lignin, affording aryl silyl ethers in which both the primary, aliphatic and benzylic alcohols are reduced to alkanes.

Reaction conditions by Cantat and co-workers:



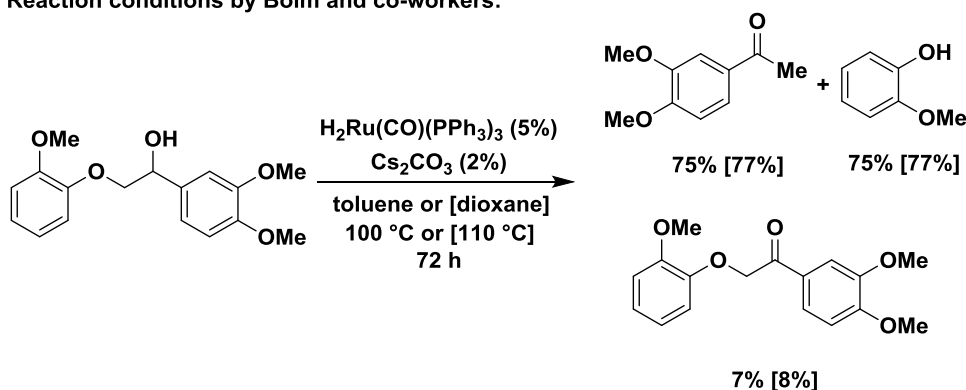
Reaction conditions by Brook and co-workers:



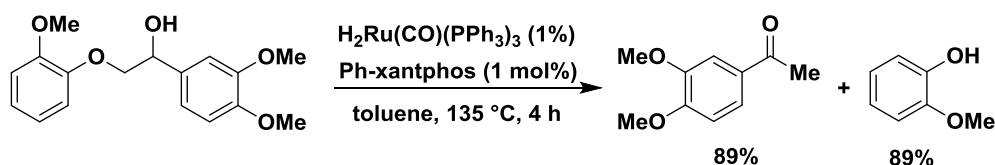
Scheme I.8. Cleavage of 1,3-dilignols under Piers-Rubinsztajn-type reaction conditions.^[32]

Apart from reductive lignin cleavage there have been several reports in which a transition metal, such as ruthenium, catalyzed transfer-hydrogenations under redox-neutral reaction conditions.^[33,34] Simultaneously, Nichols *et al.*^[33a] and Bolm and co-workers^[34] have studied the cleavage of β -O-4 monolignol model compounds with $H_2RuCO(PPh_3)_3$ as catalyst (Scheme I.9). Using 5 mol% $H_2RuCO(PPh_3)_3$ and a reaction time of 72 h, Bolm and co-workers obtained 3,4-dimethoxyacetophenone and 2-methoxyphenol in good yields (75% in toluene and 77% in dioxane). Nichols *et al.* were able to reduce the catalyst loading to 1 mol% by employing Ph-xantphos as ligand while increasing the yield for 3,4-dimethoxyacetophenone and 2-methoxyphenol to 89% after 4 h.

Reaction conditions by Bolm and co-workers:

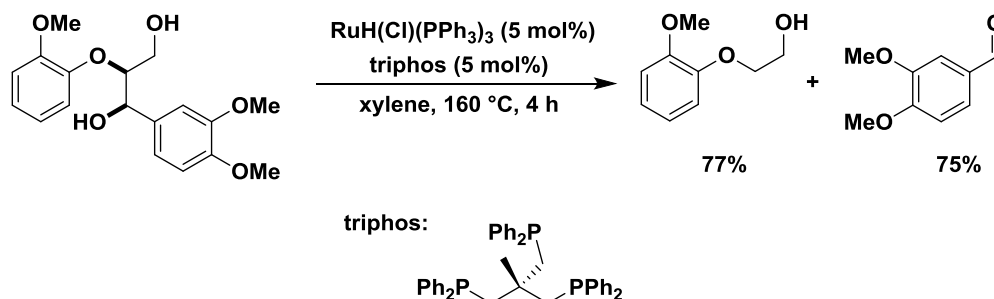


Reaction conditions by Nichols *et al.*:



Scheme I.9. Cleavage of a monolignol model compound with $H_2RuCO(PPh_3)_3$ as catalyst.^[33a,34]

Commonly, transfer-hydrogenation with ruthenium and rhodium catalysts led to C–O bond cleavage within β -O-4 model compounds. However, vom Stein *et al.* reported on the C–C bond cleavage within 1,3-dilignols in good yields when they employed a ruthenium triphos catalyst as shown in Scheme I.10.^[33e]



Scheme I.10. C–C bond cleavage with ruthenium triphos catalyst.^[33e]

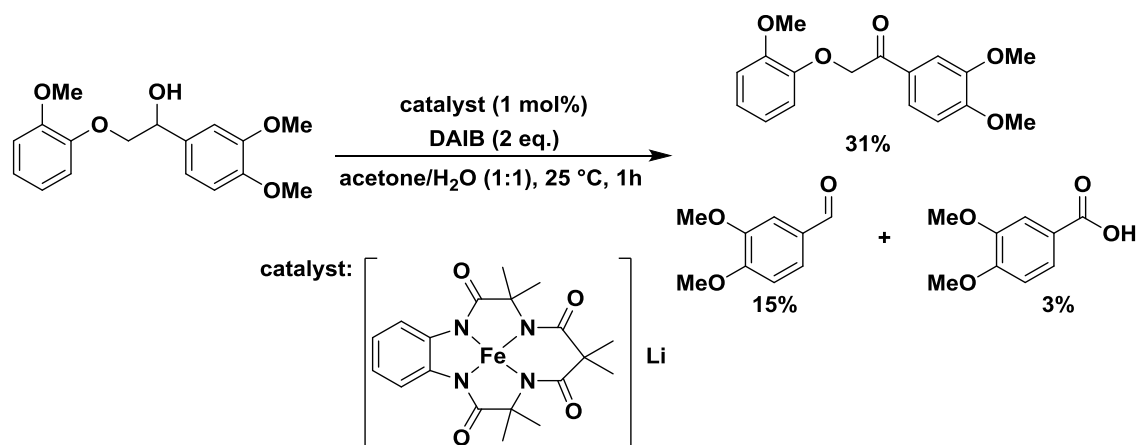
1.3.3. Homogeneously catalyzed oxidative lignin cleavage

Over many decades homogeneous catalysts have been studied extensively for the oxidative cleavage of lignin.^[8,35-38,40,41] Oxidative lignin cleavage commonly preserves more of the strong intrinsic functionalization within lignin than reductive cleavage while at the same time adding new functionality to the products. Homogeneous iron, copper and vanadium catalysts were studied over the course of this dissertation in the oxidative cleavage of lignin and catalytic systems utilizing these transition metals are now described in greater detail.

1.3.3.1. Iron-catalyzed oxidative lignin cleavage reactions

Iron has been applied in various manners as catalyst in oxidative lignin cleavage studies.^[37,38] However, considering its natural abundance and oxidation potential in organic transformations, it has thus far been underutilized.^[39]

Several different macrocyclic iron complexes have been studied in the cleavage of lignin and lignin model compounds.^[37] Shimada *et al.* employed tetraphenylporphyrinatoiron (III) chloride as catalyst in the cleavage of a β -1 lignin model compound at room temperature with TBHP as oxidant.^[37a] The main product in this reaction was an aromatic aldehyde. Wright and co-workers studied the cleavage of a 1,3-dilignol with trisodium tetra-4-sulfonatophthalocyanineiron(III) [Fe(TSPc)]. They obtained vanillin and 2-methoxyphenol as the main products. Another class of macrocycles that has been utilized in this context is tetraamido macrocyclic ligands (TAML). Collins *et al.* used Fe-TAML for the removal of lignin and lignin derivatives in pulping and waste water.^[37d] In a study with lignin model compounds, Andrioletti and co-workers demonstrated the cleavage of a β -O-4 monolignol model compound with Fe(TAML)Li as catalyst and DAIB as oxidant (Scheme I.11).^[37e] The main product in this reaction was the corresponding keto aryl ether in 31% yield. The cleavage products veratraldehyde and veratric acid were obtained in 15% and 3% yield, respectively.



Scheme I.11. Fe(TAML)Li catalyzed cleavage of a monolignol lignin model compound.^[37e]

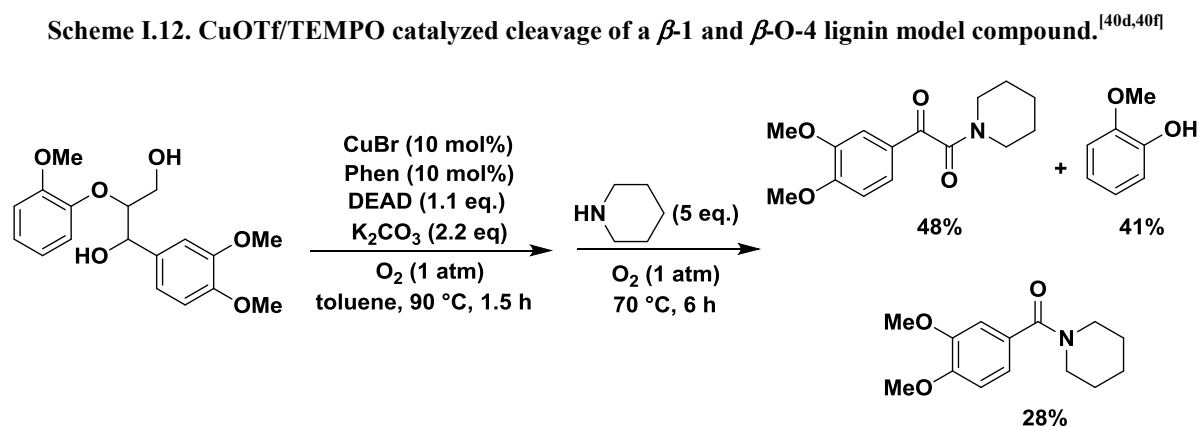
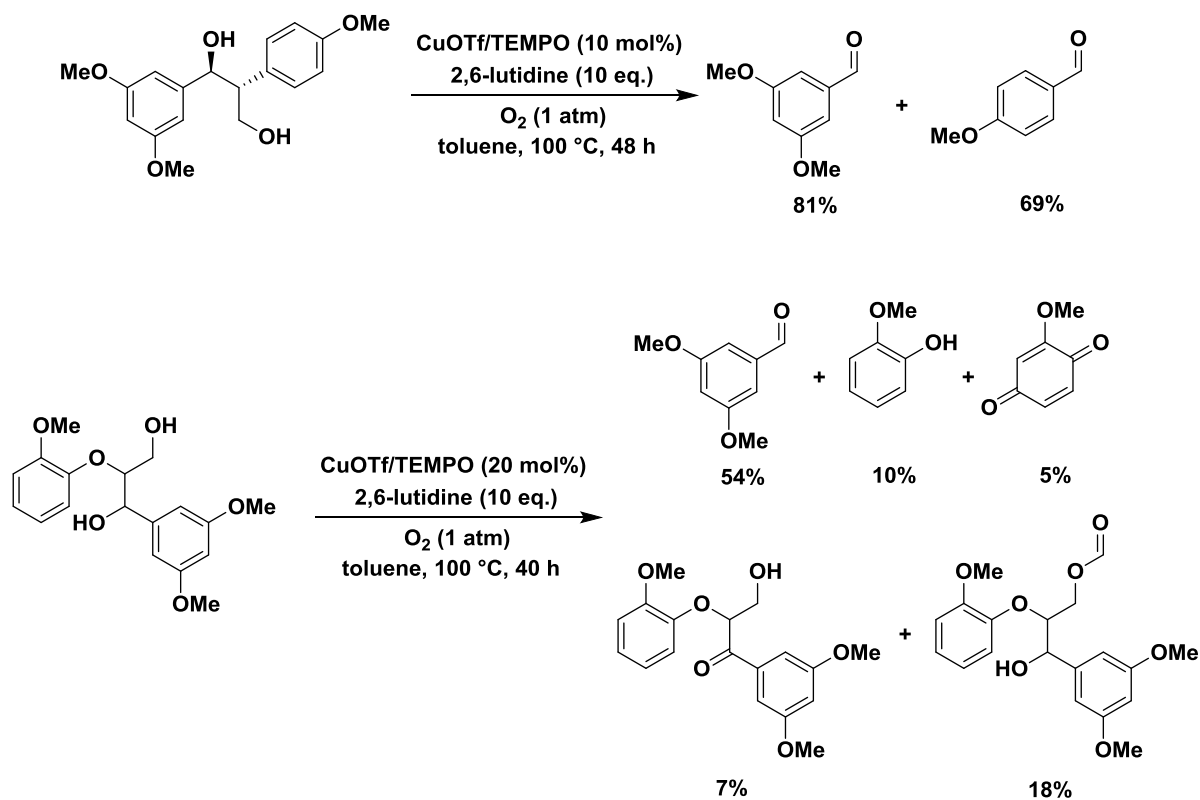
Simple iron salts have been employed under Fenton reaction conditions or at elevated temperatures in alkaline medium under dioxygen pressure.^[38] Araujo *et al.* observed that when Fenton's reagent was employed for the cleavage of kraft black liquor with low H₂O₂ concentrations, polymerization to higher masses occurred.^[38c] Higher H₂O₂ concentrations or omitting an external iron source resulted in depolymerisation to lower mass products. The activity of the reaction system without the addition of iron was attributed to iron impurities present in the kraft black liquor catalyzing the reaction. Tong and co-workers pretreated organosolv lignin under Fenton reaction conditions before cleaving it in supercritical ethanol at 250 °C under 7 MPa pressure.^[38d] An organic oil was obtained consisting of mono- and oligomeric aromatics, phenols and dicarboxylic acids.

Both Wu *et al.* and Lee and co-workers used iron (III) salts in combination with copper (II) salts for the cleavage of lignin in alkaline solution under dioxygen pressure at temperatures between 160 °C and 180 °C.^[38a,38b] The combination of both transition metals helped increase the yield of aromatic aldehydes which were obtained as the main products.

1.3.3.2. Copper-catalyzed oxidative lignin cleavage reactions

Compared to iron, copper catalysts have been studied more intensively in recent years in the oxidative cleavage of lignin.^[40] Watanabe and co-workers used copper 2,2'-dipyridylamine and copper 4-aminopyridine complexes for pulp bleaching in alkaline solution with H₂O₂ as oxidant.^[40a] Sedai *et al.* investigated the catalytic activity of a CuOTf/TEMPO catalyst under dioxygen atmosphere with 2,6-lutidine as ligand in the cleavage of β -1 and β -O-4 1,3-dilignol lignin model compounds (Scheme I.12).^[40d,40f] Aromatic aldehydes were obtained as main products in these reactions. The catalytic system was more selective and the reaction progressed faster for the cleavage of β -1 model compounds than β -O-4 model compounds. For both lignin linkages the degradation proceeded through C–C bond cleavage.

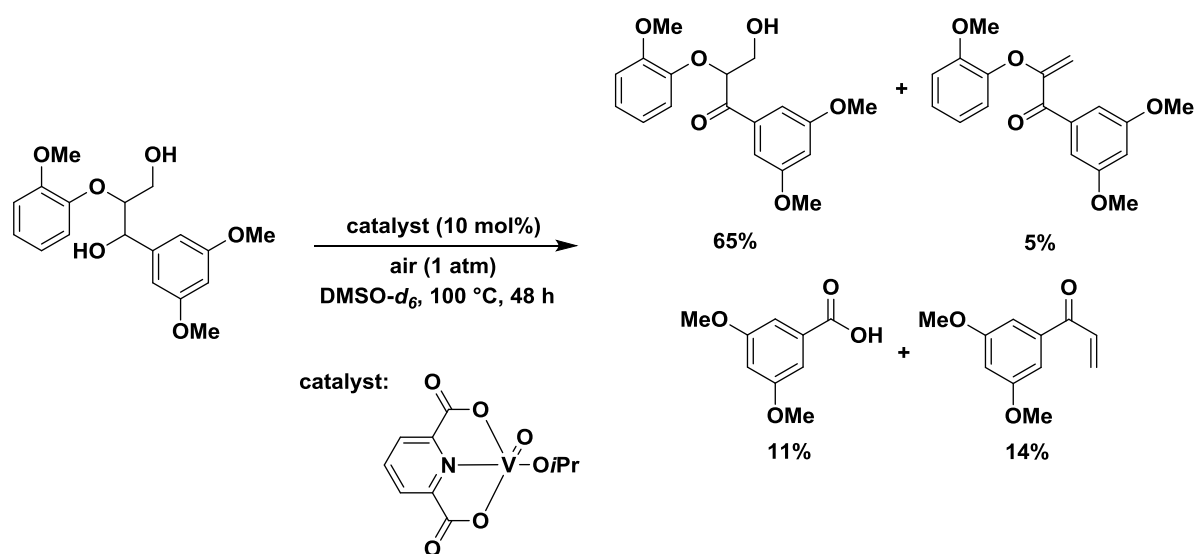
A conceptually different approach was demonstrated by Loh and co-workers.^[40c] In their cleavage studies with β -O-4 model compounds first the benzylic alcohol was oxidized to the ketone followed by a copper catalyzed aerobic amide bond formation (Scheme I.13).



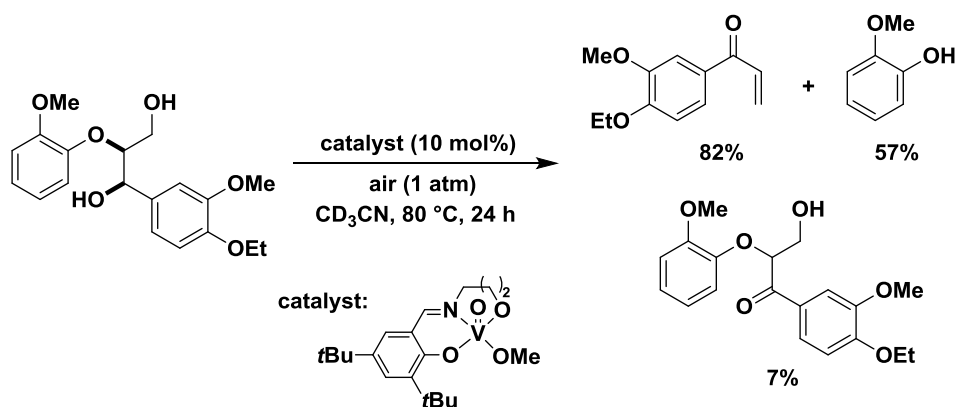
One of the key challenges in lignin cleavage is that the formed products are often more reactive than the polymeric starting material. These products are susceptible to repolymerization. To avoid random repolymerization, Saito and co-workers added 4-*tert*-butyl-2,6-dimethylphenol in a copper-catalyzed cleavage of lignin in alkaline solution under dioxygen atmosphere. 4-*tert*-Butyl-2,6-dimethylphenol reacted directly with the formed lignin cleavage products to afford more defined and shorter polymers.^[40e] Another method to prevent repolymerization or over-oxidation of the desired products was shown by Liu *et al.* in a CuSO₄ catalyzed reaction in a mixed phosphate solution.^[40g] In their reaction set-up the formed aromatic aldehyde products were continuously separated by dissociation extraction over the course of the reaction.

1.3.3.3. Vanadium-catalyzed oxidative lignin cleavage reactions

Another transition metal that has been targeted for the cleavage of lignin in recent years is vanadium.^[40b,40d,41] Initially Baker and Hanson tested the vanadium complex (dipic)V^V(O)(OiPr) in the cleavage of simple lignin model compounds and a 1,3-dilignol (Scheme I.14).^[40b,41a] In the conversion of the 1,3-dilignol model compound the benzylic alcohol was primarily oxidized. The corresponding β -hydroxy ketone was obtained in 65% yield. As cleavage products 3,5-dimethoxybenzoic acid and 1-(3,5-dimethoxyphenyl)prop-2-en-1-one were formed in 11% and 14% yield respectively. Simultaneously, Toste and co-workers investigated the cleavage of β -O-4 model compounds with vanadium salen-type complexes (Scheme I.15).^[41b] The main products in the cleavage of a 1,3-dilignol were 1-(4-ethoxy-3-methoxyphenyl)prop-2-en-1-one and 2-methoxyphenol in 82% and 57% yield respectively. As side product the corresponding β -hydroxy ketone was obtained in 7% yield. Toste proposed a redox-neutral mechanism that proceeds through a one-electron process from vanadium (V) to vanadium (IV), which in turn is reoxidized by an aryloxy radical to vanadium (V) without the need of an external oxidant. The reaction, however, proceeds slower and in lower yields without an external oxidant. This mechanism is in contrast to the one observed by Hanson *et al.* for the oxidation of alcohols with (dipic)V^V(O)(OiPr) in pyridine.^[42] They propose a two electron oxidation mechanism from vanadium (V) to vanadium (III).



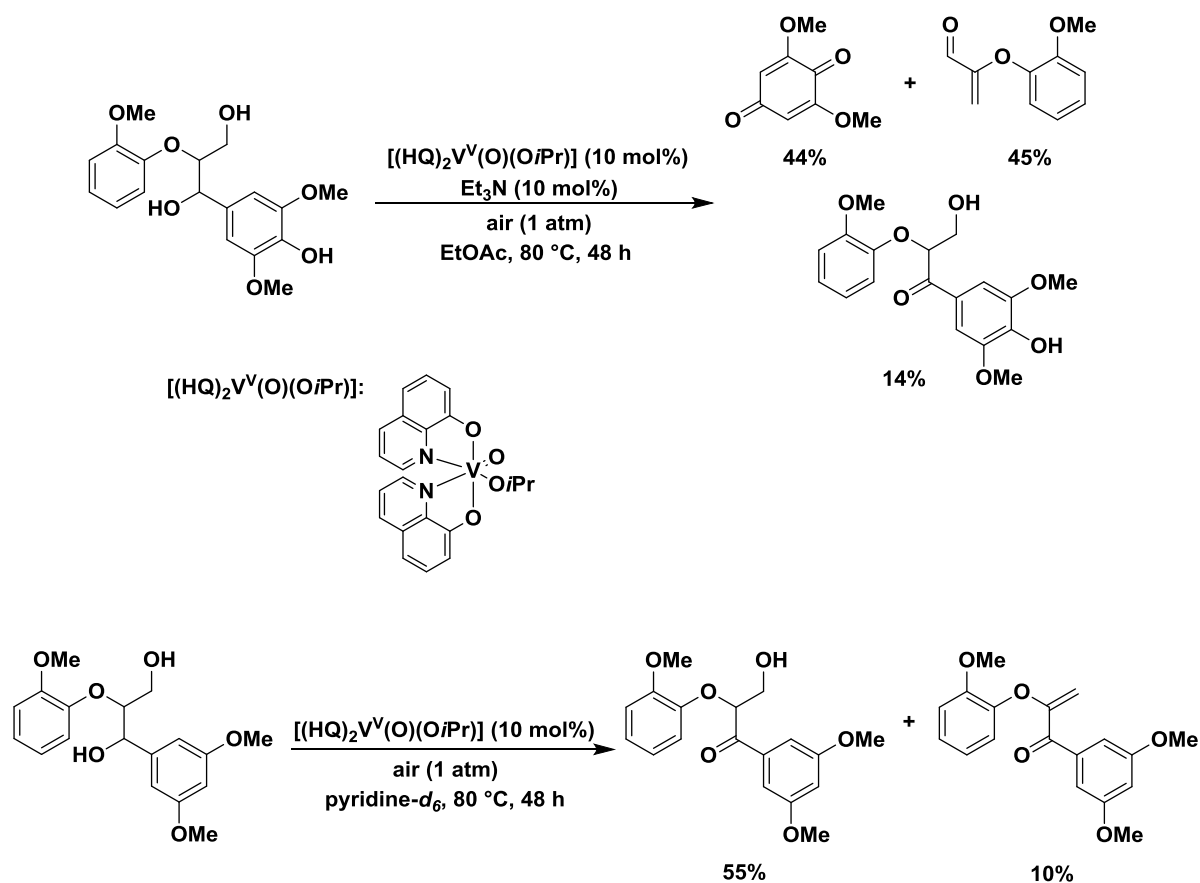
Scheme I.14. [(dipic)V^V(O)(OiPr)] catalyzed oxidation of a 1,3-dilignol.^[40b]



Scheme I.15. Vanadium catalyzed cleavage of a 1,3-dilignol by Toste and co-workers.^[41b]

Hanson and co-workers modified their previously employed [(dipic)V^V(O)(O*i*Pr)] complex by substituting dipicolinate with 8-quinolinate. The corresponding vanadium bis(quinolinate) catalyst, [(HQ)₂V^V(O)(O*i*Pr)], displayed distinctly different selectivity than the previous vanadium complexes in the cleavage of a phenolic 1,3-dilignol (Scheme I.16).^[41c] They observed C–C bond cleavage between the benzylic carbon and the phenylic carbon, affording 2,6-dimethoxybenzoquinone and an acrolein derivative in 44% and 45% yield. For a non-phenolic 1,3-dilignol [(HQ)₂V^V(O)(O*i*Pr)] was less active furnishing the corresponding β-hydroxy ketone in 55% yield with an overall conversion of 65%.

Toste and co-workers tested both his previously employed vanadium salen-type complexes and [(HQ)₂V^V(O)(O*i*Pr)] in the cleavage of various organosolv lignin samples.^[41d] Both classes of vanadium complexes showed similar activity for lignin degradation. 2D-NMR (HSQC) experiments revealed that unprotected β-O-4 linkages within lignin were completely degraded. However, acetylated or otherwise protected β-O-4 linkages, which are ubiquitous in various organosolv lignin sources, as for example from the Alcell process, remained unaffected.

Scheme I.16. $[(\text{HQ})_2\text{V}^{\text{V}}(\text{O})(\text{OiPr})]$ catalyzed cleavage of 1,3-dilignols by Hanson and co-workers.^[41c]

1.3.4. Heterogeneously catalyzed oxidative lignin cleavage

Heterogeneous transition metal catalysts have been used for the oxidative lignin cleavage, albeit less frequently than for example homogeneous catalysts.^[43-46] The goal in many of these studies was the nonselective removal of lignin and lignin derivatives in pulping and waste water streams.^[44] One approach for the selective degradation of lignin was to utilize immobilized homogeneous catalysts that have been successfully tested in homogenous reactions. Along those lines Crestini *et al.* immobilized methyltrioxorhenium (MTO) in various manners and tested them in the cleavage of lignin model compounds and lignin with H_2O_2 as oxidant.^[45a] The immobilized MTO catalysts showed both activity in the cleavage of model compounds and for the degradation of various lignin sources.

In this dissertation primarily heterogeneous catalysts were screened that used dioxygen as oxidant. Both Sales *et al.* and Lin and co-workers employed dioxygen as oxidant in their studies, investigating catalytic wet aerobic lignin oxidation in alkaline solution.^[46] They obtained aromatic aldehydes as their main products. Sales *et al.* employed $\text{Pd}/\gamma\text{-Al}_2\text{O}_3$ as catalyst at reaction temperatures between $100\text{ }^\circ\text{C}$ and $120\text{ }^\circ\text{C}$ with 20 bar pressure and a partial dioxygen pressure of 2 to 10 bar. Lin and co-workers utilized Pervoskite-type oxides containing either manganese, copper, iron or cobalt.^[46b-46e] After 3 h at $120\text{ }^\circ\text{C}$ and 20 bar pressure with a partial dioxygen pressure of 5 bar they observed that 67% of the lignin was converted. However, when the catalyst was omitted under the same reaction conditions 42%

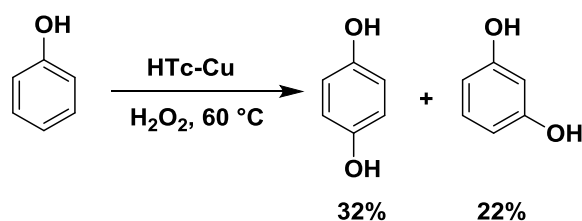
conversion was obtained. This observation is not surprising, considering that the cleavage of lignin in alkaline solution under dioxygen pressure at elevated temperatures has been studied for several decades.^[47] Furthermore, it implies that for both catalytic systems in alkaline solution the effect of the catalyst is rather minor.

1.4. Hydrotalcite-like catalysts in organic synthesis

Hydrotalcites, also known as layered double hydroxides or anionic clays, are crystalline materials composed of positively charged two-dimensional sheets that are charge compensated by exchangeable counteranions and water in their interlayers.^[48] In nature hydrotalcite has the structure $\text{Mg}_6\text{Al}_2\text{CO}_3(\text{OH})_{16}\cdot 4\text{H}_2\text{O}$. The general formula for natural and synthetic hydrotalcites is $[\text{M}^{2+}_{1-x}\text{M}^{3+}_x(\text{OH})_2]^{x+} (\text{A}^{n-}_{x/n})\cdot m\text{H}_2\text{O}$ and they display a brucite-like structure ($\text{Mg}(\text{OH})_2$). Synthetic hydrotalcites, commonly referred to as hydrotalcite-like catalysts, can also contain other bivalent (Ni, Cu, Co) and trivalent cations (Fe, Cr). Positive excess charge of layers is induced by the exchange of a bivalent cation with a trivalent cation of similar radius.^[48c] The acidity and basicity of hydrotalcites can be adjusted through the types of ions that are incorporated. Generally the basicity decreases when magnesium and aluminum ions are exchanged by other di- and trivalent transition metals. Furthermore, the Mg:Al ratio determines the density and strength of basic sites.

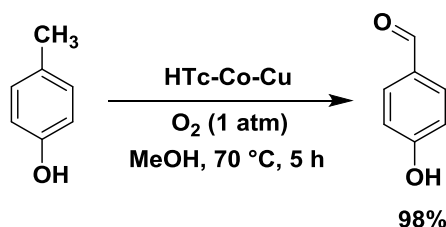
Hydrotalcite-like catalysts can be synthesized by various techniques such as co-precipitation, urea hydrolysis, sol-gel and microwave irradiation.^[48b] The most frequently employed methodology is co-precipitation. Aqueous solutions of inorganic salts (usually nitrates) are commonly slowly combined with alkaline solutions of hydroxides and carbonates at a fixed pH under stirring and inert atmosphere.^[48c] After finishing the addition, the hydrotalcite-like catalysts are further modified by ageing of the reaction slurry. Subsequent calcination at temperatures of up to 700 °C often increases the catalytic activity by raising the surface area and narrowing the pore size distribution. Furthermore the loss of water and anions leads to the formation of Lewis basic $\text{O}^{2-}\text{M}^{n+}$ pairs and O^{2-} ions.

As mentioned earlier in this chapter, transition metal catalysts were targeted for the oxidative cleavage of lignin. Transition metal containing hydrotalcite-like catalysts have shown interesting properties in oxidative transformations.^[49] Zhu *et al.* employed copper containing hydrotalcite-like catalysts (HTc-Cu) in the hydroxylation of phenol with H_2O_2 as oxidant (Scheme I.17).^[49a]

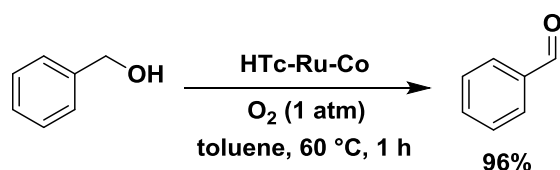
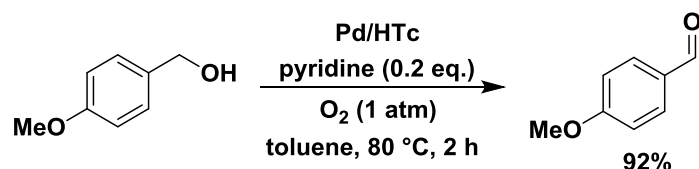


Scheme I.17. HTc-Cu catalyzed hydroxylation of phenol with H₂O₂.^[49a]

Yue and co-workers utilized cobalt-copper hydrotalcite-like catalysts (HTc-Co-Cu) in the oxidation of *p*-cresol to *p*-hydroxybenzaldehyde under dioxygen atmosphere (Scheme I.18).^[49b]

**Scheme I.18. HTc-Co-Cu catalyzed oxidation of *p*-cresol to *p*-hydroxybenzaldehyde with dioxygen.^[49b]**

Hydrotalcite-like catalysts have also been successfully employed in alcohol oxidations.^[49c-49e] This is of note because it increases the probability that they can be successfully applied for the oxidative cleavage of lignin bonds such as the β -O-4. Kaneda and co-workers demonstrated the oxidation of allylic and benzylic alcohols with ruthenium and ruthenium-cobalt hydrotalcite-like catalysts (HTc-Ru and HTc-Ru-Co) (Scheme I.19).^[49c,49d] Furthermore, Nishimura *et al.* reported the oxidation of alcohols with palladium supported on hydrotalcite in toluene with pyridine as additive under dioxygen atmosphere (Scheme I.20).^[49e]

**Scheme I.19. HTc-Ru-Co catalyzed oxidation of alcohols with dioxygen.^[49d]****Scheme I.20. Pd/HTc catalyzed oxidation of alcohols with dioxygen.^[49e]**

1.5. Research aim

The aim of this research is to investigate the selective cleavage of lignin with transition metal catalysts. Furthermore the emphasis is placed on oxidative reaction conditions. In this context both homogeneous and heterogeneous catalysts are studied. The catalysts that are utilized have been described in literature but for distinctly different transformations. To assess the activity and selectivity of the reaction systems, as well as to elaborate mechanistical aspects, lignin model compounds are used. Organosolv lignin and kraft lignin are utilized as lignin sources for studies with the natural polymer.

II. Results and Discussion

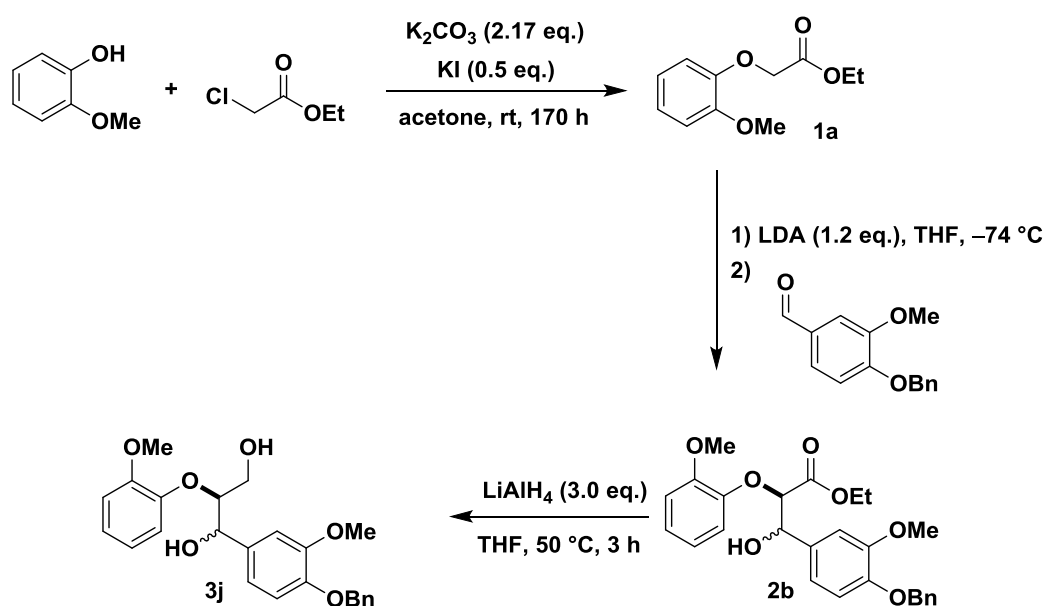
1. Synthesis of lignin model compounds

As mentioned in the previous chapter the goal of this research is to find new catalytic systems that enable the selective cleavage of lignin. Due to the complexity of lignin and its challenging analytics every initial catalyst screening described in this chapter was performed with lignin model compounds. In the introductory part of this thesis several synthetic strategies for the synthesis of 1,3-dilignol model compounds have been described. These protocols, however, have the drawback of requiring multiple synthetic steps with a low overall yield or the separation of the formed diastereomers was very challenging making them not easily accessible in their diastereomerically pure form. The development of a superior synthetic protocol for diastereomerically pure 1,3-dilignols is now discussed which gives access to both their *erythro* and *threo* forms.

1.1. Synthesis of diastereomerically pure 1,3-dilignol β -O-4 model compounds

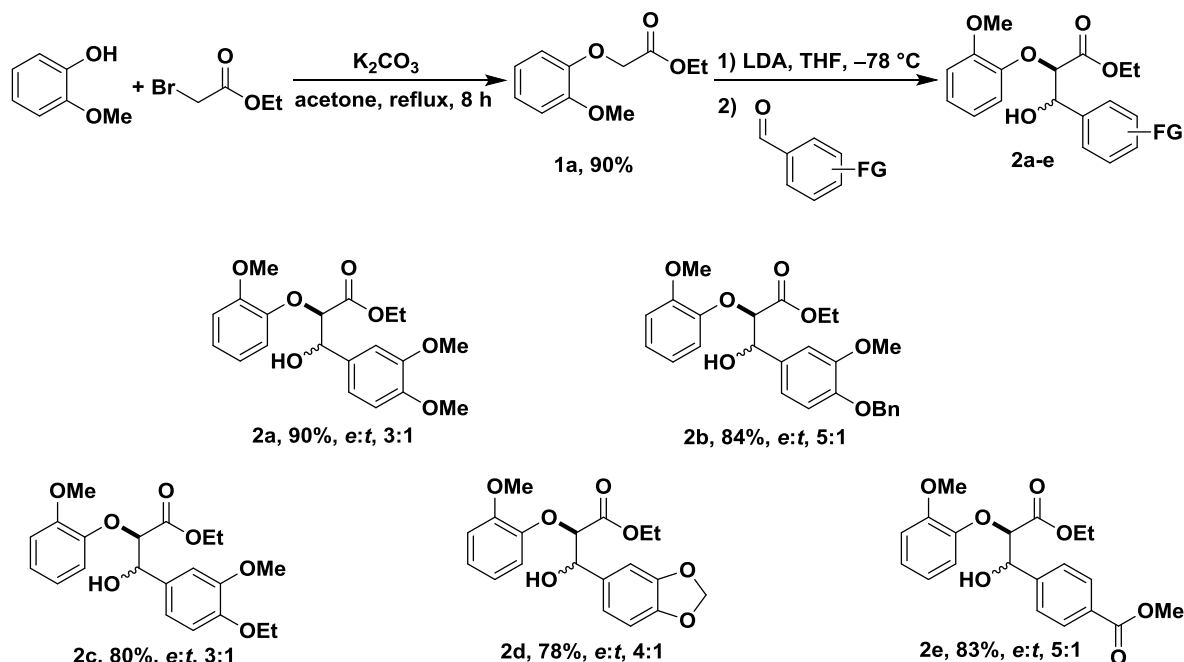
The results presented here were obtained in collaboration with Buendia.^[50] In the following discussion numerous compounds are shown that have only been synthesized by Buendia and are therefore not included in the experimental part.

The starting point for the optimization process was a synthetic protocol described by Nakatsubo *et. al.* which has been mentioned in the introduction and is shown again in Scheme II.1.^[21] In the first step, commercially available ethyl chloroacetate and 2-methoxyphenol were set to react in the presence of K_2CO_3 and KI at room temperature for 170 h. The corresponding aryloxy ester **1a** was obtained in 90% yield.



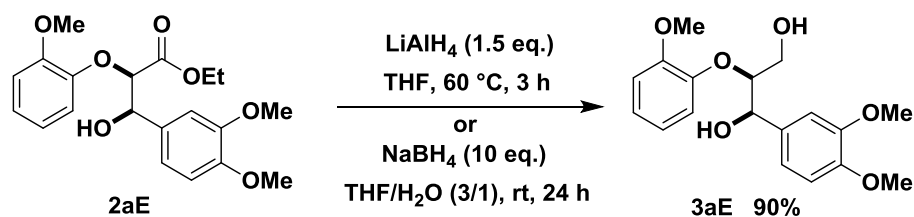
Scheme II.1. Synthesis of 1,3-dilignols using the reaction conditions of Nakatsubo *et. al.*^[21]

However, for rapid syntheses of 1,3-dilignols a reaction time of 170 h was not desirable. Therefore the more reactive ethyl bromoacetate was chosen as starting material. A screening of reaction conditions led to a significant decrease in reaction time while maintaining excellent yields. After 8 h at reflux aryloxy ester **1a** was obtained in 90% yield (Scheme II.2) independent of the reaction scale.



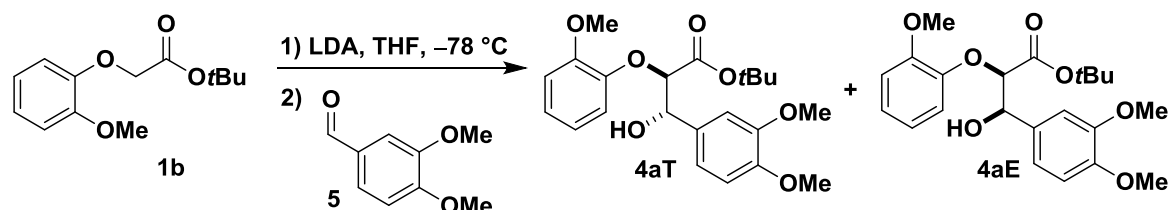
Scheme II.2. Optimized reaction conditions for the synthesis of β -hydroxy ester **2a-e**.

In the next step the corresponding lithium enolate of aryloxy ester **1a** reacted with benzaldehyde derivatives in a 1,2-addition to form β -hydroxy esters **2a-e**. The observed diastereomeric selectivities were in accordance to those previously reported in literature.^[17,21-23,51] The formation of the *erythro* diastereomers was always favored over the *threo* diastereomers giving *e:t* ratios of 3:1 to 5:1, depending on the employed aldehyde. Separation of the diastereomers by column chromatography was very cumbersome and only rendered the *erythro* products diastereomerically pure in low yields. Gratifyingly, for β -hydroxy ester **2a** the *erythro* diastereomer could be obtained diastereomerically pure (*erythro:threo* > 98:2) after recrystallization in ethyl acetate in 52% yield. Recrystallization had not been reported for this product before and the yield of the diastereomerically pure product was higher than those previously mentioned in literature.^[17,21-23,51] In addition, this reaction could be upscaled (up to 0.2 mol reaction scale was tested) without significant decrease in yields, making **2aE** easily accessible in large quantities. Recrystallization was also possible for β -hydroxy ester **2b** furnishing the diastereomerically pure (*erythro:threo* > 98:2, crystallization from ethanol/hexane) **2bE** in 30% yield.

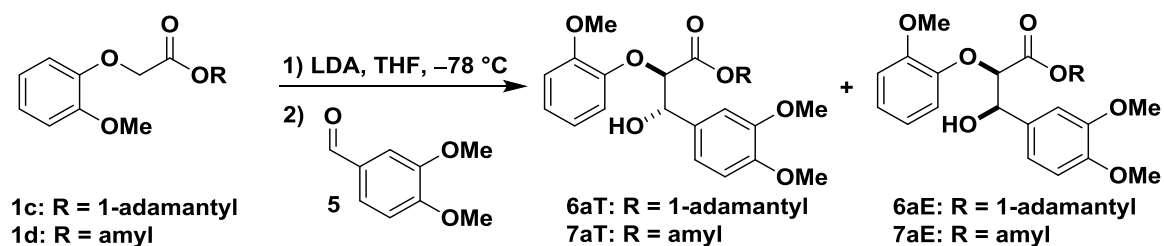
Scheme II.3. Reaction conditions for the reduction of 2bE with NaBH₄ or LiAlH₄.

The final step of the Nakatsubo protocol involved a reduction of the β -hydroxy ester with LiAlH₄ (3.0 eq.) to the desired 1,3-dilignol. The reduction was performed with NaBH₄ (10 eq.) or with LiAlH₄ (1.5 eq.) affording 1,3-dilignol **3aE** in 90% yield without change in stereochemistry (Scheme II.3).

Despite a good synthetic availability of the *erythro* 1,3-dilignols derived from **2aE** and **2bE** now, their *threo* diastereomers and differently functionalized 1,3-dilignols remained inaccessible in their diastereomerically pure form in a satisfying manner. Previous efforts in the synthesis of 1,3-dilignols have mostly utilized methyl or ethyl aryloxy esters which favor the formation of *erythro* products. Sterically hindered aryloxy esters, however, have not been tested in this context. Therefore the corresponding *tert*-butyl aryloxy ester **1b** was screened in the 1,2-addition with veratraldehyde (**5**) under the hypothesis that it could enhance the formation of the *threo* diastereomer (Scheme II.4).

Scheme II.4. 1,2-addition of *tert*-butyl aryloxy ester **1b** to β -hydroxy esters **4aE** and **4aT**.

Gratifyingly, both diastereomers were formed in a 1:1 ratio and a yield of 90%. In addition, both isomers could completely be separated from each other by column chromatography. Encouraged by these findings aryloxy esters with even greater steric hindrance containing either a 1-adamantyl, **1c**, or amyl functionality, **1d**, were synthesized. The subsequent 1,2-addition with veratraldehyde (**5**) afforded the corresponding β -hydroxy esters **6a** and **7a** in 80% and 76% yield, respectively, with an *erythro*:*threo* ratio of 1:1 (Scheme II.5). Once more the *erythro* and *threo* diastereomers were completely separated by column chromatography.

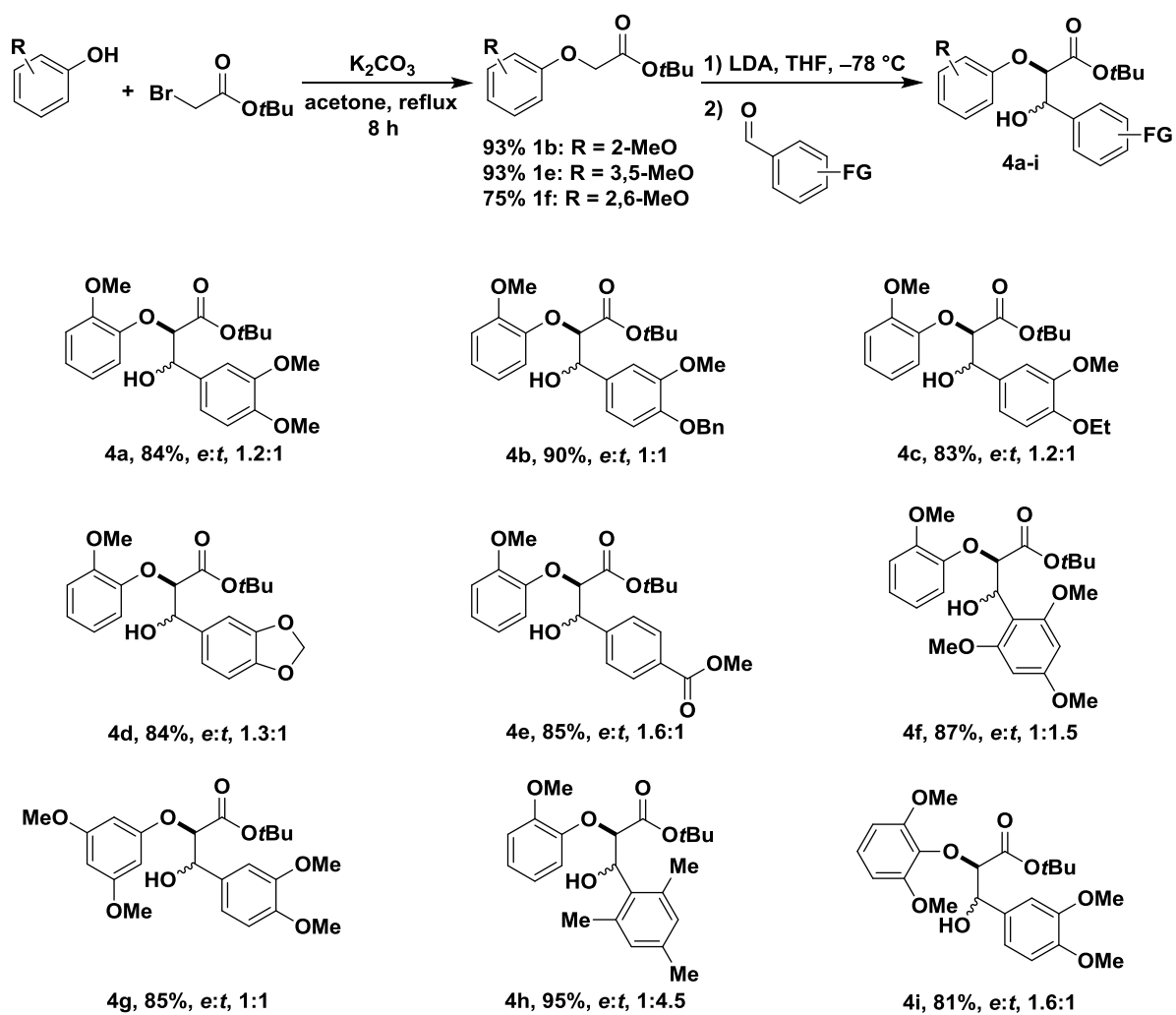


Scheme II.5. 1,2-addition with sterically more hindered aryloxy esters.

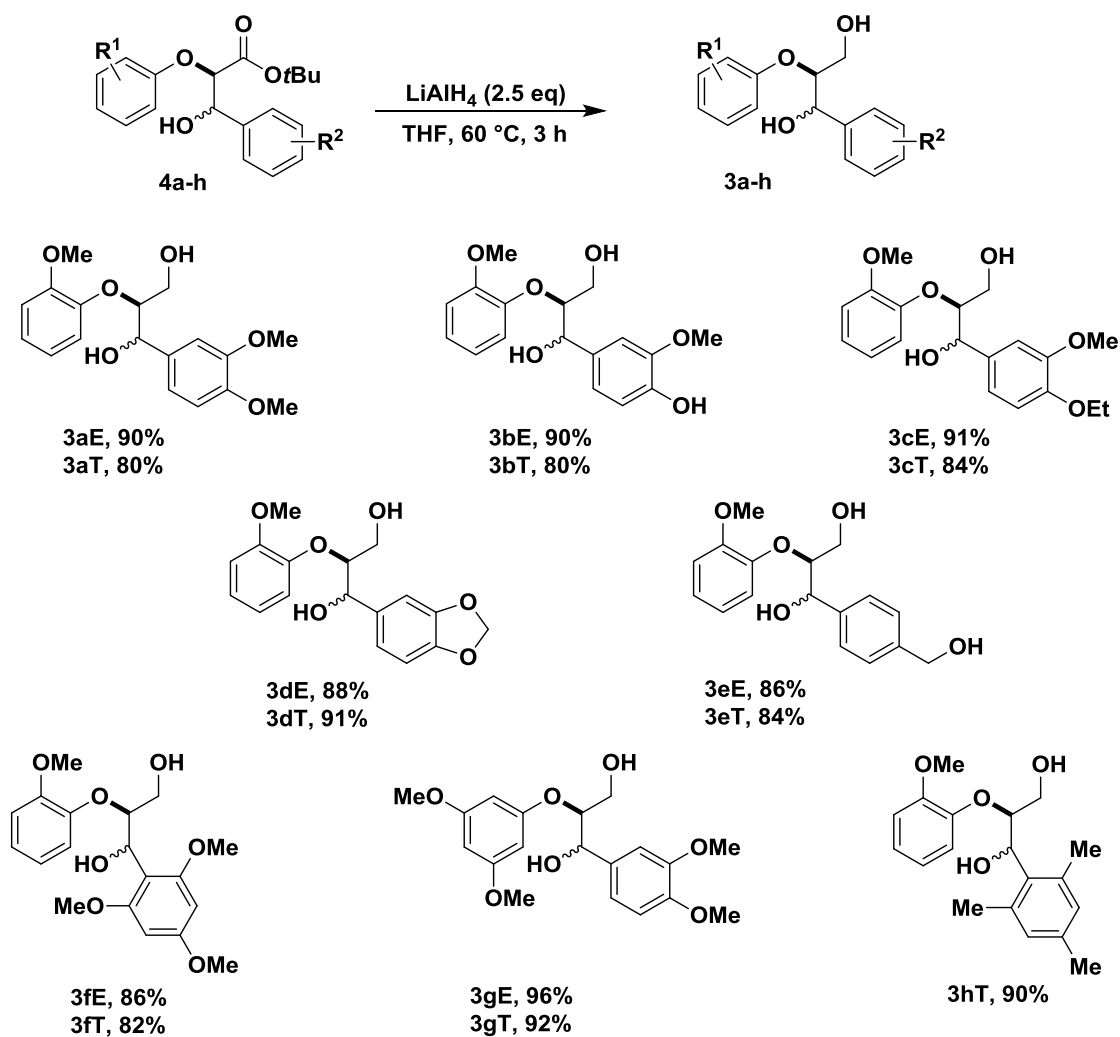
Due to the better synthetic availability of *tert*-butyl aryloxy esters from commercially available *tert*-butyl bromoacetate and the higher yield in the test reaction they were chosen for further screening reactions (Scheme II.6). The first reaction step furnished the corresponding *tert*-butyl aryloxy esters **1b**, **1e** and **1f** in very good to excellent yields of 75% to 93%. The subsequent 1,2-addition with differently functionalized benzaldehyde derivatives afforded the β -hydroxy esters **4a-i** in very good to excellent yields (81–95%). For the majority of the products the *erythro* diastereomer was formed in slight excess or in equimolar amount as the *threo* diastereomer. The only exceptions were β -hydroxy esters **4f** and **4h** where the *threo* compounds were the main product. This change in selectivity can be attributed to the greater steric hindrance of 2,4,6-trimethoxybenzaldehyde and 2,4,6-trimethylbenzaldehyde which seem to favor the *threo* transition state in the 1,2-addition. Apart from β -hydroxy esters **4i** all *erythro* and *threo* diastereomers could completely be separated from each other by column chromatography.

Next, in a likewise manner as previously described for ethyl β -hydroxy esters **2aE**, the reduction of the *tert*-butyl β -hydroxy esters **4aE** was investigated with NaBH₄ or LiAlH₄ as reducing agents. Unfortunately with NaBH₄ (10 eq.) at 60 °C and a reaction time of 24 h no complete conversion was achieved. LiAlH₄ (2.5 eq.), however, afforded 1,3-dilignol **3aE** in 90% yield after a reaction time of 3 h at 60 °C without change in stereochemistry. The reduction of all β -hydroxy esters proceeded smoothly furnishing the diastereomerically pure 1,3-dilignols **3a-h** in very good to excellent yields (80–96%) (Scheme II.7). For β -hydroxy esters **4eE** and **4eT** 5 equivalents of LiAlH₄ were employed because of the presence of a second ester group. β -Hydroxy esters **4bE** and **4bT** were directly deprotected with hydrogen and Pd/C after reduction with LiAlH₄ without prior purification by column chromatography. **3bE** and **3bT** were obtained in 90% and 80% yield, respectively, after two steps.

II. Results and Discussion



Scheme II.6. Synthesis of *tert*-butyl β -hydroxy esters.



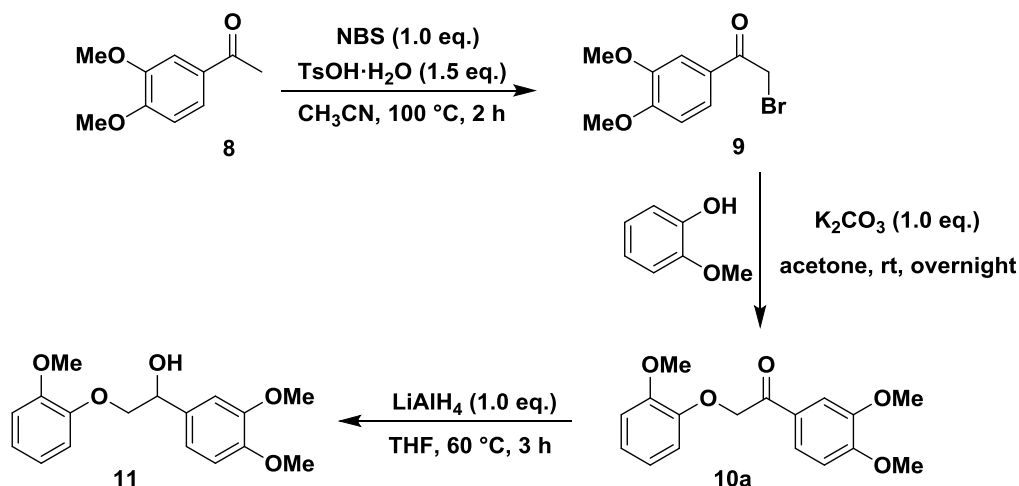
Scheme II.7. Reduction of *tert*-butyl β -hydroxy esters to 1,3-dilignols.

The easier accessibility of 1,3-dilignols, especially that of dilignol **3aE** on a large reaction scale, facilitated the transition metal catalyzed lignin cleavage studies described later in this chapter.

1.2. Synthesis of other lignin model compounds

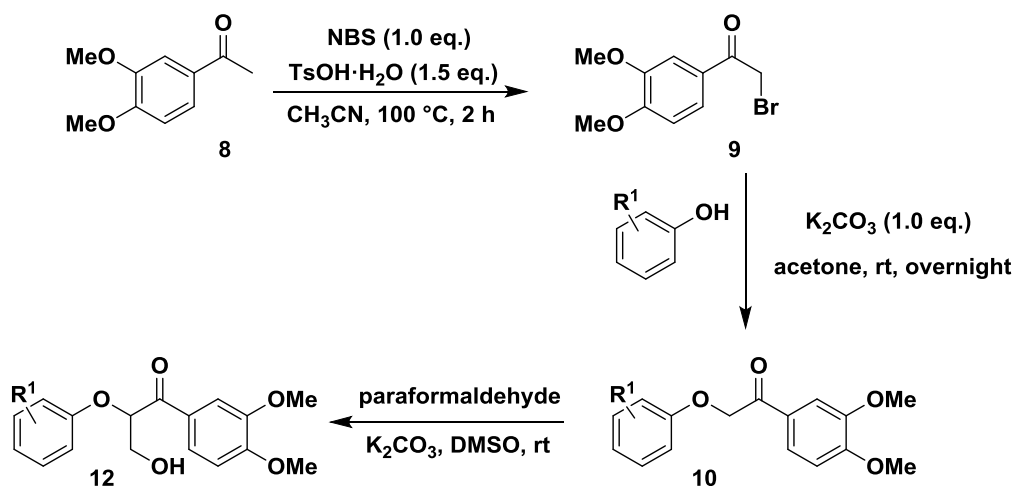
During the course of this dissertation not only 1,3-dilignols were utilized as lignin model compounds. One of the employed model compounds was monolignol **11** which does not contain a primary alcohol group. The synthesis has been reported in various sources in literature.^[22,33a] The starting point in these syntheses was generally commercially available 3,4-dimethoxyacetophenone (**8**) which in turn was brominated to 2-bromo-1-(3,4-dimethoxyphenyl)ethan-1-one (**9**). Frequently elemental bromine was used as the bromine source in the synthesis of lignin model compounds.^[22,23,41b,52] Due to its high toxicity and unselective reaction behavior in this bromination the halogen source was changed to *N*-bromosuccinimide (NBS). Lee *et. al.* have described the bromination of other acetophenone derivatives with *N*-bromosuccinimide in the presence of *p*-toluenesulfonic acid monohydrate.^[53] With a slightly modified procedure bromide **9** could be obtained in 82%

yield (Scheme II.8). Concomitantly also the di-brominated product, 2,2-dibromo-1-(3,4-dimethoxyphenyl)ethan-1-one, was formed in small amounts. The separation of this undesired byproduct proceeded smoothly by column chromatography with DCM as eluent.



Scheme II.8. Synthesis of monolignol 11.

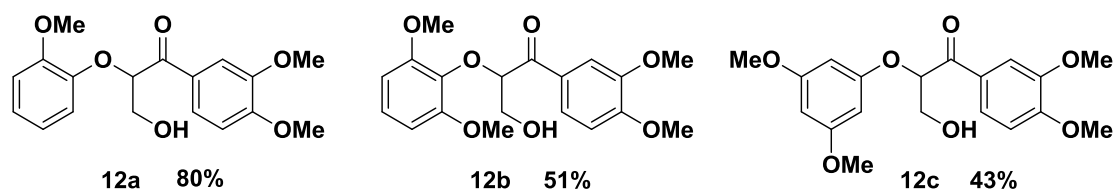
The second step was a nucleophilic substitution with 2-methoxyphenol in the presence of K_2CO_3 . The reaction conditions were in accordance to those given by Pardini *et. al.* and yielded keto aryl ether **10a** in 88%.^[22] In the final step **10a** was reduced with $LiAlH_4$ (1.0 eq.) using the same reaction conditions as previously described for the reduction of the β -hydroxy esters. Monolignol **11** was obtained in 81% yield.



Scheme II.9. Synthesis of β -hydroxy ketones.

In the oxidative cleavage studies with 1,3-dilignols later discussed in this chapter β -hydroxy ketones were frequently obtained as main or by-products. For the purpose of HPLC calibration and further mechanistic studies β -hydroxy ketones **12a-c** were synthesized in a three-step synthesis starting from commercially available 3,4-dimethoxyacetophenone (**8**) (Scheme II.9).

The first two synthetic steps used the same reaction conditions previously described for the synthesis of monolignol **11**. In the last step differently substituted keto aryl ethers reacted with paraformaldehyde in DMSO using a modified procedure by Cho *et. al.*^[23] For β -hydroxy ketone **12a** and **12c** only 0.05 eq. instead of 1.0 eq. of K_2CO_3 were used because higher amounts of base promoted the formation of an alkene byproduct through elimination. The yields were moderate to very good (43-80%) depending on the steric hindrance and the substitution pattern at the aromatic ring adjacent to the aryl ether bond (Scheme II.10).

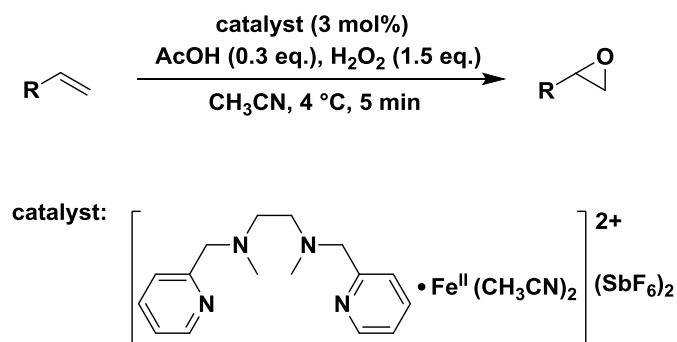


Scheme II.10. Synthesized β -hydroxy ketones.

2. Oxidative cleavage of lignin model compounds with nonheme iron complexes

One of the goals of these investigations was finding catalytic systems that would employ abundant transition metals in homogeneously catalyzed lignin cleavage reactions. A potentially suitable transition metal for the oxidative cleavage of lignin is iron. As elaborated in the introduction iron has not been applied as frequently in lignin cleavage reactions as its natural abundance might suggest.^[24b,24c,30,37,38] This is surprising considering its great potential in oxidation reactions.^[39]

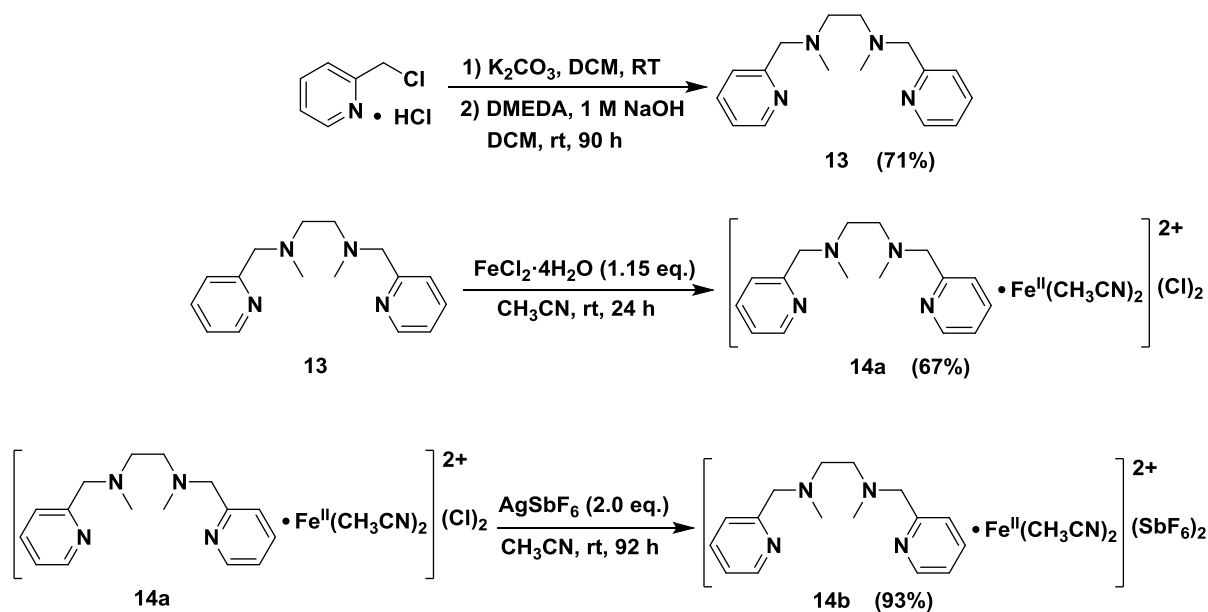
Nonheme iron catalysts seemed like promising candidates for lignin cleavage studies, they have frequently been utilized in epoxidation reactions of alkenes. Recently Tsogoeva and co-workers have written an extensive review summarizing the innovations made with nonheme iron catalysts for the epoxidation and aziridination reactions of terminal alkenes.^[39] The focus in many of these studies has been on asymmetric oxidations using chiral iron catalysts. For the cleavage of lignin, however, no asymmetric induction is needed which is why the focus was set on achiral catalysts. Along those lines White and Jacobsen reported the epoxidation of alkenes with $[\text{Fe}^{\text{II}}(\text{mep})(\text{CH}_3\text{CN})_2](\text{SbF}_6)_2$ (mep = *N,N'*-dimethyl-*N,N'*-bis(2-pyridylmethyl)-ethane-1,2-diamine) (Scheme II.11).^[54]



Scheme II.11. Iron catalyzed epoxidation of alkenes by White *et al.*^[54]

2.1. Synthesis of nonheme iron catalysts

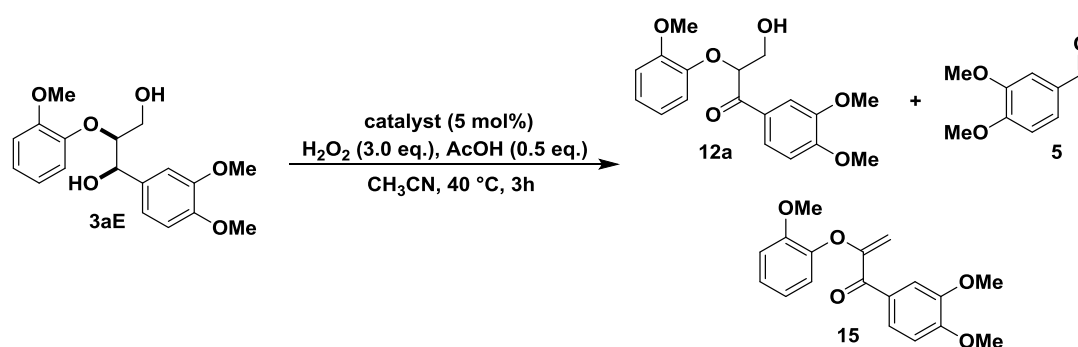
Therefore, $[\text{Fe}^{\text{II}}(\text{mep})(\text{CH}_3\text{CN})_2]\text{X}_2$ ($\text{X} = \text{Cl}$ or SbF_6) were chosen as catalyst for screening reactions. Starting from commercially available 2-(chloromethyl)pyridine hydrochloride and *N,N'*-dimethyl ethylenediamine, $[\text{Fe}(\text{mep})(\text{CH}_3\text{CN})_2](\text{Cl})_2$ was synthesized in a two-step synthesis. In the first step 2-(chloromethyl)pyridine hydrochloride was deprotonated in the presence of K_2CO_3 to 2-(chloromethyl)pyridine and then set to react with DMEDA to form *N,N'*-dimethyl-*N,N'*-bis(2-pyridylmethyl)-ethane-1,2-diamine (mep, **13**) in 71% yield (Scheme II.12). Next, mep reacted with $\text{FeCl}_2 \cdot 4\text{H}_2\text{O}$ yielding $[\text{Fe}^{\text{II}}(\text{mep})(\text{CH}_3\text{CN})_2](\text{Cl})_2$ **14a** in 67%. In order to determine whether the nature of the counter ion had an influence on the reactivity also $[\text{Fe}^{\text{II}}(\text{mep})(\text{CH}_3\text{CN})_2](\text{SbF}_6)_2$ **14b** was synthesized in one step from $[\text{Fe}^{\text{II}}(\text{mep})(\text{CH}_3\text{CN})_2](\text{Cl})_2$ and AgSbF_6 in 93% yield.

Scheme II.12. Synthesis of $[\text{Fe}(\text{mep})(\text{CH}_3\text{CN})_2](\text{X})_2$ (**14**).

2.2. Cleavage studies of dilignol 3aE and nonheme iron catalysts

The screening reactions for the nonheme iron catalysts were performed with *erythro* dilignol **3aE** as starting material on a 0.25 mmol scale. In the initial reactions, using modified reaction conditions by White and co-workers,^[55] $[\text{Fe}^{\text{II}}(\text{mep})(\text{CH}_3\text{CN})_2](\text{Cl})_2$ **14a** and $[\text{Fe}^{\text{II}}(\text{mep})(\text{CH}_3\text{CN})_2](\text{SbF}_6)_2$ **14b** were tested as catalysts (Table II.1). The catalyst loading in these reactions was 5 mol% using 3.0 equivalents of H_2O_2 , 0.5 equivalents of AcOH, 0.5 mL of acetonitrile as solvent and a reaction time of 3 h. The conversion was determined by HPLC with 3,4-dimethoxybenzyl alcohol as internal standard. The progression of the reactions was also monitored by ^1H NMR. However in this research project, in contrast to the catalytic systems described in part 3, 4 and 5 of this chapter, the overall carbon balance for the identified products and remaining starting material was poor. The ratio in the ^1H NMR of the prior identified products with the sum of the products and the starting material shall be referred to in this dissertation as “product factor”.

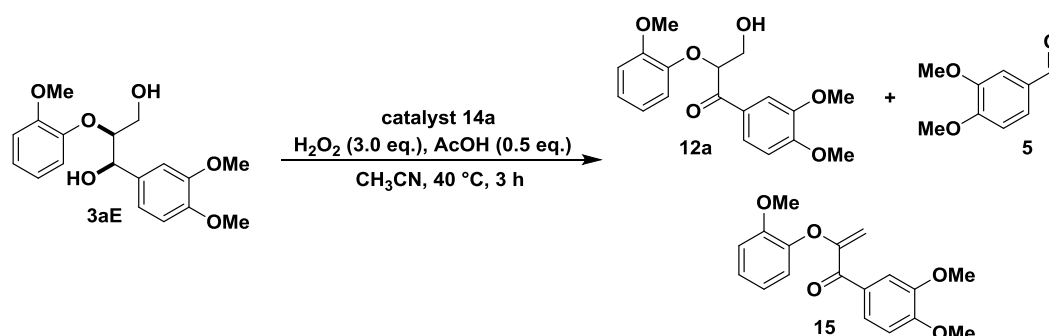
$[\text{Fe}^{\text{II}}(\text{mep})(\text{CH}_3\text{CN})_2](\text{Cl})_2$ **14a** and $[\text{Fe}^{\text{II}}(\text{mep})(\text{CH}_3\text{CN})_2](\text{SbF}_6)_2$ **14b** gave similar conversions with 64% and 68%, respectively, indicating that the counter ion had a negligible effect on the activity of the catalyst. The HPLC chromatograms and the ^1H NMR spectra showed that ketone **12a**, enol ether enone **15** and aldehyde **5** were formed as products, albeit in less than 5% yield. When the catalyst was omitted under the same reaction conditions no conversion was observed.

Table II.1: Nonheme iron catalyst screening.^[a]

catalyst	conversion [%] ^[b]
[Fe ^{II} (mep)(CH ₃ CN) ₂](Cl) ₂ 14a	64 (19 ^[c])
[Fe(mep)(CH ₃ CN) ₂](SbF ₆) ₂ 14b	68
-	0

[a] Reaction conditions: **3aE** (0.25 mmol), catalyst (5 mol%), CH₃CN (0.5 mL), H₂O₂ (3.0 eq.), AcOH (0.5 eq.), 40 °C, 3 h; [b] conversion determined by HPLC with 3,4-dimethoxybenzyl alcohol as internal standard; [c] product factor determined by ¹H NMR [product/(product+starting material)]*100.

Considering the minor influence of the counter ion, further test reactions were only performed with [Fe^{II}(mep)(CH₃CN)₂](Cl)₂ **14a**. Table II.2 shows the product factor with a catalyst loading of 5 mol% and 20 mol%. A catalyst loading of 20 mol% did not lead to an increase in the product factor. Even higher catalyst loadings (not shown in Table II.2) did not lead to greater product factors. Furthermore higher amounts of solvent were necessary to ensure a complete dissolution of the catalyst which was not beneficial for the product factor when the same reaction time was employed.

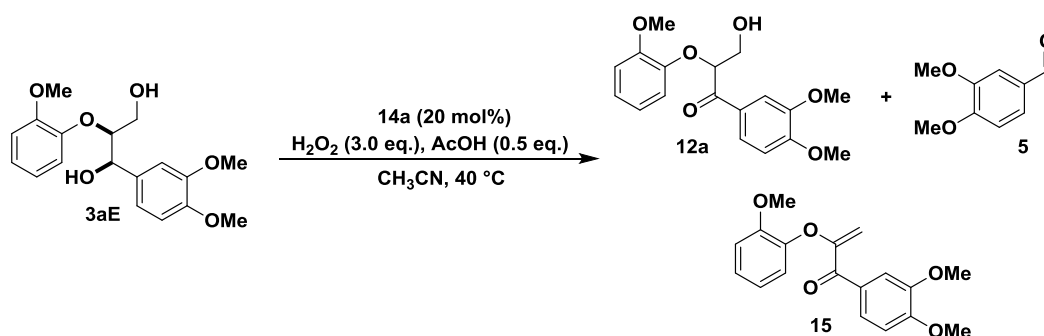
Table II.2: Variation of the catalyst loading for [Fe^{II}(mep)(CH₃CN)₂](Cl)₂ **14a**.^[a]

catalyst loading (mol%)	product factor by ¹ H NMR ^[b]
5	19
20	19

[a] Reaction conditions: **3aE** (0.25 mmol), $[\text{Fe}^{\text{II}}(\text{mep})(\text{CH}_3\text{CN})_2](\text{Cl})_2$ **14a**, CH_3CN (0.5 mL), H_2O_2 (3.0 eq.), AcOH (0.5 eq.), 40 °C, 3 h; [b] $[\text{product}/(\text{product}+\text{starting material})]*100$.

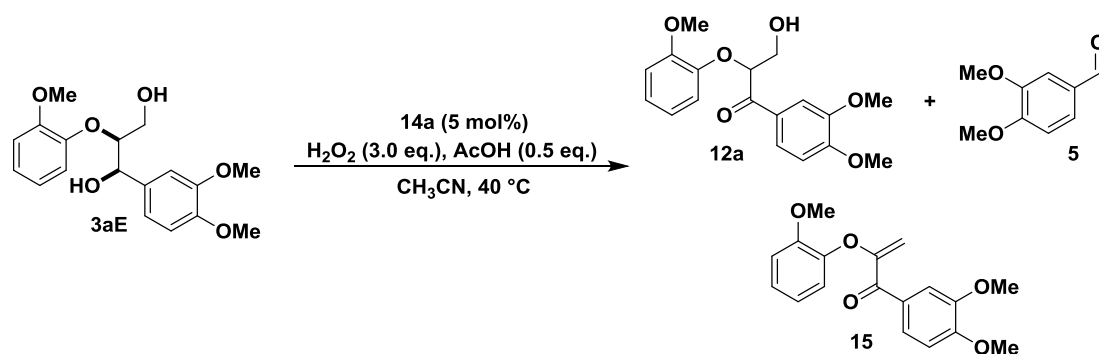
Next, the influence of the reaction time was analyzed. The reactions were either carried out using 20 mol% or 5 mol% catalyst loading (Table II.3 and Table II.4, respectively). 2.5 mL of acetonitrile were used for the 24 h and 65 h reactions, with 20 mol% of catalyst, due to the loss of solvent that occurred over longer reaction times even in the presence of a reflux condenser. The product factor increased from 9 to 19 when the reaction time was changed from 2 h to 3 h. A decrease in the product factor was observed for a reaction time of 24 h when larger amounts of solvent were used. When the reaction time was further extended to 65 h, the product factor increased to 22. Reactions with 5 mol% catalyst loading, while employing 0.5 mL of solvent, showed that the conversion increased from 64% after 3 h to 70% after 24 h. However, because the improvement in conversion after 24 h was not significant, further screening reactions were performed with a reaction time of 3 h.

Table II.3: Influence of the reaction time with 20 mol% $[\text{Fe}(\text{mep})(\text{CH}_3\text{CN})_2](\text{Cl})_2$ **14a.^[a]**



time [h]	product factor by $^1\text{H NMR}$ ^[c]
2	9
3	19
24 ^[b]	11
65 ^[b]	22

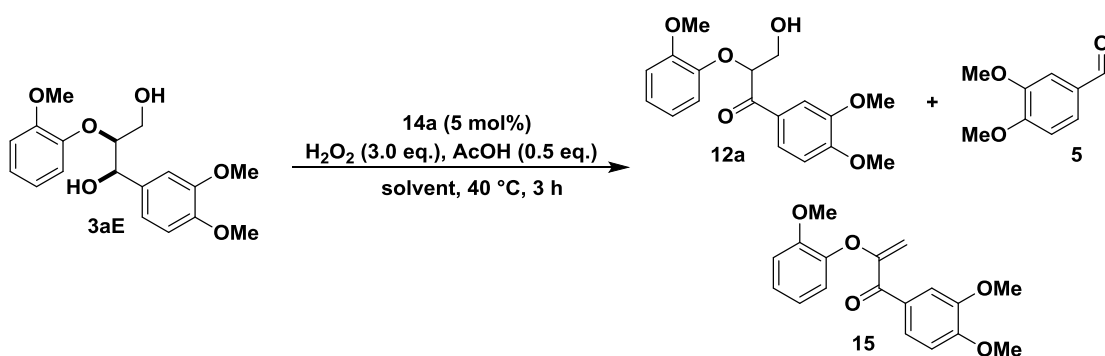
[a] Reaction conditions: **3aE** (0.25 mmol), $[\text{Fe}^{\text{II}}(\text{mep})(\text{CH}_3\text{CN})_2](\text{Cl})_2$ **14a** (20 mol%), CH_3CN (0.5 mL), H_2O_2 (3.0 eq.), AcOH (0.5 eq.), 40 °C; [b] 2.5 mL CH_3CN ; [c] $[\text{product}/(\text{product}+\text{starting material})]*100$.

Table II.4: Influence of the reaction time with 5 mol% $[\text{Fe}^{\text{II}}(\text{mep})(\text{CH}_3\text{CN})_2](\text{Cl})_2$ 14a.^[a]

time [h]	conversion by HPLC [%] ^[b]
3	64
24	70

[a] Reaction conditions: **3aE** (0.25 mmol), $[\text{Fe}^{\text{II}}(\text{mep})(\text{CH}_3\text{CN})_2](\text{Cl})_2$ (5 mol%), CH_3CN (0.5 mL), H_2O_2 (3.0 eq.), AcOH (0.5 eq.), 40 °C; [b] conversion determined by HPLC with 3,4-dimethoxybenzyl alcohol as internal standard.

To determine the influence of the solvent, dioxane, dimethyl carbonate, DMF, pyridine, THF and toluene as well as mixtures of acetonitrile and water were tested (see Table II.5). Unfortunately, none of the aforementioned solvents or solvent mixtures had a positive effect on the reaction system. Pyridine afforded the highest product factor of any non-acetonitrile containing system with 7.

Table II.5: Solvent screening for $[\text{Fe}^{\text{II}}(\text{mep})(\text{CH}_3\text{CN})_2](\text{Cl})_2$ 14a.^[a]

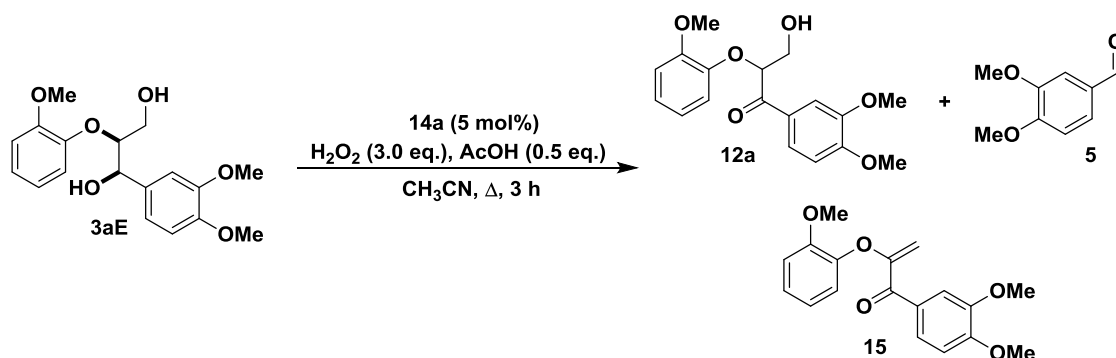
solvent	product factor by $^1\text{H NMR}$ ^[b]
acetonitrile	19
acetonitrile/water 3:1	7
acetonitrile/water 1:1	8

dioxane	2
DMC	4
DMF	2
pyridine	7
THF	1
toluene	2

[a] Reaction conditions: **3aE** (0.25 mmol), $[\text{Fe}^{\text{II}}(\text{mep})(\text{CH}_3\text{CN})_2](\text{Cl})_2$ **14a** (5 mol%), solvent (0.5 mL), H_2O_2 (3.0 eq.), AcOH (0.5 eq.), 40 °C, 3 h;
 [b] $[\text{product}/(\text{product}+\text{starting material})]*100$.

One of the final parameters that was screened in this reaction system was the temperature. For the reaction performed at 100 °C 1 mL of acetonitrile was used, due to the refluxing of the solvent. An increase of the reaction temperature from 40 °C to 60 °C led to a slightly higher product factor of 22. Even higher reaction temperatures of 80 °C or refluxing at 100 °C had no beneficial effect on the product factor.

Table II.6: Temperature dependency with $[\text{Fe}^{\text{II}}(\text{mep})(\text{CH}_3\text{CN})_2](\text{Cl})_2$ **14a as catalyst.^[a]**



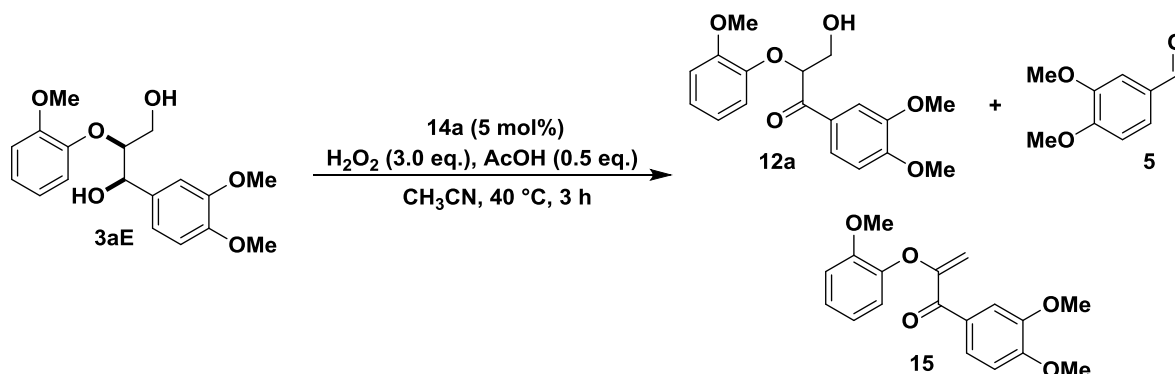
temperature [°C]	product factor by $^1\text{H NMR}^{[b]}$
40	19
60	22
80	10
100	12

[a] Reaction conditions: **3aE** (0.25 mmol), $[\text{Fe}^{\text{II}}(\text{mep})(\text{CH}_3\text{CN})_2](\text{Cl})_2$ **14a** (5 mol%), CH_3CN (0.5 mL), H_2O_2 (3.0 eq.), AcOH (0.5 eq.), 3 h;
 [b] $[\text{product}/(\text{product}+\text{starting material})]*100$.

After having screened various reaction conditions, the conversion remained more or less constant unless the solvent was changed or the catalyst was omitted. One factor that had not been taken into consideration thus far was the decomposition of H_2O_2 by the iron catalyst without the desired oxidation.^[56] To counter this potential effect the addition sequence was

changed. At the beginning of the reaction, after 1 h and after 2 h 1.0 equivalent of H₂O₂ was added instead of adding 3.0 equivalents at the beginning. This led to an increase of the conversion from 64% to 78% (Table II.7). However, even with the higher conversion the yields for ketone **12a**, aldehyde **5** and enol ether enone **15** remained below 5%.

Table II.7: Influence of the addition rate of the oxidant.^[a]



addition of H ₂ O ₂	conversion by HPLC [%] ^[b]
3.0 eq. at the beginning	64
1.0 eq. per hour	78

[a] Reaction conditions: **3aE** (0.25 mmol), [Fe^{II}(mep)(CH₃CN)₂](Cl)₂ **14a** (5 mol%), solvent (0.5 mL), H₂O₂ (3.0 eq.), AcOH (0.5 eq.), 40 °C, 3 h; [b] conversion determined by HPLC with 3,4-dimethoxybenzyl alcohol as internal standard.

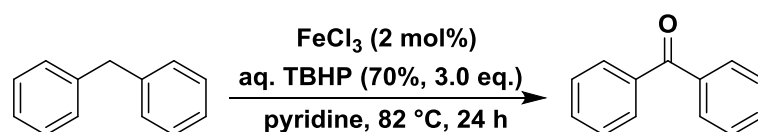
Changing the reaction atmosphere to oxygen had no effect on the conversion and omitting acetic acid lead to a decrease in conversion.

Considering the poor selectivity and the low yields for cleavage products such as veratraldehyde (**5**) the two options moving forward were either to screen other nonheme iron catalysts with a different ligand back bone in hope of better selectivity, or to search for other reaction systems. Other nonheme iron catalysts commonly employ considerably more expensive ligands. This, however, does not seem reasonable in the context of lignin degradation where the long term goal is to find catalysts that are suitable for a multi ton feedstock. Therefore the focus was shifted to other catalytic systems.

3. Oxidative cleavage of lignin model compounds with FeCl₃-derived iron complexes

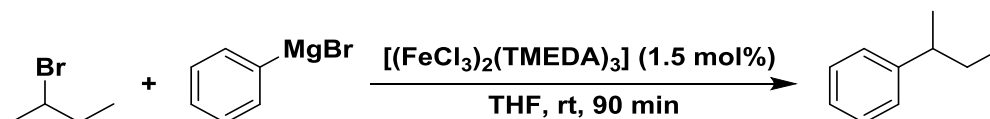
In the introduction of this dissertation several examples were presented regarding the use of iron catalysts in cleavage studies with both lignin model compounds and extracted lignin.^[24b,24c,30,37,38] However, these reaction systems required either rigorous reaction conditions with high reaction temperatures and pressure, expensive solvents or complex ligands.

In a protocol published by the Bolm group, FeCl₃ and *tert*-butyl hydroperoxide (TBHP) in pyridine were utilized for benzylic oxidations (Scheme II.13).^[57]



Scheme II.13. Benzylic oxidation with FeCl₃ by Bolm and co-workers.

Since previous lignin cleavage studies utilizing FeCl₃ required quite harsh reaction conditions it was envisaged that inexpensive nitrogen ligands could potentially increase the catalytic activity. One FeCl₃-derived iron complex that fulfilled the desired profile was [(FeCl₃)₂(TMEDA)₃]. Cahiez and co-workers employed this complex in the iron catalyzed alkylation of aromatic Grignard reagents (Scheme II.14).^[58]

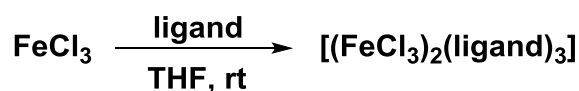


Scheme II.14. Iron catalyzed alkylation of aromatic Grignard reagents by Cahiez *et al.*^[58]

Many of the following results with FeCl₃-derived iron complexes have also been presented in the master's thesis of Rinesch which was scientifically accompanied by Bolm and myself during the course of this dissertation.^[59]

3.1 Synthesis and characterization of FeCl₃-derived iron complexes

As described by Cahiez *et al.*, [(FeCl₃)₂(TMEDA)₃] was synthesized in a one-step synthesis from anhydrous FeCl₃ and TMEDA in dry THF at room temperature.^[58] The yield after a reaction time of 1 h was 65% which was significantly lower than the reported 97% in literature. To improve the yield the reaction time was increased. After testing shorter reaction times the reaction was stirred for 65 h and [(FeCl₃)₂(TMEDA)₃] was obtained in 91% yield. In addition to TMEDA, other inexpensive bi- and tridentate nitrogen ligands were employed in this one-step synthesis (Scheme II.15 and Table II.8).

Scheme II.15. Synthesis of FeCl₃ based iron complexes.

Depending on the ligand, the reaction time had to be varied. DABCO and PMDTA afforded the corresponding complexes after 1 h in excellent yields of 97% and 93%, respectively (Table II.8). HMTA and 1,4-dimethylpiperazine furnished the respective FeCl₃-derived complexes in 93% and 64%, respectively, after stirring for 16 h. Even longer reaction times (65 h) for [(FeCl₃)₂(1,4-dimethylpiperazine)₃] increased the yield only marginally to 72%. The reaction for [(FeCl₃)₂(HMTA)₃] was performed on a 15 mmol instead of a 5 mmol scale.

Table II.8: Yields for the FeCl₃-based iron complexes.^[a]

ligand	proposed catalyst formula	yield [%]
tetramethylethylenediamine (TMEDA)	[(FeCl ₃) ₂ (TMEDA) ₃]	91 ^[b]
hexamethylenetetramine (HMTA)	[(FeCl ₃) ₂ (HMTA) ₃]	93 ^[c]
1,4-diazabicyclo[2.2.2]octane (DABCO)	[(FeCl ₃) ₂ (DABCO) ₃]	97
<i>N,N,N',N',N''</i> - pentamethyldiethylenetriamine (PMDTA)	[(FeCl ₃) ₂ (PMDTA) ₂ ·2H ₂ O]	93
1,4-dimethylpiperazine	[(FeCl ₃) ₂ (1,4- dimethylpiperazine) ₃]	64 ^[d]

[a] Reaction conditions: FeCl₃ (5 mmol), amine (7.5 mmol), THF (50 mL), rt, 1 h; [b] 65 h; [c] FeCl₃ (15 mmol), amine (22.5 mmol), THF (150 mL), rt, 16 h; [d] 16 h.

Despite proposing a stoichiometry for the FeCl₃-derived complex [(FeCl₃)₂(TMEDA)₃], Cahiez and co-workers did not provide any spectroscopic data to support this structure.^[58] Initial attempts to characterize the complexes by ESI-MS and IR spectroscopy did not provide any conclusive evidence about the nature of the complexes.

In order to confirm the formation of new iron complexes that differed from FeCl₃, EPR measurements of all the complexes and FeCl₃ were conducted. As can be seen in Figure II.1, all the formed complexes showed different EPR signals from FeCl₃. Unfortunately, the spectra did not provide conclusive evidence about the exact nature of the complexes.

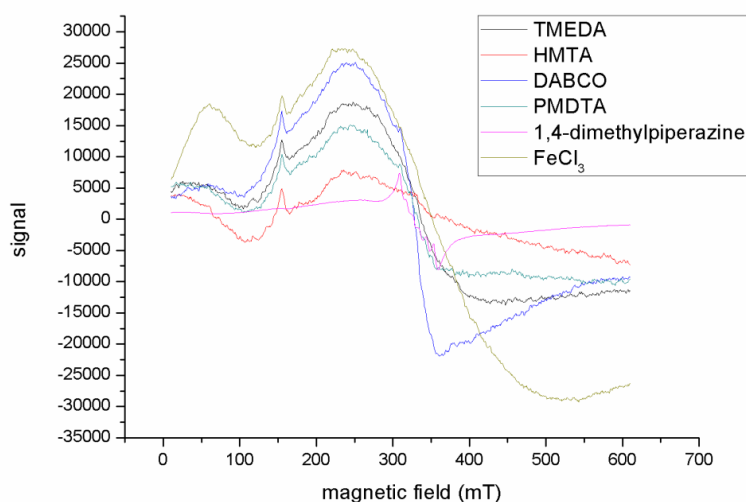


Figure II.1. EPR spectra of FeCl_3 and FeCl_3 -derived complexes.

Therefore, elemental analysis was chosen to provide more insight on the composition of the catalysts (Table II. 9). With the hypothesis that all the iron complex had the stoichiometry $[(\text{FeCl}_3)_2(\text{ligand})_3]$, it was observed that the C- and N-contents were lower than theoretical values would suggest. Based on the experimental values of the elemental analysis, $[(\text{FeCl}_3)_2(\text{PMDTA})_2 \cdot 2\text{H}_2\text{O}]$ was proposed as possible structure for the PMDTA containing iron complex.

Table II.9: Elemental analysis and ICP-OES of the FeCl_3 -derived complexes

catalyst		Fe [%]	C [%]	H [%]	N [%]
$[(\text{FeCl}_3)_2(\text{TMEDA})_3]$	Theo.	16.59	32.12	7.19	12.49
	Exp.	13.10	27.82	6.80	10.63
$[(\text{FeCl}_3)_2(\text{DABCO})_3]$	Theo.	16.90	32.71	5.49	12.72
	Exp.	13.42	27.30	5.91	10.52
$[(\text{FeCl}_3)_2(\text{HMTA})_3]$	Theo.	15.00	29.02	4.87	22.56
	Exp.	12.00	27.82	5.34	21.29
$[(\text{FeCl}_3)_2(\text{PMDTA})_2]$	Theo.	16.65	32.22	6.91	12.52
	Exp.	9.92	30.78	7.52	11.85
$[(\text{FeCl}_3)_2(1,4\text{-dimethylpiperazine})_3]$	Theo.	16.75	32.42	6.35	12.60
	Exp.	11.47	28.11	7.49	10.83

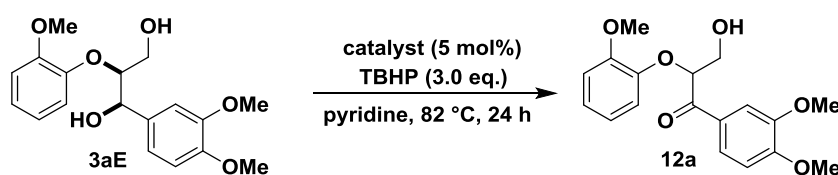
To determine the iron content of the complexes ICP-OES measurements were performed (Table II.9). Again a deviation from the theoretically expected iron content was observed with all iron values being lower than expected for the proposed structures. Both the results of the elemental analysis and the ICP-OES indicate that certain amounts of solvent or water have been incorporated into the iron complexes. Attempts to obtain single crystals from these complexes for X-ray crystal structure analysis to unequivocally determine the structure in solid state remained unsuccessful.

In the following discussion all the FeCl₃-derived iron complexes are referred to as {Fe-ligand}. Due to feasibility reasons with regard to calculating the catalyst loading for the reaction screening the proposed structure by Cahiez and co-workers was used. During the reaction optimization process I was aware that the actual iron loading was always slightly lower than indicated. The following results, however, display that these slight deviations in the theoretical and experimental iron loading do not have a crucial effect on the catalytic activity and selectivity, as the catalyst loading was not a decisive factor for the reactivity in the optimized reaction conditions (see Table II.20).

3.2. Cleavage studies of dilignol **3aE** with FeCl₃-derived iron catalysts

The screening reactions for the FeCl₃-derived iron catalysts were performed with *erythro* dilignol **3aE** as starting material on a 0.25 mmol scale. Initial tests used modified reaction conditions by Nakanishi *et al.* with a catalyst loading of 5 mol%, 3.0 equivalents of TBHP as oxidant, pyridine as a solvent at a reaction temperature of 82 °C and a reaction time of 24 h.^[57]

Table II.10: Iron catalyst screening for the cleavage of dilignol **3aE in pyridine and TBHP as oxidant.^[a]**



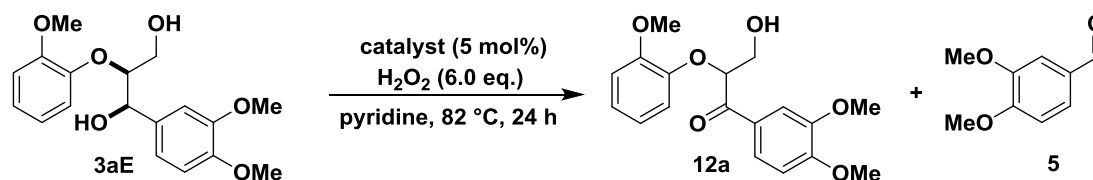
catalyst	conversion [%] ^[b]	12a [%] ^[b]
FeCl ₃	43	15
FeCl ₃ ^[c]	45	20
{Fe-TMEDA}	48	17
{Fe-DABCO}	57	21
{Fe-HMTA}	52	15
{Fe-PMDTA}	48	18
{Fe-1,4-dimethylpiperazine}	48	12

[a] Reaction conditions: **3aE** (0.25 mmol), catalyst (5 mol%), pyridine (1.0 mL), TBHP (3 eq.), 82 °C, 24 h; [b] conversion and yield determined by HPLC with 3,4-dimethoxybenzyl alcohol as internal standard; [c] 10 mol% catalyst.

When FeCl₃ was employed as a catalyst 43% conversion of **3aE** was obtained. The main product was ketone **12a** in 15% yield. Increasing the catalyst loading to 10 mol% increased the conversion marginally to 45% and the yield of ketone **12a** increased to 20%. A change in catalyst to the FeCl₃-derived complexes led to an increase in conversion. {Fe-DABCO} gave the highest conversion with 57% and afforded ketone **12a** in 21% yield.

Since the reactions with TBHP as oxidant afforded ketone **12a** as the main product, tests with H₂O₂ were then conducted in order to determine whether a change in oxidant would lead to an enhancement of cleavage products (Table II.11). In those reactions the amount of oxidant was increased to 6 equivalents.

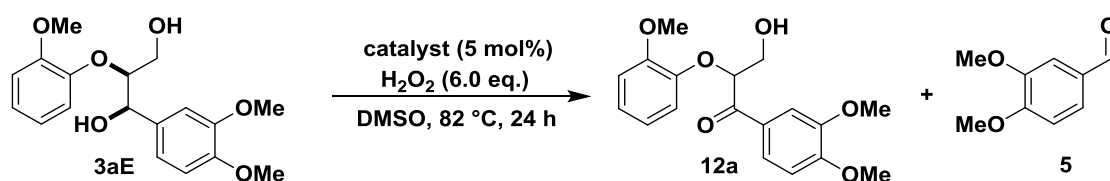
Table II.11: Iron catalyst screening for the cleavage of dilignol 3aE in pyridine and H₂O₂ as oxidant.^[a]



catalyst	conversion [%] ^[b]	12a [%] ^[b]	5 [%] ^[b]
{Fe-TMEDA}	19	11	8
{Fe-DABCO}	10	6	4
{Fe-HMTA}	15	9	6
{Fe-PMDTA}	10	6	4
{Fe-1,4-dimethylpiperazine}	13	8	5

[a] Reaction conditions: **3aE** (0.25 mmol), catalyst (5 mol%), pyridine (1.0 mL), H₂O₂ (6 eq.), 82 °C, 24 h; [b] conversion and yields determined by HPLC with 3,4-dimethoxybenzyl alcohol as internal standard.

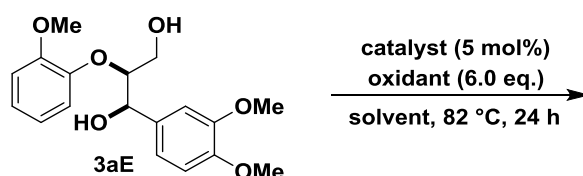
As can be seen in Table II.11 the conversions for all the FeCl₃-derived complexes were very similar ranging from 10% to 19%. Under these reaction conditions {Fe-TMEDA} showed the highest activity with 19% conversion. The main product in all reactions was ketone **12a** with yields of 6% to 11%. Despite these low conversions, the yields for the cleavage product veratraldehyde (**5**) were now higher than previously observed with TBHP. To enhance both the conversion and the yield of cleavage products the solvent was changed from pyridine to DMSO. A detailed solvent screening is presented at a later stage in this chapter (Table II.18).

Table II.12: Iron catalyst screening for the cleavage of dilignol **3aE** in DMSO and H₂O₂ as oxidant.^[a]

catalyst	conversion [%] ^[b]	12a [%] ^[b]	5 [%] ^[b]
{Fe-TMEDA}	30	13	4
{Fe-DABCO}	41	14	5
{Fe-HMTA}	35	15	2
{Fe-PMDTA}	38	14	5
{Fe-1,4-dimethylpiperazine}	32	11	3

[a] Reaction conditions: **3aE** (0.25 mmol), catalyst (5 mol%), DMSO (1.0 mL), H₂O₂ (6 eq.), 82 °C, 24 h; [b] conversion and yields determined by HPLC with 3,4-dimethoxybenzyl alcohol as internal standard.

The change in solvent to DMSO led to the desired enhancement in conversions ranging from 30% to 41% (Table II.12). As previously observed for the reaction system with pyridine and TBHP, {Fe-DABCO} was the most active catalyst with 41% conversion. The main product was still ketone **12a** in yields of 11% to 15%, depending on the catalyst. The yield for aldehyde **5**, however, remained low (2% to 5%). Considering the fact that {Fe-DABCO} gave the highest conversion and furnished the highest yields in the synthesis of all the FeCl₃-derived complexes it was chosen as catalyst for further screening reactions.

Table II.13: Influence of the oxidants and catalyst on the conversion of dilignol **3aE**.^[a]

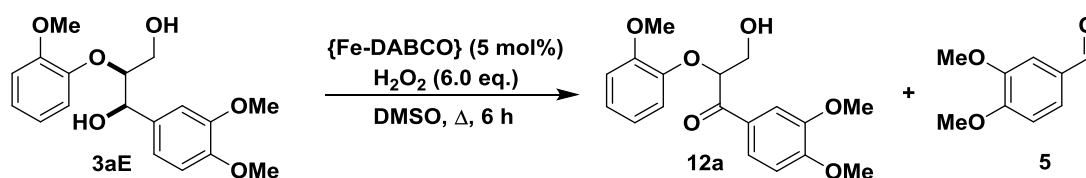
catalyst	oxidant	solvent	conversion [%] ^[b]
-	-	pyridine	0
-	-	DMSO	0
-	H ₂ O ₂	pyridine	0
-	H ₂ O ₂	DMSO	0
-	TBHP	pyridine	9 ^[c]
-	TBHP	pyridine	11

-	TBHP	DMSO	10
{Fe-DABCO}	-	DMSO	0

[a] Reaction conditions: **3aE** (0.25 mmol), catalyst (5 mol%), solvent (1.0 mL), oxidant (6 eq.), 82 °C, 24 h; [b] conversion determined by HPLC with 3,4-dimethoxybenzyl alcohol as internal standard; [c] 3 eq. oxidant.

To verify that no uncatalyzed background reactions were occurring, several reactions were conducted without the addition of a catalyst or an oxidant (Table II.13). In DMSO and pyridine no conversion was observed when both the catalyst and the oxidant were omitted. Likewise, no reaction occurred when only H₂O₂ was added as an oxidant or {Fe-DABCO} employed without the addition of an oxidant. However with TBHP as oxidant and no catalyst, independent of the solvent, 9% to 11% conversion was recorded. This uncatalyzed reaction did not increase significantly with more equivalents of oxidant as 9% conversion were observed with 3 equivalents of TBHP and 11% conversion with 6 equivalents of TBHP.

Table II.14: Temperature dependency for the cleavage of dilignol **3aE** in DMSO with H₂O₂ as oxidant.^[a]



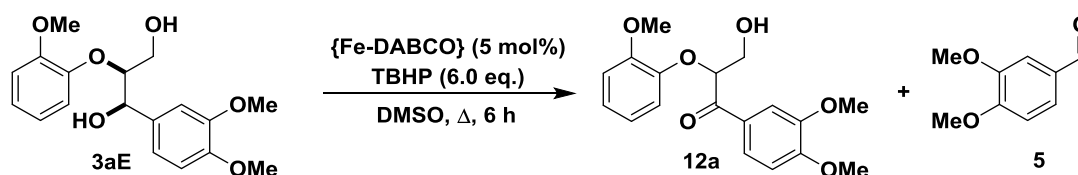
temperature	conversion [%] ^[b]	12a [%] ^[b]	5 [%] ^[b]
RT	0	0	0
50 °C	1	1	0
60 °C	2	2	0
70 °C	13	13	0
82 °C	37	19	5
90 °C	58	21	5
100 °C	64	30	15

[a] Reaction conditions: **3aE** (0.25 mmol), {Fe-DABCO} (5 mol%), DMSO (1.0 mL), H₂O₂ (6 eq.), 6 h; [b] conversion and yields determined by HPLC with 3,4-dimethoxybenzyl alcohol as internal standard.

After having established that both the catalyst and the oxidant were important for the activity, a temperature screening was performed for both H₂O₂ and TBHP as oxidant in DMSO with a reaction time of 6 h. At temperatures below 70 °C, no conversion or only trace amounts of starting material were converted with H₂O₂ as oxidant (Table II.14). This changed at 70 °C in which ketone **12a** was obtained as the only product in 13% yield. Further increasing the reaction temperature enhanced both the conversion and the product formation. At 100 °C, 64% conversion of **3aE** was observed. Gratifyingly, the yield of both ketone **12a** and

aldehyde **5** increased. Ketone **12a** was still the main product with 30% but aldehyde **5** was now formed in 15% yield.

Table II.15: Temperature dependency for the cleavage of dilignol 3aE in DMSO with TBHP as oxidant.^[a]



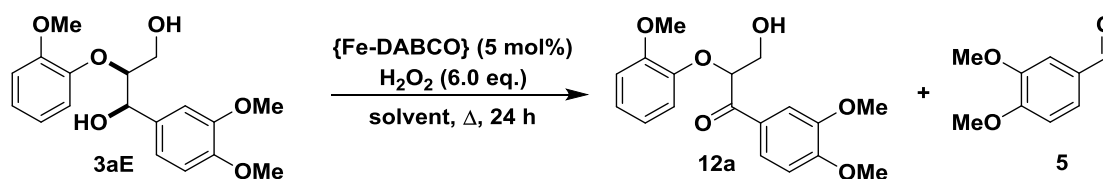
temperature	conversion [%] ^[b]	12a [%] ^[b]	5 [%] ^[b]
RT	1	1	0
50 °C	16	16	0
60 °C	28	28	0
70 °C	40	40	0
82 °C	59	31	3
90 °C	37	36	1
100 °C	35	33	2

[a] Reaction conditions: **3aE** (0.25 mmol), {Fe-DABCO} (5 mol%), DMSO (1.0 mL), TBHP (6 eq.), 6 h; [b] conversion and yields determined by HPLC with 3,4-dimethoxybenzyl alcohol as internal standard.

In contrast to H₂O₂, TBHP already afforded 16% conversion of **3aE** at 50 °C. The catalytic activity was highest at 82 °C and decreased with higher reaction temperatures. However, the highest yield for ketone **12a** was achieved at 70 °C with 40%. Aldehyde **5** always remained a minor product with yields of 3% or lower.

Studies in which the oxidants were added sequentially with 1.0 equivalent per hour instead of the entire amount at the beginning of the reaction did not lead to significant improvements in the activity. Furthermore, a change in the reaction atmosphere from air to oxygen or argon had a negligible effect on the reactivity. The amount of solvent employed in the reactions was also not crucial for the activity. However, switching to a 1:1 mixture of DMSO/H₂O led to a significant increase in conversion (Table II.16). After 24 h at 82 °C with 6.0 equivalents of H₂O₂ as oxidant the conversion increased from 41% in pure DMSO to 74% with a 1:1 mixture of DMSO/H₂O. The yield for both ketone **12a** and aldehyde **5** rose slightly to 17% and 7%, respectively. This trend was also observed with higher reaction temperatures. At 100 °C the conversion increased from 84% in pure DMSO to 94% in a 1:1 mixture of DMSO/H₂O. Furthermore the yield for aldehyde **5** increased from 20% to 24%.

Table II.16: Comparison of DMSO and DMSO/H₂O in the cleavage of dilignol 3aE with H₂O₂ as oxidant.^[a]

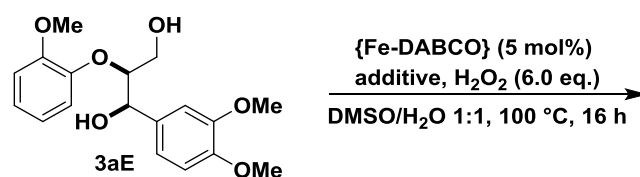


solvent	T [°C]	conversion [%] ^[b]	12a [%] ^[b]	5 [%] ^[b]
DMSO	82	41	14	5
DMSO/H ₂ O	82	74	17	7
DMSO	100	84	11	20
DMSO/H ₂ O	100	94	12	24

[a] Reaction conditions: **3aE** (0.25 mmol), {Fe-DABCO} (5 mol%), solvent (1.0 mL), H₂O₂ (6 eq.), 24 h; [b] conversion and yields determined by HPLC with 3,4-dimethoxybenzyl alcohol as internal standard.

During the optimization process the question arose why the reactions with H₂O₂ as oxidant displayed significantly more activity in DMSO than in pyridine. A possible explanation is given in reports by Swern and Norman and co-workers.^[60-62] At elevated temperatures the disproportionation of H₂O₂ leads to formation of the hydroxyl radical. The hydroxyl radical in turn reacts with DMSO to form a methyl radical and methanesulfonic acid. This methyl radical could be a reactive species in the cleavage mechanism. Bertilsson *et al.* have shown that methyl radicals generated from H₂O₂ and DMSO with iron catalysts in acidic conditions can be employed in organic synthesis for the methylation of 1,3,5-trinitrobenzene and *p*-benzoquinone.^[63]

With regard to these reports in literature, several acids were then screened as additives since the formation of hydroxyl radicals in Fenton reactions is favored at an acidic pH which would concomitantly increase the production of methyl radicals (Table II.17).^[64] Additionally two bases were also tested as control experiment.

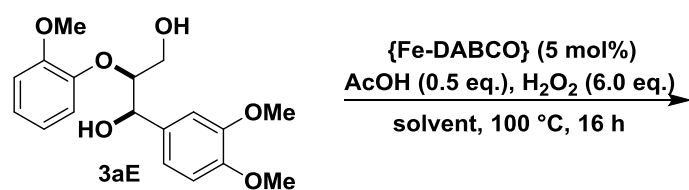
Table II.17: Influence of an additive for the cleavage of dilignol **3aE** in DMSO with H₂O₂ as oxidant.^[a]

additive	equivalents	conversion [%] ^[b]
acetic acid	0.1	90
acetic acid	0.5	97
acetic acid	5	88
boric acid	0.5	86
benzoic acid	0.5	91
H ₃ PO ₄	0.5	61
NaOH	0.5	72
Cs ₂ CO ₃	0.5	0

[a] Reaction conditions: **3aE** (0.25 mmol), {Fe-DABCO} (5 mol%), DMSO/H₂O 1:1 (1.0 mL), H₂O₂ (6 eq.), additive, 100 °C, 16 h; [b] conversion determined by HPLC with 3,4-dimethoxybenzyl alcohol as internal standard.

Acetic acid, boric acid, benzoic acid and H₃PO₄ were screened as acid additives. Of the four acids tested only H₃PO₄ had a notably negative effect on the activity with a conversion of 61%. Acetic acid, however, led to an increase in conversion with 97% even though a shorter reaction time of 16 h had been employed in the additive screening. Furthermore the yield for aldehyde **5** increased to 32% while affording ketone **12a** in 15%. These results favor the hypothesis that the methyl radical is indeed an important reactive species in this reaction. The highest activity was achieved with 0.5 equivalents of acetic acid as increasing or decreasing the amount of acetic acid lowered the conversion in this reaction.

When NaOH was employed as an additive the conversion decreased less than initially expected (72%). Changing the additive to Cs₂CO₃ led to a complete inhibition of the reaction. Considering reports by Swern and co-workers who made similar observations with a DMSO-based reaction system in the oxidation of benzyl alcohol to benzaldehyde in the presence of sodium carbonate, this is not surprising.^[62] To further elucidate the crucial influence of DMSO on this reaction, THF, NMP, 1,4-dioxane, toluene, DMF and dimethyl carbonate were screened as solvents for this reaction (Table II.18). As hypothesized the conversions decreased significantly.

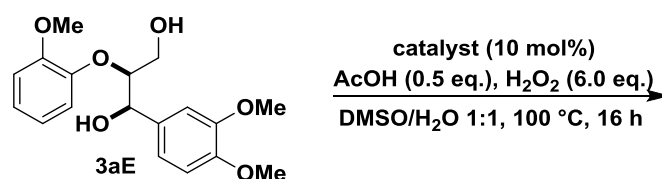
Table II.18: Solvent screening for the cleavage of dilignol **3aE** with H₂O₂ as oxidant.^[a]

solvent	conversion [%] ^[b]
DMSO/H ₂ O 1:1	97
THF	2
NMP	10
1,4-dioxane	0
toluene	29
DMF	27
dimethyl carbonate	8

[a] Reaction conditions: **3aE** (0.25 mmol), {Fe-DABCO} (5 mol%), solvent (1.0 mL), H₂O₂ (6 eq.), AcOH (0.5 eq.), 100 °C, 16 h; [b] conversion determined by HPLC with 3,4-dimethoxybenzyl alcohol as internal standard.

Since these results suggest that the main function of the catalyst is to generate the corresponding reactive radical species it was considered whether ligands that can potentially stabilize iron at higher oxidation states are actually necessary. Therefore, other iron salts were screened under the optimized conditions (Table II.19). The conversions for these iron salts varied from 54% to 82%. The most active iron salts were anhydrous FeCl₃ and Fe(NO₃)₃ with 81% and 82% conversion, respectively. In a control experiment FeCl₃ and DABCO were also added individually instead of the preformed complex. The conversion decreased to 77%. All these findings indicate that the nature of the iron source for this reaction is not very crucial as the activity from the salts does not vary greatly from the FeCl₃-derived complexes and the differences stem most likely from a different solubility.

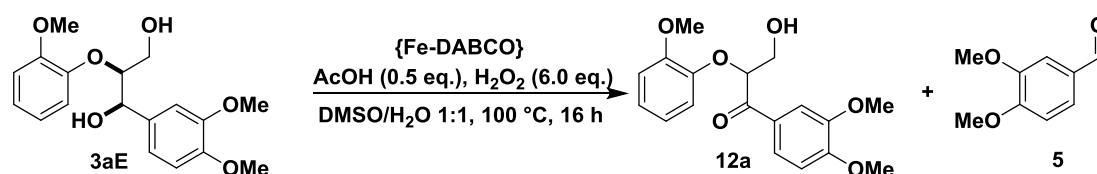
Furthermore, other transition metal salts that are known to be active in Fenton reactions were also screened (Table II.19).^[56] CuBr₂ was used as a copper source and it was less active than the iron salts with a conversion of 52%. The activity decreased even more when Mn(OAc)₃·2H₂O and Co(OAc)₃·4H₂O were employed as catalyst with conversions of 25% and 10%, respectively.

Table II.19: Metal salt screening for the cleavage of dilignol 3aE with H₂O₂ as oxidant.^[a]

catalyst	conversion [%] ^[b]
FeCl ₃ ·6 H ₂ O	65
FeCl ₃	81
FeCl ₂ ·4 H ₂ O	54
Fe(NO ₃) ₃	82
Fe(acac) ₃	76
FeC ₆ H ₅ O ₇ ·3 H ₂ O	62
FeCl ₃ + DABCO ^[c]	77
CuBr ₂	52
Mn(OAc) ₃ ·2H ₂ O	25
Co(OAc) ₃ ·4H ₂ O	10

[a] Reaction conditions: **3aE** (0.25 mmol), catalyst (10 mol%), DMSO/H₂O 1:1 (1.0 mL), H₂O₂ (6 eq.), AcOH (0.5 eq.), 100 °C, 16 h; [b] conversion determined by HPLC with 3,4-dimethoxybenzyl alcohol as internal standard; [c] 15 mol% of DABCO.

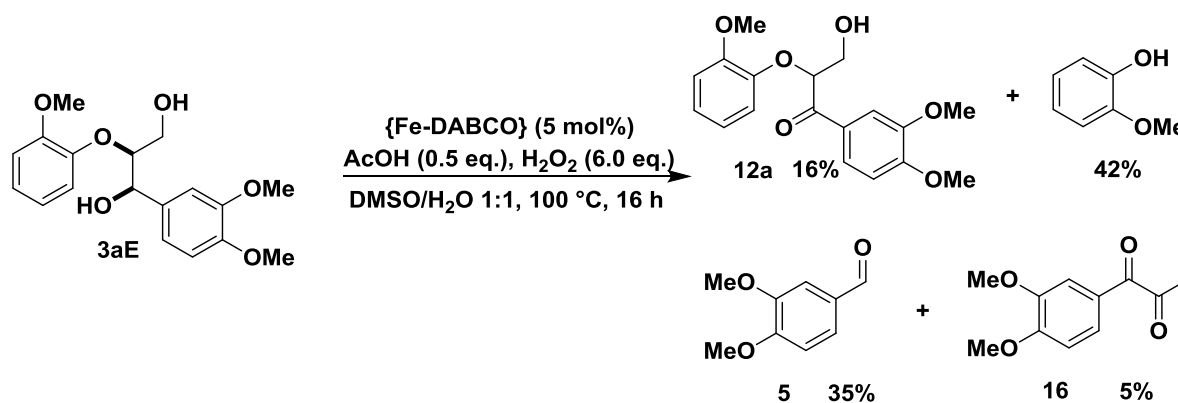
The final reaction parameter that was investigated was the influence of the catalyst loading. As already mentioned earlier in this chapter the catalyst loading was not crucial for the activity. Both decreasing the catalyst loading to 2.5 mol% and increasing it to 10 mol% slightly lowered the conversion to 88% and 86%, respectively. The yields for both ketone **12a** and aldehyde **5** with 2.5 mol% instead of 5 mol% {Fe-DABCO} were slightly lower with 12% and 26%, respectively. When 10 mol% of {Fe-DABCO} were employed the yield for the aldehyde **5** did not differ from the one with 5 mol% but the yield for ketone **12a** was a little lower with 9%.

Table II.20: Influence of the catalyst loading for the cleavage of dilignol 3aE with {Fe-DABCO}.^[a]

catalyst loading [mol%]	conversion [%] ^[b]	12a [%] ^[b]	5 [%] ^[b]
-------------------------	-------------------------------	------------------------	----------------------

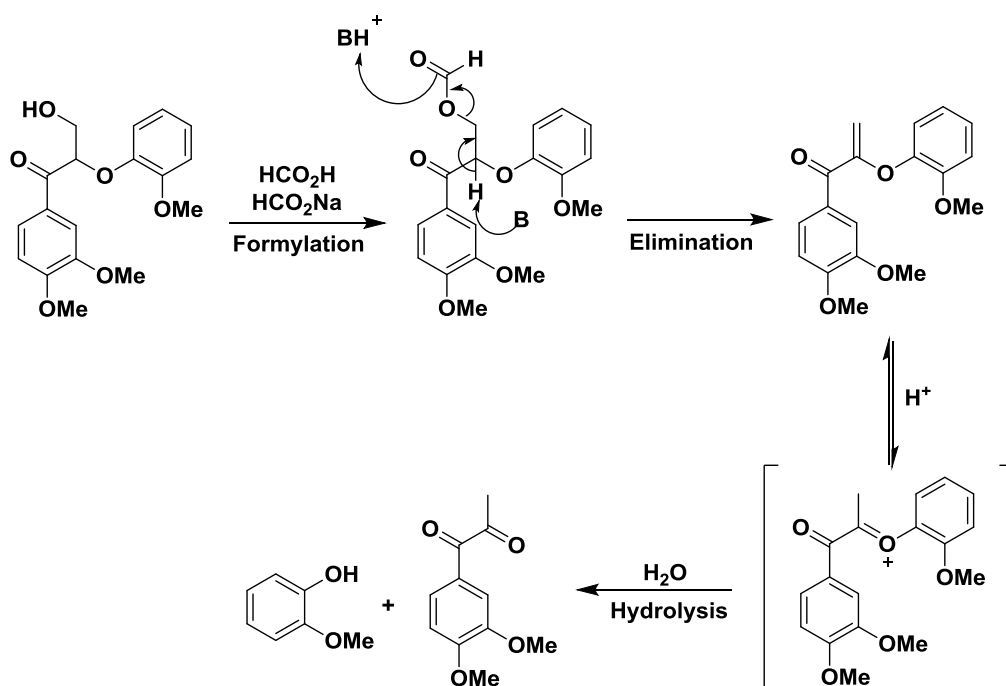
2.5	88	12	26
5.0	97	15	32
10.0	86	9	31

[a] Reaction conditions: **3aE** (0.25 mmol), {Fe-DABCO}, DMSO/H₂O 1:1 (1.0 mL), H₂O₂ (6 eq.), AcOH (0.5 eq.), 100 °C, 16 h; [b] conversion and yields determined by HPLC with 3,4-dimethoxybenzyl alcohol as internal standard.



Scheme II.16. Optimized reaction conditions for the {Fe-DABCO} catalyzed cleavage.

With the optimized reaction conditions in hand, the reaction was performed on a 1.00 mmol scale to isolate all the formed products (Scheme II.16). After column chromatography aldehyde **5** was obtained in 35% and ketone **12a** in 16% yield. As a side product diketone **16** was isolated in 5%. The main product of the reaction is 2-methoxyphenol with 42% yield. It is most likely concomitantly formed both in the cleavage of dilignol **3aE** to aldehyde **5** and in the cleavage of ketone **12a** to diketone **16**. Stahl and co-workers have postulated a mechanism for the cleavage of **12a** to diketone **16** and 2-methoxyphenol in the presence of formic acid and sodium formate (Scheme II.17).^[65] A similar mechanism seems plausible for acetic acid which is present in the optimized reaction conditions shown in Scheme II.16.



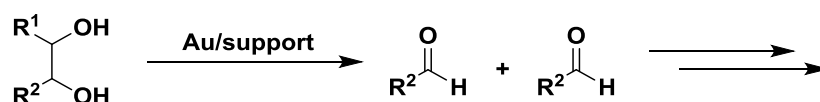
Scheme II.17. Proposed mechanism by Stahl and co-workers for the cleavage of **12a**.^[65]

The optimized reaction conditions were also applied with TBHP as oxidant. 68% conversion was achieved in that reaction and ketone **12a** was the main product in 42% yield. The yield for the aldehyde **5** remained low with 4%.

Further studies investigating the substrate scope with other model compounds and extracted lignin samples as well as EPR studies on the radical species present in the reaction are described in the article “Iron-catalysed oxidative cleavage of lignin and β -O-4 lignin model compounds using peroxides in DMSO” which has been published in the journal Green Chemistry and will be discussed in detail in the dissertation of Rinesch.^[66]

4. Oxidative cleavage of lignin model compounds with supported gold catalysts

The research goal of this dissertation was not only to examine suitable homogeneous transition metal catalysts but also heterogeneous catalysts. With regard to this incentive, supported gold catalysts were chosen for further investigations. Supported gold catalysts have been successfully employed in alcohol oxidations making them also potentially applicable for the oxidative cleavage of lignin bonds such as the β -O-4.^[67-69] Furthermore, Corma and co-workers utilized them in the synthesis of quinoxalines from biomass-derived glycols and 1,2-dinitrobenzene derivatives.^[70] A side reaction in this transformation was the oxidative cleavage of 1,2-diols to aldehydes, which, in turn reacted further to unwanted side products (Scheme II.18.).

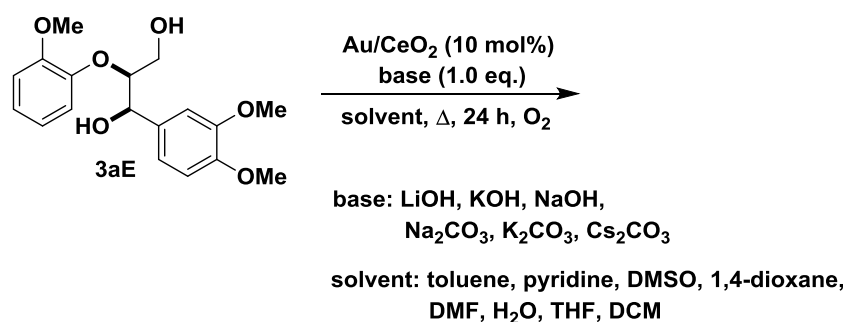


Scheme II.18. Side reaction observed by Corma and co-workers in the synthesis of quinoxalines.

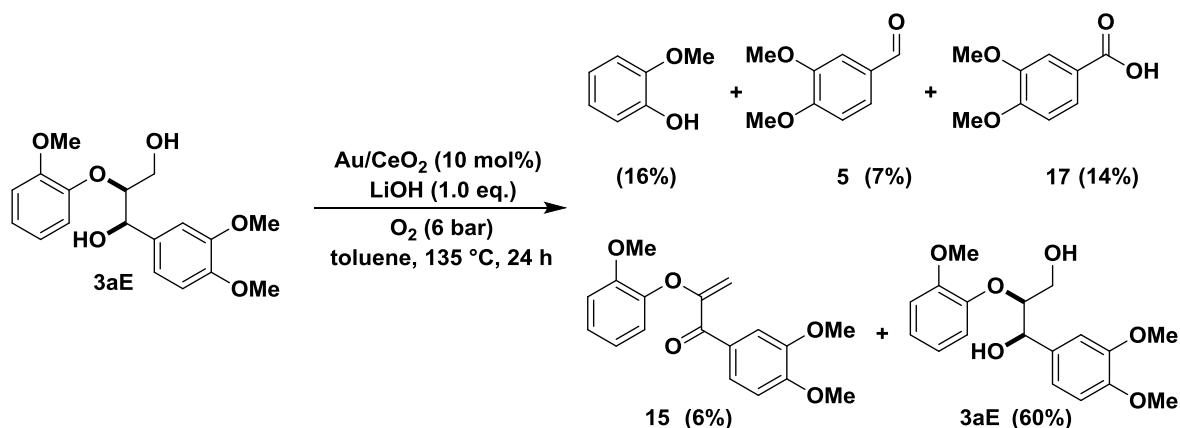
Due to the structural similarity of these 1,2-diols and the 1,3-diol motif in the β -O-4 linkage it was envisaged that this side reaction could be amplified to facilitate lignin cleavage. The initial experiments were performed during my stay at the ITQ in Valencia, Spain under the supervision of Corma. In the first reactions, gold nanoparticles supported on cerium oxide were used as catalyst which had been synthesized during that time. This catalyst was calcined under air as described in the experimental section. The other gold catalysts on various supports were synthesized by Juárez or Alós and either reduced with H_2 or 1-phenylethanol. The gold loading for all the employed catalysts was around 1% in weight.

4.1. Cleavage studies of dilignol 3aE with air calcined Au/CeO₂

The screening reactions were once more conducted with *erythro* dilignol **3aE** as starting material. The initial test reactions were performed using a modified procedure by Corma and co-workers for the oxidation of alcohols.^[68] For the oxidation of alcohols with supported gold catalysts, as well as the oxidative depolymerization of lignin, basic reaction conditions have been reported to be favorable.^[46,69,71] Therefore numerous bases and solvents as well as different temperatures and dioxygen pressures were tested as shown in Scheme II.19. The progression of these reactions was monitored by ¹H NMR. The highest conversions were obtained with toluene, pyridine and water, with the former two giving better selectivities for cleavage products. Furthermore, toluene gave higher conversions than pyridine. Of all the tested bases LiOH gave the highest and most reproducible conversion.

Scheme II.19. Screening of reaction conditions for air calcined Au/CeO₂.

To quantify the yields, the reaction in toluene and with LiOH as base was repeated on a 1.00 mmol scale and the products were separated by column chromatography (Scheme II.20). 2-Methoxyphenol was isolated as the main product in 16% yield. Veratraldehyde (**5**) and veratric acid (**17**) were obtained in 7% and 14% yield, respectively. Enol ether enone **15** was formed as a side product in 6% and the starting material was re-isolated in 60%.

Scheme II.20. Cleavage of **3aE** with air calcined Au/CeO₂ in toluene with LiOH.

A control reaction without catalyst showed that there was also conversion of **3aE** without the gold catalyst, albeit to a lower degree. In another control experiment without catalyst the base was switched to K_2CO_3 to assess whether carbonates were also active under these reaction conditions. However, no conversion of **3aE** was observed.

Since the activity of the air calcined Au/CeO₂ catalyst was not as high as originally hoped for, the focus was shifted to differently calcined gold catalysts and transition metal-containing hydrotalcite-like catalysts. These transition metal-containing hydrotalcite-like catalysts combine favorable basicity for cleavage reactions with oxidation potential and the obtained results are discussed in greater detail in part 5 of this chapter.

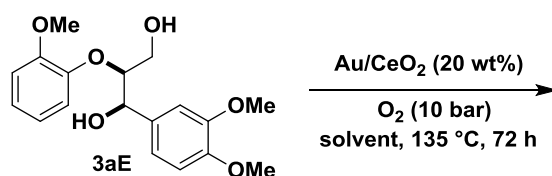
4.2. Cleavage studies of diglycol **3aE** with reduced supported gold catalysts

Here are now shown the results for the supported gold catalysts that were either reduced with H_2 or 1-phenylethanol before use. Furthermore not only CeO₂ but also hydrotalcite (HTc), TiO₂, MgO and ZrO₂ were used as support for the gold nanoparticles. Starting material was once more *erythro* diglycol **3aE**. The conversion was determined by HPLC with

3,4-dimethoxybenzyl alcohol as internal standard. The progression of the reactions was also monitored by ^1H NMR. The ratio in the ^1H NMR of the prior identified products with the sum of the products and the starting material is referred to as “product factor”. In contrast to the results described in part 2 of this chapter there was not a large discrepancy between the conversion determined by HPLC and the product factor determined by ^1H NMR because the selectivities for this reaction system were superior.

To assess whether reduced supported gold catalyst would lead to a higher activity, the initial experiments were conducted with Au/CeO₂. The reaction conditions, however, were modified from the previous ones. The dioxygen pressure was increased to 10 bar, a catalyst loading of 20 wt% was utilized and the reaction time was extended to 72 h. The most promising solvents in the previous study had been toluene and pyridine. Additionally to these two solvents, dimethyl carbonate (DMC) was screened (Table II.21).

Table II.21: Solvent screening for reduced Au/CeO₂ catalysts.^[a]



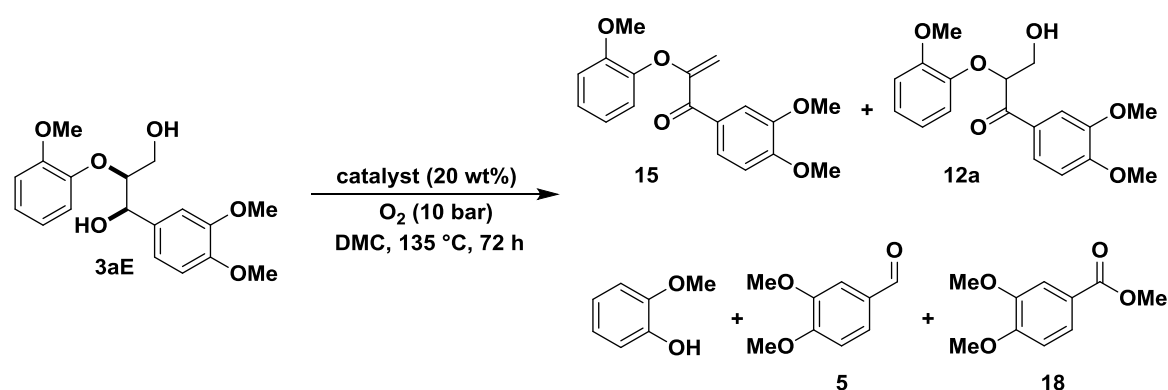
reduction method	solvent	conversion [%] ^[b]
H ₂	pyridine	0 ^[c,d]
H ₂	toluene	31
H ₂	DMC	100
1-phenylethanol	pyridine	0 ^[c,d]
1-phenylethanol	toluene	59
1-phenylethanol	DMC	100

[a] Reaction conditions: **3aE** (0.25 mmol), Au/CeO₂ (20 wt%), O₂ (10 bar), solvent (0.2 M), 72 h; [b] conversion determined by HPLC with 3,4-dimethoxybenzyl alcohol as internal standard; [c] product factor determined by ^1H NMR [product/(product+starting material)]*100; [d] performed on a 0.30 mmol scale.

Au/CeO₂ was not active in pyridine regardless of whether the catalyst was reduced with H₂ or 1-phenylethanol. This changed when either toluene or dimethyl carbonate was employed as solvent. In toluene a clear difference in activity was observed depending on how Au/CeO₂ had been reduced. The conversion increased from 31% with H₂ reduction to 59% with 1-phenylethanol reduction. A control experiment with CeO₂ was performed to determine whether or not the catalytic activity originated from gold nanoparticles. CeO₂ converted **3aE** to 34%. This indicates that only for 1-phenylethanol reduced Au/CeO₂ a little of the catalytic activity stems from the gold nanoparticles.

When dimethyl carbonate was employed as solvent the conversion of **3aE** increased for both the H₂ and 1-phenylethanol reduced Au/CeO₂ to 100%. The control experiment with CeO₂ showed that CeO₂ by itself was also very active converting **3aE** to 92%. CeO₂, however, displayed a different selectivity than both Au/CeO₂ catalysts (Table II.22). Ketone **12a** was only formed in 2% yield with CeO₂ as compared to 32% and 34% yield with 1-phenylethanol and H₂ reduced Au/CeO₂. Veratraldehyde (**5**) was one of the two main products for the CeO₂ catalyzed reaction with 18% yield. With 1-phenylethanol and H₂ reduced Au/CeO₂ as catalyst aldehyde **5** was formed in 13% and 5% yield, respectively. A different cleavage product, methyl 3,4-dimethoxybenzoate (**18**), was identified and obtained in 18% yield with CeO₂, 15% yield for H₂ reduced Au/CeO₂, and 14% yield for 1-phenylethanol reduced Au/CeO₂.

Table II.22: Product selectivities for Au/CeO₂ and CeO₂ in DMC.^[a]



catalyst	reduction method	conversion [%] ^[b]	12a [%] ^[b]	5 [%] ^[b]	18 [%] ^[b]
Au/CeO ₂	H ₂	100	34	5	15
Au/CeO ₂	1-phenylethanol	100	32	13	14
CeO ₂	-	92	2	18	18

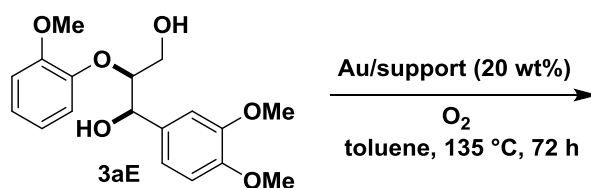
[a] Reaction conditions: **3aE** (0.25 mmol), catalyst (20 wt%), O₂ (10 bar), DMC (1.25 mL), 72 h; [b] yields determined by HPLC with 3,4-dimethoxybenzyl alcohol as internal standard.

With regard to the findings with Au/CeO₂, gold catalysts supported on HTc, MgO, ZrO₂ and TiO₂ were tested both in toluene and dimethyl carbonate. Table II.23 shows the activity of the supported gold catalyst in toluene. In order to determine whether the activity of the catalyst actually stemmed from the gold nanoparticles or just from the support, control reactions in toluene were made using just the supports (Table II.24). Au/HTc furnished a conversion of 33% when it was reduced before use with H₂. The corresponding 1-phenylethanol reduced catalyst was significantly more active, converting **3aE** to 86%. The main products in this reaction were veratric acid (**17**) in 23% and ketone **12a** in 22% yield. As side products veratraldehyde (**5**) was obtained in 11% and enol ether enone **15** in 6% yield. A lower dioxygen pressure of 6 bar decreased the conversion slightly to 77%. The control experiment with HTc afforded only trace conversion of **3aE**. This implies that the catalytic activity originates from the gold nanoparticles.

Employing MgO as support did not have a beneficial effect on the activity of the gold nanoparticles. With both Au/MgO catalysts only trace conversions of **3aE** were observed. MgO without Au was not tested because the corresponding gold catalysts already showed no relevant catalytic activity. Au/TiO₂ was very active and converted **3aE** under the standard reaction conditions to >99% when it had been reduced with H₂. 1-Phenylethanol reduced Au/TiO₂ showed similar catalytic activity with a conversion of 96%. The control experiment with TiO₂ however revealed that the activity originated mostly from the support. **3aE** was converted to 97% with TiO₂ as catalyst under the same reaction conditions as employed for Au/TiO₂. Despite the high activity for all the TiO₂ derived catalysts, the selectivity towards the known cleavage products and standard oxidations products was low in each case.

The final gold catalysts that were tested in toluene were supported on ZrO₂. H₂ reduced Au/ZrO₂ displayed relatively low activity with 19% conversion of **3aE**. Again the corresponding 1-phenylethanol reduced catalyst was more active converting **3aE** to 50% after 72 h. The control experiment with ZrO₂ revealed that the catalytic activity for both Au/ZrO₂ catalysts originated from the gold nanoparticles as ZrO₂ afforded only trace conversion. Similar to Au/TiO₂ the selectivity for cleavage products was low with less than 5%.

Table II.23: Cleavage of 3aE with supported gold catalysts in toluene.^[a]

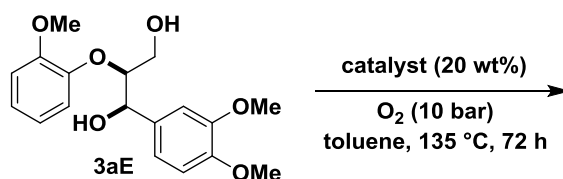


support	reduction method	O ₂ pressure [bar]	conversion [%] ^[b]
HTc	H ₂	10	33
HTc	1-phenylethanol	10	86
HTc	1-phenylethanol	6	77 ^[c]
MgO	H ₂	10	traces
MgO	1-phenylethanol	10	traces
TiO ₂	H ₂	10	>99
TiO ₂	1-phenylethanol	10	96
ZrO ₂	H ₂	10	19
ZrO ₂	1-phenylethanol	10	50
CeO ₂	H ₂	10	31
CeO ₂	1-phenylethanol	10	59

[a] Reaction conditions: **3aE** (0.25 mmol), Au/support (20 wt%), O₂, toluene (1.25 mL), 72 h; [b] conversion determined by HPLC with 3,4-dimethoxybenzyl alcohol as internal

standard; [c] reaction performed in a glass autoclave (25 mL) instead of a steel autoclave (20 mL).

Table II.24: Cleavage of 3aE with the support as catalyst in toluene.^[a]

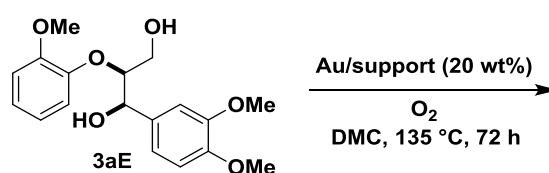


catalyst	time [h]	O ₂ pressure [bar]	conversion [%] ^[b]
HTc	72	10	traces
TiO ₂	72	10	97
ZrO ₂	72	10	traces
CeO ₂	72	10	34

[a] Reaction conditions: **3aE** (0.25 mmol), catalyst (20 wt%), O₂, dimethyl carbonate (1.25 mL); [b] conversion determined by HPLC with 3,4-dimethoxybenzyl alcohol as internal standard.

As previously observed with Au/CeO₂, the reaction behavior for the different supported gold catalysts changed significantly when dimethyl carbonate was employed as a solvent instead of toluene (Table II.25). Au/HTc afforded a product factor of 100 even when the dioxygen pressure was reduced to 1 bar and independently of how the gold nanoparticles had been reduced. Similar observations were made for gold on MgO. For the H₂ reduced Au/MgO a product factor of 85 was obtained with 1 bar of dioxygen pressure and for the corresponding 1-phenylethanol reduced catalyst a product factor of 90. The product factors did not increase with 10 bar of dioxygen pressure (not shown). The activity decreased considerably when gold catalysts were employed in which the support was less basic. Independent of the prior reduction method, Au/TiO₂ showed no catalytic activity with 1 bar of dioxygen pressure. When the dioxygen pressure was increased to 10 bar Au/TiO₂ became catalytically active. Furthermore, a clear difference in activity was observed depending on which reduction method had been utilized. The 1-phenylethanol reduced Au/TiO₂ afforded a product factor of 70 as compared to a product factor of 20 with H₂ reduced Au/TiO₂. No increased activity with higher dioxygen pressures was observed for Au/ZrO₂ as the results with 1 bar and 10 bar of dioxygen were almost identical. Furthermore, similar to the results with the other gold catalysts, a higher product factor was obtained when Au/ZrO₂ was reduced with 1-phenylethanol, affording a product factor of 33.

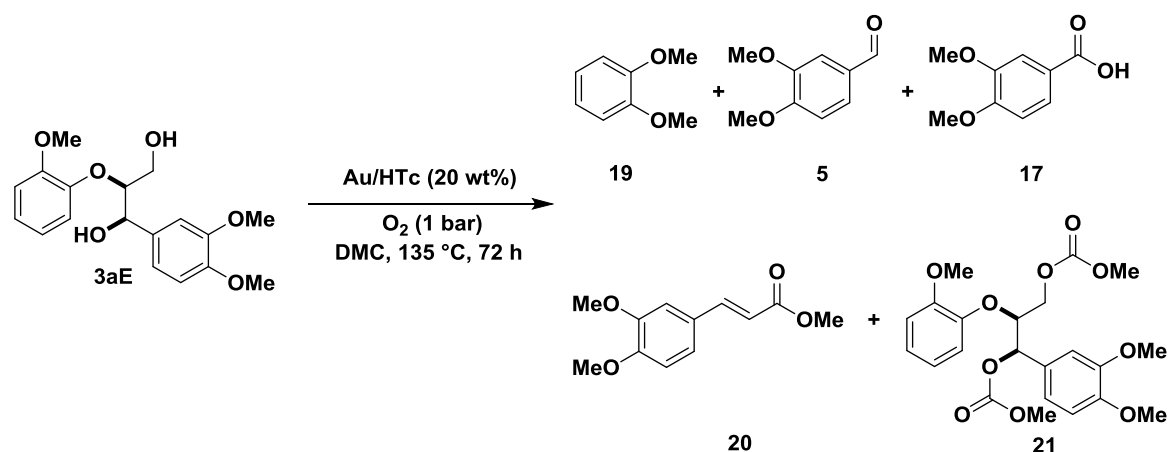
Table II.25: Cleavage of 3aE with supported gold catalysts in dimethyl carbonate.^[a]



support	reduction method	O ₂ pressure [bar]	product factor by ¹ H NMR ^[b]
HTc	H ₂	1	100 ^[c]
HTc	1-phenylethanol	1	100 ^[c]
MgO	H ₂	1	85 ^[c]
MgO	1-phenylethanol	1	90 ^[c]
TiO ₂	H ₂	1	0
TiO ₂	1-phenylethanol	1	0
TiO ₂	H ₂	10	20
TiO ₂	1-phenylethanol	10	70
ZrO ₂	H ₂	1	traces
ZrO ₂	1-phenylethanol	1	30
ZrO ₂	H ₂	10	traces
ZrO ₂	1-phenylethanol	10	33
CeO ₂	H ₂	1	35 ^[c]
CeO ₂	1-phenylethanol	1	45 ^[c]
CeO ₂	H ₂	10	100 ^[d]
CeO ₂	1-phenylethanol	10	100 ^[d]

[a] Reaction conditions: **3aE** (0.25 mmol), Au/support (20 wt%), O₂, toluene (1.25 mL), 70 h; [b] [product/(product+starting material)]*100; [c] performed on a 0.30 mmol scale; [d] conversion determined by HPLC with 3,4-dimethoxybenzyl alcohol as internal standard.

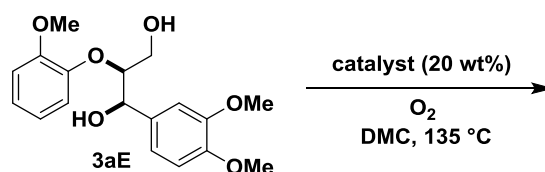
Strikingly, the observed product selectivities were different for each supported gold catalyst. In order to isolate the formed products by column chromatography the reaction with 1-phenylethanol reduced Au/HTc was repeated on a 1.00 mmol scale (Scheme II.21). The main product in this reaction was biscarbonate **21**. Trace amounts of veratraldehyde (**5**) and veratric acid (**17**) were obtained as side products. Instead of 2-methoxyphenol the corresponding methylated derivative veratrol (**19**) was isolated in small quantities. Another by-product was methyl (*E*)-3-(3,4-dimethoxyphenyl)acrylate (**20**). The formation of biscarbonate **21** as main product is not surprising considering that dimethyl carbonate is utilized in organic synthesis as a carboxymethylating and methylating reagent at temperatures higher than 90 °C in the presence of catalytic amounts of base.^[72]



Scheme II.21. Cleavage of 3aE with 1-phenylethanol reduced Au/HTc in dimethyl carbonate.

To further elucidate whether the activity of the reaction system in dimethyl carbonate stemmed only from the support acting as a base, several test reactions were made with various supports and other inorganic bases (Table II.26). HTc already furnished a product factor of 100 after 2 h at 135 °C under ambient atmosphere. The product factors for TiO₂, ZrO₂ and CeO₂ with 1 bar of dioxygen pressure and a reaction time of 72 h were almost identical to the ones with the corresponding supported gold catalysts. When the catalyst was omitted entirely no product formation was observed after 72 h. NaOH and K₂CO₃ were tested as catalyst with a reaction time of 16 h and 1 bar of dioxygen pressure. In both cases a product factor of 100 was achieved. These results indicate that the gold nanoparticles are not responsible for the catalytic activity in dimethyl carbonate when only 1 bar of dioxygen pressure is employed. An extensive study which further elaborates these initial findings on base catalyzed lignin cleavage is presented in the article “Base-catalysed cleavage of lignin β-O-4 model compounds in dimethyl carbonate” that has been published in the journal Green Chemistry and will be discussed in detail in the dissertation of Dabral.^[26]

Table II.26: Cleavage of 3aE with the support or base in dimethyl carbonate.^[a]



catalyst	time [h]	O ₂ pressure [bar]	product factor by ¹ H NMR ^[b]
HTc	72	1	100
HTc	72	-	100
HTc	16	1	100
HTc	2	-	100
TiO ₂	72	1	0
ZrO ₂	72	1	35

CeO ₂	72	1	49
-	48	1	0
-	72	-	0
NaOH	16	1	100
K ₂ CO ₃	16	1	100

[a] Reaction conditions: **3aE** (0.25 mmol), catalyst (20 wt%), O₂, dimethyl carbonate (1.25 mL);

[b] [product/(product+starting material)]*100.

In summary, the most active reaction system found during these investigations, HTc in dimethyl carbonate, actually did not require gold nanoparticles for its catalytic activity. The highest reactivity for a gold catalyst, in which the catalytic activity originated only from the gold and not from the support or the solvent, was observed for 1-phenylethanol reduced Au/HTc in toluene. Under the optimized conditions (Table II.23) 86% conversion was achieved with ketone **12a** and acid **17** as the main products. A significant effect of the reduction method was observed for the majority of the supported gold catalyst. All the 1-phenylethanol reduced gold catalysts were more or at least as active as the corresponding H₂ reduced gold catalyst.

5. Oxidative cleavage of lignin with hydrotalcite-like catalysts and $V(\text{acac})_3/\text{Cu}(\text{NO}_3)_2 \cdot 3\text{H}_2\text{O}$ as catalyst

In part 4 of this chapter it was alluded to that transition metal-containing hydrotalcite-like catalysts combine favorable basicity for lignin cleavage reactions with oxidation potential. They have been employed in a variety of oxidation reactions in organic synthesis which has been described in the introduction of this dissertation.^[49] Copper, iron, cobalt and vanadium containing hydrotalcite-like catalysts were chosen for screening reactions as these transition metals have displayed good activity in homogeneously catalyzed lignin cleavage studies.^[35,37,38,40,41] All of the employed hydrotalcite-like catalysts were synthesized by Puche. The initial experiments were conducted at the ITQ in Valencia, Spain under the supervision of Corma.

5.1. Cleavage studies of dilignol **3aE** with hydrotalcite-like catalysts

For the screening of the hydrotalcite-like catalysts *erythro* dilignol **3aE** was used as the starting material under similar reaction conditions as described in part 4 of this chapter for the supported gold catalysts. Table II.27 shows the conversion in toluene with 6 bar of dioxygen pressure and a reaction temperature of 130 °C or 135 °C. Iron, cobalt and zinc containing HTcs converted only trace amounts of **3aE**. The copper containing hydrotalcite (HTc-Cu) afforded a product factor of 50 (determined by ¹H NMR) after 40 h with cleavage products veratraldehyde (**5**) and veratric acid (**17**) as the main products. Yet, at a later stage of this investigation, those results could never be reproduced and only trace conversions of **3aE** with HTc-Cu were obtained. When vanadium was introduced into the interlayers of the HTcs as vanadate, the catalysts became catalytically active. Iron-vanadium and copper-vanadium hydrotalcite-like catalysts (HTc-Fe-V and HTc-Cu-V) converted **3aE** to >99% after 13 h. Again the formation of cleavage products such as veratraldehyde (**5**) and veratric acid (**17**) was observed. These reactions, however, were rather unselective and furnished numerous products. Similar selectivities were observed with vanadium and cobalt-vanadium hydrotalcite-like catalysts (HTc-V and HTc-Co-V) but the conversions were lower with 72% and 71%, respectively.

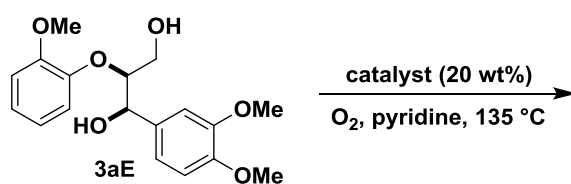
Table II.27: Hydrotalcite-like catalyst screening with dilignol **3aE** in toluene.^[a]

catalyst	T [°C]	time [h]	conversion [%] ^[b]
HTc-Fe	130	40	traces
HTc-Co	135	72	traces

HTc-Zn-Co	135	72	traces
HTc-Cu	135	72	traces
HTc-Zn	135	72	traces
HTc	135	72	traces
HTc-Fe-V	135	13	>99
HTc-Co-V	135	13	71
HTc-Cu-V	135	13	>99
HTc -V	135	13	72

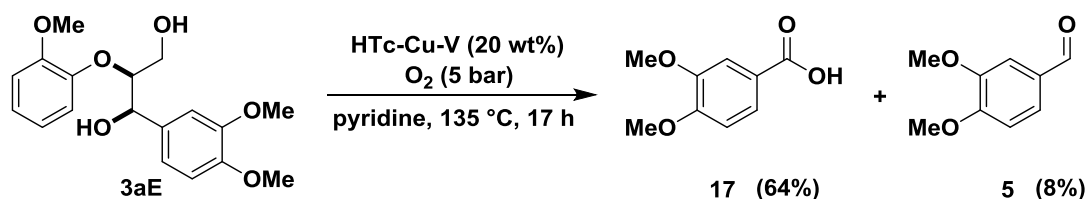
[a] Reaction conditions: **3aE** (0.25 mmol), catalyst (20 wt%), toluene (1.25 mL), O₂ (6 bar), 600 rpm; [b] conversion determined by HPLC with 3,4-dimethoxybenzyl alcohol as internal standard.

When pyridine was employed as solvent both HTc-Fe and HTc afforded only trace conversions of **3aE** (Table II.28). HTc-Cu on the other hand was active in pyridine with 77% conversion after 72 h. The cleavage products veratraldehyde (**5**) and veratric acid (**17**) were the main products. The best activity and selectivity for the formation of cleavage products was obtained when either HTc-Cu-V or HTc-Zn-Cu-V was utilized as catalyst. The reaction time could be reduced in both cases to 17 h with 5 bar of dioxygen pressure, converting **3aE** to >99%. Scheme II.22 shows the yields with HTc-Cu-V as catalyst on a 0.25 mmol reaction scale. Veratric acid (**17**) was the main product in 64% yield and veratraldehyde (**5**) was obtained as a side product in 8%. To reach similar conversions with HTc-V the dioxygen pressure had to be increased to 6 bar. Despite the high conversion HTc-V furnished lower yields for aldehyde **5** and acid **17** than either HTc-Cu-V or HTc-Zn-Cu-V. Changing the oxidant from dioxygen to air slightly reduced the conversion to 92% with HTc-Cu-V being used as catalyst.

Table II.28: Hydrotalcite-like catalyst screening with dilignol 3aE in pyridine.^[a]

catalyst	time [h]	O ₂ pressure [bar]	conversion [%] ^[b]
HTc-Fe	72	6	traces
HTc-Cu	72	6	77
HTc	40	6	traces
HTc-Cu-V	17	5	>99
HTc-Zn-Cu-V	17	5	>99
HTc-V	17	6	98
HTc-Cu-V	17	5 ^[c]	92

[a] Reaction conditions: **3aE** (0.25 mmol), catalyst (20 wt%), pyridine (1.25 mL), O₂, 600 rpm; [b] conversion determined by HPLC with 3,4-dimethoxybenzyl alcohol as internal standard; [c] air (5 bar) instead of O₂.



Scheme II.22. Cleavage of 3aE with HTc-Cu-V in pyridine on a 0.25 mmol scale.

All of the reactions thus far described in this part were performed in a 25 mL glass autoclave. To elucidate the effect of the oxidant and the employed reaction vessel, test reactions were also made in 25 mL two-necked round bottom flasks equipped with a reflux condenser and a gas storage balloon (Table II.29). The progression of these reactions was determined by ¹H NMR. After a reaction time of 13 h a product factor of only 7 was observed when the reaction was run under reflux with air as oxidant from a gas storage balloon. When the oxidant was changed to dioxygen while also employing a reflux condenser and gas storage balloon the product factor increased to 33. In both reactions ketone **12a** and enol ether enone **15** were the main products. The selectivity for the formation of the cleavage products aldehyde **5** and acid **17** was substantially higher when the reaction was performed under 1 bar of dioxygen pressure in a 25 mL glass autoclave. After a reaction time of 24 h a product factor of 70 was obtained. The higher yields for the cleavage products can only be partially attributed to the longer reaction time because later in this chapter it will be shown that the

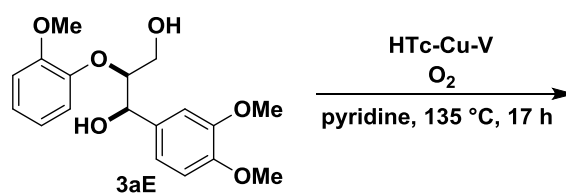
yields for aldehyde **5** were always higher after shorter reaction times. The effect of different autoclave volumes on the activity will be discussed later on in this chapter.

Table II.29: Influence of the oxidant and the reaction vessel on the conversion of dilignol **3aE.**^[a]

oxidant	time [h]	product factor by ¹ H NMR ^[b]
dioxygen	24	70
air ^[c]	13	7
dioxygen ^[c]	13	33

[a] Reaction conditions: **3aE** (0.25 mmol), HTc-Zn-Cu-V (20 wt%), pyridine (1.25 mL), oxidant (1 bar), 600 rpm; [b] [product/(product+starting material)]*100; [c] under reflux in a 25 mL two-necked round bottom flask with a gas storage balloon.

After having distinguished the influence of the oxidant and the reaction vessel, different catalyst loadings were tested. 5 wt% of HTc-Cu-V and a dioxygen pressure of 6 bar afforded 83% conversion of **3aE** after 17 h. The conversion increased to 98% when 10 wt% of HTc-Cu-V were employed. When the dioxygen pressure was reduced to 5 bar the conversion with 10 wt% catalyst decreased slightly to 89%. These results indicate that the catalyst loading can indeed be reduced but in order to maintain high activity the dioxygen pressure would have to be increased. As described earlier, 20 wt% of HTc-Cu-V and a dioxygen pressure of 5 bar afforded >99% conversion after 17 h. Therefore in all further studies 20 wt% of catalyst were used.

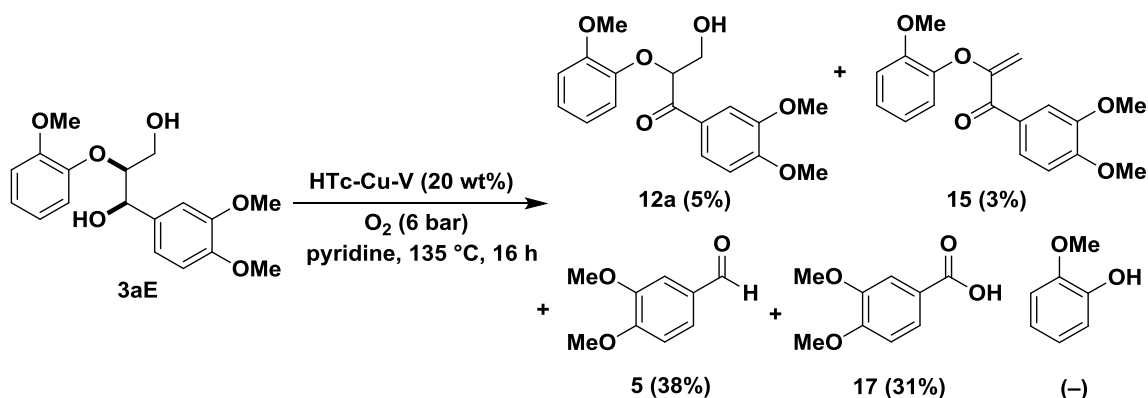
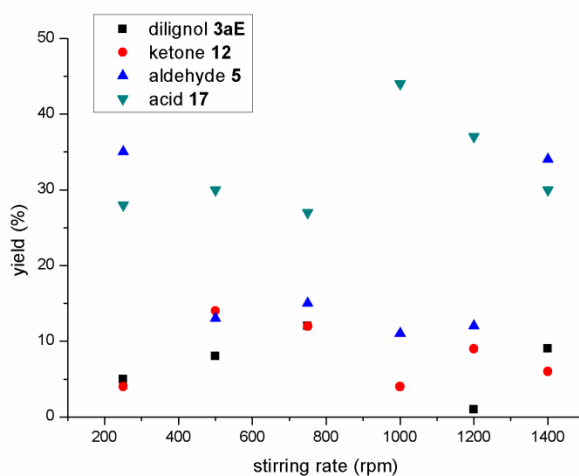
Table II.30: Influence of the catalyst loading on the conversion of dilignol **3aE**.^[a]

catalyst loading [wt%]	pressure [bar]	conversion [%] ^[b]
5	6	83
10	5	89
10	6	98
20	5	>99

[a] Reaction conditions: **3aE** (0.25 mmol), HTc-Cu-V, pyridine (1.25 mL), O₂, 600 rpm; [b] conversion determined by HPLC with 3,4-dimethoxybenzyl alcohol as internal standard.

Dimethyl carbonate was also tested as a solvent because it had shown interesting activity in the cleavage studies described in part 4 of this chapter. Using HTc-Cu-V as catalyst and a dioxygen pressure of 6 bar 92% of **3aE** was converted after 17 h. The main product in this reaction, however, was ketone **12a** with aldehyde **5** and acid **17** formed as side products.

With the optimized reaction conditions in hand, the reaction with 20 wt% of HTc-Cu-V was repeated on a 1.00 mmol scale to facilitate the isolation and characterization of the formed products (Scheme II.23). The dioxygen pressure had to be increased to 6 bar to ensure complete conversion of **3aE** under the upscaled reaction conditions. After column chromatography veratraldehyde (**5**) and veratric acid (**17**) were obtained as main products in 38% and 31% yield, respectively. As side products ketone **12a** was isolated in 5% and enol ether enone **15** in 3% yield. The fact that aldehyde **5** and acid **17** were formed in almost equimolar amounts was surprising considering the results on a 0.25 mmol scale. Initially it was suspected that the different dioxygen uptake could be responsible for this altered selectivity. Therefore the influence of the stirring rate was investigated (Figure II.2). However, no general trend was observed that would support this hypothesis. Considering the results on metal leaching that will be discussed in detail in part 5.2., the changes in selectivity are most likely caused by a difference in the ratio of active copper and vanadium species that have gone into solution on a 0.25 mmol and on a 1.00 mmol scale.

Scheme II.23. Cleavage of **3aE** with HTc-Cu-V in pyridine on a 1.00 mmol scale.Figure II.2. Influence of the stirring on the conversion of **3aE**.

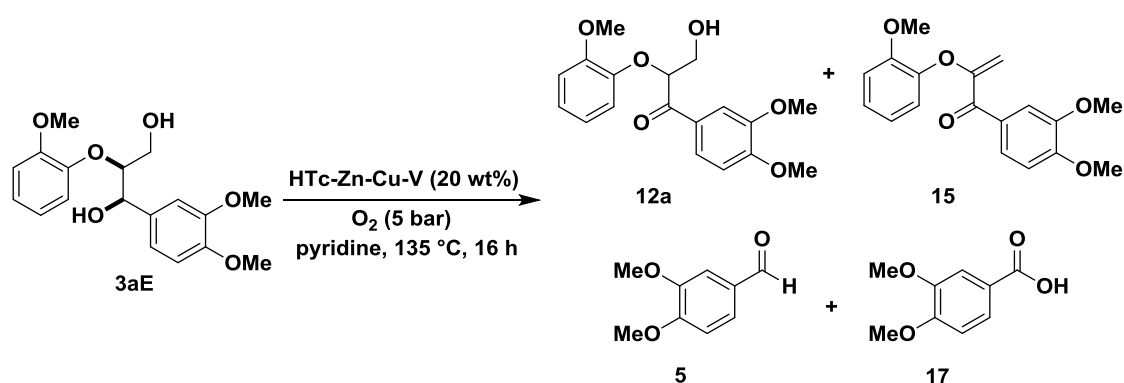
During the entire investigation with transition metal-containing hydrotalcite-like catalysts 2-methoxyphenol was never detected as a product. This was surprising since in part 3 and 4 of this chapter it was formed concomitantly in the cleavage of **3aE** to aldehyde **5**. An explanation for this observation is given by Alejandro *et al.* who reported that copper hydrotalcite-like catalysts oxidized phenol derivatives to organic acids and CO₂ with benzoquinone derivatives as intermediates.^[73] To further validate this report 2-methoxyphenol was subjected to the reaction conditions shown in Scheme II.22. Under these conditions 2-methoxyphenol was completely degraded to numerous products confirming previous observations.

5.2. Catalyst recycling and catalyst leaching studies

Having found a catalyst system that displayed good activity and selectivity it was of fundamental interest to see whether the catalyst remained active after being reused for several reactions (Table II.31). HTc-Zn-Cu-V was used as catalyst and a dioxygen pressure of 5 bar was employed. These conditions were chosen to avoid full conversion and thus help detect changes in the activity. In the first two runs the conversion of **3aE** remained almost constant with 89% and 91%, respectively. The activity in the third run, however, decreased with a

conversion of 76%. In all three runs veratraldehyde (**5**) and veratric acid (**17**) were the main products with ketone **12a** and enol ether enone **15** being formed as side products. The yields for ketone **12a** and enol ether enone **15** remained almost constant in all three runs. The yield for aldehyde **5** decreased in each run from 30% in the first run, to 26% in the second and 22% in the third. A potential explanation for the decreasing catalyst activity was leaching of the heterogeneous catalyst into solution. Furthermore to be able to provide a reasonable explanation as to why the yields for aldehyde **5** declined with every additional run some of the obtained results will be revealed now. In Figure II.8 to Figure II.12 reaction kinetics with homogeneous copper and vanadium are presented. In these it can be seen that copper enhances the formation of aldehyde **5**. At the same time, as shown in Figure II.3, the amount of copper from the heterogeneous catalyst that leached into solution continuously rose over the course of the reaction. Thus with every consecutive run there was less and less copper still present in the catalyst to help facilitate the formation of aldehyde **5** and therefore the yields for **5** steadily decreased.

Table II.31: Catalyst recycling experiments with HTc-Zn-Cu-V.^[a]



run	yield [%] ^[b]				
	3aE ^[c]	12	15	5	17
1 st	11	8	2	30	22
2 nd	9	5	2	26	32
3 rd	24	7	3	22	14

[a] Reaction conditions: **3aE** (1.00 mmol), HTc-Zn-Cu-V (20 wt%), pyridine (5.0 mL), O₂ (5 bar), 600 rpm; [b] after column chromatography; [c] reisolated starting material.

When initially investigating potential leaching of the heterogeneous catalysts, a control experiment was made in which HTc-Cu-V was filtered off from the hot reaction solution after 2 h and the resulting clear solution was then subjected to the original reaction conditions for additional 15 h. The conversion after 2 h was 38% and after the additional 15 h 82%. This clearly showed that catalytically active species had gone into solution. Since the conversion was lower than under the standard reaction conditions it still remained to be seen whether

these leached species were less active than the heterogeneous catalyst or if they deactivated over time due to agglomeration or a resting state of the catalyst. The amount of leached copper and vanadium was quantified by ICP-OES. After a reaction time of 2 h and hot filtration 111.9 mg/L copper and 251.0 mg/L vanadium had gone into solution. This corresponds to 6.4% of the original vanadium and 10% of the original copper content in HTc-Cu-V.

In order to determine whether there was just initial leaching or a continuous release of metal species, the concentration of the metal species in solution after hot filtration was monitored by ICP-OES over the course of the reaction (Figure II.3). The same reaction conditions were employed as shown in Scheme II.22. Copper was continuously released over the entire course of the reaction. Within the first 4 h the copper concentration in solution increased faster than after longer reaction times. For vanadium high initial leaching was observed but then the concentration remained more or less constant over the course of the reaction with a slight decline at the end. The significantly lower vanadium value after 4 h most likely represents an outlier. The decline at the end could potentially be attributed to agglomerates because in the previous experiment with hot filtration after 2 h the formation of precipitates from the initially clear solution was observed during the 15 h of additional reaction time.

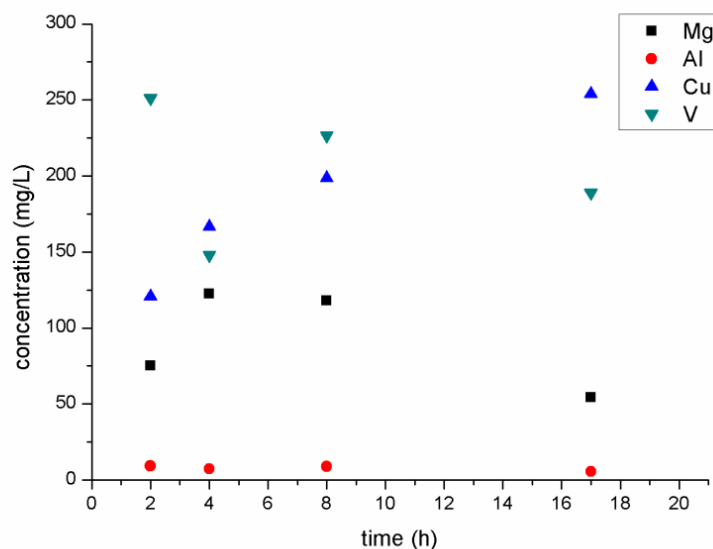


Figure II.3. By ICP-OES determined concentration of leached metal species from HTc-Cu-V over the course of the reaction.

After having investigated the extent of the leaching in solution it was studied whether the leaching had influenced the morphology of the solid catalyst. Figure II.4 shows the XRD patterns of HTc-Cu-V before and after a reaction time of 17 h. Here it can be clearly seen that no significant structural changes had occurred. The same observations were made when HTc-Cu-V was analyzed by Raman spectroscopy before and after a reaction of 17 h (Figure II.5). All the characteristic metal-oxygen stretching vibrations (317 , 338 cm^{-1}) and metal-oxygen-metal vibrations (867 and 943 cm^{-1}) were present before and after the reaction.

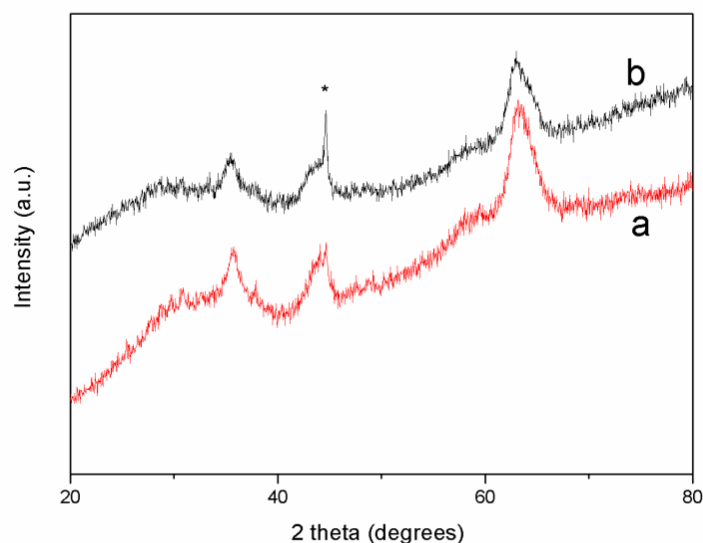


Figure II.4. XRD spectra of HTc-Cu-V a) before and b) after a reaction time of 17 h; * peak caused by the sample holder.

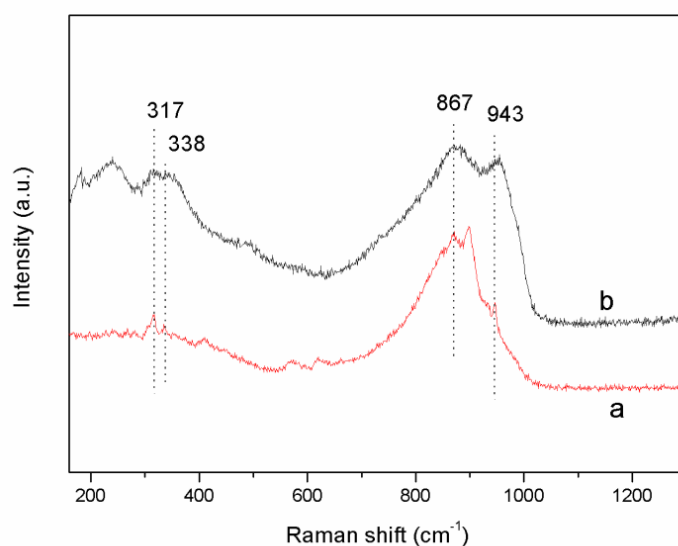


Figure II.5. Raman spectra of HTc-Cu-V a) before and b) after 17 h of reaction.

To gain a better understanding of the general activity of homogeneous copper and vanadium, both individually and together, additional experiments were conducted with a copper and a vanadium salt. As a copper source $\text{Cu}(\text{NO}_3)_2 \cdot 3\text{H}_2\text{O}$ and as a vanadium source $\text{V}(\text{acac})_3$ were used. In the previous ICP-OES measurements 251.0 mg/L vanadium were detected in solution after 2 h. This translates to 2.5 mol% vanadium. Correspondingly, 111.9 mg/L copper were found in solution after 2 h which correlates to 1.0 mol%. Therefore, to assess whether the activity was similar to the leached components, 2.5 mol% of $\text{V}(\text{acac})_3$ and 1.0 mol% of $\text{Cu}(\text{NO}_3)_2 \cdot 3\text{H}_2\text{O}$ were employed in the test experiment under the reaction conditions shown in Scheme II.22. After a reaction time of 17 h 97% of **3aE** was converted and veratric acid (**17**)

and veratraldehyde (**5**) were the main products in 39% and 26% yield, respectively. When $V(acac)_3$ (2.5 mol%) was employed without $Cu(NO_3)_2 \cdot 3H_2O$ the conversion remained high with 96%. The yield for veratric acid (**17**) stayed the same with 39% but the yield for aldehyde **5** decreased to 15% as described earlier in this chapter. $Cu(NO_3)_2 \cdot 3H_2O$ without $V(acac)_3$ did not display high activity. Even when the catalyst loading was increased to 5 mol% or 10 mol% only 20% conversion after 17 h was obtained. Detailed kinetics and rate constants for reaction systems using $V(acac)_3$ and $Cu(NO_3)_2 \cdot 3H_2O$ will be presented in part 5.3 of this chapter.

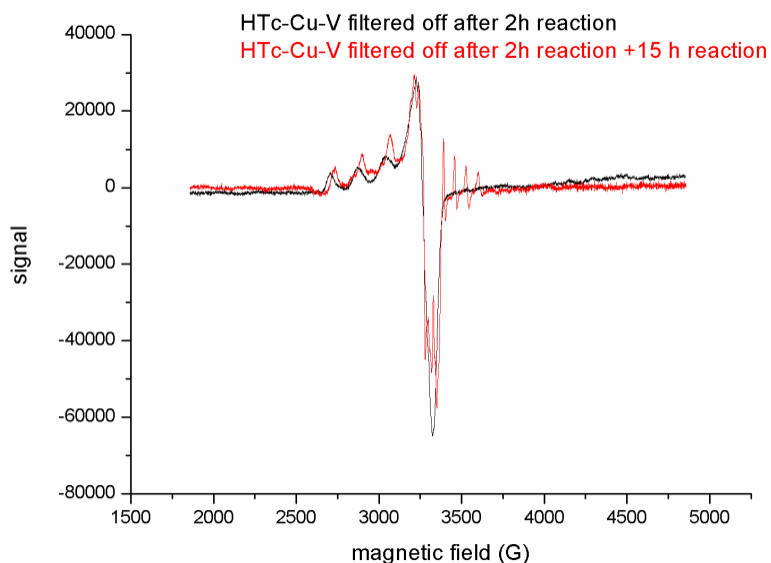


Figure II.6. EPR spectra of the reaction solution after hot filtration of HTc-Cu-V.

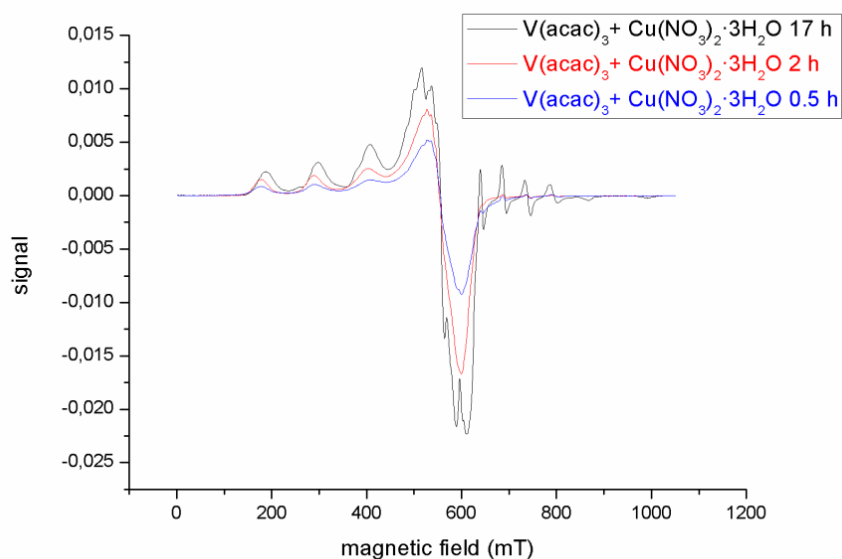


Figure II.7. EPR spectra of the reaction solution using 5 mol% of $V(acac)_3/Cu(NO_3)_2 \cdot 3H_2O$.

After having established that homogeneous copper and vanadium together were very active for the conversion of **3aE** I wanted to verify whether there was a correlation between the nature of the active homogeneous copper and vanadium species in the $V(acac)_3/Cu(NO_3)_2 \cdot 3H_2O$ catalyst and the leached metal species that had gone into solution from the HTc-Cu-V catalyst. To enable such a correlation additional experiments with $V(acac)_3/Cu(NO_3)_2 \cdot 3H_2O$ and HTc-Cu-V were performed that were monitored by EPR spectroscopy. Figure II.6 shows the results that were obtained for the leached species of HTc-Cu-V. In these experiments HTc-Cu-V was set to react under the reaction conditions shown in Scheme II.22. Similar to the initial leaching experiment, HTc-Cu-V was filtered off hot after a reaction time of 2 h. The resulting reaction solution was analyzed by EPR spectroscopy. The EPR spectrum showed a strong signal typical for copper (II) and none for vanadium (IV). This experiment was repeated but the resulting solution after the hot filtration was again subjected to the original reaction conditions for additional 15 h and then examined by EPR. The spectrum not only showed a signal for copper (II) but also a distinct signal for vanadium (IV) (to have a reference of a pure vanadium (IV) EPR spectrum, the spectrum of 5 mol% $V(acac)_3$ dissolved at room temperature in pyridine is included in the experimental part).

Next, $V(acac)_3/Cu(NO_3)_2 \cdot 3H_2O$ was investigated (Figure II.7). The experiments with this catalyst system were performed with a catalyst loading of 5 mol%. The EPR spectra after 0.5 h and 2 h displayed a strong signal for copper (II) and only a very weak signal for vanadium (IV). These results correlate to the ones with HTc-Cu-V after 2 h. The signal intensity for vanadium (IV) increased significantly after a reaction time of 17 h similar to HTc-Cu-V after 15 h of additional reaction time. On the basis of these and the previously presented results it is reasonable to postulate that the homogeneous copper and vanadium species from the leached HTc-Cu-V and $V(acac)_3/Cu(NO_3)_2 \cdot 3H_2O$ are most likely very similar in their nature. Furthermore, the EPR results suggest that vanadium (IV) is not the catalytically active species in both reaction systems and potentially represents a resting state of the catalyst. The kinetics for 5 mol% $V(acac)_3/Cu(NO_3)_2 \cdot 3H_2O$ shown later in Figure II.10 demonstrate that the reaction system is most active at the beginning of the reaction when almost no vanadium (IV) is present. As the reaction system becomes less active the amount of vanadium (IV) increases. These findings are in accordance with reports by Hanson *et al.* who propose a two electron oxidation mechanism from vanadium (V) to vanadium (III) in the alcohol oxidations with dipicolinate vanadium (V) in the presence of pyridine.^[42] With regard to all the results presented in part 5.2 of this chapter it can be concluded that HTc-Cu-V and HTc-Zn-Cu-V act to a significant degree as a dispenser of the catalytically active homogeneous species that are continuously released. These leached species deactivate over time either through agglomeration or a resting state of the catalyst.

5.3. Reaction kinetics and reaction pathways

To gain a better understanding of the reactivity and selectivity of both the homogeneous reaction system with $V(acac)_3/Cu(NO_3)_2 \cdot 3H_2O$ and the hydrotalcite-like catalysts a series of kinetics were conducted. All the kinetics presented in part 5.3 were performed at a reaction

temperature of 135 °C and 5 bar of dioxygen pressure. Figure II.8 and Figure II.9 show the kinetics of $V(acac)_3/Cu(NO_3)_2 \cdot 3H_2O$ with a catalyst loading of 20 mol% and 10 mol%, respectively. The activity with regard to the conversion of **3aE** was almost identical, demonstrating that a higher catalyst loading did not lead to a faster conversion. Ketone **12a** was initially formed in 26% yield under both reaction conditions after a reaction time of 2 h and was then consumed over time. The yield for aldehyde **5** remained more or less constant between the reaction times of 2 h to 17 h, but with 10 mol% $V(acac)_3/Cu(NO_3)_2 \cdot 3H_2O$ the yields were in average 5% higher than those obtained with 20 mol% $V(acac)_3/Cu(NO_3)_2 \cdot 3H_2O$. After a reaction time of 17 h veratric acid (**17**) was obtained in 54% yield independently of the catalyst loading (10 mol% or 20 mol%). In both cases the yield for acid **17** had reached a plateau at the end of the reaction.

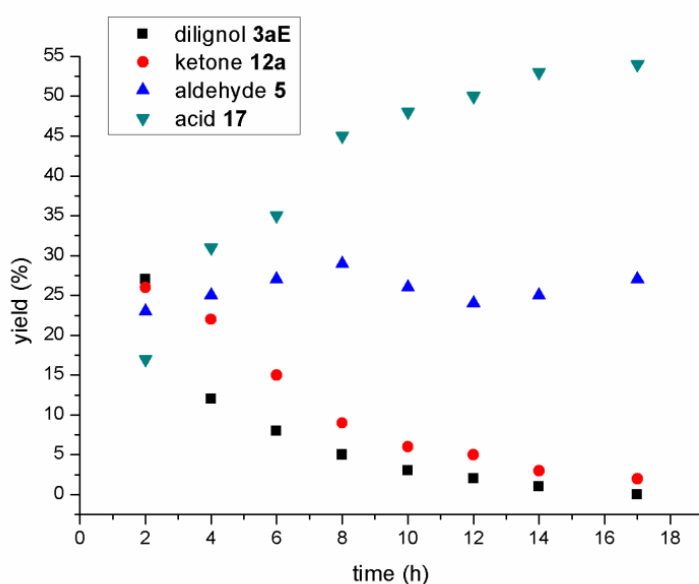


Figure II.8. Reaction kinetics for **3aE** using 20 mol% of $V(acac)_3/Cu(NO_3)_2 \cdot 3H_2O$.

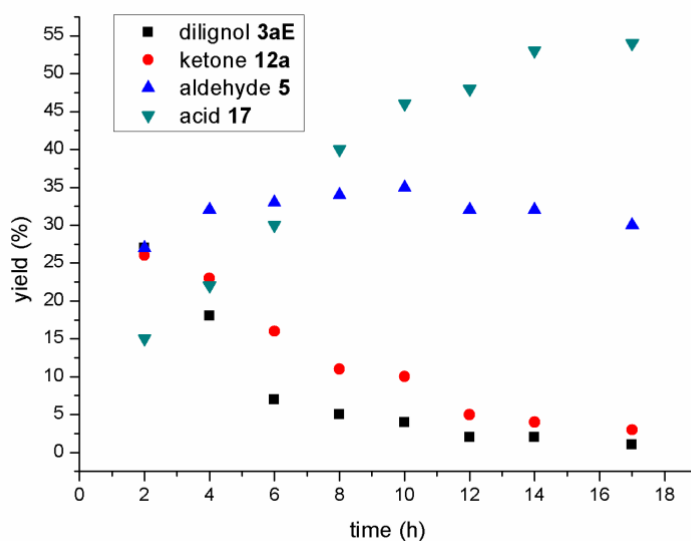


Figure II.9. Reaction kinetics for **3aE** using 10 mol% of $V(acac)_3/Cu(NO_3)_2 \cdot 3H_2O$.

For the kinetics with 5 mol% $V(acac)_3/Cu(NO_3)_2 \cdot 3H_2O$ the yields after 0.5 h and 1.0 h were determined in order to calculate the rate constant for the initial 4 h (Figure II.10). After making the approximation that the degradation of **3aE** followed a first order decay, the formula for integrated first order kinetics was used:

$$\ln[A]_t = -kt + \ln[A]_0$$

The rate constant $-k$ was obtained after plotting $\ln([A]_t/[A]_0)$ versus the reaction time t (Figure II.11). Accordingly, the rate constant k for the degradation of dilignol **3aE** within the first 4 h was 0.53 h^{-1} . Despite the high rate constant a reaction time of 20 h was needed to reach full conversion. The yield for acid **17** during that time increased almost linearly with a yield of 62% after 20 h. Compared to 10 mol% and 20 mol% $V(acac)_3/Cu(NO_3)_2 \cdot 3H_2O$, the yield for acid **17** was slightly higher after 17 h with 56%. The yield for aldehyde **5** after 17 h was almost identical for 5 mol% and 10 mol% $V(acac)_3/Cu(NO_3)_2 \cdot 3H_2O$ with 31% and 30%, respectively.

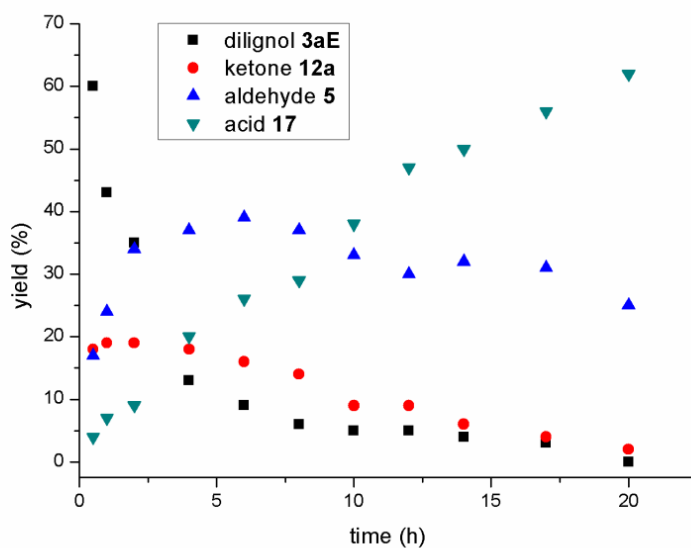


Figure II.10. Reaction kinetics for 3aE using 5 mol% of $V(acac)_3/Cu(NO_3)_2 \cdot 3H_2O$.

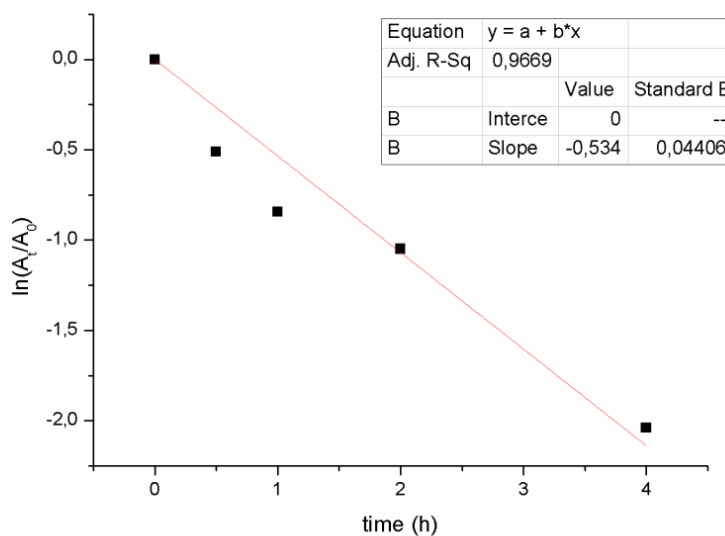


Figure II.11. Rate constant $-k$ for the first 4 h with 5 mol% of $V(acac)_3/Cu(NO_3)_2 \cdot 3H_2O$.

In part 5.2 of this chapter it was mentioned that $V(acac)_3/Cu(NO_3)_2 \cdot 3H_2O$ was also very active with lower catalyst loadings. **3aE** was converted to 97% with 2.5 mol% $V(acac)_3/Cu(NO_3)_2 \cdot 3H_2O$ after 17 h. This conversion was identical to the one with 2.5 mol% $V(acac)_3$ and 1.0 mol% $Cu(NO_3)_2 \cdot 3H_2O$ after the same reaction time. However, a difference in selectivity was observed between these two reaction conditions. As previously reported 2.5 mol% $V(acac)_3$ and 1.0 mol% $Cu(NO_3)_2 \cdot 3H_2O$ afforded veratric acid (**17**) and veratraldehyde (**5**) in 39% and 26% yield, respectively. 2.5 mol% of $V(acac)_3/Cu(NO_3)_2 \cdot 3H_2O$ furnished acid **17** in 53% and aldehyde **5** in 35% yield (Figure II.12). Despite the low activity of $Cu(NO_3)_2 \cdot 3H_2O$ by itself (see Figure II.15), increasing its loading from 1.0 mol% to 2.5 mol% helped raise the selectivity towards the cleavage products veratric acid (**17**) and

veratraldehyde (**5**) from 67% to 91%. The rate constant k for the degradation of dilignol **3aE** within the first 4 h was 0.45 h^{-1} and therefore slightly lower than with a catalyst loading of 5 mol%.

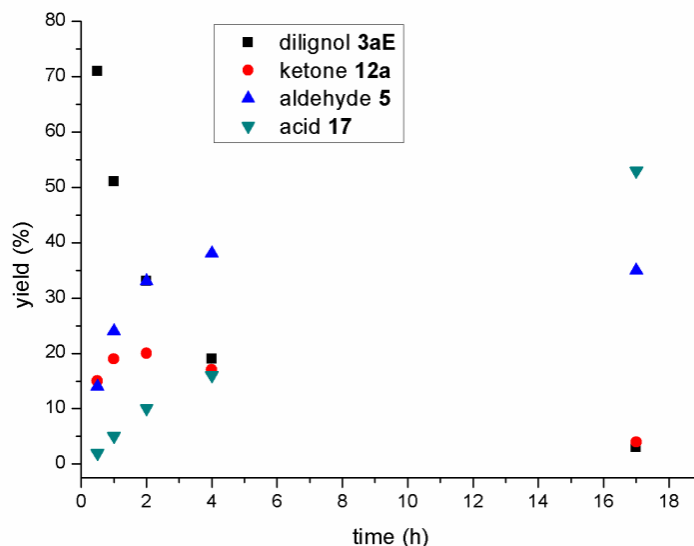


Figure II.12. Reaction kinetics for **3aE** using 2.5 mol% of $\text{V}(\text{acac})_3/\text{Cu}(\text{NO}_3)_2 \cdot 3\text{H}_2\text{O}$.

To extend the scope of the kinetic investigation the initial kinetics and rate constants for 5.0 mol% and 2.5 mol% of $\text{V}(\text{acac})_3$ were determined (Figure II.13 and Figure II.14). Table II.32 summarizes the rate constants for all homogeneous reaction systems. The rate constant for the degradation of **3aE** within the first 4 h with 5 mol% $\text{V}(\text{acac})_3$ was 0.40 h^{-1} and therefore lower than with 2.5 mol% $\text{V}(\text{acac})_3/\text{Cu}(\text{NO}_3)_2 \cdot 3\text{H}_2\text{O}$. These observations were a little surprising considering that vanadium is primarily responsible for the catalytic activity when evaluating the two metals individually. A combined effect of $\text{V}(\text{acac})_3$ together with $\text{Cu}(\text{NO}_3)_2 \cdot 3\text{H}_2\text{O}$ appears to occur which leads to a noticeably higher rate constant than what the sum of the individual rate constant for $\text{V}(\text{acac})_3$ and $\text{Cu}(\text{NO}_3)_2 \cdot 3\text{H}_2\text{O}$ would suggest. Accordingly, the rate constant with 2.5 mol% $\text{V}(\text{acac})_3$ during the first 4 h of the reaction was 0.32 h^{-1} and therefore lower than with 2.5 mol% $\text{V}(\text{acac})_3/\text{Cu}(\text{NO}_3)_2 \cdot 3\text{H}_2\text{O}$. The yield for acid **17** after 17 h with 5 mol% $\text{V}(\text{acac})_3$ was the same as for 5 mol% $\text{V}(\text{acac})_3/\text{Cu}(\text{NO}_3)_2 \cdot 3\text{H}_2\text{O}$ with 56%. Again the yields for aldehyde **5** differed more strongly from each other with 17% and 31%, respectively. When employing 2.5 mol% $\text{V}(\text{acac})_3$ the yields for acid **17** and aldehyde **5** after 17 h were 39% and 15% which were both lower than with 2.5 mol% $\text{V}(\text{acac})_3/\text{Cu}(\text{NO}_3)_2 \cdot 3\text{H}_2\text{O}$.

Table II.32: Rate constants k for the degradation of **3aE** within the first 4 h of reaction.^[a]

$\text{V}(\text{acac})_3$ [mol%]	$\text{Cu}(\text{NO}_3)_2 \cdot 3\text{H}_2\text{O}$ [mol%]	rate constant k [h^{-1}]
5.0	5.0	0.53
2.5	2.5	0.45

5.0	-	0.40
2.5	-	0.32
-	5.0	0.01

[a] Reaction conditions: **3aE** (0.25 mmol), V(acac)₃, Cu(NO₃)₂·3H₂O, pyridine (1.25 mL), O₂ (5 bar), 135 °C, 600 rpm.

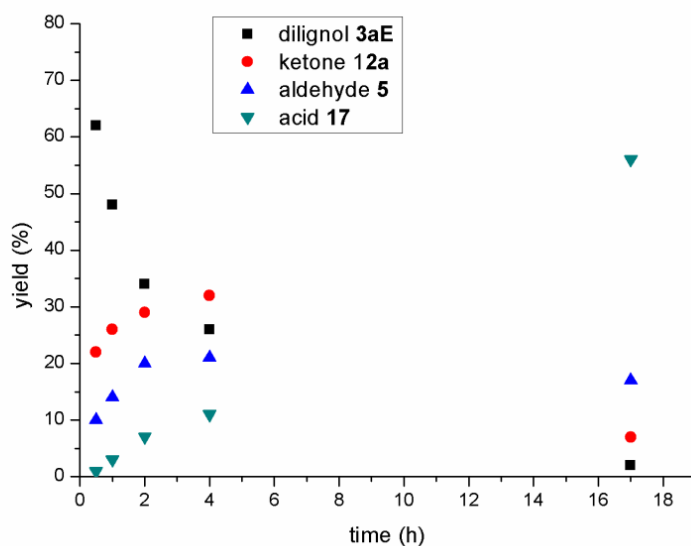


Figure II.13. Reaction kinetics for **3aE** using 5 mol% of V(acac)₃.

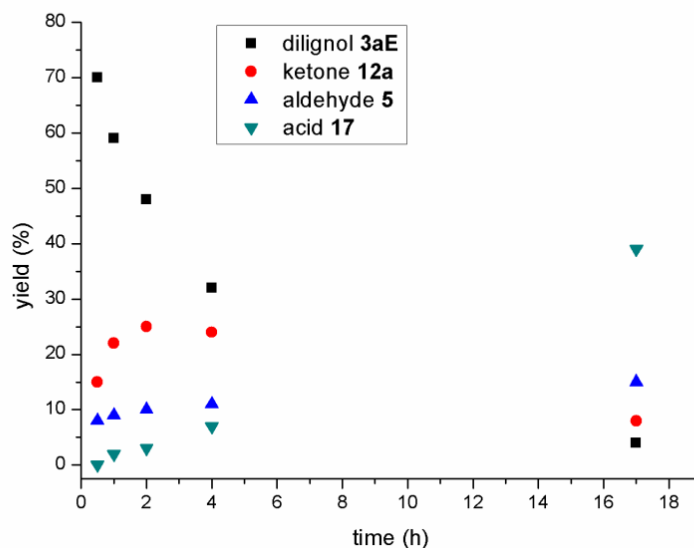


Figure II.14. Reaction kinetics for **3aE** using 2.5 mol% of V(acac)₃.

For a final comparison the initial kinetics and rate constants for 5 mol% Cu(NO₃)₂·3H₂O were determined. As alluded to earlier Cu(NO₃)₂·3H₂O was not very active by itself. In order to provide a comparison with the previously described reaction systems the rate constant within

the first 4 h of the reaction was calculated for first order kinetics, obtaining a value of 0.01 h^{-1} . Realistically, however, the reaction of $\text{Cu}(\text{NO}_3)_2 \cdot 3\text{H}_2\text{O}$ follows zero order kinetics. After 17 h only 21% of **3aE** had been converted. Aldehyde **5** and acid **17** were both obtained in 4% yield.

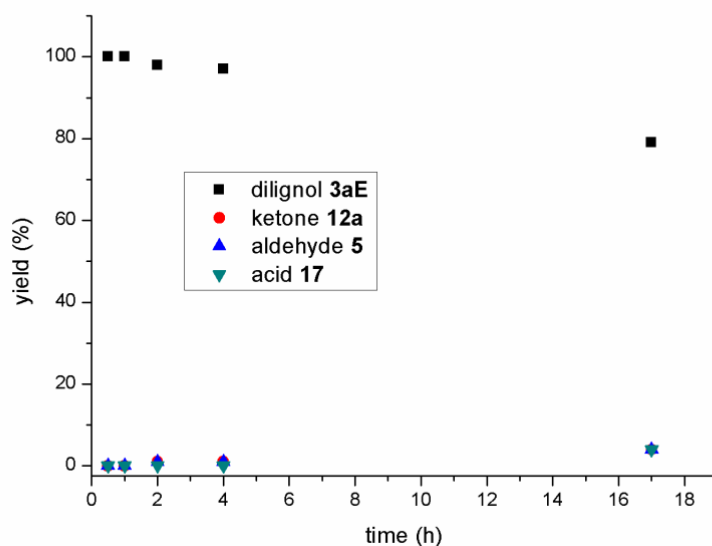


Figure II.15. Reaction kinetics for **3aE** using 5 mol% $\text{Cu}(\text{NO}_3)_2 \cdot 3\text{H}_2\text{O}$.

To also gain a better understanding of the HTc-Cu-V catalyzed reaction system kinetic studies were performed for both dilignol **3aE** and ketone **12a**. In both kinetic studies 20 wt% of HTc-Cu-V were employed with 5 bar of dioxygen pressure at a reaction temperature of $135 \text{ }^\circ\text{C}$. The obtained yields and rate constants cannot be compared in a direct manner with the previous kinetic investigations because they were performed in 20 mL steel autoclaves instead of 25 mL glass autoclaves. The smaller reactor volume led to slightly higher pressures during the reaction which is why the reactions in the steel autoclave proceeded marginally faster than in the glass autoclave. The general trend, however, is very much comparable.

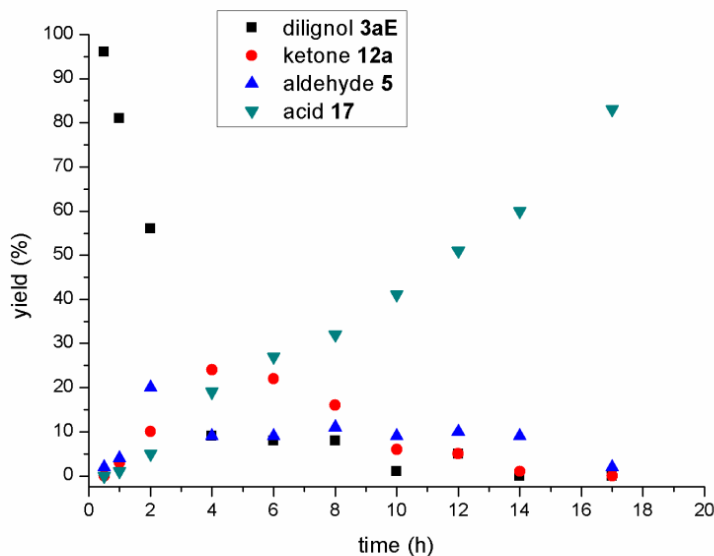


Figure II.16. Reaction kinetics for 3aE using 20 wt% HTc-Cu-V in a steel autoclave.

Figure II.16 shows the kinetics for dilignol **3aE**. Within the first 2 h of the reaction with HTc-Cu-V the conversion of **3aE** proceeded markedly slower than with all the homogeneous reaction systems apart from $\text{Cu}(\text{NO}_3)_2 \cdot 3\text{H}_2\text{O}$. Accordingly, the initial rate constant within the first 2 h of the reaction is quite low with 0.26 h^{-1} . But when taking into account the first 4 h of the reaction, the rate constant doubles to 0.52 h^{-1} . In part 5.2 it was shown that a continuous release of homogeneous copper species and a fast initial leaching of homogeneous vanadium species by HTc-Cu-V occurred. The increase in the rate constant from 2 h to 4 h can therefore most likely be attributed to the catalytic activity of the leached homogeneous copper and vanadium species that are then present in sufficient concentration in the reaction solution to significantly accelerate the progression of the reaction. The early reactivity within the first 2 h probably stems from the heterogeneous catalyst that is less active than the homogeneous species.

The evolution of the reaction products over time was very similar to the homogeneous systems. Ketone **12a** was formed at the beginning of the reaction reaching its maximum yield after 4 h in 24% yield. After reaching its maximum, **12a** was slowly consumed over the course of the reaction. Aldehyde **5** also had an early maximum after 2 h with 20%. Between a reaction time of 4 h and 14 h the yield remained almost constant around 10% before decreasing at the very end. The yield for acid **17** increased more or less linearly during the entire reaction similar to the kinetics with 5 mol% $\text{V}(\text{acac})_3/\text{Cu}(\text{NO}_3)_2 \cdot 3\text{H}_2\text{O}$. The 83% yield of acid **17** after 17 h is most likely an outlier as the HPLC yields for veratric acid with yields higher than 50% were subject to a greater variance than with other products. The general credibility of the yields determined by HPLC had been previously established in the homogeneous kinetics where the highest yields for veratric acid were confirmed by yields after column chromatography.

In the kinetics of dilignol **3aE** with both the homogeneous catalysts and HTc-Cu-V it was seen that ketone **12a** was formed initially as a product in over 20% yield before being

consumed over longer reaction times. The kinetics for ketone **12a** were determined to verify whether it acted as an intermediate product that was subsequently cleaved to veratric acid or veratraldehyde. Figure II.17 shows that ketone **12a** was converted following a first order decay. Furthermore, acid **17** was almost exclusively formed as product. The yield for veratric acid increased almost linearly before reaching a plateau after 10 h. The yield between 10 h and 17 h remained almost constant at about 70%. Aldehyde **5** on the other hand was only formed in minute quantities and its yields stayed between 1% and 2% over the entire reaction. The initial rate constant within the first 4 h of the reaction was 0.19 h^{-1} . The comparison of the rate constants shows that the conversion of ketone **12a** proceeds markedly slower than the conversion of dilignol **3aE**. When the conversion of **12a** was monitored by ^1H NMR it was seen that only trace amounts of enol ether enone **15** were formed in this reaction.

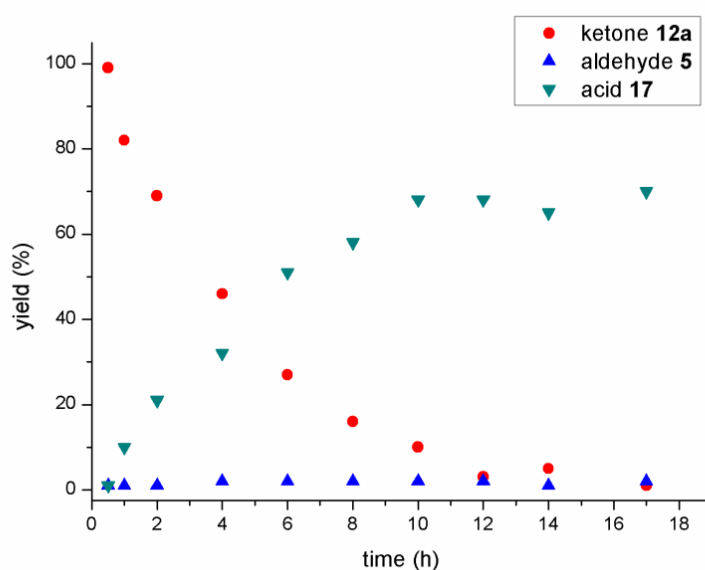
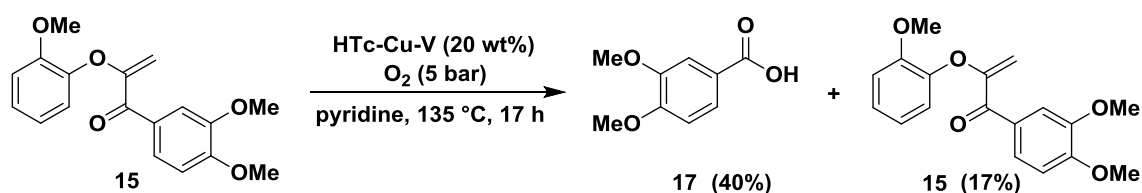


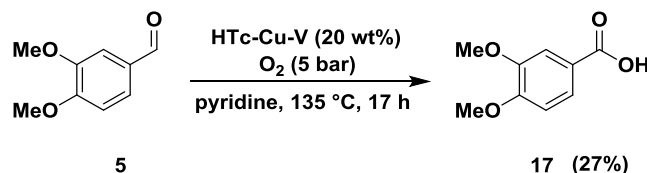
Figure II.17. Reaction kinetics for **12a** using 20 wt% HTc-Cu-V in a steel autoclave.

After proving that ketone **12a** is a key intermediate in the formation of veratric acid (**17**) from dilignol **3aE** it was still of interest to see whether the cleavage products **17** and **5** were also formed from enol ether enone **15**, another side product in this reaction. Due to the limited stability of enol ether enone **15** at room temperature no kinetic studies were performed with this substrate. After preparing it freshly from ketone **12a**, enol ether enone **15** was directly employed in a reaction on a 1.00 mmol scale with 20 wt% of HTc-Cu-V, 5 bar of dioxygen pressure at 135 °C and a reaction time of 17 h (Scheme II.24). Acid **17** was again the main product in 40% yield. The transformation of **15** was a bit more sluggish as 17% of **15** were reisolated and it proceeded less selectively with two other by-products being observed.



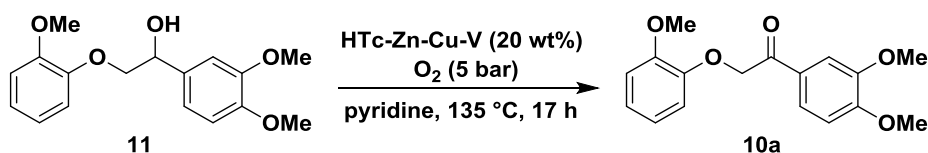
Scheme II.24. Cleavage of **15** with HTc-Cu-V on a 1.00 mmol scale in a steel autoclave.

Therefore, aldehyde **5** seems to be formed either directly by C–C bond cleavage from **3aE**, or through an unknown intermediate directly at the beginning of the reaction. To elucidate to what extent the over-oxidation of aldehyde **5** contributed to the yield of acid **17** another control experiment was performed (Scheme II.25). On a 1.00 mmol scale veratraldehyd (**5**) was set to react under the standard reaction condition with HTc-Cu-V as catalyst. After 17 h veratric acid (**17**) was isolated in 27% yield. This result confirms that over oxidation of aldehyde **5** to acid **17** indeed occurs but proceeds slowly.



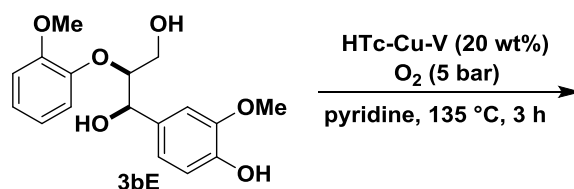
Scheme II.25. Oxidation of **5** with HTc-Cu-V on a 1.00 mmol scale in a glass autoclave.

The final mechanistic studies of this chapter investigated the influence when monolignol **11**, lacking the primary hydroxyl group (Scheme II.26) or dilignol **3bE**, containing a phenolic moiety, were employed as substrates (Scheme II.27).



Scheme II.26. Cleavage of monolignol **11** with HTc-Zn-Cu-V.

Under the standard reaction conditions monolignol **11** was significantly less reactive. After 17 h a product factor of only 15 was obtained (determined by $^1\text{H-NMR}$) and the corresponding ketone **10a** was the main product while almost no cleavage products were observed. This implies that the primary hydroxyl group is very important for the different oxidation and cleavage pathways. However, since the structural motif of the monolignol **11** is not present in natural lignin it does not represent a limitation for applications in the natural polymer.



Scheme II.27. Cleavage of dilignol **3bE** with HTc-Cu-V.

When dilignol **3bE** was utilized as starting material with HTc-Cu-V as catalyst, after 3 h complete conversion was already achieved. The reaction, however, was far less selective leading to a large mixture of different products. Therefore in future applications lignin sources should be used with a lower content of phenolic moieties.

5.4. Lignin cleavage studies

After studying model based systems it was investigated whether these results would translate to extracted lignin sources. In the lignin cleavage studies two different organosolv beech lignin and two different kraft lignin sources were utilized. The first organosolv beech lignin (MPI lignin) had been extracted from beech wood chips at the MPI für Kohlenforschung, Mülheim a.d.R., Germany, by Stiefel and Roth (both Aachener Verfahrenstechnik) using an organosolv process with ethanol/water = 50/50 without the addition of an acid catalyst. The second organosolv beech lignin (HH lignin) was also extracted from beech wood chips using an organosolv process with ethanol/water = 50/50 without the addition of an acid catalyst and was supplied by Puls from the Institut für Holztechnologie und Holzbiologie, Hamburg, Germany. Both kraft lignin #471003 and kraft lignin #370959 were purchased from Sigma Aldrich.

The initial optimization experiments were performed with MPI and HH lignin. The cleavage of the characteristic bonds within lignin was monitored by HSQC 2D-NMR. The signals for the different lignin linkages were assigned with the help of an article by Sun and co-workers.^[74] Using 100 mg of the corresponding lignin source the reactions were performed at 135 °C with 5 bar of dioxygen pressure in 1.5 mL deuterated pyridine and 20 wt% HTc-Zn-Cu-V for 14 h. In both MPI lignin and HH lignin over 90% of the β -O-4 linkages were degraded.

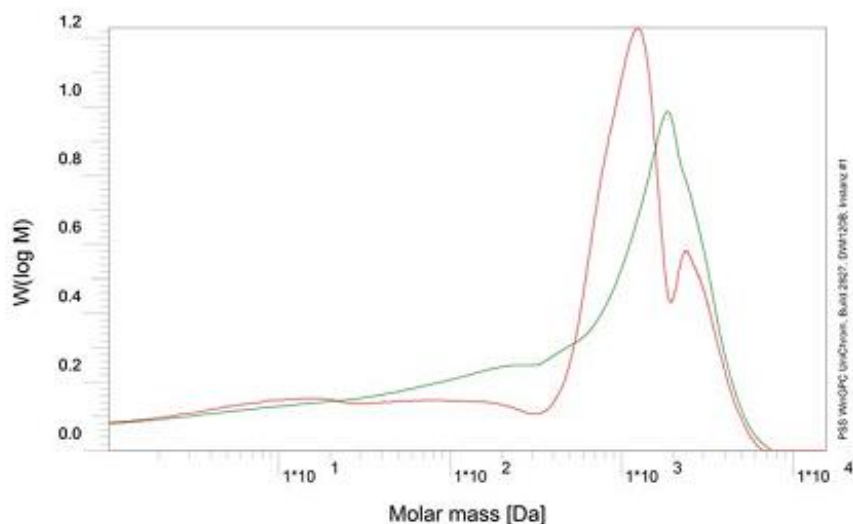


Figure II.18. Mass distribution of HH lignin before (red) and after 14 h with 20 wt% of HTc-Zn-Cu-V (green).

GPC measurements revealed that despite the significant degradation of the β -O-4 linkages the mass maximum actually shifted to slightly higher masses. Figure II.18 presents the mass distribution of HH lignin. In red is shown the mass distribution before the reaction and in green after the reaction. In all the GPC measurements discussed in this dissertation the detector response of the RI-detector was used. The GPC elugrams were recorded with 0.1 M hydrogen phosphate dibasic (Na_2HPO_4) and 0.5 g polyethylene glycol 6000 (PEG) at a pH of

12 in HPLC grade water as eluent because it provided a significantly better solubility of all product fractions than any standard organic solvent. The external calibrations for the mass distributions were performed with polystyrenesulfonate standards. These external calibrations are always subject to a certain mass deviation because even the more branched polystyrenesulfonate standards cannot provide an entirely exact mass for the very heterogeneous lignin polymers.

After these initial results the amount of pyridine for the 100 mg lignin reactions was increased from 1.5 mL to 4.5 mL ensuring a better solubilization of the lignin sources. Furthermore the dioxygen pressure was increased to 10 bar and the reaction time extended to 40 h. The HSQC spectra for MPI lignin, HH lignin and kraft lignin #370959 displaying the chemical shifts for the characteristic ether and alcohol bonds are shown in Figure II.19 to Figure II.21.

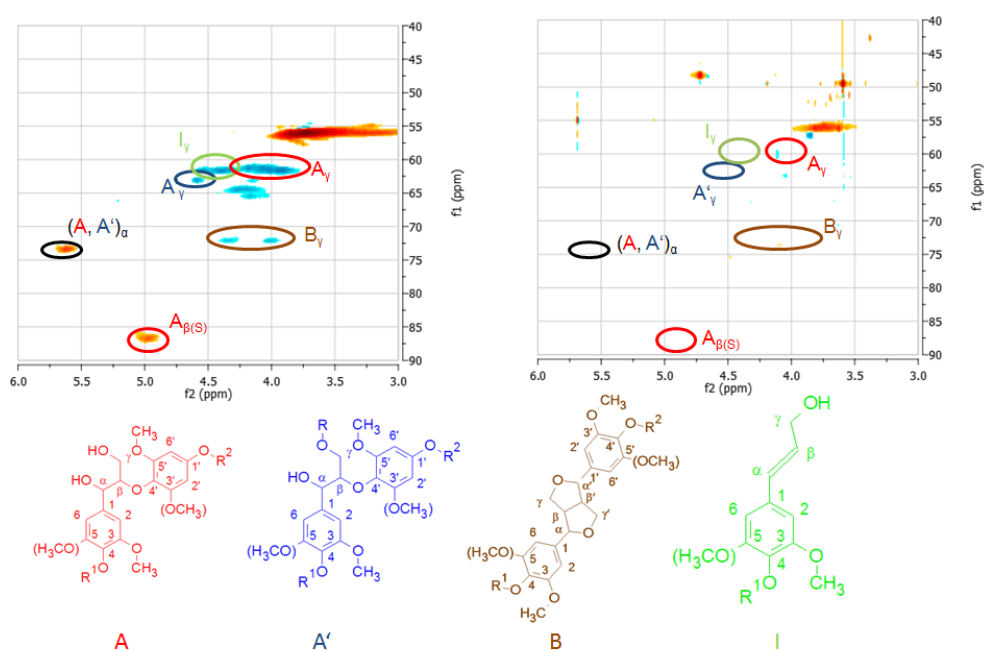


Figure II.19. Comparison of MPI lignin before (left) and after the reaction with HTc-Cu-V as catalyst after 40 h (right).

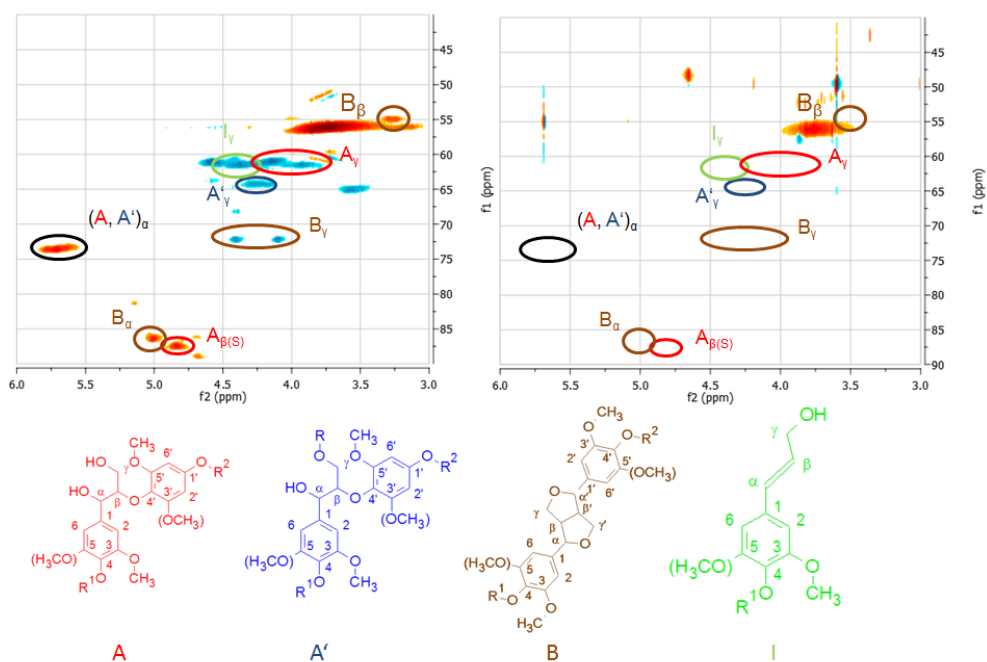


Figure II.20. Comparison of HH lignin before (left) and after the reaction with HTc-Cu-V as catalyst after 40 h (right).

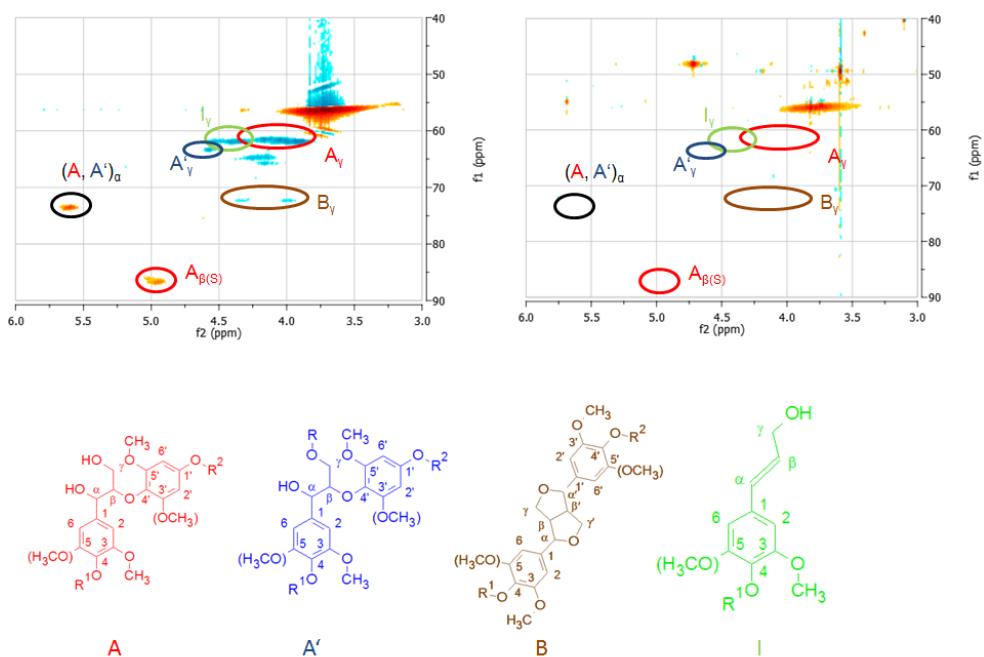


Figure II.21. Comparison of kraft lignin #370959 before (left) and after the reaction with HTc-Cu-V as catalyst after 40 h (right).

In all three lignin sources the characteristic signals for the β -O-4 and the protected β -O-4 linkages as well as the resinol structures and *p*-hydroxycinnamyl alcohols had disappeared after the reaction meaning that all of these linkages had been completely degraded. The cleavage of the resinol structure in its entirety is of special note because the here described transition metal catalysts are the first to achieve this with dioxygen as oxidant. Studies by Kleine *et al.* and Westwood and co-workers have shown that the resinol structures are a more

prominent linkage in pretreated lignin sources than previously assumed.^[75,76] The HSQC of kraft lignin #471003 is not shown because it does not contain any β -O-4 linkages to begin with due the harsher pretreatment conditions. To see whether the degradation of these prominent lignin bonds also led to depolymerization, further GPC measurements were conducted.

The GPC measurements for MPI lignin, HH lignin, kraft lignin #370959 and kraft lignin #471003 revealed that with a dioxygen pressure of 10 bar and a reaction time of 40 h significant depolymerization had occurred. In red are again shown the mass distribution before the reaction and in green the mass distribution after the reaction. For HH lignin the mass maximum shifted from around 1400 Da to about 300 Da (Figure II.22). This mass corresponds to dimer sized products. To a minor degree also the formation of products with a mass of 4000 Da to 6000 Da was observed. However, if these were indeed polymerization products or just agglomerates of lower mass products could not be answered with final certainty.

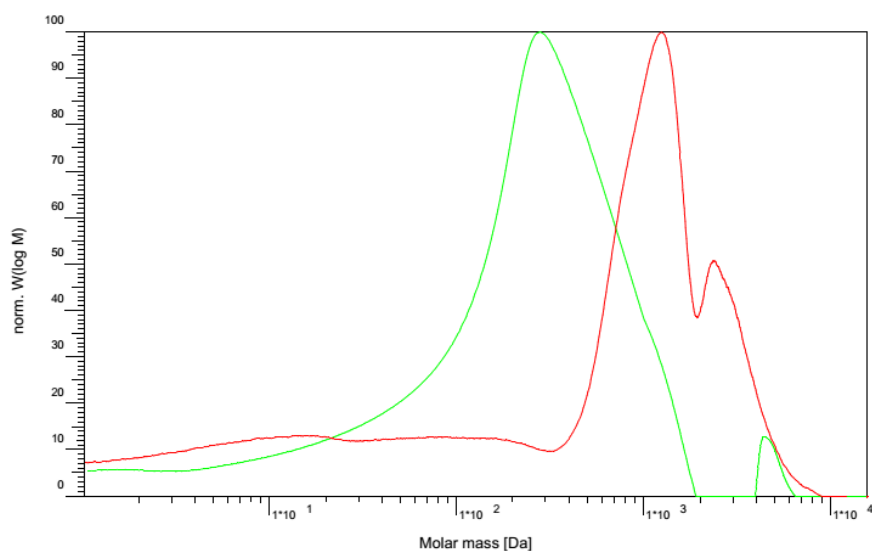


Figure II.22. Mass distribution of HH lignin before (red) and after 40 h with HTc-Cu-V (green).

The same kind of depolymerization behavior was observed for the other three lignin sources independently of whether they had been extracted by an organosolv or kraft process (Figure II.23 to Figure II.25). This is noteworthy because especially in kraft lignin significant amounts of impurities are present that frequently have a detrimental effect on transition metal catalysts. The mass maxima that are discussed in the following always refer to the mass maximum of the actual polymer. Due to the pretreatment MPI lignin and kraft lignin #471003 already contained some lower mass fractions. In all the lignin samples the mass maximum shifted from 1200 Da and 1500 Da to about 300 Da or lower. For kraft lignin #471003 these results are especially striking because no β -O-4 linkages had been observed in the HSQC. Which kind of bonds had been cleaved in kraft lignin #471003 could unfortunately not be assigned. For the other three lignin sources 75% to 86% of the original mass could be isolated as products after the reaction. Due to the poor solubility of kraft lignin #471003 in pyridine only 30% of its original mass was isolated as products.

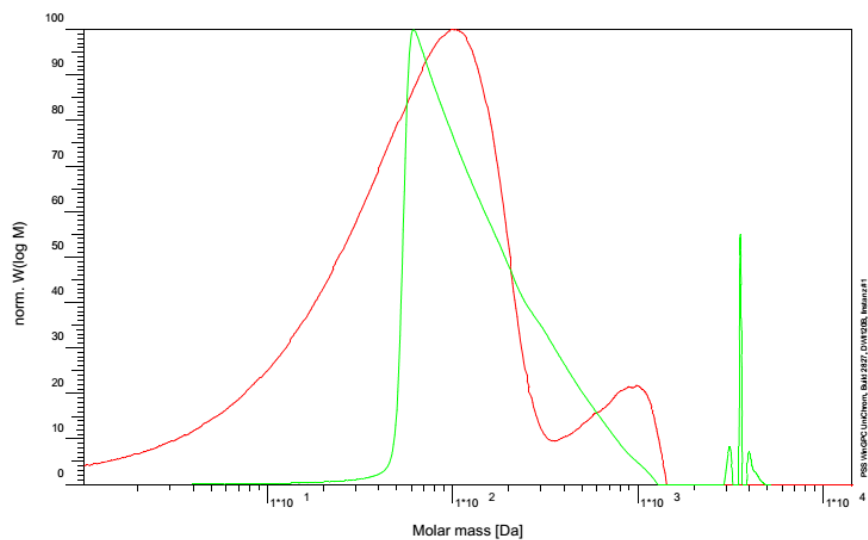


Figure II.23. Mass distribution of MPI lignin before (red) and after 40 h with HTc-Cu-V (green).

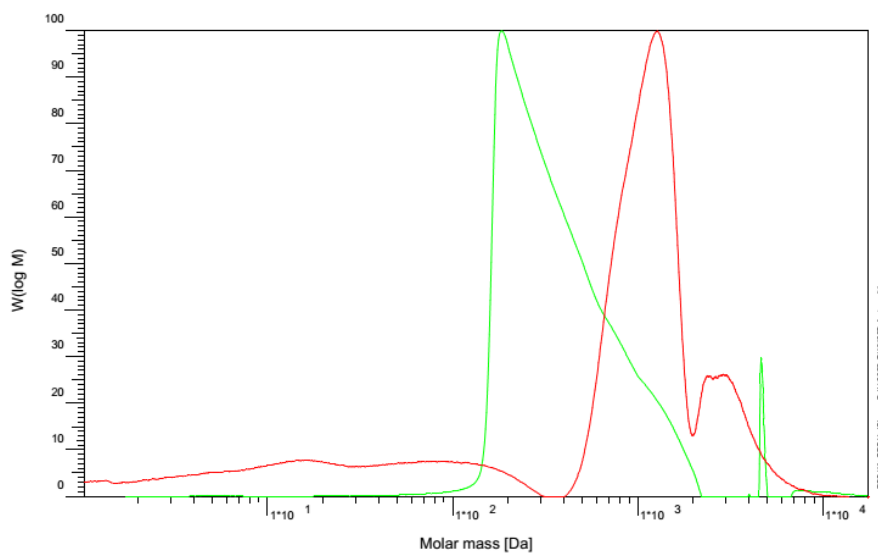


Figure II.24. Mass distribution of kraft lignin #370959 before (red) and after 40 h with HTc-Cu-V (green).

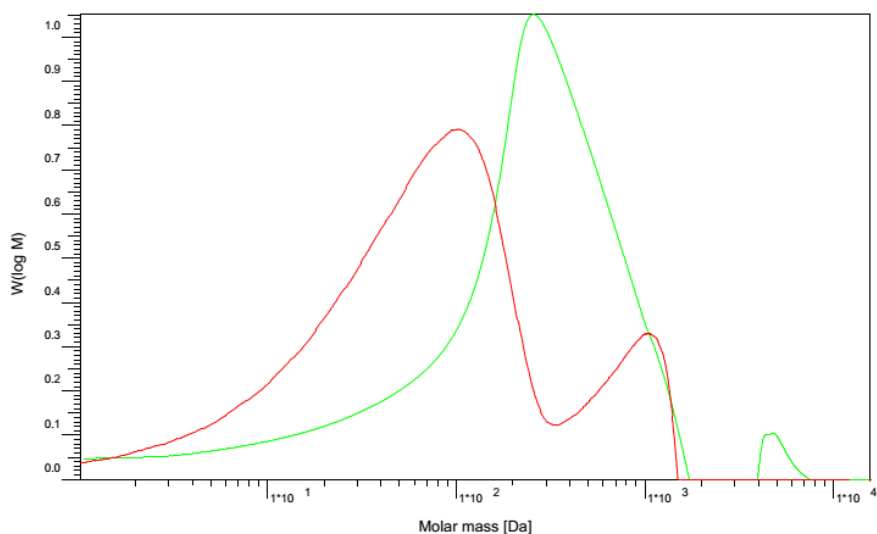


Figure II.25. Mass distribution of kraft lignin #471003 before (red) and after 40 h with HTc-Cu-V (green).

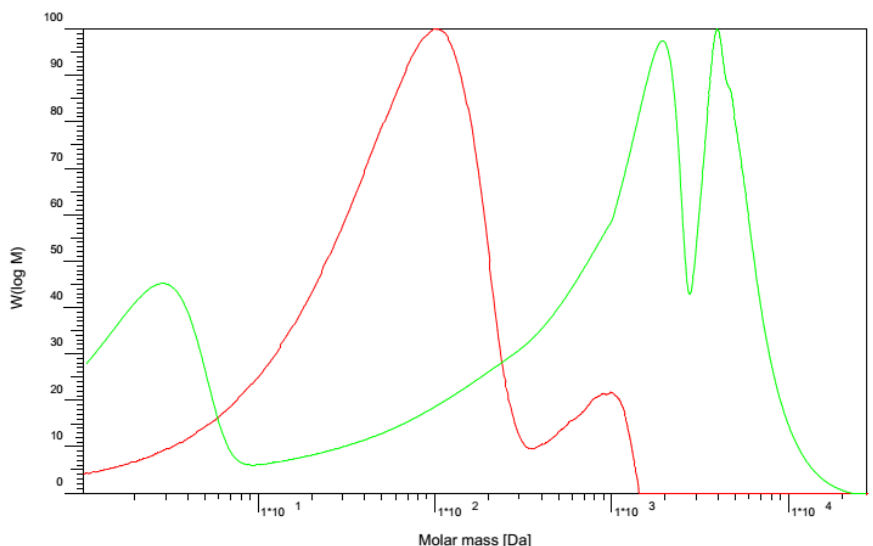


Figure II.26. Mass distribution of MPI lignin before (red) and after 40 h reaction without catalyst (green).

To validate the importance of the catalyst for the depolymerization a control experiment was conducted without catalyst (Figure II.26). The omission of the catalyst enhanced the formation of higher mass products with the mass maximum shifting to about 4000 Da.

Elemental analysis of the reaction products from MPI lignin, HH lignin and kraft lignin #370959 showed a decrease in the carbon and the hydrogen content when compared to the starting material, indicating the formation of higher oxidized products. The ¹³C NMR of MPI lignin exhibited two distinct signals at 173.5 ppm and 164.0 ppm that most likely belong to carbonyl carbons of carboxylic acids (Figure II.27). This and the results of the previous model compound studies support the hypothesis that predominantly carboxylic acids were formed as products.

II. Results and Discussion

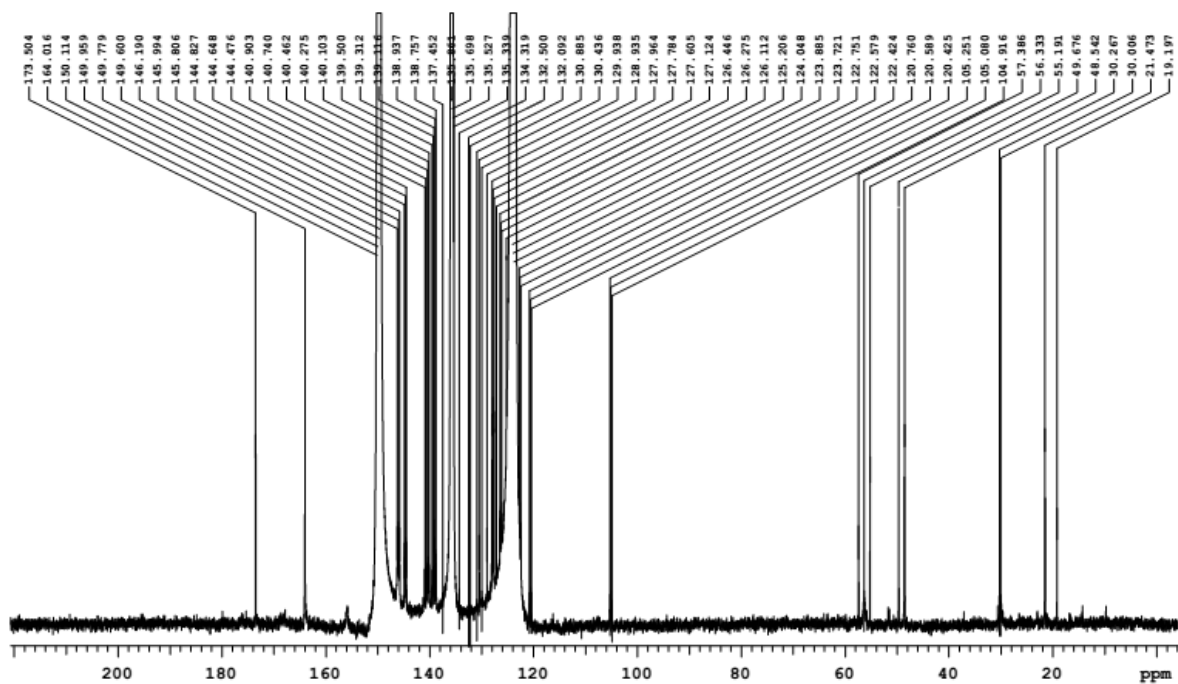


Figure II.27. ^{13}C NMR spectrum of MPI lignin after 40 h with HTc-Cu-V as catalyst.

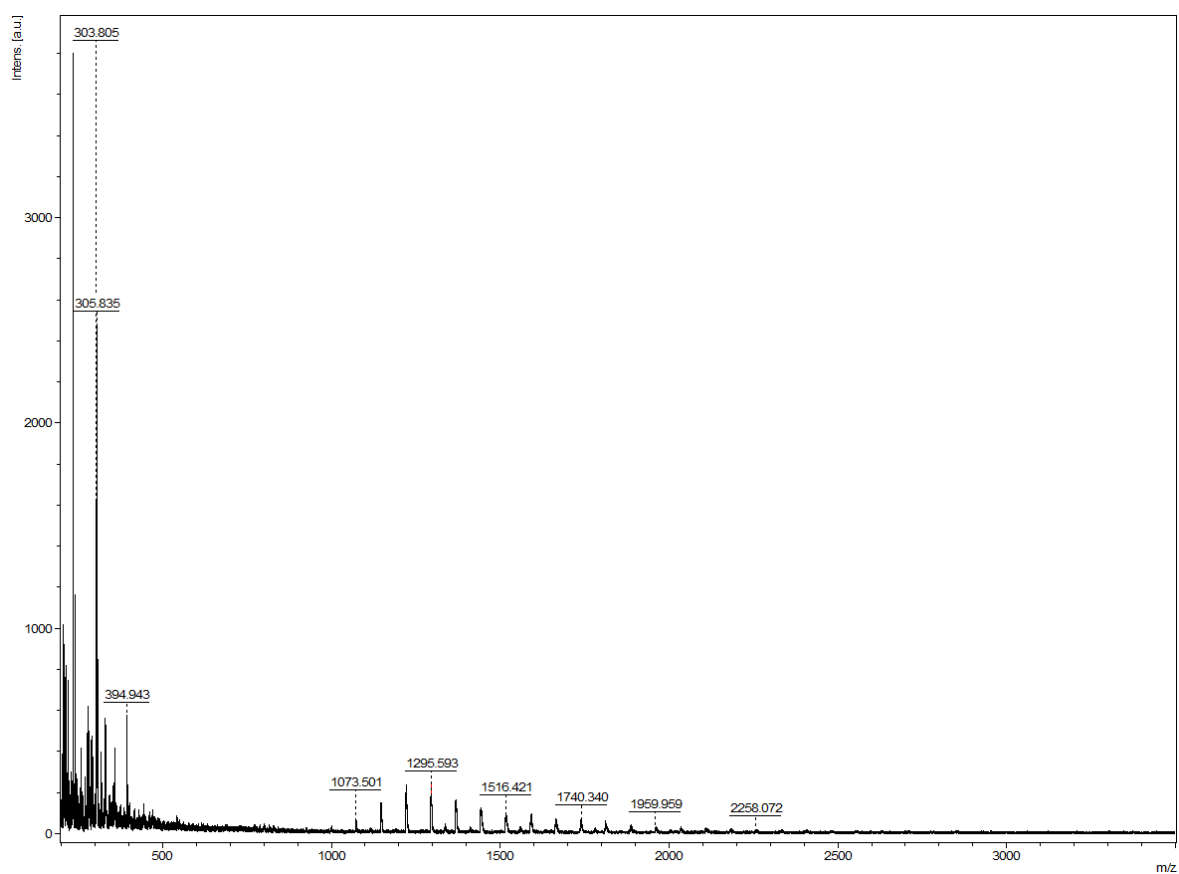


Figure II.28. MALDI spectrum of kraft lignin #370959 with matrix.

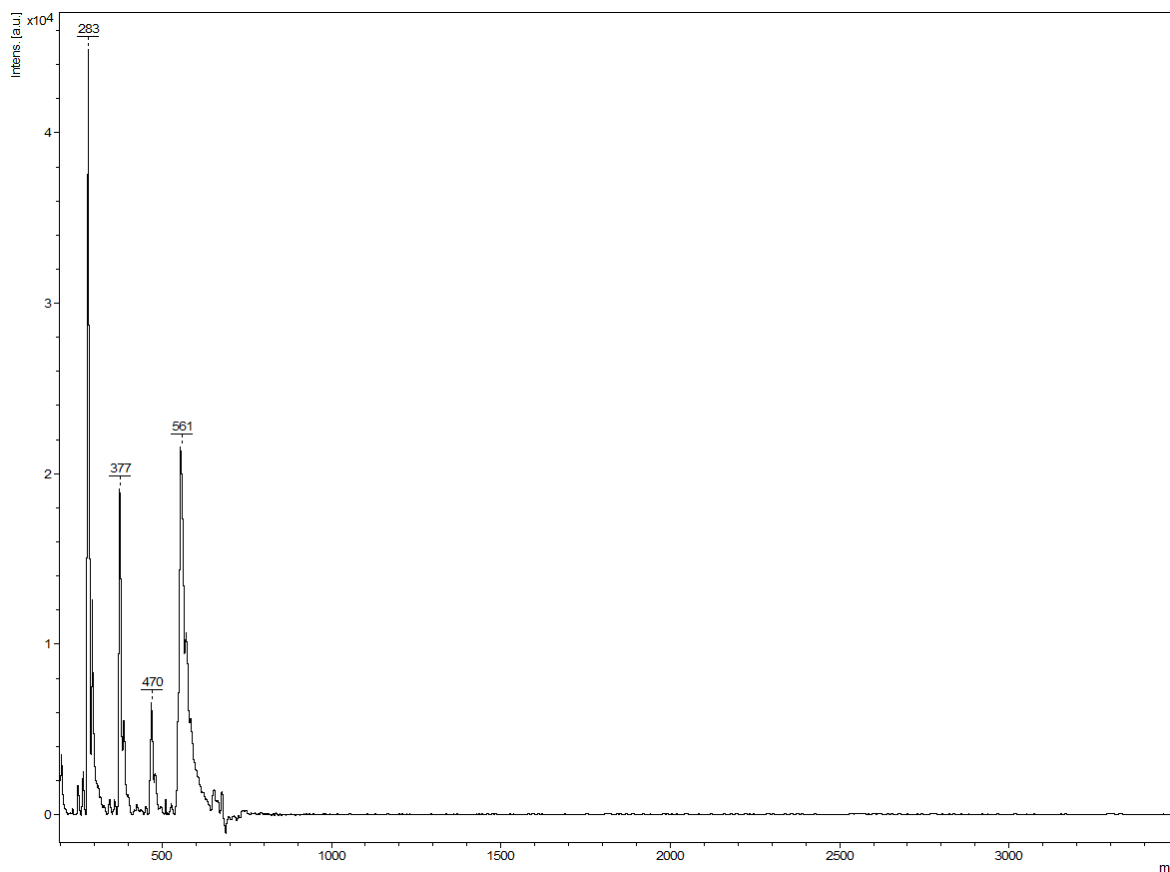


Figure II.29. MALDI spectrum of kraft lignin #370959 with matrix after 40 h with HTc-Cu-V.

To further validate the depolymerization of lignin with a second analytical method MALDI measurements were conducted of lignin before and after the reaction. Figure II.28 shows the MALDI spectrum of kraft lignin #370959 and Figure II.29 the MALDI spectrum of kraft lignin #370959 after 40 h reaction with HTc-Cu-V as catalyst. Both spectra include signals of the matrix in which they were measured which is why masses of 300 Da and below are disregarded in this discussion due to the potential overlap of signals. Before the reaction kraft lignin #370959 had a mass of 1000 Da to 2500 Da. After the reaction only products with a mass between 300 Da and 700 Da were observed. Products with masses of 4000 Da to 6000 Da were not detected. This result does not exclude their formation because the employed MALDI method becomes less and less precise for molecules with masses higher than 3000 Da. Similar results were also obtained for MPI lignin with HTc-Cu-V as catalyst, confirming the previous results (the corresponding spectra are shown in the experimental part).

Next, it was investigated whether $V(\text{acac})_3/\text{Cu}(\text{NO}_3)_2 \cdot 3\text{H}_2\text{O}$ would also display similar reactivity in the cleavage of lignin as HTc-Cu-V. In the lignin cleavage reactions 5 wt% of $V(\text{acac})_3$ and 5 wt% of $\text{Cu}(\text{NO}_3)_2 \cdot 3\text{H}_2\text{O}$ were used with 10 bar of dioxygen at 135 °C for 40 h. In accordance to the previous results with HTc-Cu-V the HSQC of MPI lignin after the reaction revealed that all the β -O-4 and the protected β -O-4 linkages as well as the resinol structures and *p*-hydroxycinnamyl alcohols had been degraded (Figure II.30). GPC measurements of MPI lignin after the reaction showed the depolymerization of lignin to lower masses (Figure II.31). This depolymerization was once more reconfirmed by MALDI

II. Results and Discussion

measurements of MPI lignin before and after the reaction (Figure II.32 and Figure II.33). Before the reaction MPI lignin had a mass of 1000 Da to 3000 Da. After the reaction almost exclusively products of 300 Da to 800 Da were detected.

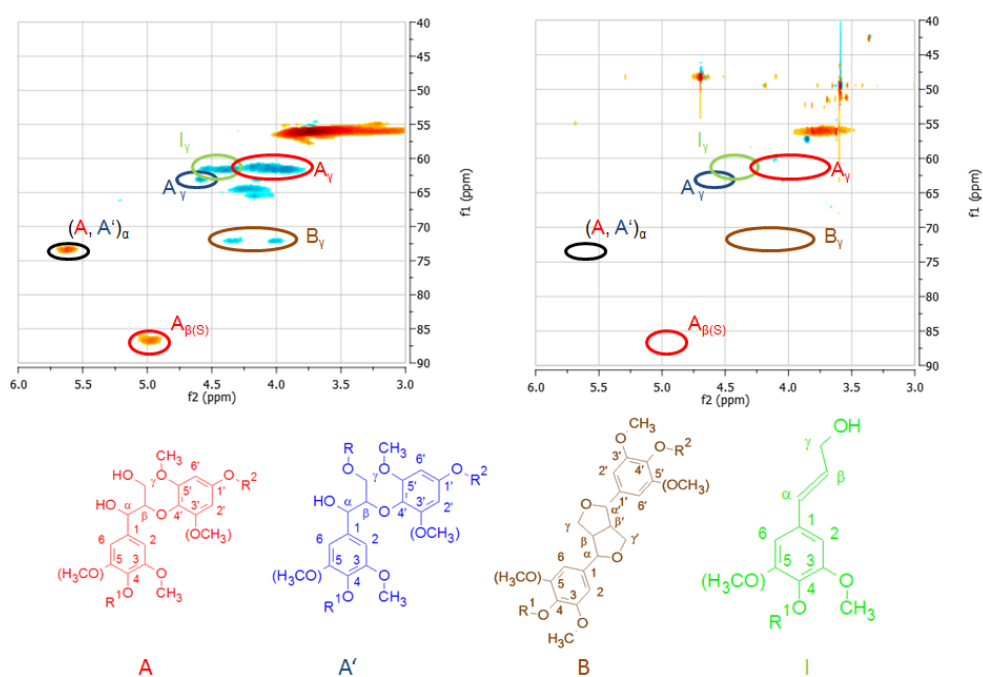


Figure II.30. Comparison of MPI lignin before (left) and after 40 h reaction with $V(acac)_3/Cu(NO_3)_2 \cdot 3H_2O$ as catalyst (right).

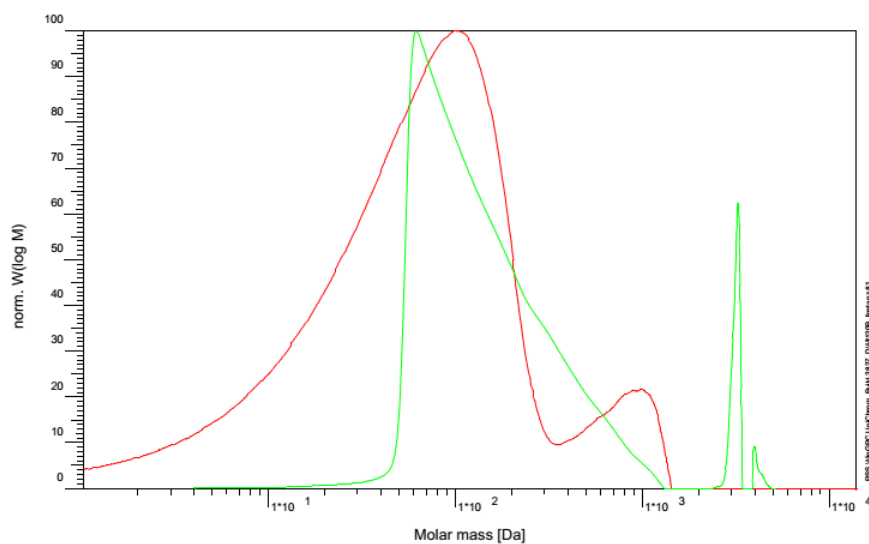


Figure II.31. Mass distribution of MPI lignin before (red) and after 40 h reaction with $V(acac)_3/Cu(NO_3)_2 \cdot 3H_2O$ as catalyst (green).

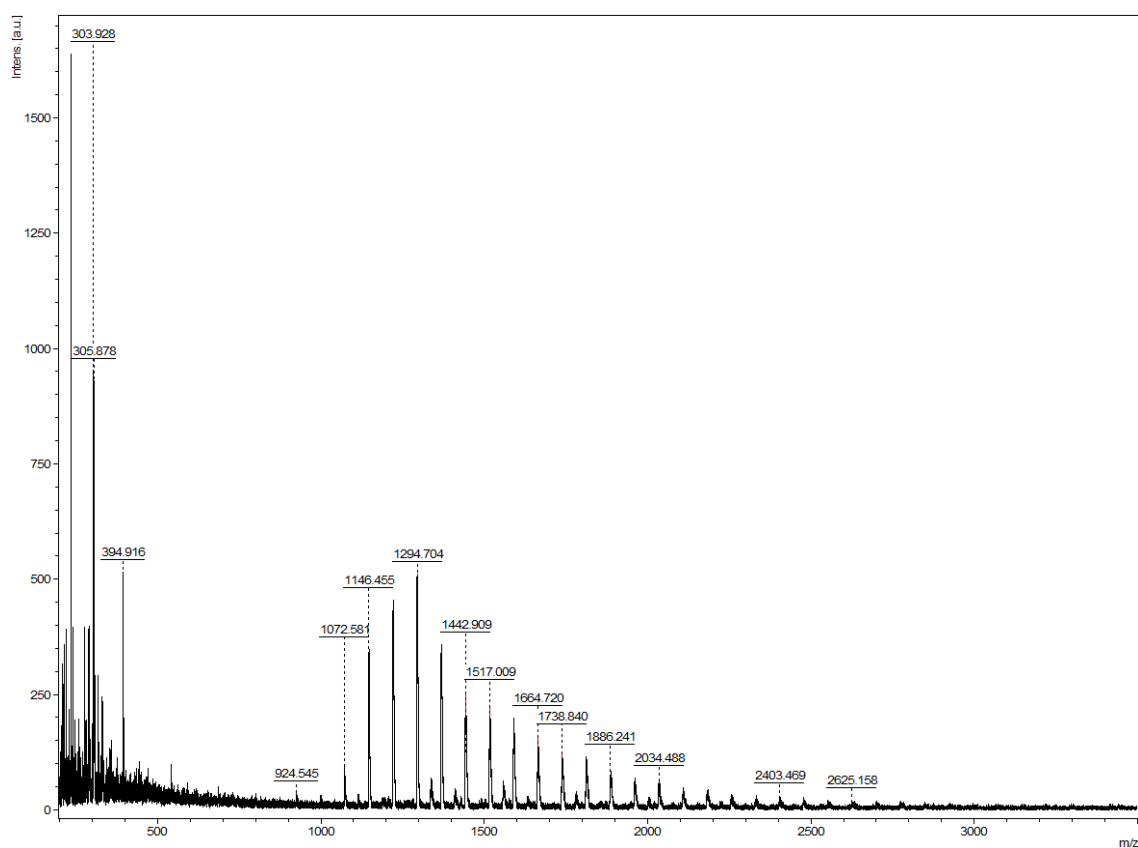


Figure II.32. MALDI spectrum of MPI lignin with matrix.

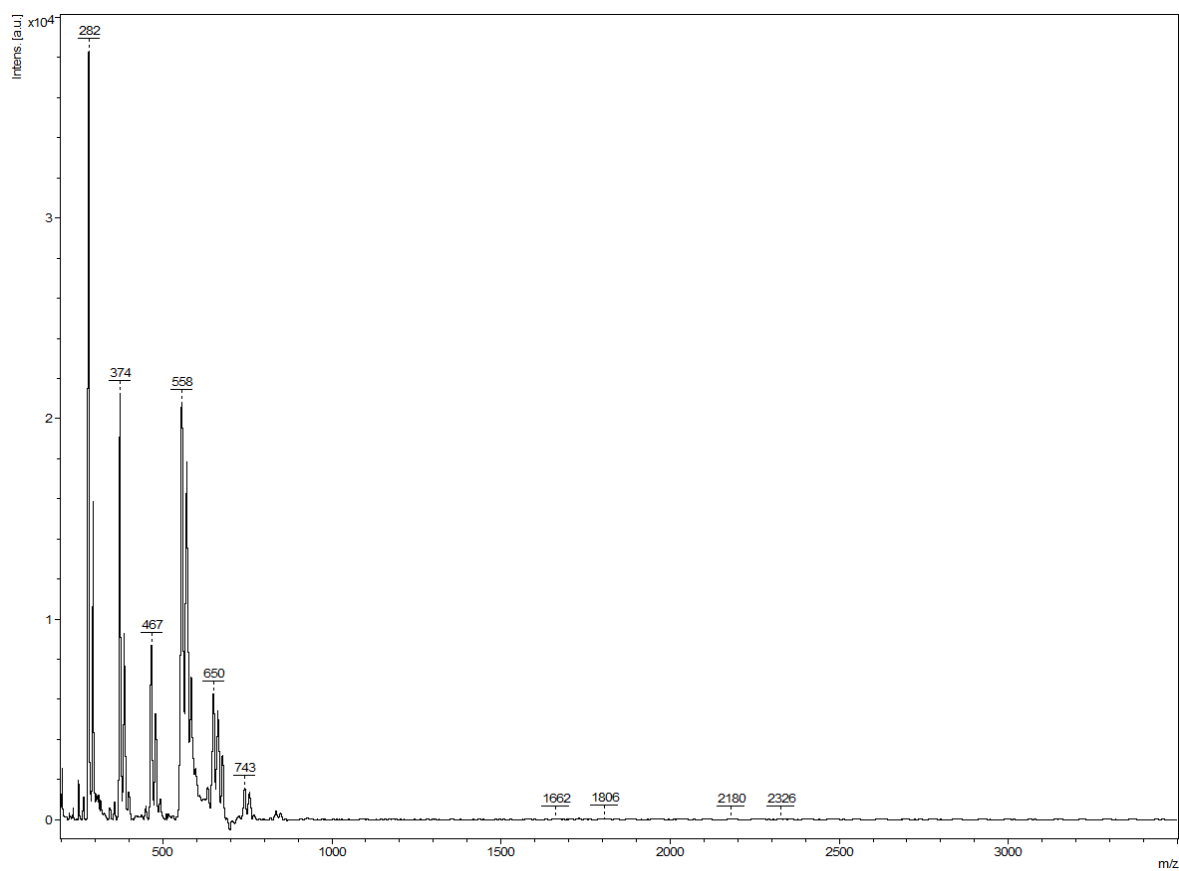


Figure II.33. MALDI spectrum of MPI lignin with matrix after 40 h reaction with $V(acac)_3/Cu(NO_3)_2 \cdot 3H_2O$.

In summary, both copper- and vanadium-containing hydrotalcite-like catalysts (HTc-Cu-V and HTc-Zn-Cu-V) and $V(acac)_3/Cu(NO_3)_2 \cdot 3H_2O$ displayed high activity and good selectivity for the oxidative cleavage of β -O-4 lignin model compound *erythro* dilignol **3aE**. The catalyst recyclability and stability of copper- and vanadium-containing hydrotalcite-like catalysts was investigated in detail and kinetic investigations for both $V(acac)_3/Cu(NO_3)_2 \cdot 3H_2O$ and HTc-Cu-V were conducted revealing a combined effect of copper together with vanadium enhancing the catalytic activity and selectivity. Studies with two different organosolv lignin and two kraft lignin sources showcased that both catalytic systems cleaved all of the β -O-4 and the protected β -O-4 linkages as well as the resinol structures and *p*-hydroxycinnamyl alcohols present in lignin, leading to dimer and trimer sized products.

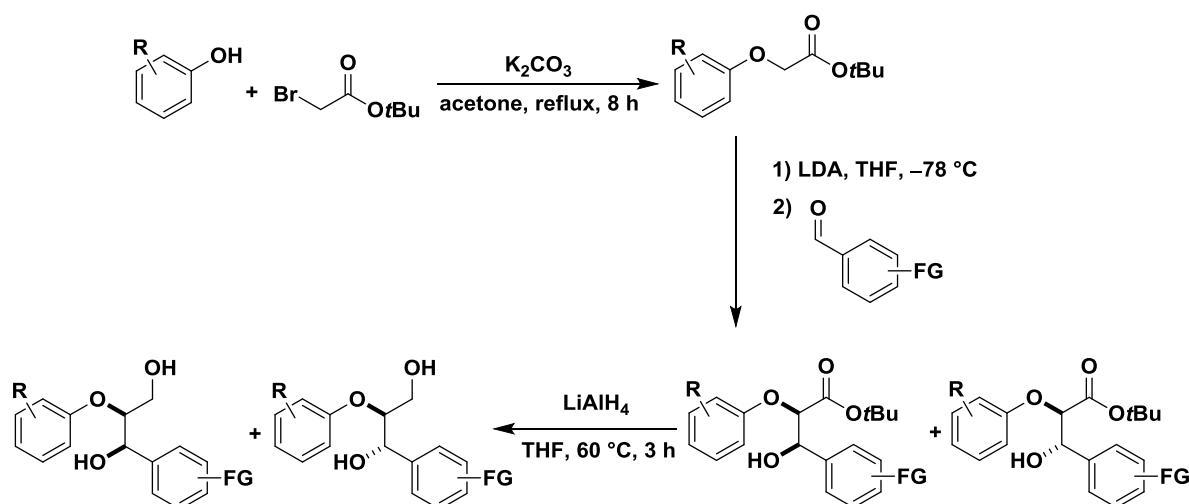
III. Summary and Outlook

1. Summary

Experimental results that were obtained with $\text{H}_2\text{Ru}(\text{CO})(\text{PPh}_3)_3$ as catalyst for the cleavage of monolignol **11** were not be discussed in this dissertation but have been published before.^[34]

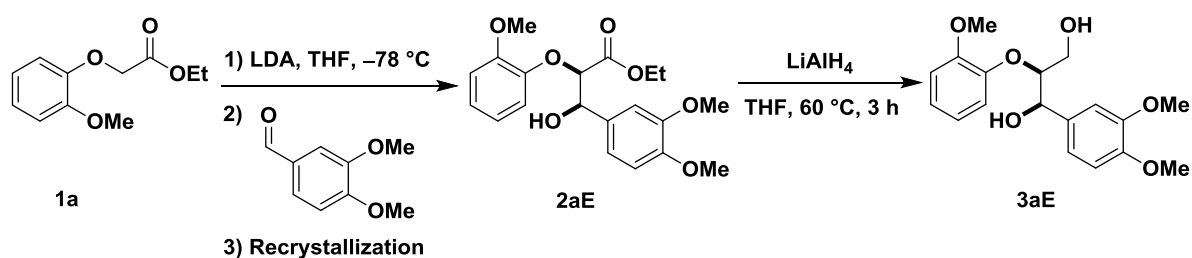
1.1. Synthesis of diastereomerically pure 1,3-dilignol β -O-4 model compounds

In collaboration with Buendia an improved protocol for the synthesis of diastereomerically pure 1,3-dilignol β -O-4 model compounds was developed.^[50] Starting from commercially available *tert*-butyl bromoacetate and phenol derivatives the corresponding *erythro* and *threo* 1,3-dilignols were obtained in good overall yields in three synthetic steps (Scheme III.1). The key step of this synthesis is the 1,2-addition of a *tert*-butyl aryloxy ester to a benzaldehyde derivative which afforded in most cases a 1:1 mixture of the corresponding *erythro* and *threo* β -hydroxy esters in very good to excellent yields. This mixture of diastereomers could completely be separated from each other by column chromatography which had been one of the main challenges in previous protocols.



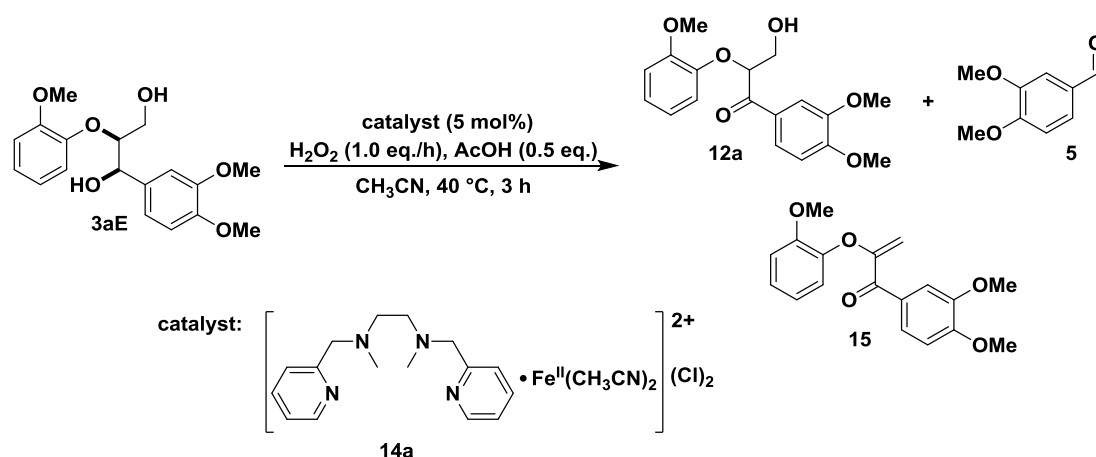
Scheme III.1. Synthesis of diastereomerically pure 1,3-dilignols.

Furthermore, a protocol is described which enables the synthesis of *erythro* 1,3-dilignol **3aE** on a large scale in a convenient manner (Scheme III.3).

Scheme III.2. Protocol for the large-scale synthesis of *erythro* 1,3-dilignol **3aE**.

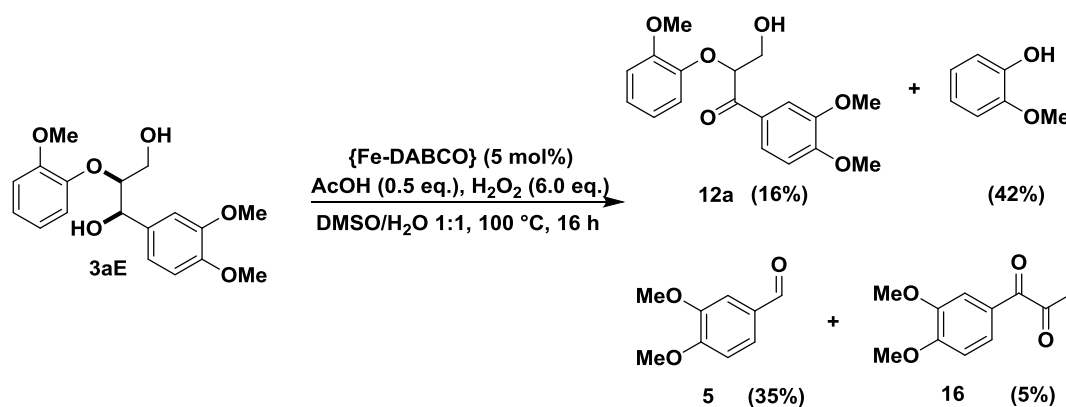
1.2. Oxidative cleavage of lignin model compounds with nonheme iron complexes

Nonheme iron catalysts were screened for the cleavage of *erythro* 1,3-dilignol **3aE**. Under the optimized reaction conditions 78% conversion of **3aE** was achieved after a reaction time of 3 h (Scheme III.3). However, the individual yields for the identified oxidation and cleavage products, ketone **12a**, aldehyde **5** and enol ether enone **15** were below 5%.

Scheme III.3. Optimized reaction conditions for the degradation of **3aE** with a nonheme iron catalyst.

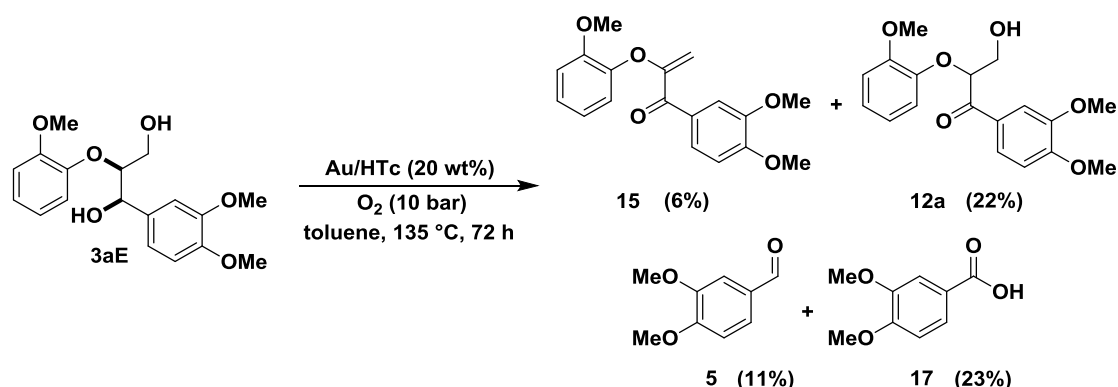
1.3. Oxidative cleavage of lignin model compounds with FeCl_3 -derived iron complexes

FeCl_3 -derived iron catalysts were utilized for the cleavage of *erythro* 1,3-dilignol **3aE**. Under the optimized reaction conditions the cleavage products 2-methoxyphenol and veratraldehyde were obtained in 42% and 35% yield, respectively (Scheme III.4). The reaction likely involves the formation of methyl radicals that are generated from DMSO and H_2O_2 .

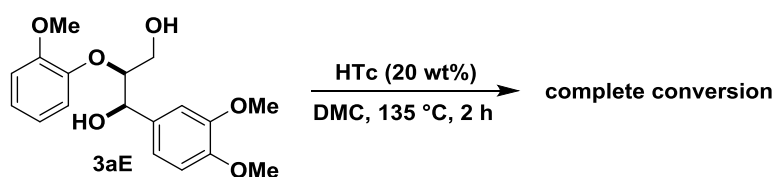
Scheme III.4. Optimized reaction conditions for the $\{\text{Fe-DABCO}\}$ catalyzed cleavage of **3aE**.

1.4. Oxidative cleavage of lignin model compounds with supported gold catalysts

Gold nanoparticles, supported on CeO_2 , HTc, MgO , ZrO_2 or TiO_2 , were studied in the oxidative cleavage of lignin model compound *erythro* 1,3-dilignol **3aE**. The most active catalyst, in which the catalytic activity stemmed from the gold nanoparticles and not from the support or the solvent, was 1-phenylethanol reduced Au/HTc in toluene (Scheme III.5).

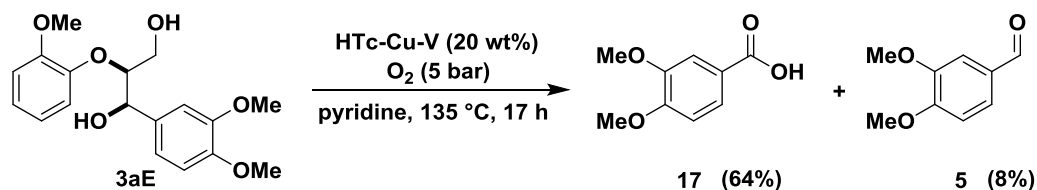
Scheme III.5. 1-Phenylethanol reduced Au/HTc catalyzed cleavage of **3aE**.

Veratric acid (**17**) and ketone **12a** were the main products in 23% and 22% yield. Veratraldehyde (**5**) and enol ether enone **15** were obtained as side products in 11% and 6% yield, respectively. The most active reaction system was with Au/HTc in dimethyl carbonate (DMC). The catalytic activity, however, did not originate from the gold nanoparticles and no dioxygen pressure was needed. With HTc as base catalyst complete conversion was achieved after 2 h (Scheme III.6).

Scheme III.6. Base catalyzed cleavage of **3aE** with HTc.

1.5. Oxidative cleavage of lignin with hydrotalcite-like catalysts

Transition metal-containing hydrotalcite-like catalysts were employed in the cleavage of lignin model compounds and different lignin sources. Copper-vanadium and copper-vanadium-zinc hydrotalcite-like catalysts (HTc-Cu-V and HTc-Zn-Cu-V) in pyridine showed high activity and good selectivity for the cleavage of *erythro* 1,3-dilignol **3aE** (Scheme III.7). Veratric acid (**17**) was the main product in 64% and veratraldehyde (**5**) was obtained in 8% yield.



Scheme III.7. HTc-Cu-V catalyzed cleavage of **3aE**.

Catalyst recycling experiments, leaching tests, reaction kinetics and EPR experiments of leached copper and vanadium revealed that copper-vanadium-containing hydrotalcite-like catalysts act to a significant degree as dispenser of the catalytically active homogeneous species that are continuously released. These leached species deactivate over time either through agglomeration or a resting state of the catalyst.

Lignin cleavage studies with different organosolv and kraft lignin sources showed that HTc-Cu-V completely degraded the β -O-4 and the protected β -O-4 linkages, as well as the resinol structures and *p*-hydroxycinnamyl alcohol motifs present in the lignin sources (Figure III.1). Furthermore, the different lignin sources were degraded to dimer and trimer size products (Figure III.2). HTc-Cu-V was catalytically active independently of the lignin pretreatment conditions employed.

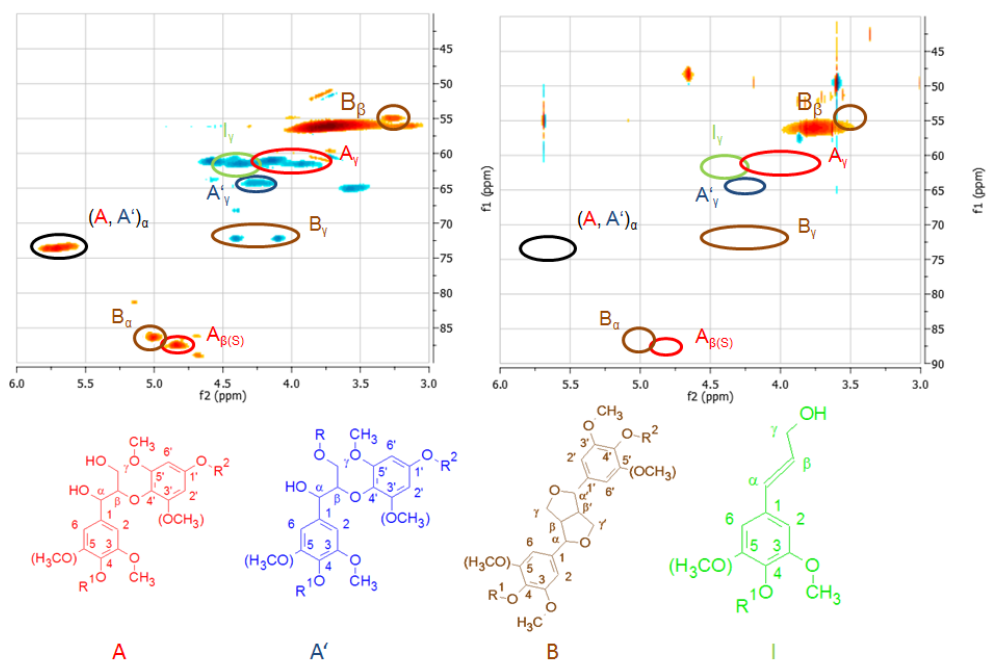


Figure III.1. HSQC of HH lignin before (left) and after the reaction with HTc-Cu-V as catalyst (right).

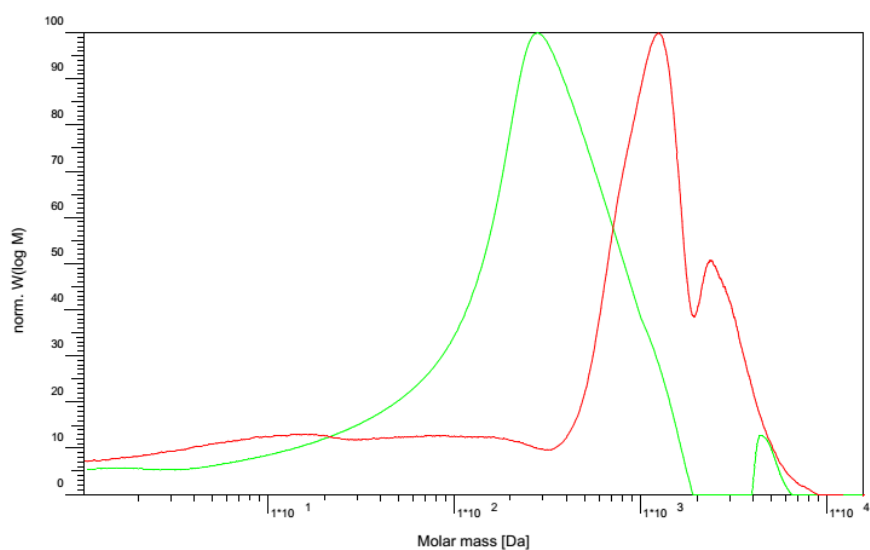
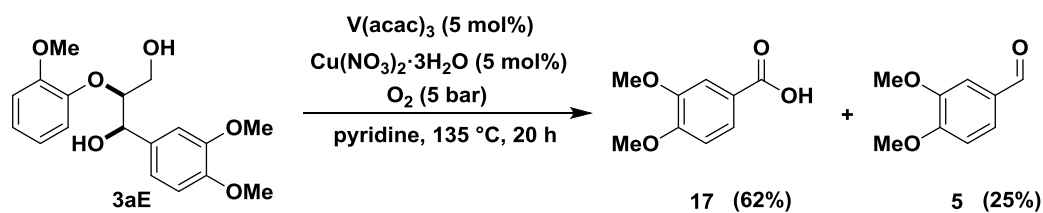


Figure III.2. Mass distribution of HH lignin before (red) and after the reaction with HTc-Cu-V (green).

1.6. Oxidative cleavage of lignin with $V(\text{acac})_3/\text{Cu}(\text{NO}_3)_2 \cdot 3\text{H}_2\text{O}$

During the leaching experiments conducted with HTc-Cu-V, $V(\text{acac})_3$ and $\text{Cu}(\text{NO}_3)_2 \cdot 3\text{H}_2\text{O}$ were tested as homogeneous vanadium and copper sources. $V(\text{acac})_3/\text{Cu}(\text{NO}_3)_2 \cdot 3\text{H}_2\text{O}$ showed high activity and good selectivity for the cleavage of *erythro* 1,3-dilignol **3aE** (Scheme III.8). Veratric acid (**17**) was the main product in 62% yield and veratraldehyde (**5**) was obtained in 25% yield.



Scheme III.8. $\text{V(acac)}_3/\text{Cu(NO}_3)_2 \cdot 3\text{H}_2\text{O}$ catalyzed cleavage of 3aE.

Studies with MPI lignin showed that $\text{V(acac)}_3/\text{Cu(NO}_3)_2 \cdot 3\text{H}_2\text{O}$ displays similar activity as HTc-Cu-V for the cleavage of lignin (Figure III.3 and Figure III.4).

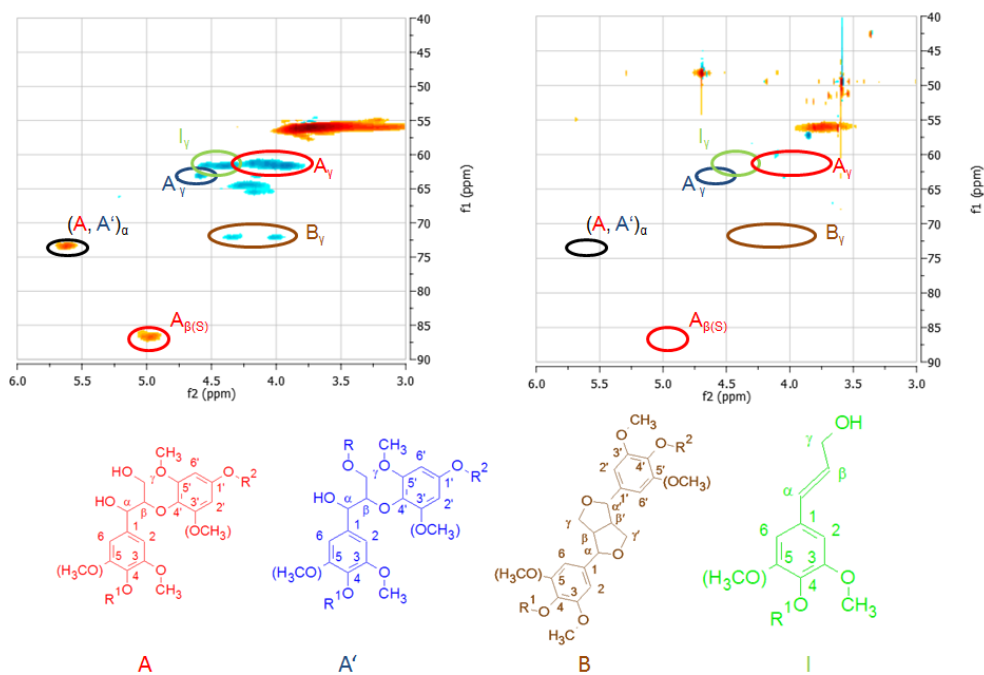


Figure III.3. HSQC of MPI lignin before (left) and after reaction with $\text{V(acac)}_3/\text{Cu(NO}_3)_2 \cdot 3\text{H}_2\text{O}$ (right).

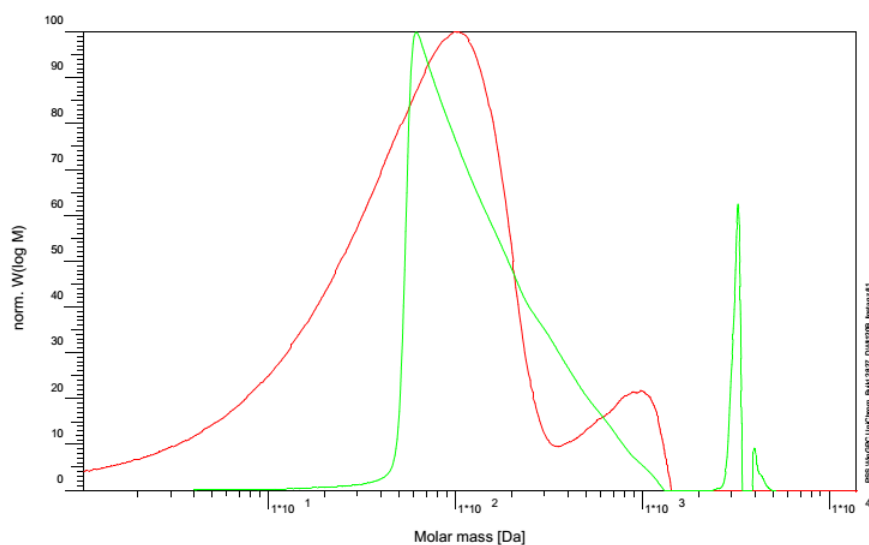


Figure III.4. Mass distribution of MPI lignin before (red) and after reaction with $\text{V(acac)}_3/\text{Cu(NO}_3)_2 \cdot 3\text{H}_2\text{O}$ (green).

2. Outlook

2.1. Oxidative cleavage of lignin model compounds with nonheme iron complexes

Nonheme iron catalysts displayed high activity under mild reaction conditions; nevertheless the selectivity was poor for identifiable cleavage products. Varying ligands to improve the selectivity has been discussed as one of the options in the previous chapter. Another option to potentially increase selectivity could be changing the transition metal from iron to manganese, since nonheme manganese complexes have displayed higher and better selectivity for some oxidations of aliphatic C-H groups.^[82]

2.2. Oxidative cleavage of lignin model compounds with FeCl₃-derived iron complexes

After having found the optimized reaction conditions for the cleavage of *erythro* 1,3-dilignol **3aE** with FeCl₃-derived catalysts, the next step is to apply the conditions for different model compounds and lignin. Furthermore, possible radical species involved in degradation should be characterized. All of these additional studies have been performed by Rinesch. The results are presented in the article “Iron-catalysed oxidative cleavage of lignin and β -O-4 lignin model compounds using peroxides in DMSO” which has been published in the journal Green Chemistry and will also be discussed in the dissertation of Rinesch.^[66]

2.3. Oxidative cleavage of lignin model compounds with supported gold catalysts

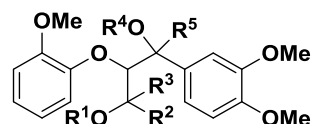
During the studies with various supported gold catalysts it was observed that 1-phenylethanol reduced catalysts generally displayed a higher activity than H₂ reduced catalysts. Studies that elucidate how the reduction method influences the particle size and distribution of gold nanoparticles are of interest because they could provide an explanation as to why the 1-phenylethanol reduced catalysts are more active.

Another important aspect is catalyst stability. Leaching and catalyst recycling experiments should provide insight as to whether the reaction is heterogeneously catalyzed and if the catalysts are suitable for multiple reuses. Furthermore, testing air as oxidant at elevated pressures is to be considered because it is less dangerous and would permit using higher reaction temperatures. To justify all of these additional experiments 1-phenylethanol reduced Au/HTc should be applied for the cleavage of extracted lignin to see whether the activity translates to the actual polymer.

The reactions of HTc, NaOH and K₂CO₃ in dimethyl carbonate for the cleavage of *erythro* 1,3-dilignol **3aE** demonstrated that base catalyzed cleavage of lignin in dimethyl carbonate could potentially be a promising reaction system. Based on these initial findings Dabral presents in the article “Base-catalysed cleavage of lignin β -O-4 model compounds in dimethyl carbonate”, that has been published in the journal Green Chemistry, a detailed screening of reaction conditions, different model substrates and organosolv lignin.^[26] Further results on this reaction system will be discussed in her dissertation.

2.4. Oxidative cleavage of lignin with hydrotalcite-like catalysts and $V(acac)_3/Cu(NO_3)_2 \cdot 3H_2O$

To conclude the model based mechanistic studies, further reactions using substrates where different protons or coordination sites are blocked could give insight on how the cleavage mechanism proceeds (Scheme III.9).



Scheme III.9. Model compounds for mechanistic studies.

A general problem in oxidative lignin cleavage, compared to reductive lignin cleavage, is the characterization of the cleavage products. 2D GC×GC-MS is able to provide good insight on the types of products that are formed in reductive lignin cleavage. The depolymerization products in oxidative lignin cleavage, however, are less volatile and therefore need to be derivatized before they can be analyzed by GC. To circumvent derivatization it is desirable to establish a 2D liquid chromatography methodology. One option is GPC×LC-MS in which the products are first separated by size and then by polarity. Another option is HPLC×LC-MS with different column interactions. The development of such a methodology would enable a better characterization of the products formed in HTc-Cu-V and $V(acac)_3/Cu(NO_3)_2 \cdot 3H_2O$ catalyzed lignin cleavage.

IV. Experimental Section

1. General Information

1.1. General

Starting materials were purchased from commercial suppliers and used without further purification. V(acac)₃ was supplied either by ABCR, 98%, or Sigma Aldrich, 97% and Cu(NO₃)₂·3H₂O by Merck, 99.5%, or Acros Organics 99%. All catalyzed reactions involving hydrotalcite-like catalysts, supported gold catalysts, Cu(NO₃)₂·3H₂O and V(acac)₃ were either performed in a 51.10201.0000 Büchi “tynyclave steel” type 1/25 mL autoclave, 6 to 20 mL glass autoclaves (ITQ) or in a 20 mL steel autoclave. THF, diethyl ether, 1,4-dioxane and toluene were dried by distillation over Solvona[®] (sodium on molecular sieves) in the presence of benzophenone and then stored under a nitrogen or argon atmosphere. CH₂Cl₂ was dried by distillation over CaH₂ and stored under argon atmosphere. Acetonitrile, pyridine, DMSO and DMF were purchased as dry solvents from Acros Organics (AcroSealTM). Flash chromatography was performed with Merck silica gel 60 (35-75 mesh). Analytical TLC was performed with aluminium sheets silica gel 60 F254 (Merck), and the products were visualized by UV detection or a cerium ammonium molybdate stain.

1.2. NMR

NMR spectra were recorded on a Varian Mercury 300 (¹H NMR: 300 MHz, ¹³C NMR: 75 MHz), Varian Inova 400 (¹H NMR: 400 MHz, ¹³C NMR: 101 MHz) or Agilent VNMRs 600 (¹H NMR: 600 MHz, ¹³C NMR: 151 MHz) spectrometer. Chemical shifts (δ) are given in ppm relative to the residual solvent peaks (CDCl₃: δ = 7.26 ppm, C₅D₅N: δ = 7.19 ppm, 7.55 ppm and 8.71 ppm, (CD₃)₂SO: δ = 2.50 ppm) as external standard. Spin-spin coupling constants (*J*) are given in Hz. NMR abbreviations are as follows: s (singlet), d (doublet), t (triplet), q (quartet), m (multiplet), bs (broad singlet), bd (broad doublet), bt (broad triplet), dd (doublet of doublets), td (triplet of doublets), ddd (doublet of doublet of doublets).

1.3. Mass spectrometry

Mass spectra were recorded on a Finnigan SSQ 7000 spectrometer (EI) and HRMS on a Finnigan MAT 95 spectrometer (ESI).

1.4. HPLC

An Agilent Infinity 1260 HPLC apparatus using an Agilent Eclipse XDB-C18 (4.6 mm ID × 150 mm, 5 μm) column with a H₂O/MeOH (60:40) eluent and a flow rate of 1.0 mL/min was employed for HPLC measurements. As internal standard 3,4-dimethoxybenzylalcohol in methanol, *c* = 0.2 mol/L, was used.

1.5. EPR

EPR measurements were either conducted at 150 K on a Bruker EMX-12 instrument operating in X-band at 9.5 GHz, a modulation amplitude of 1 G and a modulation frequency of 100 kHz or at 110 K on a X-band Bruker ESP 3220 instrument with a power of 1 mW (nonsaturation), a modulation amplitude of 3.8 G and a modulation frequency of 100 kHz.

1.6. SEC

An Agilent 1200er series instrument with an UV detector at 280 nm, a RI detector and three 100 Å Suprema columns with a particle size of 5 µm (PSS Polymer Service GmbH) was employed for size exclusion chromatography (SEC) measurements. The eluent consisted of 0.1 M hydrogen phosphate dibasic (Na₂HPO₄) and 0.5 g polyethylene glycol 6000 (PEG) at a pH of 12 in HPLC grade water. The elugrams show the detector response of the RI detector.

1.7. MALDI

MALDI spectra were measured utilizing a 1 kHz Laser Bruker ultraFlex MALDI-ToF-ToF mass spectrometer (Bruker, Bremen, Germany) with pulsed ion extraction (PIE). The polymer masses were determined in positive ion linear mode. Both samples and standard were dissolved in a 0.1 mol·L⁻¹ sodium hydroxide solution (NaOH, 99.5%, VWR chemicals), mixed with the matrix solution at a ratio of 1:5 and applied to a ground steel target by dried droplet technique. α-Cyano-4-hydroxycinnamic acid (CCA) in 0.1 mol·L⁻¹ NaOH was used as matrix. Mass calibration was performed using narrow distributed poly(ethylene glycol) with a mass at the peak of 3020 Da (Polymer Standards Service). The resulting spectra were evaluated using the Bruker flexAnalysis software (Version 3.3).

1.8. ICP-OES

ICP-OES were either recorded on a Varian 715-ES or a ‘Spektro-Flamme D’ device. The ICP-OES samples were either dissolved in a mixture of HF/HNO₃/HCl (1/1/3) or HNO₃/HCl (1/3) before measuring.

1.9. XRD

To identify the crystalline phases present in the heterogeneous catalysts, powder X-ray diffraction (XRD) was used. A CUBIX de PANalytical equipment with a PANalytical X'Celerator detector was utilized. The measurements were performed with a monochromatic CuKα1 source operated at 45 kV and 40 mA.

1.10. Raman

Raman spectra were recorded at ambient temperature with a 514 nm laser excitation on a Renishaw Raman Spectrometer (“in via”) equipped with a CCD detector. A total of 20 acquisitions were taken for each spectrum and the laser power on the sample was 25 mW.

2. Synthesis of model compounds

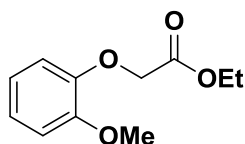
2.1. Synthesis of 1,3-dilignol β -O-4 model compounds

The synthesis of diastereomerically pure 1,3-dilignols has been published during the course of this dissertation in the article “Preparation of Diastereomerically Pure Dilignol Model Compounds” in the journal “Chemistry-A European Journal”.^[50] The following synthetic protocols closely resemble those given in reference 50 and the spectroscopic data are identical to the ones given in reference 50.

2.1.1 General procedure for the synthesis of the aryloxy esters

A dry and argon-flushed 1 L three-necked flask equipped with a magnetic stirrer, a reflux condenser, an argon inlet and a septum was charged with dry K_2CO_3 (13.82 g, 0.1 mol, 1.0 eq.), the corresponding phenol derivative (0.1 mol, 1.0 eq.) and acetone (500 mL). The mixture was stirred at ambient temperature for 15 min and then cooled to 0 °C. The desired bromoacetate derivative (0.1 mol, 1.0 eq.) was added dropwise over 5 min with a syringe and the reaction mixture was subsequently stirred at reflux over 8 h. Then, the solution was allowed to cool to ambient temperature, and filtered over a pad of celite (washed with acetone). The filtrate was evaporated under reduced pressure until almost dryness and diluted in diethyl ether (200 mL). The organic phase was washed with an aqueous NaOH solution (5% w/w, 3×50 mL), water (50 mL) and brine (50 mL). The organic phase was dried over $MgSO_4$, filtered and the solvent removed under reduced pressure. The product was purified by column chromatography (pentane/diethyl ether = 2:1).

Ethyl (2-methoxyphenoxy)acetate



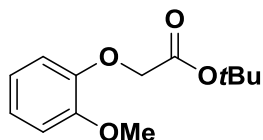
Ethyl (2-methoxyphenoxy)acetate was prepared following the general procedure for aryloxy esters and obtained in 90% yield as slightly yellow oil.

1H NMR (400 MHz, $CDCl_3$): δ = 6.97 (ddd, J = 8.0, 7.2, 1.6 Hz, 1H), 6.92–6.82 (m, 3H), 4.67 (s, 2H), 4.24 (q, J = 7.3 Hz, 2H), 3.86 (s, 3H), 1.27 (t, J = 7.3 Hz, 3H).

^{13}C NMR (101 MHz, $CDCl_3$): δ = 169.0, 149.7, 147.3, 122.5, 120.7, 114.5, 112.1, 66.6, 61.2, 55.9, 14.1.

MS (EI, 70 eV): m/z (%): 211 [$M+1$]⁺ (15), 210 [M]⁺ (100), 137 (27), 123 (27), 122 (23), 95 (15), 77 (20).

HRMS (ESI, 70 eV): m/z calcd for $C_{11}H_{14}O_4+K^+$: 249.0524 [$M+K$]⁺; found: 249.0524.

***tert*-Butyl (2-methoxyphenoxy)acetate**

The product was synthesized following the general procedure for aryloxy esters yielding the title compound in 93% as a white solid.

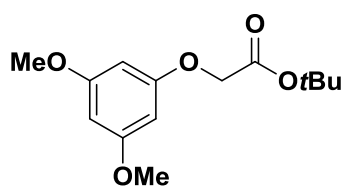
m.p.: 62-63 °C.

¹H NMR (400 MHz, CDCl₃): δ = 6.89 (ddd, J = 8.0, 7.2, 1.6 Hz, 1H), 6.86–6.77 (m, 2H), 6.74 (dd, J = 8.0, 1.6 Hz, 1H), 4.51 (s, 2H), 3.81 (s, 3H), 1.40 (s, 9H).

¹³C NMR (101 MHz, CDCl₃): δ = 167.9, 149.4, 147.3, 122.1, 120.6, 113.8, 112.1, 82.1, 66.6, 55.9, 28.1 (3C).

MS (EI, 70 eV): m/z (%): 239 [M+1]⁺ (15), 238 [M]⁺ (100), 183 (19), 182 (67), 138 (15), 137 (32), 123 (27), 122 (19), 77 (17), 57 (42).

HRMS (ESI, 70 eV): m/z calcd for C₁₃H₁₈O₄+Na⁺: 261.1097 [M+Na]⁺; found: 261.1097.

***tert*-Butyl (3,5-dimethoxyphenoxy)acetate**

tert-Butyl (3,5-dimethoxyphenoxy)acetate was prepared following the general procedure for aryloxy esters and obtained in 93% yield as a colorless oil.

¹H NMR (400 MHz, CDCl₃): δ = 6.11 (dd, J = 1.6, 1.6 Hz, 1H), 6.08 (d, J = 1.6 Hz, 2H), 4.46 (s, 2H), 3.75 (s, 6H), 1.49 (s, 9H).

¹³C NMR (101 MHz, CDCl₃): δ = 167.8, 161.4 (2C), 159.7, 93.8, 93.4 (2C), 82.3, 65.6, 55.3 (2C), 28.0 (3C).

MS (EI, 70 eV): m/z (%): 269 [M+1]⁺ (24), 268 [M]⁺ (100), 213 (17), 212 (59), 195 (10), 167 (23), 139 (15), 137 (13), 57 (24).

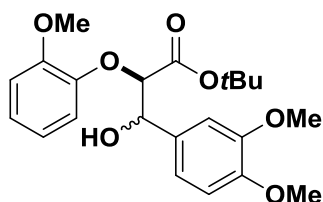
HRMS (ESI, 70 eV): m/z calcd for C₁₄H₂₀O₅+K⁺: 307.0942 [M+K]⁺; found: 307.0942.

2.1.2 General procedure for the synthesis of the β -hydroxy esters

A dry and argon flushed 250 mL three-necked flask equipped with a magnetic stirrer, an argon inlet, a septum and a dropping funnel was charged with dry THF (25 mL) and cooled to -78 °C. Diisopropylamine (1.315 g, 13 mmol, 1.3 eq.) and *n*-butyllithium in hexane (6.88 mL, 1.6 M, 11 mmol, 1.1 eq.) were added and the mixture was stirred for 1 h. The

corresponding aryloxy ester (10 mmol, 1.0 eq.), dissolved in dry THF (25 mL), was added dropwise to the mixture at $-78\text{ }^{\circ}\text{C}$ within 1 h and stirred for another 15 min. Afterwards the desired benzaldehyde derivative (10.05 mmol, 1.05 eq.), dissolved in dry THF (25 mL), was added dropwise over 30 min at $-78\text{ }^{\circ}\text{C}$. The mixture was stirred at $-78\text{ }^{\circ}\text{C}$ for 90 min and then warmed to $0\text{ }^{\circ}\text{C}$. Distilled water (60 mL) was added and the aqueous phase was extracted with ethyl acetate ($3\times 80\text{ mL}$). The combined organic phases were washed with 1 M HCl (80 mL), distilled water (80 mL) and brine (80 mL). After drying over MgSO_4 and filtration, the solvent was evaporated under reduced pressure. The products were purified by column chromatography (pentane/ethyl acetate = 5:1 to 1:1).

***tert*-Butyl 3-(3,4-dimethoxyphenyl)-3-hydroxy-2-(2-methoxyphenoxy)propanoate**



tert-Butyl 3-(3,4-dimethoxyphenyl)-3-hydroxy-2-(2-methoxyphenoxy)propanoate was synthesized following the general procedure for the synthesis of the β -hydroxy esters with *tert*-butyl (2-methoxyphenoxy)acetate and 3,4-dimethoxybenzaldehyde as starting materials. After column chromatography the *erythro* diastereomer was obtained in 46% yield as a white solid and the *threo* diastereomer in 44% yield as colorless syrup.

erythro:

m.p.: 103-104 $^{\circ}\text{C}$.

$^1\text{H NMR}$ (400 MHz, CDCl_3): δ = 7.12 (d, J = 8.0 Hz, 1H), 7.04–6.98 (m, 2H), 6.95 (dd, J = 8.0, 1.6 Hz, 1H), 6.91 (dd, J = 8.0, 1.6 Hz, 1H), 6.88–6.82 (m, 2H), 5.12 (dd, J = 6.0, 4.7 Hz, 1H), 4.68 (d, J = 4.7 Hz, 1H), 3.89 (s, 3H), 3.87 (s, 3H), 3.87 (s, 3H), 3.71 (d, J = 6.0 Hz, 1H), 1.32 (s, 9H).

$^{13}\text{C NMR}$ (101 MHz, CDCl_3): δ = 168.1, 150.5, 148.7, 148.6, 147.4, 131.8, 123.6, 121.0, 119.6, 118.5, 112.3, 110.6, 110.4, 83.8, 82.3, 73.8, 55.9, 55.8, 55.8, 27.8 (3C).

MS (EI, 70 eV): m/z (%): 404 $[\text{M}]^+$ (10), 387 (20), 331 (27), 238 (37), 182 (66), 179 (15), 167 (100), 151 (13), 139 (27), 137 (23), 108 (15), 57 (27).

HRMS (ESI, 70 eV): m/z calcd for $\text{C}_{22}\text{H}_{28}\text{O}_7+\text{Na}^+$: 427.1727 $[\text{M}+\text{Na}]^+$; found: 427.1728.

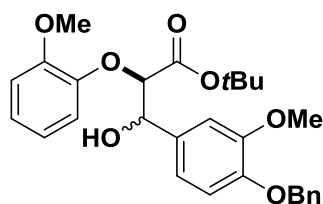
threo:

$^1\text{H NMR}$ (300 MHz, CDCl_3): δ = 7.05–6.98 (m, 2H), 6.97–6.89 (m, 3H), 6.86 (dd, J = 8.0, 1.6 Hz, 1H), 6.81 (d, J = 8.0 Hz, 1H), 5.00 (dd, J = 7.7, 2.7 Hz, 1H), 4.39 (d, J = 7.7 Hz, 1H), 3.92 (d, J = 2.7 Hz, 1H), 3.87 (s, 3H), 3.86 (s, 3H), 3.86 (s, 3H), 1.25 (s, 9H).

$^{13}\text{C NMR}$ (75 MHz, CDCl_3): δ = 168.3, 150.4, 149.1, 148.9, 147.5, 130.6, 123.7, 121.0, 120.2, 118.2, 112.2, 110.7, 110.4, 85.9, 82.1, 74.9, 55.9, 55.8 (2C), 27.7 (3C).

MS (EI, 70 eV): m/z (%): 404 $[\text{M}]^+$ (12), 387 (25), 331 (29), 238 (35), 182 (73), 179 (17), 167 (100), 151 (15), 139 (28), 137 (23), 124 (10), 108 (15), 57 (27).

HRMS (ESI, 70 eV): m/z calcd for $\text{C}_{22}\text{H}_{28}\text{O}_7+\text{K}^+$: 443.1467 $[\text{M}+\text{K}]^+$; found: 443.1468.

***tert*-Butyl 3-(4-benzyloxy-3-methoxyphenyl)-3-hydroxy-2-(2-methoxyphenoxy)propanoate**

The title compound was synthesized employing the general procedure for the synthesis of the β -hydroxy esters with *tert*-butyl (2-methoxyphenoxy)acetate and 4-(benzyloxy)-3-methoxybenzaldehyde as starting materials. After column chromatography the *erythro* diastereomer was obtained in 46% yield as a white solid and the *threo* diastereomer in 38% yield as slightly yellow syrup.

erythro:

m.p.: 107-108 °C.

$^1\text{H NMR}$ (400 MHz, CDCl_3): δ = 7.37–7.33 (m, 2H), 7.27 (tt, J = 8.0, 1.6 Hz, 2H), 7.23–7.18 (m, 1H), 7.06 (d, J = 1.6 Hz, 1H), 6.93 (ddd, J = 8.0, 7.2, 1.6 Hz, 1H), 6.88–6.84 (m, 2H), 6.83 (dd, J = 8.0, 1.6 Hz, 1H), 6.80–6.75 (m, 2H), 5.08 (s, 2H), 5.03 (bt, J = 5.2 Hz, 1H), 4.60 (d, J = 4.7 Hz, 1H), 3.82 (s, 3H), 3.77 (s, 3H), 3.65 (d, J = 6.0 Hz, 1H), 1.21 (s, 9H).

$^{13}\text{C NMR}$ (75 MHz, CDCl_3): δ = 168.4, 150.7, 149.5, 147.9, 147.6, 137.4, 132.6, 128.7 (2C), 128.0, 127.4 (2C), 123.9, 121.4, 119.7, 118.7, 113.7, 112.5, 111.1, 84.0, 82.5, 74.0, 71.1, 56.1, 56.1, 28.1 (3C).

MS (EI, 70 eV): m/z (%): 480 $[\text{M}]^+$ (7), 463 (10), 407 (12), 299 (11), 255 (17), 244 (48), 243 (91), 239 (13), 238 (59), 183 (28), 182 (99), 151 (23), 137 (41), 124 (14), 123 (15), 108 (18), 92 (11), 91 (100), 57 (19).

HRMS (ESI, 70 eV): m/z calcd for $\text{C}_{28}\text{H}_{32}\text{O}_7 + \text{Na}^+$: 503.2040 $[\text{M} + \text{Na}]^+$; found: 503.2042.

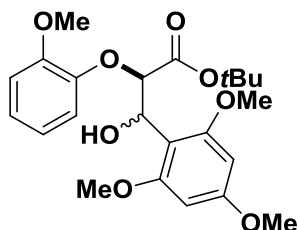
threo:

$^1\text{H NMR}$ (300 MHz, CDCl_3): δ = 7.37–7.32 (m, 2H), 7.30–7.24 (m, 2H), 7.24–7.17 (m, 1H), 6.99–6.92 (m, 2H), 6.87–6.82 (m, 2H), 6.82–6.76 (m, 2H), 6.75 (d, J = 8.0 Hz, 1H), 5.09 (s, 2H), 4.92 (dd, J = 7.7, 2.7 Hz, 1H), 4.31 (d, J = 7.7 Hz, 1H), 3.82 (s, 3H), 3.80 (s, 3H), 3.77 (d, J = 2.7 Hz, 1H), 1.14 (s, 9H).

$^{13}\text{C NMR}$ (75 MHz, CDCl_3): δ = 168.3, 150.4, 149.6, 148.1, 147.5, 137.1, 131.1, 128.5 (2C), 127.8, 127.2 (2C), 123.8, 121.0, 120.1, 118.3, 113.7, 112.2, 111.0, 85.9, 82.1, 75.0, 70.9, 56.0, 55.8, 27.7 (3C).

MS (EI, 70 eV): m/z (%): 480 $[\text{M}]^+$ (1), 244 (21), 243 (80), 238 (26), 183 (12), 182 (86), 151 (12), 137 (21), 124 (10), 108 (11), 91 (100), 57 (17).

HRMS (ESI, 70 eV): m/z calcd for $\text{C}_{28}\text{H}_{32}\text{O}_7 + \text{Na}^+$: 503.2040 $[\text{M} + \text{Na}]^+$; found: 503.2039.

***tert*-Butyl 3-hydroxy-2-(2-methoxyphenoxy)-3-(2,4,6-trimethoxyphenyl)propanoate**

tert-Butyl 3-hydroxy-2-(2-methoxyphenoxy)-3-(2,4,6-trimethoxyphenyl)propanoate was synthesized following the general procedure for the synthesis of the β -hydroxy esters with *tert*-butyl (2-methoxyphenoxy)acetate and 2,4,6-trimethoxybenzaldehyde as starting materials. After column chromatography (pentane/ethyl acetate = 4:1 to 1:1) the *erythro* diastereomer was obtained in 35% yield and the *threo* diastereomer in 52% yield. Both diastereomers were slightly yellow solids.

erythro:

m.p.: 121-123 °C.

$^1\text{H NMR}$ (400 MHz, CDCl_3): δ = 6.87 (ddd, J = 8.0, 7.2, 1.6 Hz, 1H), 6.79 (dd, J = 8.0, 1.6 Hz, 1H), 6.77–6.72 (m, 1H), 6.67 (dd, J = 8.0, 1.6 Hz, 1H), 6.12 (s, 2H), 5.55 (dd, J = 11.5, 8.3 Hz, 1H), 4.74 (d, J = 8.3 Hz, 1H), 3.80 (s, 6H), 3.79 (s, 3H), 3.76 (d, J = 11.5 Hz, 1H), 3.69 (s, 3H), 1.48 (s, 9H).

$^{13}\text{C NMR}$ (101 MHz, CDCl_3): δ = 170.1, 161.0, 159.4 (2C), 150.4, 148.3, 122.4, 120.9, 117.1, 113.5, 109.0, 91.1 (2C), 82.6, 81.5, 67.5, 56.3, 55.8 (2C), 55.3, 28.1 (3C).

MS (EI, 70 eV): m/z (%): 434 [$\text{M}]^+$ (1), 361 (10), 198 (31), 197 (100), 181 (12).

HRMS (ESI, 70 eV): m/z calcd for $\text{C}_{23}\text{H}_{30}\text{O}_8 + \text{K}^+$: 473.1572 [$\text{M} + \text{K}]^+$; found: 473.1572.

threo:

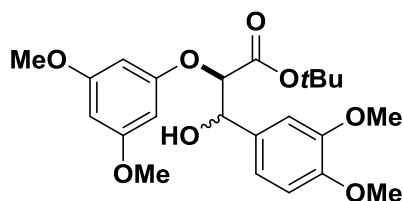
m.p.: 97-99 °C.

$^1\text{H NMR}$ (400 MHz, CDCl_3): δ = 6.95 (ddd, J = 8.0, 7.2, 1.6 Hz, 1H), 6.91–6.87 (m, 2H), 6.83 (ddd, J = 8.0, 7.2, 1.6 Hz, 1H), 6.12 (s, 2H), 5.61 (bt, J = 6.6 Hz, 1H), 4.99 (d, J = 7.6 Hz, 1H), 3.86 (s, 3H), 3.86–3.83 (m, 1H), 3.81 (s, 6H), 3.80 (s, 3H), 1.21 (s, 9H).

$^{13}\text{C NMR}$ (101 MHz, CDCl_3): δ = 168.5, 161.3, 159.6 (2C), 150.2, 148.2, 122.4, 120.7, 116.7, 112.6, 107.4, 90.9 (2C), 82.9, 81.0, 68.0, 56.0, 55.7 (2C), 55.3, 27.5 (3C).

MS (EI, 70 eV): m/z (%): 434 [$\text{M}]^+$ (1), 417 (12), 361 (19), 209 (13), 198 (34), 197 (100), 181 (15), 169 (12).

HRMS (ESI, 70 eV): m/z calcd for $\text{C}_{23}\text{H}_{30}\text{O}_8 + \text{Na}^+$: 457.1833 [$\text{M} + \text{Na}]^+$; found: 457.1832.

***tert*-Butyl 2-(3,5-dimethoxyphenoxy)-3-(3,4-dimethoxyphenyl)-3-hydroxypropanoate**

The title compound was synthesized employing the general procedure for the synthesis of the β -hydroxy esters with *tert*-butyl (3,5-dimethoxyphenoxy)acetate and 3,4-dimethoxybenzaldehyde as starting materials. After column chromatography the *erythro* diastereomer was obtained in 43% yield as yellow syrup and the *threo* diastereomer in 42% yield as colorless syrup.

erythro:

$^1\text{H NMR}$ (400 MHz, CDCl_3): δ = 7.03 (d, J = 2.0 Hz, 1H), 7.00 (dd, J = 8.0, 2.0 Hz, 1H), 6.85 (d, J = 8.0 Hz, 1H), 6.10 (dd, J = 2.0, 2.0 Hz, 1H), 6.05 (d, J = 2.0 Hz, 2H), 5.13 (dd, J = 5.6, 3.7 Hz, 1H), 4.63 (d, J = 5.6 Hz, 1H), 3.89 (s, 3H), 3.87 (s, 3H), 3.73 (s, 6H), 2.91 (d, J = 3.7 Hz, 1H), 1.35 (s, 9H).

$^{13}\text{C NMR}$ (151 MHz, CDCl_3): δ = 168.4, 161.4 (2C), 159.4, 148.8 (2C), 131.7, 119.1, 110.8, 109.8, 94.3, 94.2 (2C), 82.6, 80.9, 73.9, 55.9, 55.8, 55.3 (2C), 27.8 (3C).

MS (EI, 70 eV): m/z (%): 434 $[\text{M}]^+$ (1), 212 (22), 168 (10), 167 (100), 155 (11), 139 (19), 57 (25).

HRMS (ESI, 70 eV): m/z calcd for $\text{C}_{23}\text{H}_{30}\text{O}_8 + \text{K}^+$: 473.1572 $[\text{M} + \text{K}]^+$; found: 473.1573.

threo:

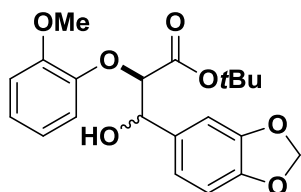
$^1\text{H NMR}$ (400 MHz, CDCl_3): δ = 7.01 (d, J = 2.0 Hz, 1H), 6.96 (dd, J = 8.0, 2.0 Hz, 1H), 6.84 (d, J = 8.0 Hz, 1H), 6.12 (dd, J = 2.0, 2.0 Hz, 1H), 6.10 (d, J = 2.0 Hz, 2H), 5.02 (dd, J = 6.4, 4.0 Hz, 1H), 4.58 (d, J = 6.4 Hz, 1H), 3.89 (s, 3H), 3.88 (s, 3H), 3.74 (s, 6H), 2.92 (d, J = 4.0 Hz, 1H), 1.28 (s, 9H).

$^{13}\text{C NMR}$ (101 MHz, CDCl_3): δ = 168.1, 161.5 (2C), 159.4, 149.3, 149.0, 130.8, 119.8, 110.9, 110.3, 94.4, 94.2 (2C), 82.6, 81.9, 74.7, 56.0, 55.9, 55.4 (2C), 27.8 (3C).

MS (EI, 70 eV): m/z (%): 434 $[\text{M}]^+$ (1), 212 (22), 168 (10), 167 (100), 155 (12), 139 (20), 57 (26).

HRMS (ESI, 70 eV): m/z calcd for $\text{C}_{23}\text{H}_{30}\text{O}_8 + \text{K}^+$: 473.1572 $[\text{M} + \text{K}]^+$; found: 473.1574.

***tert*-Butyl 3-hydroxy-2-(2-methoxyphenoxy)-3-[3,4-(methylenedioxy)phenyl]propanoate**



tert-Butyl 3-hydroxy-2-(2-methoxyphenoxy)-3-[3,4-(methylenedioxy)phenyl]propanoate was synthesized following the general procedure for the synthesis of the β -hydroxy esters with *tert*-butyl (2-methoxyphenoxy)acetate and 3,4-(methylenedioxy)benzaldehyde as starting materials. After column chromatography the *erythro* diastereomer was obtained in 47% yield as a white solid and the *threo* diastereomer in 36% yield as colorless syrup.

erythro:

m.p.: 121-123 °C.

$^1\text{H NMR}$ (600 MHz, CDCl_3): δ = 7.06 (d, J = 1.6 Hz, 1H), 7.02 (ddd, J = 8.0, 7.2, 1.6 Hz, 1H), 6.98 (dd, J = 8.0, 1.6 Hz, 1H), 6.91 (dd, J = 8.0, 1.6 Hz, 1H), 6.90 (dd, J = 8.0, 1.6 Hz, 1H), 6.86 (ddd, J = 8.0, 8.0, 1.6 Hz, 1H), 6.77 (d, J = 8.0 Hz, 1H), 5.94 (q, J = 1.6 Hz, 2H), 5.09 (dd, J = 6.6, 4.7 Hz, 1H), 4.63 (d, J = 4.7 Hz, 1H), 3.92 (d, J = 6.6 Hz, 1H), 3.88 (s, 3H), 1.34 (s, 9H).

^{13}C NMR (151 MHz, CDCl_3): $\delta = 168.3, 150.9, 147.7, 147.6, 147.4, 133.4, 124.1, 121.3, 120.9, 119.4, 112.5, 108.1, 108.0, 101.2, 84.4, 82.6, 74.0, 56.1, 28.1$ (3C).

MS (EI, 70 eV): m/z (%): 388 [$\text{M}]^+$ (8), 371 (15), 315 (29), 238 (45), 183 (10), 182 (100), 163 (15), 151 (76), 137 (46), 135 (20), 133 (10), 124 (14), 123 (18), 108 (30), 93 (19), 77 (13), 65 (11), 57 (27).

HRMS (ESI, 70 eV): m/z calcd for $\text{C}_{21}\text{H}_{24}\text{O}_7+\text{Na}^+$: 411.1414 [$\text{M}+\text{Na}]^+$; found: 411.1415.

threo:

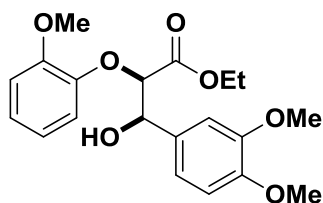
^1H NMR (600 MHz, CDCl_3): $\delta = 7.03$ (ddd, $J = 8.0, 7.2, 1.6$ Hz, 1H), 6.96 (d, $J = 1.6$ Hz, 1H), 6.93 (d, $J = 1.6$ Hz, 1H), 6.92 (d, $J = 1.6$ Hz, 1H), 6.88–6.84 (m, 2H), 6.77 (d, $J = 8.0$ Hz, 1H), 5.94 (s, 2H), 4.98 (dd, $J = 7.7, 2.4$ Hz, 1H), 4.32 (d, $J = 7.7$ Hz, 1H), 3.89 (d, $J = 2.4$ Hz, 1H), 3.88 (s, 3H), 1.28 (s, 9H).

^{13}C NMR (151 MHz, CDCl_3): $\delta = 168.5, 150.6, 147.9$ (2C), 147.6, 132.2, 124.1, 121.5, 121.2, 118.6, 112.4, 108.2, 108.1, 101.3, 86.3, 82.5, 75.1, 56.05, 28.0 (3C).

MS (EI, 70 eV): m/z (%): 238 (12), 183 (10), 182 (89), 164 (12), 163 (17), 151 (100), 137 (52), 135 (21), 133 (10), 124 (13), 123 (18), 108 (40), 93 (20), 77 (12), 57 (36).

HRMS (ESI, 70 eV): m/z calcd for $\text{C}_{21}\text{H}_{24}\text{O}_7+\text{K}^+$: 427.1154 [$\text{M}+\text{K}]^+$; found: 427.1154.

***erythro* Ethyl 3-(3,4-dimethoxyphenyl)-3-hydroxy-2-(2-methoxyphenoxy)propanoate**



A dry and argon flushed 1 L three-necked flask equipped with a magnetic stirrer, a septum, an argon inlet, and an addition funnel was charged with dry THF (140 mL) and cooled to -78 °C. Diisopropylamine (9.236 g, 91.3 mmol, 1.3 eq.) and *n*-butyllithium in hexane (48.27 mL, 1.6 M, 77.2 mmol, 1.1 eq.) were added and the mixture was stirred for 1 h. Ethyl-2-(2-methoxyphenoxy)acetate (14.76 g, 70.2 mmol, 1.0 eq.), dissolved in dry THF (120 mL), was added dropwise over 2.75 h to the mixture at -78 °C and stirred for another 15 min. Afterwards, 3,4-dimethoxybenzaldehyde (12.834 g, 77.2 mmol, 1.1 eq.), dissolved in dry THF (120 mL), was added dropwise over 1 h. The mixture was stirred at -78 °C for 90 min, warmed to 0 °C and distilled water (120 mL) was added. The aqueous phase was extracted with ethyl acetate (3×120 mL). The combined organic phases were washed with 1 M HCl (120 mL), water (120 mL) and brine (120 mL), dried over MgSO_4 , filtered, and concentrated under reduced pressure. The crude solid was recrystallized 3 times in ethyl acetate (2.5 mL of ethyl acetate for 4 g of crude material; diethyl ether was used to wash the recrystallized solid) to obtain the title compound (9.22 g, 24.5 mmol, 35%, *erythro:threo* > 98:2) as a white solid.

m.p.: 103-104 °C.

^1H NMR (400 MHz, CDCl_3): $\delta = 7.06$ (d, $J = 8.0$ Hz, 1H), 7.05–6.97 (m, 2H), 6.92 (ddd, $J = 8.0, 8.0, 1.6$ Hz, 2H), 6.87–6.82 (m, 2H), 5.15 (bt, $J = 5.6$ Hz, 1H), 4.74 (d, $J = 4.7$ Hz, 1H), 4.14 (q, $J = 7.3$ Hz, 2H), 3.89 (s, 3H), 3.87 (s, 3H), 3.87 (s, 3H), 3.66 (d, $J = 6.0$ Hz, 1H), 1.16 (t, $J = 7.3$ Hz, 3H).

¹³C NMR (101 MHz, CDCl₃): δ = 169.3, 150.6, 148.8, 148.7, 147.2, 131.7, 123.9, 121.1, 119.3, 119.0, 112.3, 110.7, 110.1, 83.9, 73.8, 61.2, 55.9, 55.8, 55.8, 14.1.

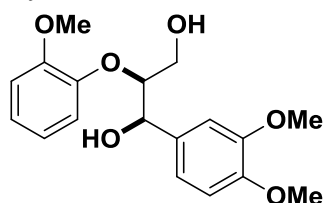
MS (EI, 70 eV): m/z (%): 376 [M]⁺ (13), 210 (48), 167 (31), 139 (29), 137 (100), 124 (10), 108 (13), 77 (15).

HRMS (ESI, 70 eV): m/z calcd for C₂₀H₂₄O₇+Na⁺: 399.1414 [M+Na]⁺; found: 399.1414.

2.1.3 General procedure for the synthesis of 1,3-diols

A dry 250 mL three-necked flask equipped with a reflux condenser, an argon inlet, a dropping funnel and a magnetic stirrer was charged with LiAlH₄ (1.139 g, 30.00 mmol, 3.0 eq.) and 25 mL of dry THF and cooled to 0 °C. The corresponding β -hydroxy ester (10.00 mmol, 1.0 eq.) was dissolved in 35 mL of dry THF and added dropwise over 15 min at 0 °C. The resulting mixture was heated to 60 °C and stirred for 3 h. Afterwards the reaction was cooled to 0 °C, quenched by slow and sequential addition of H₂O (1.139 mL), NaOH (15% w/w, 1.139 mL) and additional H₂O (3.417 mL) and stirred at room temperature for 60 min. The reaction mixture was filtered over celite and washed with DCM (4×25 mL), dried over MgSO₄, filtered and the solvent removed under reduced pressure. The desired product was obtained after column chromatography (DCM/MeOH = 100:0 to 100:3).

erythro 1-(3,4-Dimethoxyphenyl)-2-(2-methoxyphenoxy)-1,3-propanediol



The title compound was synthesized following the general procedure for the synthesis of 1,3-diols with *erythro* *tert*-butyl 3-(3,4-dimethoxyphenyl)-3-hydroxy-2-(2-methoxyphenoxy)propanoate as starting material, affording the desired product in 90%. When using *erythro* ethyl 3-(3,4-dimethoxyphenyl)-3-hydroxy-2-(2-methoxyphenoxy)propanoate, 2.0 eq. of LiAlH₄ were employed yielding the title compound in 90%. In both syntheses the product was dried by azeotropic distillation with toluene after column chromatography and the residual toluene was removed under high vacuum at 50 °C to furnish *erythro* 1-(3,4-dimethoxyphenyl)-2-(2-methoxyphenoxy)-1,3-propanediol as a white solid.

m.p.: 100-101 °C.

¹H NMR (400 MHz, CDCl₃): δ = 7.06 (ddd, J = 8.0, 7.2, 1.6 Hz, 1H), 6.99–6.88 (m, 5H), 6.83 (d, J = 8.0 Hz, 1H), 4.98 (bt, J = 4.7 Hz, 1H), 4.16 (ddd, J = 6.0, 4.7, 3.7 Hz, 1H), 3.95–3.89 (m, 1H), 3.88 (s, 3H), 3.87 (s, 3H), 3.87 (s, 3H), 3.66 (ddd, J = 12.0, 7.2, 3.7 Hz, 1H), 3.55 (bs, 1H), 2.79 (bs, 1H).

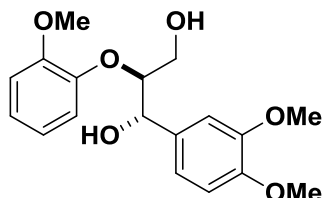
¹³C NMR (101 MHz, CDCl₃): δ = 151.6, 149.0, 148.5, 146.9, 132.4, 124.3, 121.7, 121.1, 118.4, 112.2, 111.0, 109.2, 87.5, 72.7, 60.7, 55.9 (3C).

MS (EI, 70 eV): m/z (%): 334 $[M]^+$ (7), 167 (15), 166 (12), 151 (14), 150 (100), 139 (20), 124 (10), 121 (12), 109 (10).

HRMS (ESI, 70 eV): m/z calcd for $C_{18}H_{22}O_6+Na^+$: 357.1309 $[M+Na]^+$; found: 357.1309.

HPLC (H₂O/ MeOH, 60/40): t_R = 11.9 min.

***threo* 1-(3,4-Dimethoxyphenyl)-2-(2-methoxyphenoxy)-1,3-propanediol**



threo 1-(3,4-Dimethoxyphenyl)-2-(2-methoxyphenoxy)-1,3-propanediol was prepared following the general procedure for the synthesis of 1,3-diols with *threo tert*-butyl 3-(3,4-dimethoxyphenyl)-3-hydroxy-2-(2-methoxyphenoxy)propanoate as starting material, yielding the title compound in 80% as a colorless syrup.

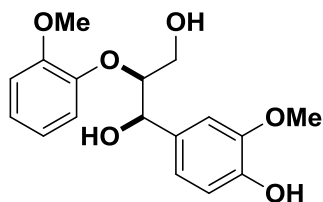
¹H NMR (400 MHz, CDCl₃): δ = 7.13 (dd, J = 8.0, 1.6 Hz, 1H), 7.07 (ddd, J = 8.0, 7.2, 1.6 Hz, 1H), 7.01–6.96 (m, 2H), 6.95 (dd, J = 8.0, 1.6 Hz, 1H), 6.93 (ddd, J = 8.0, 8.0, 1.6 Hz, 1H), 6.85 (d, J = 8.0 Hz, 1H), 4.99 (d, J = 4.7 Hz, 1H), 4.03 (dt, J = 7.7, 3.7 Hz, 1H), 3.91 (s, 3H), 3.88 (s, 3H), 3.87 (s, 3H), 3.69 (bd, J = 1.6 Hz, 1H), 3.63 (dt, J = 12.0, 3.7 Hz, 1H), 3.48 (ddd, J = 12.0, 7.7, 3.7 Hz, 1H), 2.72 (dd, J = 7.7, 4.7 Hz, 1H).

¹³C NMR (101 MHz, CDCl₃): δ = 151.3, 149.1, 148.9, 147.6, 132.1, 124.3, 121.7, 121.1, 119.6, 112.1, 111.0, 109.9, 89.5, 73.9, 61.0, 55.9 (3C).

MS (EI, 70 eV): m/z (%): 334 $[M]^+$ (14), 167 (19), 166 (13), 151 (16), 150 (100), 139 (24), 124 (13), 121 (12), 109 (10).

HRMS (ESI, 70 eV): m/z calcd for $C_{18}H_{22}O_6+Na^+$: 357.1309 $[M+Na]^+$; found: 357.1312.

***erythro* 1-(4-Hydroxy-3-methoxyphenyl)-2-(2-methoxyphenoxy)-1,3-propanediol**



The title compound was synthesized in a two-step synthesis with *erythro tert*-butyl 3-(4-benzyloxy-3-methoxyphenyl)-3-hydroxy-2-(2-methoxyphenoxy)propanoate as starting material. The first step followed the general procedure for the synthesis of 1,3-diols without purification by column chromatography. The crude product was dissolved in a 1:1 mixture of methanol and DCM, and 10 wt% of Pd/C (10% w/w) was added to the reaction mixture. The solution was stirred at room temperature under hydrogen atmosphere for 3 h, and then filtered over celite, washed with DCM and methanol and the solvent removed under reduced pressure. The product was purified by column chromatography (DCM/MeOH = 99:1 to 94:6) yielding the title compound as a sticky white solid in 90% after two steps.

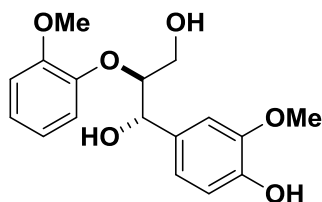
¹H NMR (400 MHz, CDCl₃): δ = 6.98 (ddd, J = 8.0, 7.2, 1.6 Hz, 1H), 6.91–6.81 (m, 4H), 6.80 (d, J = 8.0 Hz, 1H), 6.75 (dd, J = 8.0, 1.6 Hz, 1H), 5.60 (bs, 1H), 4.90 (d, J = 4.7 Hz, 1H), 4.08 (ddd, J = 6.0, 4.7, 3.2 Hz, 1H), 3.84 (dd, J = 12.0, 6.0 Hz, 1H), 3.80 (s, 3H), 3.79 (s, 3H), 3.59 (dd, J = 12.0, 3.2 Hz, 1H), 2.94 (bs, 2H).

¹³C NMR (101 MHz, CDCl₃): δ = 151.5, 146.9, 146.6, 145.1, 131.8, 124.2, 121.6, 120.9, 119.0, 114.2, 112.2, 108.7, 87.3, 72.7, 60.7, 55.9 (2C).

MS (EI, 70 eV): m/z (%): 320 [M]⁺ (1), 153 (16), 151 (15), 150 (100), 124 (15), 121 (15), 109 (17), 93 (19), 77 (15), 65 (15).

HRMS (ESI, 70 eV): m/z calcd for C₁₇H₂₀O₆+K⁺: 359.0892 [M+K]⁺; found: 359.0892.

***threo* 1-(4-Hydroxy-3-methoxyphenyl)-2-(2-methoxyphenoxy)-1,3-propanediol**



The title compound was synthesized in a two-step synthesis with *threo tert*-butyl 3-(4-benzyloxy-3-methoxyphenyl)-3-hydroxy-2-(2-methoxyphenoxy)propanoate as starting material. The first step followed the general procedure for the synthesis of 1,3-diols without purification by column chromatography. The crude product was dissolved in a 1:1 mixture of methanol and DCM, and 10 wt% of Pd/C (10% w/w) was added to the reaction mixture. The solution was stirred at room temperature under hydrogen atmosphere for 3 h, and then filtered over celite, washed with DCM and methanol and the solvent removed under reduced pressure. The product was purified by column chromatography (DCM/MeOH = 99:1 to 94:6) yielding the title compound as a sticky white solid in 80% after two steps.

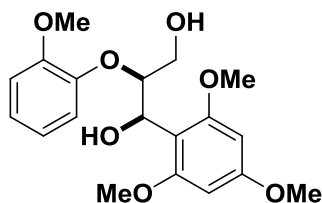
¹H NMR (400 MHz, CDCl₃): δ = 7.12 (dd, J = 8.0, 1.6 Hz, 1H), 7.09–7.03 (m, 1H), 6.99–6.89 (m, 4H), 6.88 (d, J = 8.0 Hz, 1H), 5.79–5.70 (m, 1H), 4.96 (d, J = 7.7 Hz, 1H), 4.02 (dt, J = 7.7, 3.7 Hz, 1H), 3.90 (s, 3H), 3.86 (s, 3H), 3.75–3.69 (m, 1H), 3.62 (ddd, J = 12.0, 4.7, 3.7 Hz, 1H), 3.48 (ddd, J = 12.0, 7.7, 3.7 Hz, 1H), 2.85–2.74 (m, 1H).

¹³C NMR (101 MHz, CDCl₃): δ = 151.3, 147.6, 146.7, 145.6, 131.5, 124.2, 121.7, 121.0, 120.2, 114.3, 112.2, 109.4, 89.5, 74.0, 61.0, 55.9 (2C).

MS (EI, 70 eV): m/z (%): 153 (15), 151 (14), 150 (100), 137 (29), 124 (22), 121 (13), 109 (11).

HRMS (ESI, 70 eV): m/z calcd for C₁₇H₂₀O₆+K⁺: 359.0892 [M+K]⁺; found: 359.0895.

***erythro* 2-(2-Methoxyphenoxy)-1-(2,4,6-trimethoxyphenyl)-1,3-propanediol**



erythro 2-(2-Methoxyphenoxy)-1-(2,4,6-trimethoxyphenyl)-1,3-propanediol was prepared following the general procedure for the synthesis of 1,3-diols with *erythro tert*-butyl 3-hydroxy-2-(2-methoxyphenoxy)-3-(2,4,6-trimethoxyphenyl)propanoate as starting material, yielding the title compound in 86% as a white solid.

m.p.: 125-127 °C.

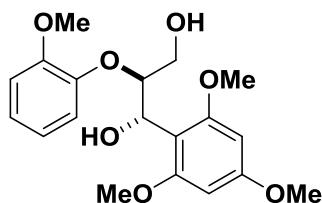
¹H NMR (400 MHz, CDCl₃): δ = 6.90 (ddd, *J* = 8.0, 7.2, 1.6 Hz, 1H), 6.80 (dd, *J* = 8.0, 1.6 Hz, 1H), 6.77–6.72 (m, 1H), 6.65 (dd, *J* = 8.0, 1.6 Hz, 1H), 6.10 (s, 2H), 5.40 (dd, *J* = 11.0, 7.4 Hz, 1H), 4.45 (ddd, *J* = 7.4, 6.2, 3.9 Hz, 1H), 4.06–3.88 (m, 2H), 3.79 (s, 3H), 3.78 (s, 3H), 3.77 (s, 6H), 3.72 (d, *J* = 11.0 Hz, 1H), 3.19 (dd, *J* = 7.4, 6.2 Hz, 1H).

¹³C NMR (101 MHz, CDCl₃): δ = 160.9, 159.1 (2C), 150.9, 148.3, 122.8, 121.0, 119.6, 111.9, 109.0, 91.0 (2C), 85.5, 67.3, 63.0, 55.8 (3C), 55.4.

MS (EI, 70 eV): *m/z* (%): 198 (11), 197 (100), 150 (22), 77 (15).

HRMS (ESI, 70 eV): *m/z* calcd for C₁₉H₂₄O₇+Na⁺: 387.1414 [*M*+Na]⁺; found: 387.1414.

***threo* 2-(2-Methoxyphenoxy)-1-(2,4,6-trimethoxyphenyl)-1,3-propanediol**



threo 2-(2-Methoxyphenoxy)-1-(2,4,6-trimethoxyphenyl)-1,3-propanediol was prepared following the general procedure for the synthesis of 1,3-diols with *threo tert*-butyl 3-hydroxy-2-(2-methoxyphenoxy)-3-(2,4,6-trimethoxyphenyl)propanoate as starting material, yielding the title compound in 82% as a slightly yellow syrup.

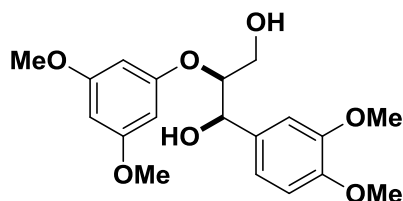
¹H NMR (400 MHz, CDCl₃): δ = 7.26–7.20 (m, 1H), 7.00 (ddd, *J* = 8.0, 7.2, 1.6 Hz, 1H), 6.94–6.86 (m, 2H), 6.13 (s, 2H), 5.39 (dd, *J* = 9.0, 8.0 Hz, 1H), 4.58 (ddd, *J* = 8.0, 7.0, 3.3 Hz, 1H), 3.89 (s, 3H), 3.80 (s, 3H), 3.80 (s, 6H), 3.71 (d, *J* = 9.0 Hz, 1H), 3.61 (ddd, *J* = 12.0, 7.0, 4.1 Hz, 1H), 3.45 (ddd, *J* = 12.0, 9.0, 3.3 Hz, 1H), 3.08 (dd, *J* = 9.0, 4.1 Hz, 1H).

¹³C NMR (101 MHz, CDCl₃): δ = 161.1, 159.0 (2C), 150.9, 149.1, 123.1, 121.4, 120.6, 112.0, 108.4, 91.1 (2C), 87.8, 67.8, 62.6, 55.9, 55.8 (2C), 55.3.

MS (EI, 70 eV): *m/z* (%): 198 (10), 197 (100), 150 (32).

HRMS (ESI, 70 eV): *m/z* calcd for C₁₉H₂₄O₇+K⁺: 403.1154 [*M*+K]⁺; found: 403.1150.

***erythro* 2-(3,5-Dimethoxyphenoxy)-1-(3,4-dimethoxyphenyl)-1,3-propanediol**



The title compound was prepared following the general procedure for the synthesis of 1,3-diols with *erythro tert*-butyl 2-(3,5-dimethoxyphenoxy)-3-(3,4-dimethoxyphenyl)-3-hydroxypropanoate as starting material, affording *erythro* 2-(3,5-dimethoxyphenoxy)-1-(3,4-dimethoxyphenyl)-1,3-propanediol in 96% yield as a colorless syrup.

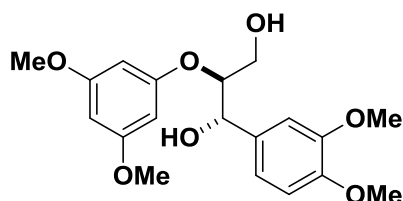
¹H NMR (400 MHz, CDCl₃): δ = 6.98–6.92 (m, 2H), 6.84 (d, J = 8.0 Hz, 1H), 6.09 (dd, J = 2.0, 2.0 Hz, 1H), 6.07 (d, J = 2.0 Hz, 2H), 5.03 (dd, J = 4.7, 3.7 Hz, 1H), 4.36 (dt, J = 4.7 Hz, 1H), 3.98–3.87 (m, 2H), 3.86 (bs, 6H), 3.72 (s, 6H), 2.87 (bs, 1H), 2.29 (bs, 1H).

¹³C NMR (101 MHz, CDCl₃): δ = 161.5 (2C), 159.5, 149.0, 148.7, 133.0, 118.7, 111.1, 109.5, 95.3 (2C), 94.0, 81.8, 73.9, 61.5, 55.9 (2C), 55.3 (2C).

MS (EI, 70 eV): m/z (%): 364 [M]⁺ (1), 210 (21), 181 (14), 180 (100), 167 (33), 155 (24), 151 (19), 139 (33), 138 (12).

HRMS (ESI, 70 eV): m/z calcd for C₁₉H₂₄O₇+Na⁺: 387.1414 [M+Na]⁺; found: 387.1413.

threo 2-(3,5-Dimethoxyphenoxy)-1-(3,4-dimethoxyphenyl)-1,3-propanediol



The title compound was prepared following the general procedure for the synthesis of 1,3-diols with *threo tert*-butyl 2-(3,5-dimethoxyphenoxy)-3-(3,4-dimethoxyphenyl)-3-hydroxypropanoate as starting material, affording *threo* 2-(3,5-dimethoxyphenoxy)-1-(3,4-dimethoxyphenyl)-1,3-propanediol in 92% yield as a colorless syrup.

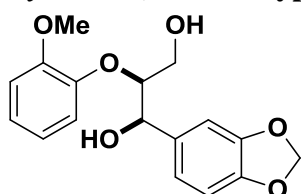
¹H NMR (400 MHz, CDCl₃): δ = 6.98 (d, J = 2.0 Hz, 1H), 6.96 (dd, J = 8.0, 2.0 Hz, 1H), 6.84 (d, J = 8.0 Hz, 1H), 6.15 (d, J = 2.0 Hz, 2H), 6.11 (dd, J = 2.0, 2.0 Hz, 1H), 4.97 (dd, J = 6.4, 2.0 Hz, 1H), 4.36 (dt, J = 6.4, 4.0 Hz, 1H), 3.86 (s, 3H), 3.86 (s, 3H), 3.74 (s, 6H), 3.82 (dt, J = 12.0, 4.0 Hz, 1H), 3.61–3.53 (m, 1H), 2.94 (bs, 1H), 2.03 (bs, 1H).

¹³C NMR (101 MHz, CDCl₃): δ = 161.6 (2C), 159.9, 149.0, 148.9, 132.3, 119.2, 111.0, 109.9, 95.2 (2C), 93.9, 82.8, 73.5, 61.1, 55.9 (2C), 55.3 (2C).

MS (EI, 70 eV): m/z (%): 364 [M]⁺ (2), 181 (14), 180 (100), 167 (29), 151 (18), 139 (28), 138 (10).

HRMS (ESI, 70 eV): m/z calcd for C₁₉H₂₄O₇+Na⁺: 387.1414 [M+Na]⁺; found: 387.1413.

erythro 2-(2-Methoxyphenoxy)-1-[3,4-(methylenedioxy)phenyl]-1,3-propanediol



erythro 2-(2-Methoxyphenoxy)-1-[3,4-(methylenedioxy)phenyl]-1,3-propanediol was synthesized following the general procedure for the synthesis of 1,3-diols with *erythro tert-butyl* 3-hydroxy-2-(2-methoxyphenoxy)-3-[3,4-(methylenedioxy)phenyl]propanoate as starting material, yielding the title compound in 88% as a white solid.

m.p.: 94-95 °C.

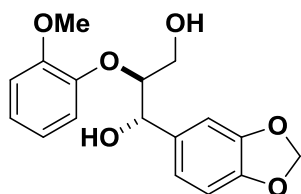
¹H NMR (400 MHz, CDCl₃): δ = 6.97 (ddd, *J* = 8.0, 7.2, 1.6 Hz, 1H), 6.89 (dd, *J* = 8.0, 1.6 Hz, 1H), 6.87–6.80 (m, 3H), 6.75 (dd, *J* = 8.0, 1.6 Hz, 1H), 6.69 (d, *J* = 8.0 Hz, 1H), 5.86 (q, *J* = 1.2 Hz, 2H), 4.87 (d, *J* = 4.7 Hz, 1H), 4.05 (ddd, *J* = 6.0, 4.7, 3.7 Hz, 1H), 3.83 (dt, *J* = 12.0, 6.0 Hz, 1H), 3.79 (s, 3H), 3.57 (dd, *J* = 12.0, 3.7 Hz, 1H), 2.92 (bs, 2H).

¹³C NMR (101 MHz, CDCl₃): δ = 151.5, 147.7, 147.0, 146.8, 133.9, 124.2, 121.6, 120.9, 119.5, 112.2, 108.1, 106.7, 101.0, 87.2, 72.7, 60.6, 55.9.

MS (EI, 70 eV): *m/z* (%): 318 [M]⁺ (5), 151 (22), 150 (100), 124 (11), 121 (14), 109 (10), 93 (14), 65 (11).

HRMS (ESI, 70 eV): *m/z* calcd for C₁₇H₁₈O₆+Na⁺: 341.0996 [M+Na]⁺; found: 341.0999.

threo 2-(2-Methoxyphenoxy)-1-(3,4-methylenedioxyphenyl)-1,3-propanediol



threo 2-(2-Methoxyphenoxy)-1-[3,4-(methylenedioxy)phenyl]-1,3-propanediol was synthesized following the general procedure for the synthesis of 1,3-diols with *threo tert-butyl* 3-hydroxy-2-(2-methoxyphenoxy)-3-[3,4-(methylenedioxy)phenyl]propanoate as starting material, yielding the title compound in 91% as a colorless syrup.

¹H NMR (400 MHz, CDCl₃): δ = 7.05 (dd, *J* = 8.0, 1.6 Hz, 1H), 7.02–6.96 (m, 1H), 6.90–6.81 (m, 4H), 6.71 (d, *J* = 8.0 Hz, 1H), 5.87 (s, 2H), 4.88 (d, *J* = 7.7 Hz, 1H), 3.92 (dt, *J* = 7.7, 3.2 Hz, 1H), 3.83 (s, 3H), 3.56 (dd, *J* = 12.0, 3.2 Hz, 1H), 3.43–3.36 (m, 1H), 2.78 (bs, 2H).

¹³C NMR (101 MHz, CDCl₃): δ = 151.3, 147.8, 147.5, 147.4, 133.5, 124.3, 121.7, 121.0, 120.7, 112.2, 108.2, 107.4, 101.0, 89.4, 73.8, 60.9, 55.9.

MS (EI, 70 eV): *m/z* (%): 318 [M]⁺ (3), 151 (22), 150 (100), 124 (13), 121 (14), 109 (11), 93 (13), 65 (10).

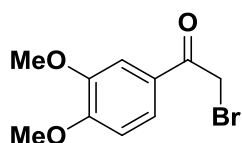
HRMS (ESI, 70 eV): *m/z* calcd for C₁₇H₁₈O₆+Na⁺: 341.0996 [M+Na]⁺; found: 341.0995.

2.2. Synthesis of monolignol and β-hydroxy ketones

The synthesis of 2-bromo-1-(3,4-dimethoxyphenyl)ethan-1-one, keto aryl ethers and β-hydroxy ketones has been published during the course of this dissertation in the journal “ChemSusChem” as part of the article “From Gene Towards Selective Biomass Valorization:

Bacterial β -Etherases with Catalytic Activity on Lignin-Like Polymers”.^[77] Likewise, the synthetic protocol for the synthesis of monolignol **11** has been published during the course of this dissertation in the journal “Green Chemistry” as part of the article “Base-catalysed cleavage of lignin β -O-4 model compounds in dimethyl carbonate”.^[26] The following synthetic protocols closely resemble those given in reference 26 and 77 and the spectroscopic data are identical to the ones given in reference 26 and 77.

2-Bromo-1-(3,4-dimethoxyphenyl)ethan-1-one



A dry and argon-flushed three-necked flask equipped with a magnetic stirrer, a reflux condenser, an argon inlet and a septum was charged with 3,4-dimethoxyacetophenone (1.530 g, 8.5 mmol, 1.0 eq.), *p*-toluenesulfonic acid monohydrate (2.420 g, 12.7 mmol, 1.5 eq.) and dry acetonitrile (200 mL). Subsequently, a solution of *N*-bromosuccinimide (1.507 g, 8.5 mmol, 1.0 eq.) in dry acetonitrile (50 mL) was added by syringe. Upon completion of the addition the reaction mixture was heated to 100 °C and stirred for 2 h. Afterwards the solution was cooled to room temperature and the solvent was removed under reduced pressure. The crude mixture was redissolved in DCM (200 mL), washed with distilled water (2×80 mL), dried over MgSO₄, filtered and the solvent removed under reduced pressure. The product was purified by column chromatography (DCM) yielding 2-bromo-1-(3,4-dimethoxyphenyl)ethan-1-one (1.790 g, 6.9 mmol, 82%) as a white solid.

m.p.: 81-82 °C.

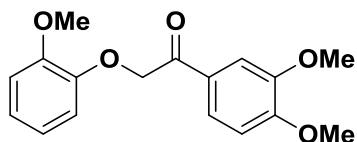
¹H NMR (600 MHz, CDCl₃): δ = 7.61 (dd, *J* = 8.4, 2.0 Hz, 1H), 7.54 (d, *J* = 2.0 Hz, 1H), 6.91 (d, *J* = 8.4 Hz, 1H), 4.41 (s, 2H), 3.96 (s, 3H), 3.94 (s, 3H).

¹³C NMR (151 MHz, CDCl₃): δ = 190.2, 154.2, 149.5, 127.2, 124.0, 111.0, 110.2, 56.3, 56.2, 30.5.

MS (EI, 70 eV): *m/z* (%): 260 [M+1]⁺ (24), 259 [M]⁺ (3), 258 (23), 166 (10), 165 (100), 151 (21), 107 (11), 79 (19), 51 (30).

2.2.1 General procedure for the synthesis of keto aryl ethers

2-Bromo-1-(3,4-dimethoxyphenyl)ethan-1-one (5.21 g, 20.1 mmol, 1.0 eq.), anhydrous K₂CO₃ (2.78 g, 20.1 mmol, 1.0 eq.) and the corresponding phenol derivative (20.1 mmol, 1.0 eq.) were dissolved in acetone (50 mL). Afterwards the solution was stirred at room temperature overnight. Next, the reaction mixture was filtered, washed with DCM and the solvent removed under reduced pressure. The crude mixture was redissolved in DCM and washed with distilled water (2×100 mL) and brine (90 mL). The organic phase was dried over MgSO₄, filtered and evaporated under reduced pressure. Purification by column chromatography (pentane/ethyl acetate = 5:1 to 2:1) yielded the desired product.

1-(3,4-Dimethoxyphenyl)-2-(2-methoxyphenoxy)ethan-1-one

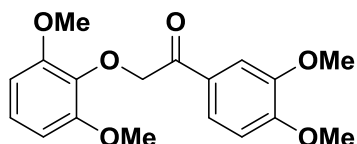
The title compound was synthesized following the general procedure for keto aryl ethers, affording 1-(3,4-dimethoxyphenyl)-2-(2-methoxyphenoxy)ethan-1-one in 88% yield as a white solid.

m.p.: 94-95 °C.

¹H NMR (400 MHz, CDCl₃): δ = 7.67 (dd, J = 8.4, 2.0 Hz, 1H), 7.59 (d, J = 2.0 Hz, 1H), 6.96–6.84 (m, 5H), 5.28 (s, 2H), 3.94 (s, 3H), 3.93 (s, 3H), 3.88 (s, 3H).

¹³C NMR (101 MHz, CDCl₃): δ = 193.4, 153.9, 149.8, 149.3, 147.7, 128.0, 122.9, 122.5, 120.9, 114.8, 112.3, 110.6, 110.3, 72.2, 56.2, 56.1, 56.0.

MS (EI, 70 eV): m/z (%): 303 [M+1]⁺ (10), 302 [M]⁺ (53), 165 (100), 151 (11), 77 (14), 51 (11).

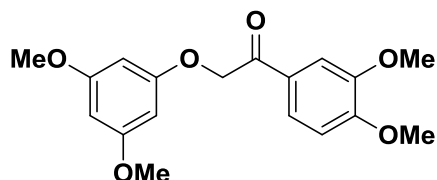
2-(2,6-Dimethoxyphenoxy)-1-(3,4-dimethoxyphenyl)ethan-1-one

2-(2,6-dimethoxyphenoxy)-1-(3,4-dimethoxyphenyl)ethan-1-one was prepared following the general procedure for keto aryl ethers yielding the title compound in 85% as a colorless oil.

¹H NMR (400 MHz, CDCl₃): δ = 7.72 (dd, J = 8.4, 1.8 Hz, 1H), 7.64 (d, J = 1.8 Hz, 1H), 7.01 (t, J = 8.4 Hz, 1H), 6.89 (d, J = 8.4 Hz, 1H), 6.58 (d, J = 8.4 Hz, 2H), 5.15 (s, 2H), 3.94 (s, 3H), 3.94 (s, 3H), 3.81 (s, 6H).

¹³C NMR (101 MHz, CDCl₃): δ = 193.7, 153.4 (2C), 153.2, 149.0, 136.6, 128.4, 124.1, 123.0, 110.6, 110.0, 105.3 (2C), 75.3, 56.1 (2C), 56.0 (2C).

MS (EI, 70 eV): m/z (%): 332 [M]⁺ (30), 166 (10), 165 (100), 153 (11), 152 (10), 151 (29), 107 (11).

2-(3,5-Dimethoxyphenoxy)-1-(3,4-dimethoxyphenyl)ethan-1-one

The title compound was synthesized following the general procedure for keto aryl ethers yielding 2-(3,5-dimethoxyphenoxy)-1-(3,4-dimethoxyphenyl)ethan-1-one in 90% as a white solid.

m.p.: 110-111 °C.

¹H NMR (400 MHz, CDCl₃): δ = 7.63 (dd, J = 8.4, 1.8 Hz, 1H), 7.55 (d, J = 1.8 Hz, 1H), 6.90 (d,

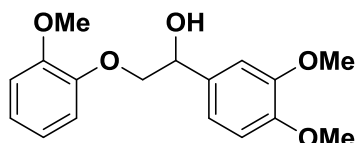
$J = 8.4$ Hz, 1H), 6.13 (d, $J = 2.1$ Hz, 2H), 6.11 (t, $J = 2.1$ Hz, 1H), 5.18 (s, 2H), 3.96 (s, 3H), 3.94 (s, 3H), 3.75 (s, 6H).

^{13}C NMR (101 MHz, CDCl_3): $\delta = 192.7, 161.5$ (2C), 159.9, 153.9, 149.3, 127.7, 122.7, 110.3, 110.1, 93.9, 93.7, 93.6, 70.6, 56.1, 56.0, 55.4 (2C).

MS (EI, 70 eV): m/z (%): 332 $[\text{M}]^+$ (23), 166 (10), 165 (100).

HRMS (ESI, 70 eV): m/z calcd for $\text{C}_{18}\text{H}_{20}\text{O}_6 + \text{Na}^+$: 355.1145 $[\text{M} + \text{Na}]^+$; found: 355.1152.

1-(3,4-Dimethoxyphenyl)-2-(2-methoxyphenoxy)ethan-1-ol



A dry 250 mL three-necked flask equipped with a reflux condenser, an argon inlet, a dropping funnel and a magnetic stirrer was charged with LiAlH_4 (0.469 g, 12.4 mmol, 1.0 eq.) and dry THF (31 mL) and cooled to 0 °C. 1-(3,4-Dimethoxyphenyl)-2-(2-methoxyphenoxy)ethan-1-one (3.74 g, 12.4 mmol, 1.0 eq.) was dissolved in dry THF (43 mL) and added dropwise over 15 min under cooling (0 °C). The resulting solution was heated to 60 °C and stirred for 3 h. Upon completion of the reaction it was cooled to 0 °C and quenched by the sequential and dropwise addition of water (0.470 mL), aqueous NaOH solution (15% w/w, 0.470 mL) and additional water (1.410 mL). Afterwards the mixture was stirred for 1 h at room temperature. Then the reaction solution was filtered over celite, washed with DCM (150 mL), dried over MgSO_4 , and the solvent removed under reduced pressure. The product was purified by column chromatography (pentane/ethyl acetate = 1:1) yielding 1-(3,4-dimethoxyphenyl)-2-(2-methoxyphenoxy)ethan-1-ol (3.06 g, 10.1 mmol, 81%) as a white solid.

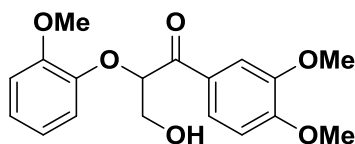
m.p.: 133-134 °C.

^1H NMR (400 MHz, CDCl_3): $\delta = 7.03$ –6.88 (m, 6H), 6.86 (d, $J = 8.2$ Hz, 1H), 5.05 (dd, $J = 9.4, 2.9$ Hz, 1H), 4.17 (dd, $J = 10.0, 3.0$ Hz, 1H), 3.97 (t, $J = 9.4$ Hz, 1H), 3.90 (s, 3H), 3.89 (s, 3H), 3.88 (s, 3H), 3.44 (bs, 1H).

^{13}C NMR (101 MHz, CDCl_3): $\delta = 150.1, 149.0, 148.7, 147.9, 132.2, 122.5, 121.0, 118.6, 116.9, 111.9, 110.9, 109.3, 76.3, 72.0, 55.9, 55.8, 55.7$.

MS (EI, 70 eV): m/z (%): 305 $[\text{M} + 1]^+$ (48), 304 $[\text{M}]^+$ (90), 288 (14), 287 (55), 181 (10), 180 (56), 168 (18), 167 (100), 164 (10), 151 (73), 149 (28), 139 (90), 138 (80), 137 (10), 124 (43), 122 (16), 121 (15), 109 (19), 108 (11), 95 (11), 77 (30), 65 (10).

1-(3,4-Dimethoxyphenyl)-3-hydroxy-2-(2-methoxyphenoxy)propan-1-one



A 100 mL flask was charged with 1-(3,4-dimethoxyphenyl)-2-(2-methoxyphenoxy)ethanone (1.980 g, 6.550 mmol, 1.0 eq.), paraformaldehyde (0.240 g, 7.860 mmol, 1.2 eq.), anhydrous

K_2CO_3 (0.045 g, 0.328 mmol, 0.05 eq.) and dry DMSO (17 mL). The resulting mixture was stirred at room temperature for 1 h. To quench the reaction ethyl acetate (40 mL) and distilled water (20 mL) were added and the aqueous phase was extracted with ethyl acetate (20 mL). The organic phase was washed with brine (20 mL), dried over $MgSO_4$, filtered and the solvent removed under reduced pressure. The product was purified by column chromatography (DCM/MeOH = 200:1 to 100:3) yielding 1-(3,4-dimethoxyphenyl)-3-hydroxy-2-(2-methoxyphenoxy)propan-1-one (1.740 g, 5.235 mmol, 80%) as a white solid.

m.p.: 116-117 °C.

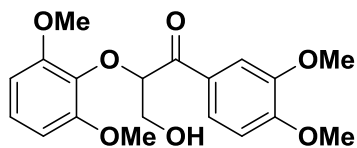
1H NMR (600 MHz, $CDCl_3$): δ = 7.75 (dd, J = 8.4, 2.0 Hz, 1H), 7.62 (d, J = 2.0 Hz, 1H), 7.00 (td, J = 8.0, 1.4 Hz, 1H), 6.94–6.86 (m, 3H), 6.82 (td, J = 8.0, 1.4 Hz, 1H), 5.40 (t, J = 5.3 Hz, 1H), 4.07 (d, J = 5.3 Hz, 2H), 3.95 (s, 3H), 3.92 (s, 3H), 3.86 (s, 3H).

^{13}C NMR (151 MHz, $CDCl_3$): δ = 195.0, 153.9, 150.5, 149.2, 146.9, 128.0, 123.7, 123.6, 121.2, 118.5, 112.2, 110.9, 110.1, 84.6, 63.7, 56.1, 56.0, 55.8.

MS (EI, 70 eV): m/z (%): 333 $[M+1]^+$ (7), 332 $[M]^+$ (31), 166 (11), 165 (100), 150 (30), 77 (11).

HPLC ($H_2O/MeOH$, 60/40): t_R = 24.0 min.

2-(2,6-Dimethoxyphenoxy)-1-(3,4-dimethoxyphenyl)-3-hydroxypropan-1-one



A 100 ml flask was charged with 2-(2,6-dimethoxyphenoxy)-1-(3,4-dimethoxyphenyl)ethan-1-one (1.255 g, 3.688 mmol, 1.0 eq.), paraformaldehyde (0.222 g, 7.377 mmol, 2.0 eq.), anhydrous K_2CO_3 (0.510 g, 3.688 mmol, 1.0 eq.) and dry DMSO (12 mL). The resulting mixture was stirred at room temperature for 20 h. To quench the reaction ethyl acetate (40 mL) and distilled water (20 mL) were added and the aqueous phase was extracted with ethyl acetate (20 mL). The organic phase was washed with brine (20 mL), dried over $MgSO_4$, filtered and the solvent removed under reduced pressure. The product was purified by column chromatography (DCM/MeOH = 200:1) yielding 2-(2,6-dimethoxyphenoxy)-1-(3,4-dimethoxyphenyl)-3-hydroxypropan-1-one (0.685 g, 1.890 mmol, 51%) as a colorless oil.

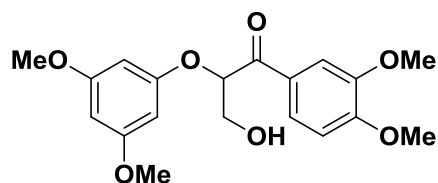
1H NMR (600 MHz, $CDCl_3$): δ = 7.69 (dd, J = 8.4, 1.8 Hz, 1H), 7.63 (d, J = 1.8 Hz, 1H), 6.98 (t, J = 8.4 Hz, 1H), 6.85 (d, J = 8.4 Hz, 1H), 6.54 (d, J = 8.4 Hz, 2H), 5.07 (dd, J = 7.8, 3.6 Hz, 1H), 4.01–3.92 (m, 2H), 3.91 (s, 3H), 3.91 (s, 3H), 3.83–3.77 (m, 1H), 3.69 (s, 6H).

^{13}C NMR (151 MHz, $CDCl_3$): δ = 194.9, 153.4, 152.7 (2C), 149.0, 136.6, 128.6, 124.3, 123.4, 110.8, 110.0, 105.2 (2C), 87.4, 63.6, 56.0 (2C), 55.9 (2C).

MS (EI, 70 eV): m/z (%): 362 $[M]^+$ (30), 180 (47), 166 (11), 165 (100), 154 (46), 153 (23), 151 (14), 110 (10), 77 (12).

HRMS (ESI, 70 eV): m/z calcd for $C_{19}H_{23}O_7^+$: 363.1437 $[M+H]^+$; found: 363.1438.

2-(3,5-Dimethoxyphenoxy)-1-(3,4-dimethoxyphenyl)-3-hydroxypropan-1-one



A 100 ml flask was charged with 2-(3,5-dimethoxyphenoxy)-1-(3,4-dimethoxyphenyl)ethan-1-one (0.590 g, 1.775 mmol, 1.0 eq.), paraformaldehyde (0.053 g, 1.775 mmol, 1.0 eq.), anhydrous K_2CO_3 (0.012 g, 0.088 mmol, 0.05 eq.) and dry DMSO (5 mL). The resulting mixture was stirred at room temperature for 25 h. To quench the reaction ethyl acetate (20 mL) and distilled water (10 mL) were added and the aqueous phase was extracted with ethyl acetate (20 mL). The organic phase was washed with brine (10 mL), dried over $MgSO_4$, filtered and the solvent removed under reduced pressure. The product was purified by column chromatography (DCM/MeOH = 200:1) yielding 2-(3,5-dimethoxyphenoxy)-1-(3,4-dimethoxyphenyl)-3-hydroxypropan-1-one (0.280 g, 0.773 mmol, 43%) as a white solid.

m.p.: 133-134 °C.

1H NMR (600 MHz, $CDCl_3$): δ = 7.72 (dd, J = 8.4, 1.9 Hz, 1H), 7.55 (d, J = 1.9 Hz, 1H), 6.87 (d, J = 8.4 Hz, 1H), 6.07 (s, 3H), 5.50 (dd, J = 6.2, 4.1 Hz, 1H), 4.11 (ddd, J = 18.4, 12.1, 5.2 Hz, 2H), 3.94 (s, 3H), 3.89 (s, 3H), 3.70 (s, 6H), 2.53 (bs, 1H).

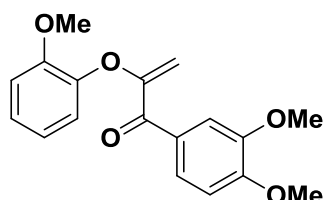
^{13}C NMR (151 MHz, $CDCl_3$): δ = 194.7, 161.6 (2C), 159.1, 154.1, 149.3, 127.8, 123.5, 110.8, 110.2, 94.1 (2C), 93.9, 80.6, 63.4, 56.1, 55.9, 55.3 (2C).

MS (EI, 70 eV): m/z (%): 362 $[M]^+$ (24), 180 (37), 166 (17), 165 (100), 155 (12), 77 (12).

HRMS (ESI, 70 eV): m/z calcd for $C_{19}H_{23}O_7^+$: 363.1439 $[M+H]^+$; found: 363.1438.

2.3. Synthesis 1-(3,4-dimethoxyphenyl)-2-(2-methoxyphenoxy)prop-2-en-1-one

1-(3,4-dimethoxyphenyl)-2-(2-methoxyphenoxy)prop-2-en-1-one



1-(3,4-Dimethoxyphenyl)-3-hydroxy-2-(2-methoxyphenoxy)propan-1-one (1.002 g, 3.015 mmol, 1.0 eq.) was dissolved in dry DMSO (42 mL). Anhydrous K_2CO_3 (0.833 g, 6.027 mmol, 2.0 eq.) was added and the reaction mixture was stirred at room temperature overnight. After 20 h the reaction was stopped by the addition of ethyl acetate (60 mL) and distilled water (60 mL). The aqueous phase was extracted with ethyl acetate (3×20 mL). The

combined organic phases were then washed with brine (100 mL), dried over MgSO₄, filtered and evaporated under reduced pressure. The product was purified by column chromatography (DCM) yielding 1-(3,4-dimethoxyphenyl)-2-(2-methoxyphenoxy)prop-2-en-1-one (0.748 g, 2.380 mmol, 79%) as a pale yellow oil.

¹H NMR (600 MHz, CDCl₃): δ = 7.83 (dd, J = 8.4, 1.9 Hz, 1H), 7.64 (d, J = 1.8 Hz, 1H), 7.14 (td, J = 7.2, 1.5 Hz, 1H), 7.08 (dd, J = 7.9, 1.5 Hz, 1H), 6.98 (dd, J = 8.4, 1.0 Hz, 1H), 6.93 (td, J = 7.8, 1.5 Hz, 1H), 6.90 (d, J = 8.4 Hz, 1H), 5.21 (d, J = 2.4 Hz, 1H), 4.71 (d, J = 2.4 Hz, 1H), 3.95 (s, 3H), 3.93 (s, 3H), 3.87 (s, 3H).

¹³C NMR (151 MHz, CDCl₃): δ = 189.2, 158.1, 153.5, 151.1, 148.8, 143.4, 129.2, 125.9, 125.2, 121.8, 121.4, 113.0, 112.4, 110.0 (2C), 56.2, 56.1, 56.0.

MS (EI, 70 eV): m/z (%): 315 [M+1]⁺ (6), 314 [M]⁺ (28), 166 (11), 165 (100), 163 (17), 77 (11).

HRMS (ESI, 70 eV): m/z calcd for C₁₈H₁₈O₅+Na⁺: 337.1046 [M+Na]⁺; found: 337.1046.

3. Synthesis and catalysis with iron catalysts

3.1. Synthesis of FeCl₃-derived iron complexes

All iron complexes were synthesized following the protocol described by Cahiez *et. al.*^[58] Depending on the added nitrogen ligand the reaction time was extended to facilitate the precipitation of the formed complexes.

3.1.1 General procedure for the synthesis of FeCl₃-derived iron complexes

A dry 100 mL Schlenk flask was charged with anhydrous FeCl₃ (0.811 g, 5 mmol, 1.0 eq.) which was dissolved in 50 mL dry THF. Subsequently, the respective amine (7.5 mmol, 1.5 eq.) was added and the reaction mixture stirred for 1 h at room temperature. Upon completion, the reaction mixture was filtered, the resulting solid washed with THF (3×5 mL) and pentane (3×5 mL) and dried overnight under high vacuum.

{Fe-TMEDA}

The title compound was prepared using the general procedure for the synthesis of FeCl₃-derived iron complexes except that the reaction time was extended to 65 h. TMEDA was used as amine giving {Fe-TMEDA} in 91% yield as an orange to brown solid.

ICP-OES: 131.0 mg/g Fe

Elem. Anal. calcd. for C₁₈H₄₈Cl₆Fe₂N₆ (673.01): C = 32.12, H = 7.19, N = 12.49; found: C = 27.04, H = 6.84, N = 10.31.

{Fe-HMTA}

The title compound was synthesized using the general procedure for the synthesis of FeCl₃-derived iron complexes on a threefold higher reaction scale and a reaction time of 16 h. HMTA was used as amine to give {Fe-HMTA} in 93% as a brown solid.

ICP-OES: 120.0 mg/g Fe

Elem. Anal. calcd. for C₁₈H₃₆Cl₆Fe₂N₁₂ (744.96): C = 29.02, H = 4.87, N = 22.56; found: C = 27.82, H = 5.34, N = 21.29.

{Fe-DABCO}

The title compound was prepared using the general procedure for the synthesis of FeCl₃-derived iron complexes with DABCO as amine giving {Fe-DABCO} in 97% yield as a brown solid.

ICP-OES: 134.2 mg/g Fe

Elem. Anal. calcd. for C₁₈H₃₆Cl₆Fe₂N₆ (660.92): C = 32.71, H = 5.49, N = 12.72; found: C = 27.30, H = 5.91, N = 10.52.

{Fe-PMDTA}

The title compound was prepared using the general procedure for the synthesis of FeCl₃-derived iron complexes with PMDTA as amine giving {Fe-PMDTA} in 93% yield as a brown solid.

ICP-OES: 99.2 mg/g Fe

Elem. Anal. calcd. for $C_{18}H_{50}Cl_6Fe_2N_9O_2$ (707.03): C = 30.58, H = 7.13, N = 11.89; found: C = 30.78, H = 7.52, N = 11.85.

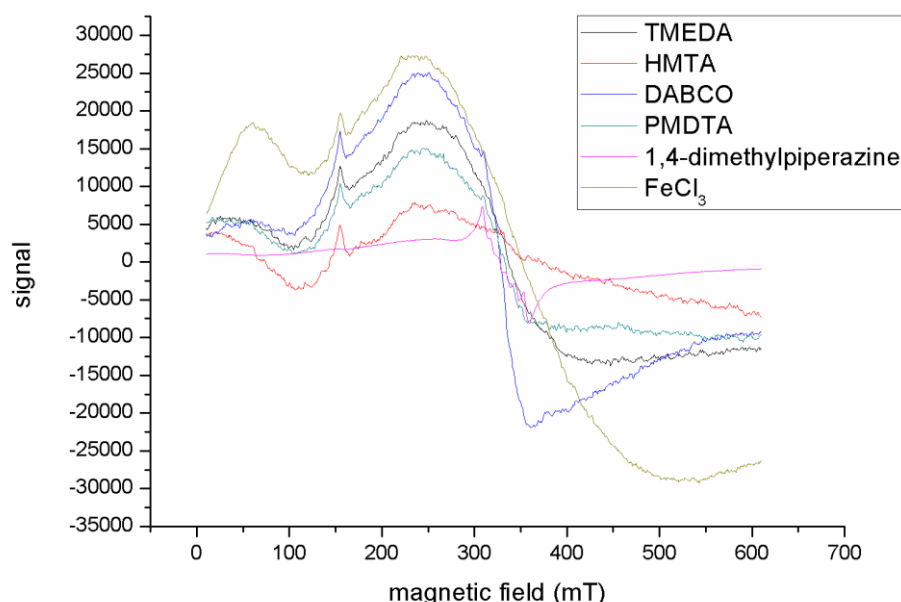
{Fe-1,4-dimethylpiperazine}

The title compound was prepared using the general procedure for the synthesis of $FeCl_3$ -derived iron complexes except that the reaction time was extended to 16 h. 1,4-Dimethylpiperazine was used as amine giving {Fe-1,4-dimethylpiperazine} in 64% yield as a brown solid.

ICP-OES: 114.7 mg/g Fe

Elem. Anal. calcd. for $C_{18}H_{42}Cl_6Fe_2N_6$ (666.97): C = 32.42, H = 6.35, N = 12.60; found: C = 28.11, H = 7.49, N = 10.83.

EPR Spectra of the Iron complexes and $FeCl_3$



3.2. Catalysis reaction with $FeCl_3$ -derived iron complexes

3.2.1 General reaction condition for the catalysis reactions with $FeCl_3$ -derived iron complexes

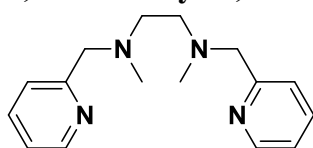
A flask 25 mL was charged with dilignol **3aE** (0.0836 g, 0.250 mmol, 1.0 eq.), the respective iron catalyst and the desired additive and dissolved in the corresponding solvent. Subsequently, either H_2O_2 or TBHP were added as oxidant. Next, the flask was equipped with a reflux condenser and heated to the desired reaction temperature. Upon completion of the respective reaction time, the mixture was cooled to room temperature and the reaction quenched by the addition of 1 M HCl (20 mL). If the reaction was to be analyzed by HPLC, 1.000 mL of a standard-solution (3,4-dimethoxybenzylalcohol in methanol, $c = 0.2$ mol/L) was added with an Eppendorf-pipette to the reaction solution. The aqueous phase was extracted with DCM (3×20 mL). The combined organic phases were washed with brine

(20 mL), distilled H₂O (20 mL) and additional brine (20 mL), dried over MgSO₄, filtered and the solvent was removed under reduced pressure. For HPLC measurements three samples were taken by weighing 2.0 to 3.0 mg of the reaction product into a vial. Then, 0.5 mL of ethyl acetate and 0.5 mL of acetonitrile were added to the vial and after the complete dissolution of all products, the solution was filtered into a HPLC vial.

3.3. Synthesis of nonheme iron complexes

All nonheme iron complexes were synthesized using a modified protocol by White *et. al.*^[54].

N,N'-Dimethyl-*N,N'*-bis(2-pyridylmethyl)-ethane-1,2-diamine (mep)



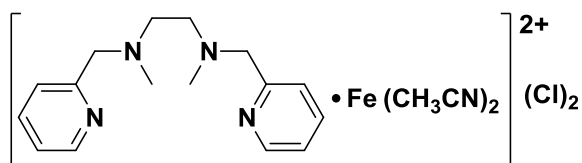
2-(Chloromethyl)pyridine hydrochloride (3.0 g, 18.3 mmol, 2.1 eq.) was dissolved in 100 mL DCM and K₂CO₃ (5.1 g, 37.0 mmol, 4.2 eq.) was added. The solution was washed with water, dried over MgSO₄ and the solvent removed under reduced pressure yielding 2-(chloromethyl)pyridine. Subsequently, it was redissolved in 10 mL DCM and *N,N'*-dimethyl ethylenediamine (0.771 g, 8.75 mmol, 1.0 eq.), dissolved in 25 mL DCM, was added. Then 20 mL of a 1 M NaOH solution was added and the reaction stirred for 90 h at room temperature. The reaction mixture was diluted with 50 mL 1 M NaOH and extracted with DCM (3×40 mL). The combined organic phases were dried over MgSO₄, filtered and the solvent removed under reduced pressure. The product was purified by column chromatography (DCM/MeOH/Et₃N = 95:5:1), then dissolved in acetonitrile overlaid with diethyl ether and kept in the freezer. Overnight the residual impurities precipitated and the clear solution was decanted off. Under reduced pressure the solvent was removed yielding the title compound (1.68 g, 6.22 mmol, 71%) as a yellow oil.

¹H NMR (400 MHz, CDCl₃): δ = 8.54–8.47 (m, 2H), 7.60 (td, *J* = 7.7 Hz, 1.8 Hz, 2H), 7.39 (d, *J* = 7.8 Hz, 2H), 7.15–7.10 (m, 2H), 3.67 (s, 4H), 2.64 (s, 4H), 2.25 (s, 6H).

¹³C NMR (101 MHz, CDCl₃): δ = 159.1 (2C), 149.0 (2C), 136.4 (2C), 123.2 (2C), 122.0 (2C), 64.1 (2C), 55.3 (2C), 42.8 (2C).

MS (EI, 70 eV): *m/z* (%): 270 [M]⁺ (3), 148 (22), 135 (100), 93 (28), 92 (56), 65 (17).

[Fe(mep)(CH₃CN)₂](Cl)₂

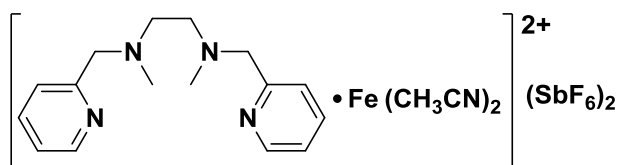


A dry 100 mL Schlenk flask equipped with a magnetic stirrer was charged with *N,N'*-dimethyl-*N,N'*-bis(2-pyridylmethyl)-ethane-1,2-diamine (mep) (1.08 g, 4.00 mmol,

1.0 eq.) and dissolved in 25 mL dry acetonitrile. $\text{FeCl}_2 \cdot 4\text{H}_2\text{O}$ (0.92 g, 4.60 mmol, 1.15 eq.) was added and the solution stirred for 24 h at room temperature. 25 mL of diethyl ether were added to the solution and the orange precipitant was filtered and washed with diethyl ether. The product was dried under an argon flow for 4 h yielding the title compound (1.29 g, 2.69 mmol, 67%) as an orange solid.

MS (ESI): m/z calcd for $\text{C}_{16}\text{H}_{22}\text{ClFeN}_4^+$: 361.09 $[\text{Fe}(\text{mep})\text{Cl}]^+$; found: 361.09.

$[\text{Fe}(\text{mep})(\text{CH}_3\text{CN})_2](\text{SbF}_6)_2$



A flame dried schlenk flask was charged in the glove box with AgSbF_6 (0.210 g, 0.611 mmol, 2.0 eq.). Under an argon atmosphere $[\text{Fe}(\text{mep})(\text{CH}_3\text{CN})_2](\text{Cl})_2$ (0.147 g, 0.306 mmol, 1.0 eq) and dry acetonitrile (6 mL) were added. The mixture was stirred at room temperature for 92 h under light exclusion. Upon completion the solution was filtered twice over celite. Then the solvent was removed under reduced pressure and dried under an argon current for 5 h. The title compound (0.251 g, 0.285 mmol, 93%) was obtained as a purple solid.

ESI-MS did not provide conclusive evidence about the structure of the complex.

3.4. Catalysis reaction with nonheme iron complexes

3.4.1 General reaction condition for the catalysis reactions with nonheme iron complexes

Dilignol **3aE** (0.0836 g, 0.250 mmol, 1.0 eq.) and the respective iron catalyst were dissolved in the corresponding solvent. Subsequently, AcOH (0.007 mL, 0.125 mmol, 0.5 eq) and the corresponding amount of H_2O_2 as oxidant were added. Next, the flask was equipped with a reflux condenser and heated to the desired reaction temperature. Upon completion of the respective reaction time, the mixture was cooled to room temperature and the reaction quenched by the addition of DCM (15 mL) and 1 M HCl (50 mL). The aqueous phase was extracted with DCM (3×20 mL) and the combined organic phases were washed with 1M HCl and brine, dried over MgSO_4 , filtered and the solvent removed under reduced pressure. The crude product was then analyzed by ^1H NMR in CDCl_3 .

4. Synthesis and catalysis with supported gold catalysts

4.1. Synthesis of supported gold catalysts

4.1.1 Synthesis of air calcined gold on cerium oxide catalyst

An 800 mL beaker equipped with a magnetic stirrer was charged with 500 mL of Milli-Q water and heated to 70 °C. $\text{HAuCl}_4 \cdot 3\text{H}_2\text{O}$ (0.0393 g, 0.10 mmol) dissolved in Milli-Q water was added. Next, the pH was adjusted from 3.5 to 5.9 with a 0.2 M NaOH solution. Then CeO_2 (Rhodia) (0.570 g, 3.31 mmol) was added rapidly, the pH was adjusted to 8.2 and stirred for 30 minutes. During that time the pH dropped to 7.5. Upon completion the mixture was cooled to 0 °C and centrifuged three times at 12000 rpm for 10 minutes. Each time the solution was discarded and deionized water added to the solid before centrifugation. Afterwards the catalyst was filtered off and dried under vacuum and light exclusion overnight. The catalyst was calcined at 400 °C under air for 8 h with a heating rate of 5 °C/min. Au/ CeO_2 was obtained in 34% yield (0.195 g, 1.13 mmol).

ICP-OES: 8.9 mg/g Au

4.1.2 Synthesis of reduced supported gold catalysts

All reduced supported gold catalysts were synthesized by Alós or Juárez at the Instituto de Tecnología Química (UPV-CSIC), Valencia, Spain. The gold loading for all the employed catalysts was around 1% in weight.

Au/HTc

3 g of hydrotalcite ($\text{Mg}/\text{Al} = 3$), 370 mL of HAuCl_4 ($5 \cdot 10^{-4}$ M) and urea (1.115 g, 18.56 mmol, ratio $c_{\text{urea}}/c_{\text{Au}}$, $\sim 100/1$) were stirred at 80 °C for 1 h. Upon completion the mixture was 4 times centrifuged at 12000 rpm for 10 min and washed with deionized water. The absence of chloride was monitored by adding some drops of a AgNO_3 solution to the last washing solution. Afterwards the sample was dried at room temperature under vacuum for 12 h. Au/HTc was either reduced using the general procedure for H_2 or 1-phenylethanol reduction.

Au/ CeO_2

CeO_2 (Rhodia) was calcined under air at 450 °C for 8 h with a slope of 2 °C/min. A 500 mL flask was charged with HAuCl_4 (0.050 g, 0.147 mmol) and 125 mL of Milli-Q water and stirred at 400 rpm. The pH of the resulting solution was measured (pH = 3.01) and adjusted to 10 by adding a 0.2 M NaOH solution. Once pH 10 was reached and stabilized, calcined CeO_2 (2.5 g, 14.5 mmol) was added. During the next 30 minutes the pH of the mixture was measured and maintained at 10 with a 0.2 M NaOH solution. The flask was closed and the mixture stirred overnight for 18 h. Upon completion the pH was measured and once more adjusted to 10. The sample was filtered with a nylon 0.45 μL filter and washed with 4 L of deionized water and acetone. Afterwards the solid was dried overnight at room temperature. Au/ CeO_2 was either reduced using the general procedure for H_2 or 1-phenylethanol reduction.

Au/MgO

MgO (Nanoscale) was calcined under N_2 at 450 °C for 5.5 h with a slope of 5 °C/min. A 500 ml flask was charged with HAuCl_4 (0.050 g, 0.147 mmol) and 125 ml of Milli-Q water

and stirred at 400 rpm. The pH of this solution was measured (pH = 2.99) and calcined MgO (2.5 g, 62.0 mmol) was added. After the addition the pH rose to 11.2 and after 40 minutes it decreased to 10.8. The flask was closed and the mixture stirred overnight for 18 h. Upon completion the mixture was 3 times centrifuged at 10000 rpm for 15 min at 10 °C and washed with Milli-Q water. Afterwards the sample was dried under vacuum at room temperature for 12 h. Au/MgO was either reduced using the general procedure for H₂ or 1-phenylethanol reduction.

General procedure for the reduction of supported gold catalyst with H₂

1 g of the corresponding supported gold catalyst was reduced at 400 °C for 4 h (slope = 5 °C/min) with a H₂ flow of 100 mL/min.

General procedure for the reduction of supported gold catalyst with 1-phenylethanol

1 g of the corresponding supported gold catalyst was reduced with 12 mL of 1-phenylethanol at 160 °C for 1.5 h. The sample was filtered, washed with acetone, water and again with acetone and dried at 100 °C overnight.

4.1.3 General reaction condition for the catalysis reactions with air calcined gold on cerium oxide catalyst

A glass-autoclave was charged with dilignol **3aE** (0.084 g, 0.250 mmol, 1.0 eq.), Au/CeO₂ (0.004 g, 0.025 mmol, 0.1 eq.), base (0.25 mmol, 1.0 eq.) and a magnetic stirrer. Subsequently, 1.25 mL of the desired solvent was added. The autoclave was purged three times with oxygen, charged with 5 or 6 bar of oxygen and stirred in a preheated oil bath at corresponding reaction temperature. After the expiration of the desired reaction time the autoclave was taken out of the oil bath and cooled to room temperature. The remaining oxygen pressure was released and the autoclave opened. The reaction mixture was filtered and the autoclave rinsed with DCM (20 mL). The organic phase was washed with 1 M HCl (20 mL) and brine (20 mL), dried over MgSO₄, filtered and the solvent removed under reduced pressure. The crude product was then analyzed by ¹H NMR in CDCl₃.

4.1.4 General reaction condition for the catalysis reactions with reduced supported gold catalysts

A 25 mL glass-autoclave or 20 mL steel autoclave was charged with dilignol **3aE** (83.6 mg, 0.250 mmol, 1.0 eq.), the respective supported gold catalyst (16.7 mg, 20 wt%) and a magnetic stirrer. Subsequently, 1.25 mL of the desired solvent was added. The autoclave was purged three times with oxygen, charged with the respective oxygen pressure and stirred in a preheated oil bath at 135 °C. After the expiration of the desired reaction time the autoclave was taken out of the oil bath and cooled to room temperature. The remaining oxygen pressure was released and the autoclave opened. If the reaction was to be analyzed by HPLC, 1.000 mL of a standard-solution (3,4-dimethoxybenzylalcohol in methanol, c = 0.2 mol/L) was added with an Eppendorf-pipette to the reaction solution. The reaction mixture was filtered into 50 mL of a 1 M HCl solution, the autoclave rinsed with DCM (10 mL) and the catalyst was washed with DCM (20 mL). The aqueous phase was then extracted with DCM (4×20 mL). Next, the combined organic phases were washed with 1 M HCl (50 mL) and brine (50 mL), dried over MgSO₄, filtered and the solvent removed under reduced pressure. A minimum of three samples was taken from each reaction for HPLC measurements. For each

sample 2.0 to 3.0 mg of the reaction product were weighed into a vial. Then, 0.5 mL of ethyl acetate and 0.5 mL of acetonitrile were added to the vial and after the complete dissolution of all products, the solution was filtered into a HPLC vial.

4.1.5 General reaction condition for the catalysis reactions in DMC

A 25 mL two-necked flask was charged with dilignol **3aE** (0.0836 g, 0.250 mmol, 1.0 eq.) and the respective supported gold catalyst or base (0.0167 g, 20 wt%). 1.25 mL dimethyl carbonate was added, the flask equipped with a reflux condenser and the reaction mixture put under a dioxygen atmosphere of 1 atm by using a gas storage balloon. Next, the reaction was heated to 135 °C and stirred for the desired reaction time. Upon completion the mixture was cooled to room temperature, filtered into 50 mL of a 1 M HCl solution, the autoclave rinsed with DCM (10 mL) and the catalyst was washed with DCM (20 mL). The aqueous phase then was extracted with DCM (3×20 mL), the combined organic phases washed with 1M HCl (25 mL) and brine (25 mL), dried over MgSO₄, filtered and the solvent removed under reduced pressure. The crude product was then analyzed by ¹H NMR in CDCl₃.

5. Synthesis and catalysis with hydrotalcite-like catalysts

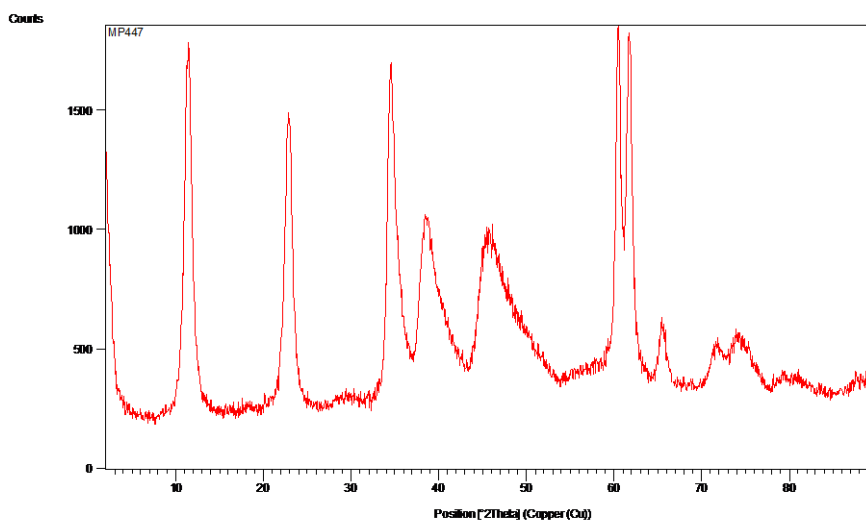
All hydrotalcite-like catalysts (HTc) were synthesized by Puche at the Instituto de Tecnología Química (UPV-CSIC), Valencia, Spain. The synthesis of all hydrotalcite-like catalysts is described in the article “Copper- and Vanadium-Catalyzed Oxidative Cleavage of Lignin using Dioxygen” which has been published in the journal “ChemSusChem” during the course of this dissertation.^[78] The following spectroscopic data and synthetic procedures involving HTc as catalyst are identical to those given in reference 78. The molar ratio in all hydrotalcite-like catalysts is $M^{2+}/M^{3+} = 3$.

5.1. Spectroscopic data for the hydrotalcite-like catalysts

HTc:

ICP-OES: 248.1 mg/g Mg, 94.1 mg/g Al.

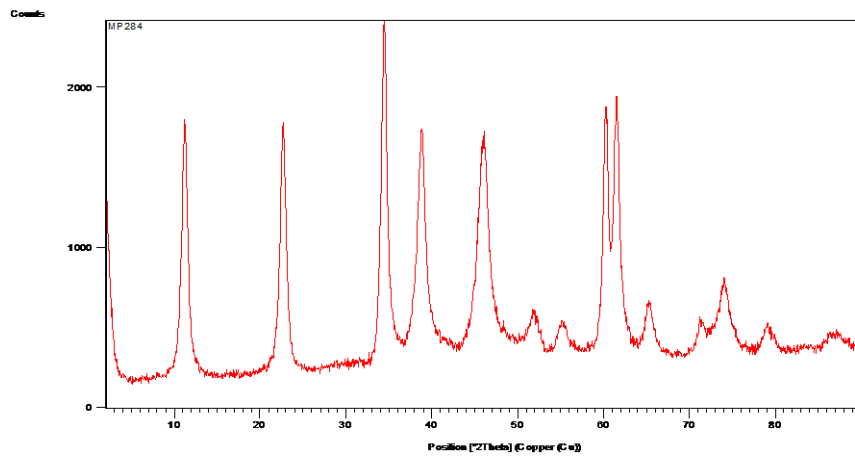
XRD:



HTc-Zn:

ICP-OES: 235.8 mg/g Mg, 95.3 mg/g Al, 7.4 mg/g Zn.

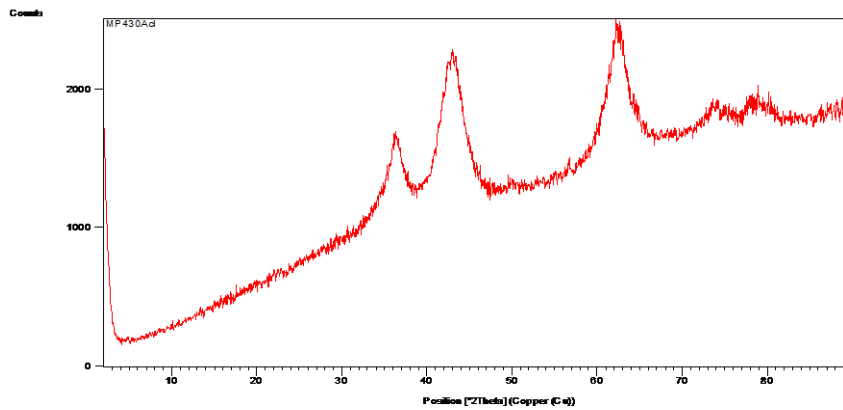
XRD:



HTc-Cu:

ICP-OES: 353.0 mg/g Mg, 150.9 mg/g Al, 156.3 mg/g Cu.

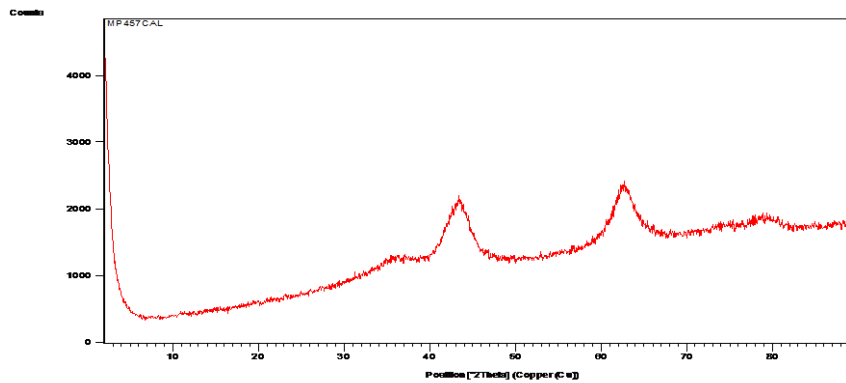
XRD:



HTc-Zn-Cu:

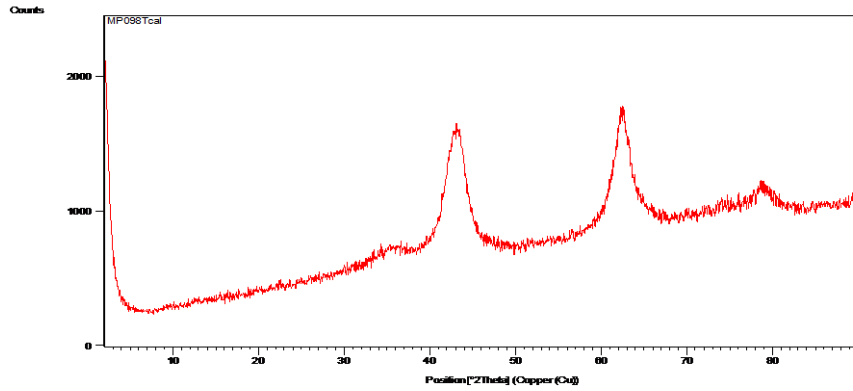
ICP-OES: 265.3 mg/g Mg, 130.9 mg/g Al, 32.1 mg/g Zn, 142.1 mg/g Cu.

XRD:

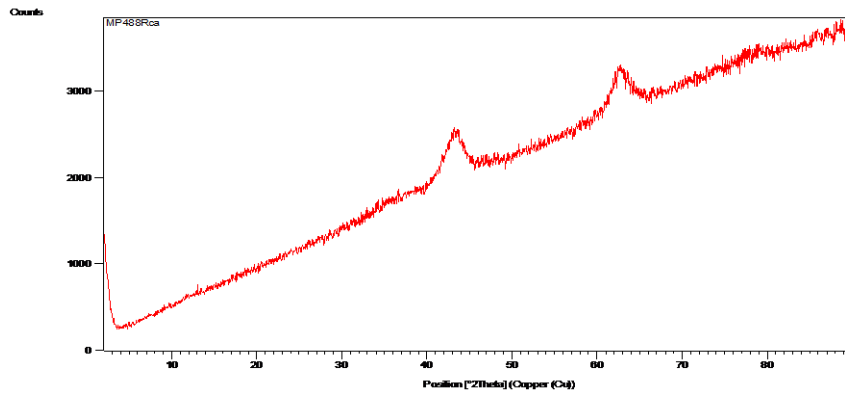


HTc-Fe:

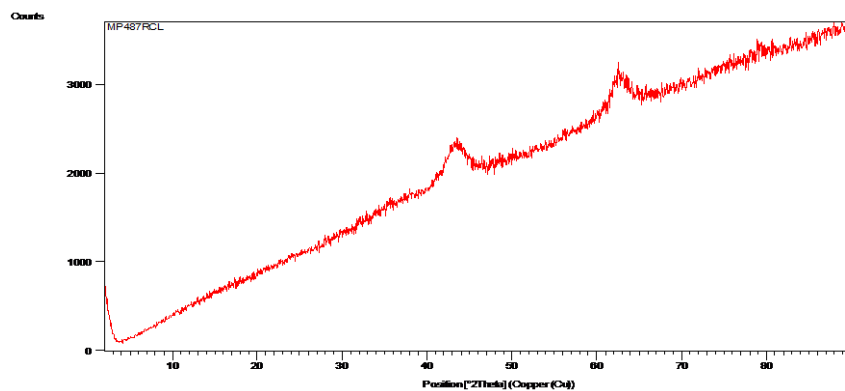
ICP-OES: 433.0 mg/g Mg, 109.3 mg/g Al, 68.7 mg/g Fe.

XRD:**HTc-Co:**

ICP-OES: 292.6 mg/g Mg, 141.3 mg/g Al, 141.5 mg/g Co.

XRD:**HTc-Zn-Co:**

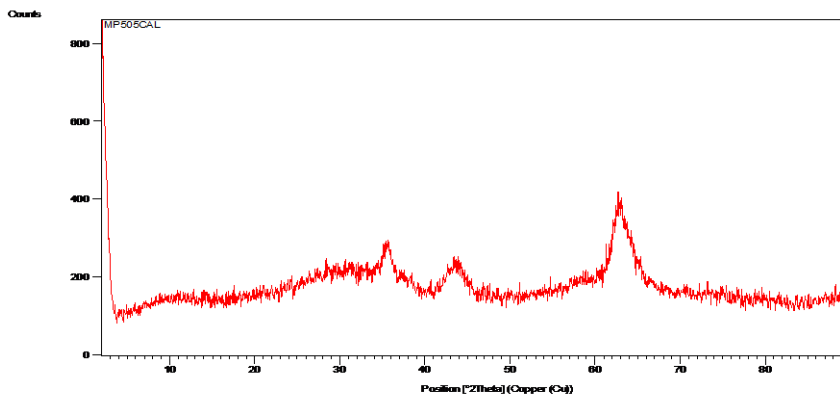
ICP-OES: 271.3 mg/g Mg, 123.7 mg/g Al, 123.7 mg/g Co, 33.3 mg/g Zn

XRD:

HTc-V:

ICP-OES: 207.0 mg/g Mg, 82.14 mg/g Al, 178.9 mg/g V

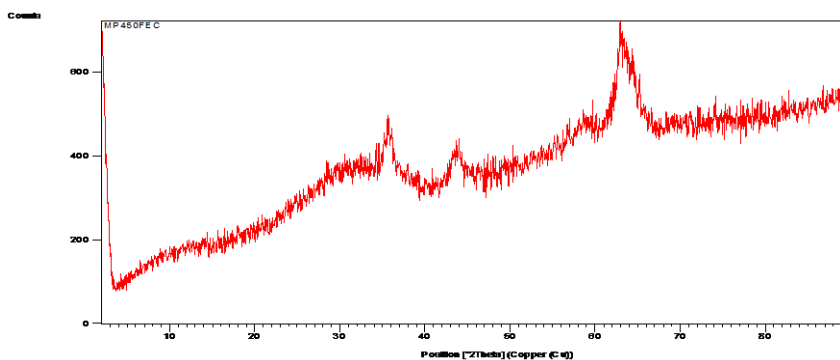
XRD:



HTc-Cu-V:

ICP-OES: 142.4 mg/g Mg, 84.2 mg/g Al, 91.6 mg/g Cu, 286.4 mg/g V.

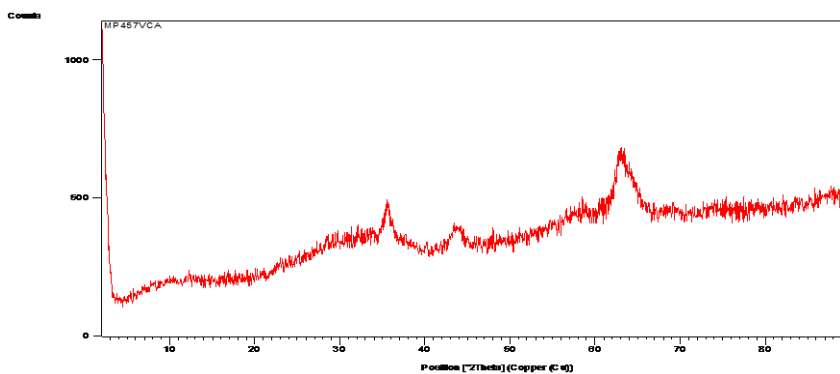
XRD:



HTc-Zn-Cu-V:

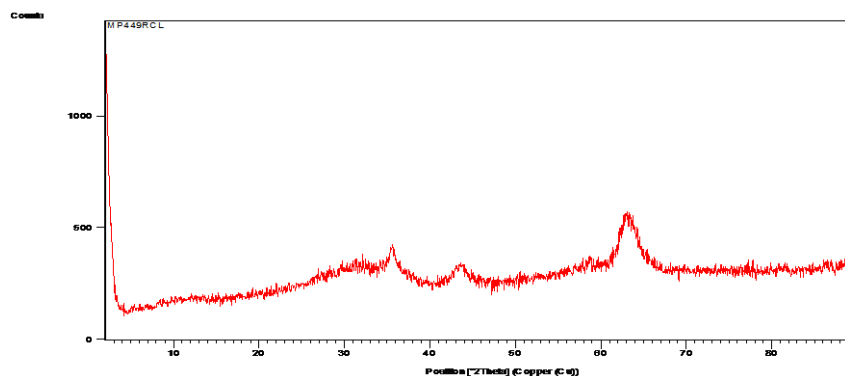
ICP-OES: 121.8 mg/g Mg, 80.20 mg/g Al, 20.1 mg/g Zn, 87.2 mg/g Cu, 294.5 mg/g V.

XRD:

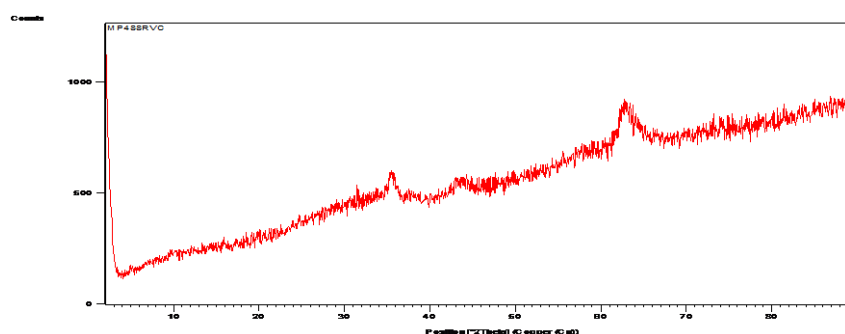


HTc-Fe-V:

ICP-OES: 153.8 mg/g Mg, 63.4 mg/g Al, 40.6 mg/g Fe, 296.4 mg/g V.

XRD:**HTc-Co-V:**

ICP-OES: 114.3 mg/g Mg, 73.1 mg/g Al, 72.7 mg/g Co, 303.1 mg/g V.

XRD:**5.2. Catalysis with hydrotalcite-like catalysts****5.2.1 Reaction conditions for the cleavage of dilignol 3aE with HTc-catalysts on a 0.250 mmol scale**

A 25 mL glass-autoclave was charged with dilignol **3aE** (83.6 mg, 0.250 mmol, 1.0 eq.), the corresponding HTc-catalyst (16.7 mg, 20 wt%) and a magnetic stirrer. Subsequently, 1.25 mL of pyridine was added. The autoclave was purged three times with oxygen, charged with 5 bar of oxygen and stirred with 600 rpm in a preheated oil bath at 135 °C. After the expiration of the desired reaction time the autoclave was taken out of the oil bath and cooled to room temperature. The remaining oxygen pressure was released and the autoclave opened. 1.000 mL of a standard-solution (3,4-dimethoxybenzylalcohol in methanol, $c = 0.2$ mol/L) was added with an Eppendorf-pipette to the reaction solution. The reaction mixture was filtered into 50 mL of a 1 M HCl solution, the autoclave rinsed with DCM (10 mL) and the catalyst was washed with DCM (20 mL). The aqueous phase was then extracted with DCM (4×20 mL). Next, the combined organic phases were washed with 1 M HCl (50 mL) and brine

(50 mL), dried over MgSO₄, filtered and the solvent removed under reduced pressure. A minimum of three samples was taken from each reaction for HPLC measurements. For each sample 2.0 to 3.0 mg of the reaction product were weighed into a vial. Then, 0.5 mL of ethyl acetate and 0.5 mL of acetonitrile were added to the vial and after the complete dissolution of all products, the solution was filtered into a HPLC vial.

5.2.2 Reaction conditions for the cleavage of dilignol 3aE with HTc-Cu-V or HTc-Zn-Cu-V on a 1.000 mmol scale

A 25 mL glass-autoclave was charged with dilignol **3aE** (334.4 mg, 1.000 mmol, 1.0 eq.), HTc-Cu-V or HTc-Zn-Cu-V (66.9 mg, 20 wt%) and a magnetic stirrer. Subsequently, 5 mL of pyridine was added. The autoclave was purged three times with oxygen, charged with 5 or 6 bar of oxygen and stirred in a preheated oil bath at 135 °C with 600 rpm. After 16 h the autoclave was taken out of the oil bath and cooled to room temperature. The remaining oxygen pressure was released and the autoclave opened. The reaction mixture was filtered into 200 mL of a 1 M HCl solution, the autoclave rinsed with DCM (20 mL) and the catalyst was washed with DCM (20 mL). The aqueous phase was extracted with DCM (4×80 mL) and the organic phase was washed with 1 M HCl (150 mL) and brine (150 mL). After drying over MgSO₄ and filtration, the solvent was evaporated under reduced pressure. The products were purified by column chromatography (DCM/MeOH = 100:0 to 100:6). HTc-Zn-Cu-V was dried under high vacuum and reused for a 2nd and 3rd catalytic cycle.

5.2.3 Reaction conditions for determining the influence of the stirring rate with HTc-Cu-V as catalyst

A 25 mL glass-autoclave was charged with dilignol **3aE** (83.6 mg, 0.250 mmol, 1.0 eq.), HTc-Cu-V (16.7 mg, 20 wt%) and a magnetic stirrer. Subsequently, 1.25 mL of pyridine was added. The autoclave was purged three times with oxygen, charged with 5 bar of oxygen and stirred in a preheated oil bath at 135 °C with the corresponding stirring velocity. After 14 h the autoclave was taken out of the oil bath and cooled to room temperature. The remaining oxygen pressure was released and the autoclave opened. 1.000 mL of a standard-solution (3,4-dimethoxybenzylalcohol in methanol, c = 0.2 mol/L) was added with an Eppendorf-pipette to the reaction solution. The reaction mixture was filtered into 50 mL of a 1 M HCl solution, the autoclave rinsed with DCM (10 mL) and the catalyst was washed with DCM (20 mL). The aqueous phase was then extracted with DCM (4×20 mL). Next, the combined organic phases were washed with 1 M HCl (50 mL) and brine (50 mL), dried over MgSO₄, filtered and the solvent removed under reduced pressure. A minimum of three samples was taken from each reaction for HPLC measurements. For each sample 2.0 to 3.0 mg of the reaction product were weighed into a vial. Then, 0.5 mL of ethyl acetate and 0.5 mL of acetonitrile were added to the vial and after the complete dissolution of all products, the solution was filtered into a HPLC vial.

5.2.4 Reaction conditions for the kinetics of dilignol 3aE and ketone 12a with HTc-Cu-V as catalyst

A 20 mL steel autoclave was either charged with dilignol **3aE** (83.6 mg, 0.250 mmol, 1.0 eq.) or ketone **12a** (83.3 mg, 0.250 mmol, 1.0 eq.), HTc-Cu-V (16.7 mg, 20 wt%) and a magnetic stirrer. Subsequently, 1.25 mL of pyridine was added. The autoclave was purged three times

with oxygen, charged with 5 bar of oxygen and stirred with 500 rpm in a preheated oil bath at 135 °C. Upon completion of the desired reaction time the autoclave was taken out of the oil bath and cooled to room temperature. Afterwards, the remaining oxygen pressure was released and the autoclave opened. 1.000 mL of a standard-solution (3,4-dimethoxybenzylalcohol in methanol, $c = 0.2 \text{ mol/L}$) was added with an Eppendorf-pipette to the reaction solution. The reaction mixture was filtered to separate the solid catalyst from the solution and the catalyst was washed with DCM. The solution was then washed with 1 M HCl (50 mL) and the aqueous phase extracted with DCM ($2 \times 10 \text{ mL}$). The combined organic phases were dried over MgSO_4 , filtered, and the solvent was removed under reduced pressure. A minimum of two samples was taken from each reaction for HPLC measurements. For each sample 2.0 to 3.0 mg of the reaction product were weighed into a vial. Then, either 1.0 mL of acetonitrile or 0.5 mL of ethyl acetate and 0.5 mL of acetonitrile were added to the vial and after the complete dissolution of all products, the solution was filtered into a HPLC vial.

5.2.5. Reaction conditions for the oxidative cleavage of lignin with HTc-Cu-V as catalyst

A 20 mL steel autoclave was charged with 100 mg of the corresponding lignin source and 20 mg (20 wt%) of HTc-Cu-V. Subsequently, pyridine (4.5 mL) was added. The autoclave was purged three times with oxygen, charged with 10 bar of oxygen and stirred with 600 rpm in a preheated oil bath at 135 °C. After 40 h the autoclave was taken out of the oil bath and cooled to room temperature. The residual pressure was released, the reaction mixture filtered and the autoclave and catalyst washed with 20 mL of pyridine. Under reduced pressure pyridine was removed. The reaction mixture was dissolved in methanol (20 mL) and the solvent evaporated to remove residual pyridine. This process was repeated twice ($2 \times 20 \text{ mL}$). Afterwards the product was dried under high vacuum. The product was analyzed by GPC, MALDI and elemental analysis.

5.2.6 Reaction conditions for the 2D-NMRs of lignin with HTc-Cu-V as catalyst

A 20 mL steel autoclave was charged with 100 mg of the corresponding lignin source and 20 mg (20 wt%) of HTc-Cu-V. Subsequently, 4.5 mL of pyridine- d_5 was added. The autoclave was purged three times with oxygen, charged with 10 bar of oxygen and stirred in a preheated oil bath at 135 °C with 600 rpm. After 40 h the autoclave was taken out of the oil bath and cooled to room temperature. The residual pressure was released and the reaction mixture filtered into a NMR tube.

5.2.7 Reaction conditions with other model compounds and HTc-Cu-V as catalyst

A 25 mL glass autoclave was charged with corresponding lignin model compound (0.250 mmol or 1.000 mmol), HTc-Cu-V (20 wt%) and a magnetic stirrer. Subsequently either 1.25 mL or 5 mL of pyridine were added. The autoclave was purged three times with oxygen, charged with 5 or 6 bar of oxygen and stirred in a preheated oil bath at 135 °C with 600 rpm. After 17 h the autoclave was taken out of the oil bath and cooled to room temperature. The remaining oxygen pressure was released and the autoclave opened. Depending on the reaction scale the work up was performed as described in 5.2.1 or 5.2.2 in this chapter.

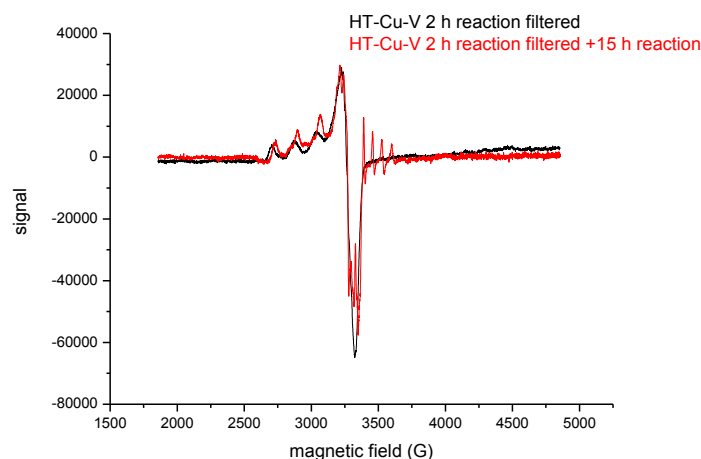
5.2.8 Reaction conditions for the leaching tests with HTc-Cu-V as catalyst

A 25 mL glass autoclave was charged with dilignol **3aE** (83.6 mg, 0.250 mmol, 1.0 eq.), HTc-Cu-V (16.7 mg, 20 wt%) and a magnetic stirrer. Subsequently, 1.25 mL of pyridine was added. The autoclave was purged three times with oxygen, charged with 5 bar of oxygen and stirred in a preheated oil bath at 135 °C with 600 rpm. Upon completion of the desired reaction time the autoclave was taken out of the oil bath, the remaining oxygen pressure released and the hot reaction mixture filtered over two pipettes with cotton into a flask. The solvent was removed under reduced pressure. To remove the residual pyridine the reaction mixture was dissolved in methanol (20 mL) and the solvent evaporated.

5.2.9 Reaction conditions for the EPR measurements with HTc-Cu-V as catalyst

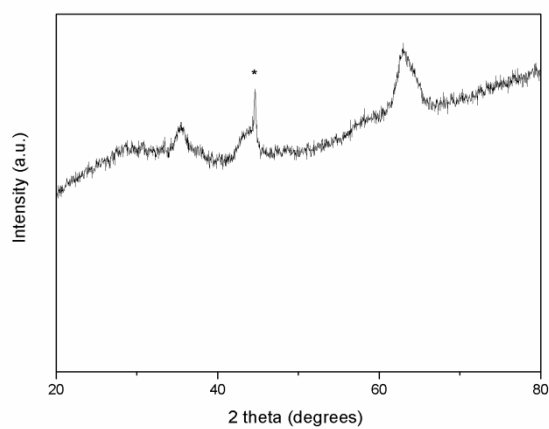
A glass autoclave was charged with dilignol **3aE** (83.6 mg, 0.250 mmol, 1.0 eq.), HTc-Cu-V (16.7 mg, 20 wt%) and a magnetic stirrer. Subsequently, 1.25 mL of pyridine was added. The autoclave was purged three times with oxygen, charged with 5 bar of oxygen and stirred in a preheated oil bath at 135 °C with 600 rpm. After 2 h the autoclave was taken out of the oil bath, the remaining oxygen pressure released and the reaction solution either filtered hot into an EPR-tube or into another glass autoclave equipped with a magnetic stirrer. The glass-autoclave was purged three times with oxygen, charged with 5 bar of oxygen and stirred in a preheated oil bath at 135 °C with 600 rpm. After 15 h the autoclave was taken out of the oil bath and cooled to room temperature. The remaining oxygen pressure was released and the reaction solution filtered into an EPR-tube.

5.2.10 EPR spectra of the reaction solution after hot filtration of HTc-Cu-V

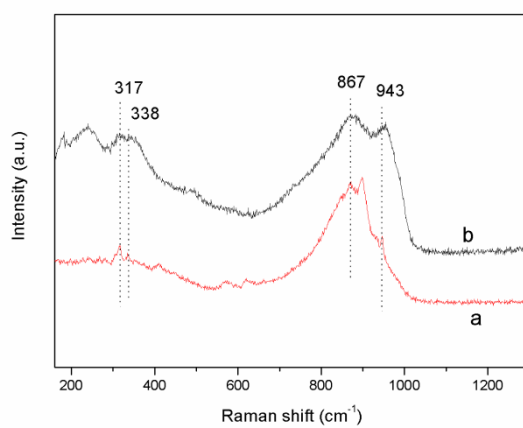


5.3. Spectroscopic data of HTc-Cu-V after reaction

5.3.1. XRD of HTc-Cu-V after 17 h of reaction; * peak caused by the sample holder



5.3.2. Raman spectra of HTc-Cu-V a) before and b) after 17 h of reaction



6. Catalysis with V(acac)₃ and Cu(NO₃)₂·3H₂O

The synthetic protocols involving V(acac)₃ and Cu(NO₃)₂·3H₂O as catalysts have been published during the course of this dissertation in the journal “ChemSusChem” as part of the article “Copper- and Vanadium-Catalyzed Oxidative Cleavage of Lignin using Dioxygen”.^[78] The following reaction conditions are identical to those given in reference 78.

6.1.1 Reaction conditions for the cleavage of dilignol 3aE with V(acac)₃ and Cu(NO₃)₂·3H₂O

A 25 mL glass autoclave was charged with dilignol **3aE** (83.6 mg, 0.250 mmol, 1.0 eq.), the corresponding amount of V(acac)₃ and Cu(NO₃)₂·3H₂O and a magnetic stirrer. Subsequently, 1.25 mL of pyridine was added. The autoclave was purged three times with oxygen, charged with 5 bar of oxygen and stirred with 600 rpm in a preheated oil bath at 135 °C. After the expiration of the desired reaction time the autoclave was taken out of the oil bath and cooled to room temperature. The remaining oxygen pressure was released and the autoclave opened. 1.000 mL of a standard solution (3,4-dimethoxybenzylalcohol in methanol, c = 0.2 mol/L) was added with an Eppendorf-pipette to the reaction solution. The reaction mixture was added to 50 mL of a 1 M HCl-solution and the autoclave rinsed with DCM (10 mL). The aqueous phase was then extracted with DCM (4×20 mL). Next, the combined organic phases were washed with 1 M HCl (50 mL) and brine (50 mL), dried over MgSO₄, filtered and the solvent removed under reduced pressure. A minimum of three samples was taken from each reaction for HPLC measurements. For each sample 2.0 to 3.0 mg of the reaction product were weighed into a vial. Then, 0.5 mL of ethyl acetate and 0.5 mL of acetonitrile were added to the vial and after the complete dissolution of all products, the solution was filtered into a HPLC vial.

6.1.2 Reaction conditions for the oxidative cleavage of lignin with V(acac)₃ and Cu(NO₃)₂·3H₂O

A 20 mL steel autoclave was charged with 100 mg of the corresponding lignin source and 5 mg (5 wt%) of V(acac)₃ and 5 mg (5 wt%) of Cu(NO₃)₂·3H₂O. Subsequently, pyridine (4.5 mL) was added. The autoclave was purged three times with oxygen, charged with 10 bar of oxygen and stirred with 600 rpm in a preheated oil bath at 135 °C. After 40 h the autoclave was taken out of the oil bath and cooled to room temperature. The residual pressure was released, the reaction mixture filtered and the autoclave and catalyst washed with 20 mL of pyridine. Under reduced pressure pyridine was removed. The reaction mixture was dissolved in methanol (20 mL) and the solvent evaporated to remove residual pyridine. This process was repeated twice (2×20 mL). Afterwards the product was dried under high vacuum. The product was analyzed by GPC, MALDI and elemental analysis.

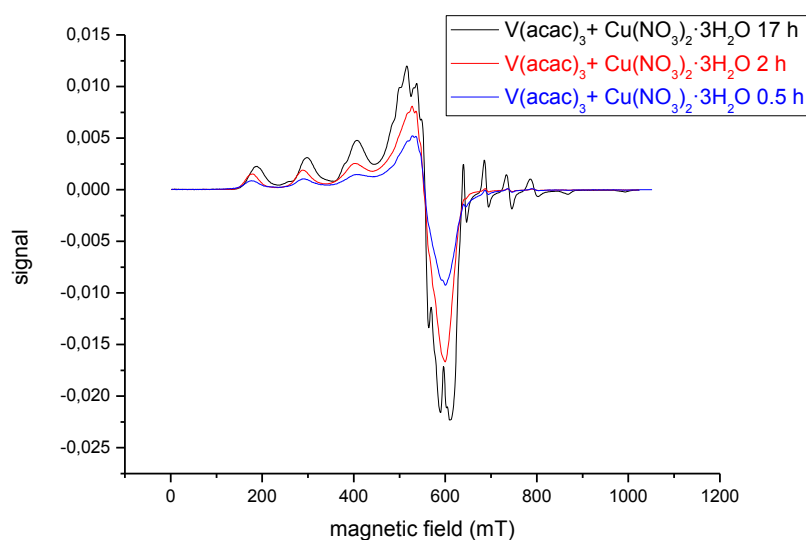
6.1.3 Reaction conditions for the 2D-NMRs of lignin with V(acac)₃ and Cu(NO₃)₂·3H₂O

A 20 mL steel autoclave was charged with 100 mg of the corresponding lignin source and 5 mg (5 wt%) of V(acac)₃ and 5 mg (5 wt%) of Cu(NO₃)₂·3H₂O. Subsequently, 4.5 mL of pyridine-*d*₅ was added. The autoclave was purged three times with oxygen, charged with 10 bar of oxygen and stirred in a preheated oil bath at 135 °C with 600 rpm. After 40 h the autoclave was taken out of the oil bath and cooled to room temperature. The residual pressure was released and the reaction mixture filtered into a NMR tube.

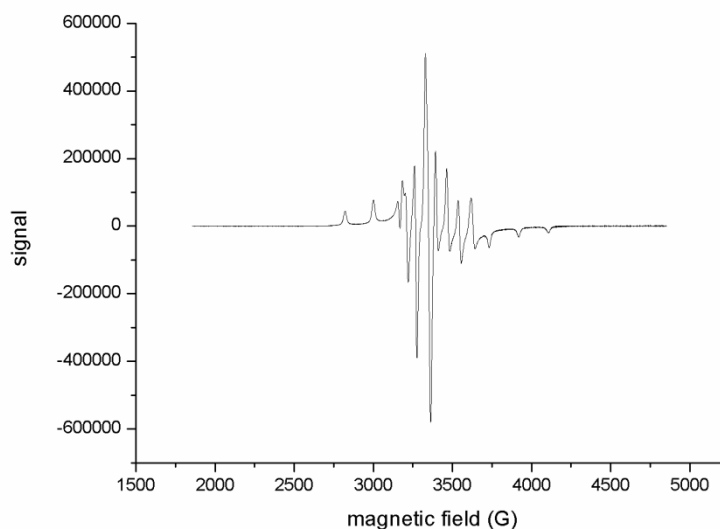
6.1.4 Reaction conditions for the EPR measurements with $V(acac)_3$ and $Cu(NO_3)_2 \cdot 3H_2O$ as catalyst

A 25 mL glass autoclave was charged with dilignol **3aE** (83.6 mg, 0.250 mmol, 1.0 eq.), $V(acac)_3$ (4.4 mg, 0.0125 mmol, 5 mol%), $Cu(NO_3)_2 \cdot 3H_2O$ (3.0 mg, 0.0125 mmol, 5 mol%) and a magnetic stirrer. Subsequently, 1.25 mL of pyridine was added. The autoclave was purged three times with oxygen, charged with 5 bar of oxygen and stirred in a preheated oil bath at 135 °C with 600 rpm. After the expiration of the desired reaction time the autoclave was taken out of the oil bath and cooled to room temperature. The remaining oxygen pressure was released and the autoclave opened. The reaction solution was filtered into an EPR-tube.

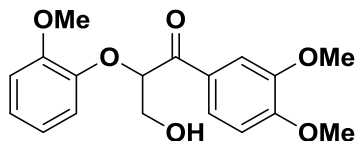
6.1.5 EPR spectra of the reaction solution using 5 mol% of $V(acac)_3/Cu(NO_3)_2 \cdot 3H_2O$



6.1.6 EPR spectrum of 5 mol% $V(acac)_3$ in pyridine at ambient pressure and room temperature



7. Spectroscopic data of isolated products

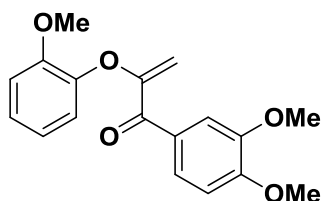
1-(3,4-Dimethoxyphenyl)-3-hydroxy-2-(2-methoxyphenoxy)propan-1-one^[36g]

¹H NMR (600 MHz, CDCl₃): δ = 7.75 (dd, J = 8.4, 2.0 Hz, 1H), 7.62 (d, J = 2.0 Hz, 1H), 7.00 (td, J = 8.0, 1.4 Hz, 1H), 6.94–6.86 (m, 3H), 6.82 (td, J = 8.0, 1.4 Hz, 1H), 5.40 (t, J = 5.3 Hz, 1H), 4.07 (d, J = 5.3 Hz, 2H), 3.95 (s, 3H), 3.92 (s, 3H), 3.86 (s, 3H).

¹³C NMR (151 MHz, CDCl₃): δ = 195.0, 153.9, 150.5, 149.2, 146.9, 128.0, 123.7, 123.6, 121.2, 118.5, 112.2, 110.9, 110.1, 84.6, 63.7, 56.1, 56.0, 55.8.

MS (EI, 70 eV): m/z (%): 333 [M+1]⁺ (7), 332 [M]⁺ (31), 166 (11), 165 (100), 150 (30), 77 (11).

HPLC (H₂O/MeOH, 60/40): t_R = 24.0 min.

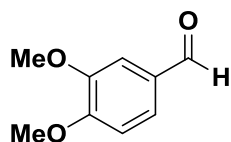
1-(3,4-Dimethoxyphenyl)-2-(2-methoxyphenoxy)prop-2-en-1-one^[79]

¹H NMR (600 MHz, CDCl₃): δ = 7.83 (dd, J = 8.4, 1.9 Hz, 1H), 7.64 (d, J = 1.8 Hz, 1H), 7.14 (td, J = 7.2, 1.5 Hz, 1H), 7.08 (dd, J = 7.9, 1.5 Hz, 1H), 6.98 (dd, J = 8.4, 1.0 Hz, 1H), 6.93 (td, J = 7.8, 1.5 Hz, 1H), 6.90 (d, J = 8.4 Hz, 1H), 5.21 (d, J = 2.4 Hz, 1H), 4.71 (d, J = 2.4 Hz, 1H), 3.95 (s, 3H), 3.93 (s, 3H), 3.87 (s, 3H).

¹³C NMR (151 MHz, CDCl₃): δ = 189.2, 158.1, 153.5, 151.1, 148.8, 143.4, 129.2, 125.9, 125.2, 121.8, 121.4, 113.0, 112.4, 110.0 (2C), 56.2, 56.1, 56.0.

MS (EI, 70 eV): m/z (%): 315 [M+1]⁺ (6), 314 [M]⁺ (28), 166 (11), 165 (100), 163 (17), 77 (11).

HRMS (ESI, 70 eV): m/z calcd for C₁₈H₁₈O₅+Na⁺: 337.1046 [M+Na]⁺; found: 337.1046.

3,4-Dimethoxybenzaldehyde^[37e]

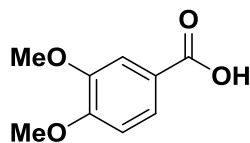
¹H NMR (600 MHz, CDCl₃): δ = 9.84 (s, 1H), 7.45 (dd, J = 8.4, 1.8 Hz, 1H), 7.40 (d, J = 1.8 Hz, 1H), 6.97 (d, J = 8.4 Hz, 1H), 3.95 (s, 3H), 3.93 (s, 3H).

¹³C NMR (151 MHz, CDCl₃): δ = 191.0, 154.6, 149.7, 130.2, 127.0, 110.5, 109.0, 56.3, 56.1.

MS (EI, 70 eV): m/z (%): 167 [M+1]⁺ (14), 166 [M]⁺ (100), 165 (48), 151 (11), 95 (17), 77 (11), 51 (14).

HPLC (H₂O/MeOH, 60/40): $t_R = 5.3$ min.

3,4-Dimethoxybenzoic acid^[37e]



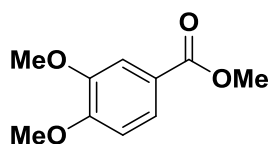
¹H NMR (600 MHz, CDCl₃): $\delta = 10.31$ (bs, 1H), 7.77 (dd, $J = 8.4, 1.9$ Hz, 1H), 7.59 (d, $J = 1.8$ Hz, 1H), 6.89 (d, $J = 8.4$ Hz, 1H), 3.94 (s, 3H), 3.93 (s, 3H).

¹³C NMR (151 MHz, CDCl₃): $\delta = 171.9, 153.5, 148.7, 124.6, 112.5, 110.4$ (2C), 56.1, 56.0.

MS (EI, 70 eV): m/z (%): 183 [M+1]⁺ (13), 182 [M]⁺ (100), 167 (25), 111 (13), 51 (13).

HPLC (H₂O/MeOH, 60/40): $t_R = 1.8$ min.

Methyl 3,4-dimethoxybenzoate^[80]



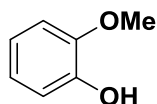
¹H NMR (600 MHz, CDCl₃): $\delta = 7.68$ (dd, $J = 8.4, 1.8$ Hz, 1H), 7.54 (d, $J = 1.8$ Hz, 1H), 6.88 (d, $J = 8.4$ Hz, 1H), 3.94 (s, 3H), 3.93 (s, 3H), 3.89 (s, 3H).

¹³C NMR (151 MHz, CDCl₃): $\delta = 166.8, 152.9, 148.5, 123.5, 122.6, 111.9, 110.2, 56.0, 55.9, 52.0$.

MS (EI, 70 eV): m/z (%): 196 [M]⁺ (100), 165 (83), 124.9 (18), 79 (25).

HPLC(H₂O/MeOH, 60/40): $t_R = 14.3$ min

2-Methoxyphenol^[65]

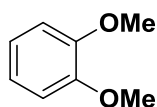


¹H NMR (600 MHz, CDCl₃): $\delta = 6.93$ (dd, $J = 8.0, 1.8$ Hz, 1H), 6.89–6.81 (m, 3H), 5.60 (s, 1H), 3.89 (s, 3H).

¹³C NMR (151 MHz, CDCl₃): $\delta = 146.5, 145.6, 121.4, 120.1, 114.5, 110.7, 55.8$.

MS (EI, 70 eV): m/z (%): 125 [M+1]⁺ (76), 124 [M]⁺ (100), 123 (10), 109 (13), 81 (14).

1,2-Dimethoxybenzene^[81]

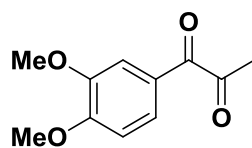


¹H NMR (600 MHz, CDCl₃): $\delta = 6.94$ –6.88 (m, 4H), 3.88 (s, 6H).

¹³C NMR (151 MHz, CDCl₃): $\delta = 149.0$ (2C), 120.8 (2C), 111.3 (2C), 55.8 (2C).

MS (EI, 70 eV): m/z (%) = 139 $[M+1]^+$ (22), 138 $[M]^+$ (100), 123 (22), 95 (26).

1-(3,4-Dimethoxyphenyl)propane-1,2-dione^[65]

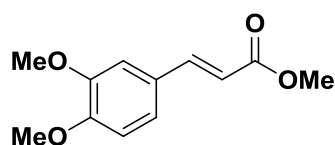


¹H NMR (600 MHz, CDCl₃): δ = 7.66 (dd, J = 8.4, 1.8 Hz, 1H), 7.57 (d, J = 1.8 Hz, 1H), 6.91 (d, J = 8.4 Hz, 1H), 3.97 (s, 3H), 3.94 (s, 3H), 2.52 (s, 3H).

¹³C NMR (151 MHz, CDCl₃): δ = 201.1, 190.2, 154.8, 149.4, 126.4, 124.7, 111.1, 110.3, 56.2, 56.0, 26.7.

MS (EI, 70 eV): m/z (%) = 208 $[M]^+$ (100), 166 (10), 165 (100), 137 (10), 79 (10).

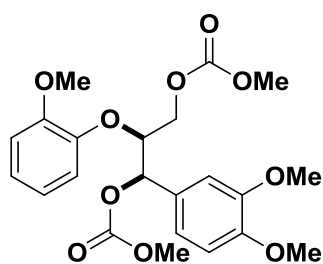
Methyl (*E*)-3-(3,4-dimethoxyphenyl)acrylate^[37e]



¹H NMR (300 MHz, CDCl₃): δ = 7.64 (d, J = 15.9 Hz, 1H), 7.10 (dd, J = 8.3, 2.0 Hz, 1H), 7.05 (d, J = 2.0 Hz, 1H), 6.86 (d, J = 8.3 Hz, 1H), 6.31 (d, J = 15.9 Hz, 1H), 3.91 (s, 6H), 3.80 (s, 3H).

MS (EI, 70 eV): m/z (%) = 223 $[M+1]^+$ (13), 222 $[M]^+$ (28), 207 (17), 191 (41), 164 (11), 147 (16), 119 (14), 91 (17), 89 (11), 77 (18), 51 (17).

***erythro*-1-(3,4-Dimethoxyphenyl)-2-(2-methoxyphenoxy)-propane-1,3-diyl dimethyl biscarbonate**



¹H NMR (600 MHz, CDCl₃): δ = 7.00–6.95 (m, 3H), 6.86–6.79 (m, 4H), 5.87 (d, J = 6.0 Hz, 1H), 4.68 (m, 1H), 4.50 (dd, J = 12.0, 5.4 Hz, 1H), 4.33 (dd, J = 12.0, 4.3 Hz, 1H), 3.86 (s, 3H), 3.85 (s, 3H), 3.77 (s, 3H), 3.76 (s, 3H), 3.75 (s, 3H).

¹³C NMR (151 MHz, CDCl₃): δ = 155.5, 154.7, 151.0, 149.2, 148.8, 146.9, 128.2, 123.6, 120.9, 120.0, 119.4, 112.5, 110.7, 110.5, 79.9, 77.8, 65.8, 55.8 (2C), 55.7, 54.9 (2C).

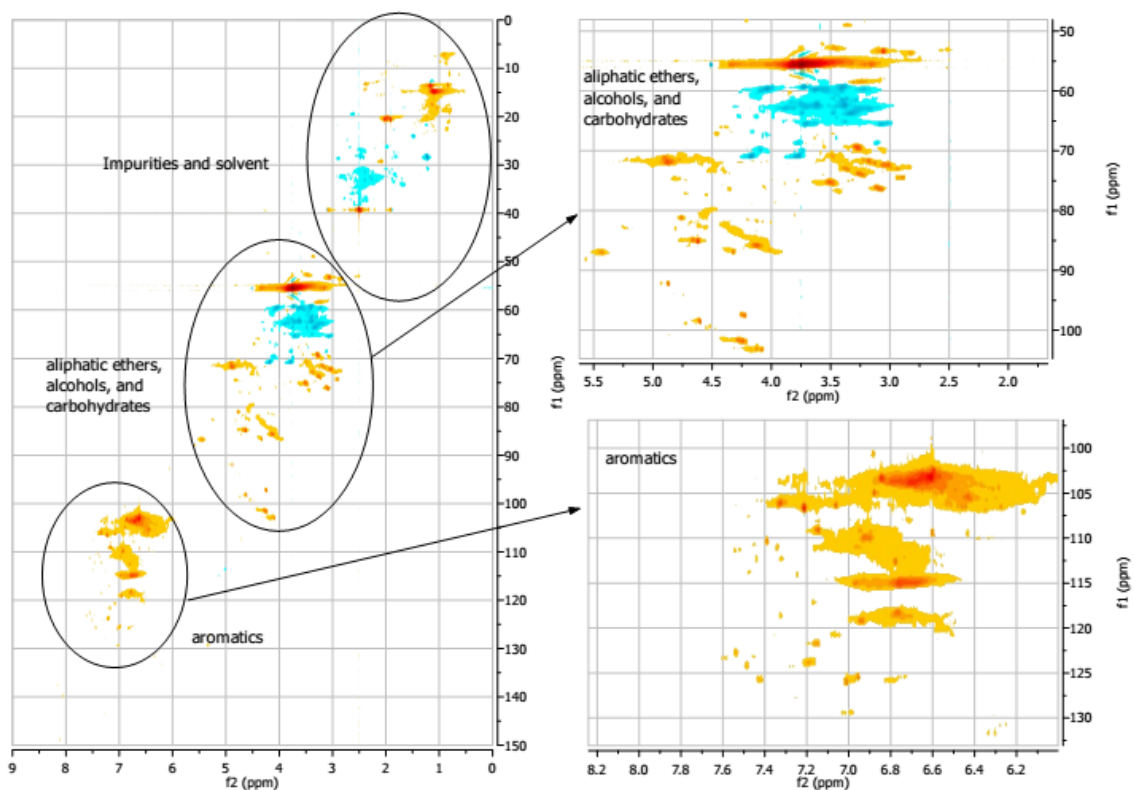
MS (EI, 70 eV): m/z (%): 451 $[M+1]^+$ (10), 450 $[M]^+$ (37), 251 (54), 225 (100), 181 (70).

HRMS (ESI, 70 eV): m/z calcd. for C₂₂H₂₆O₁₀+Na⁺: 473.14182 $[M+Na]^+$; found: 473.14166.

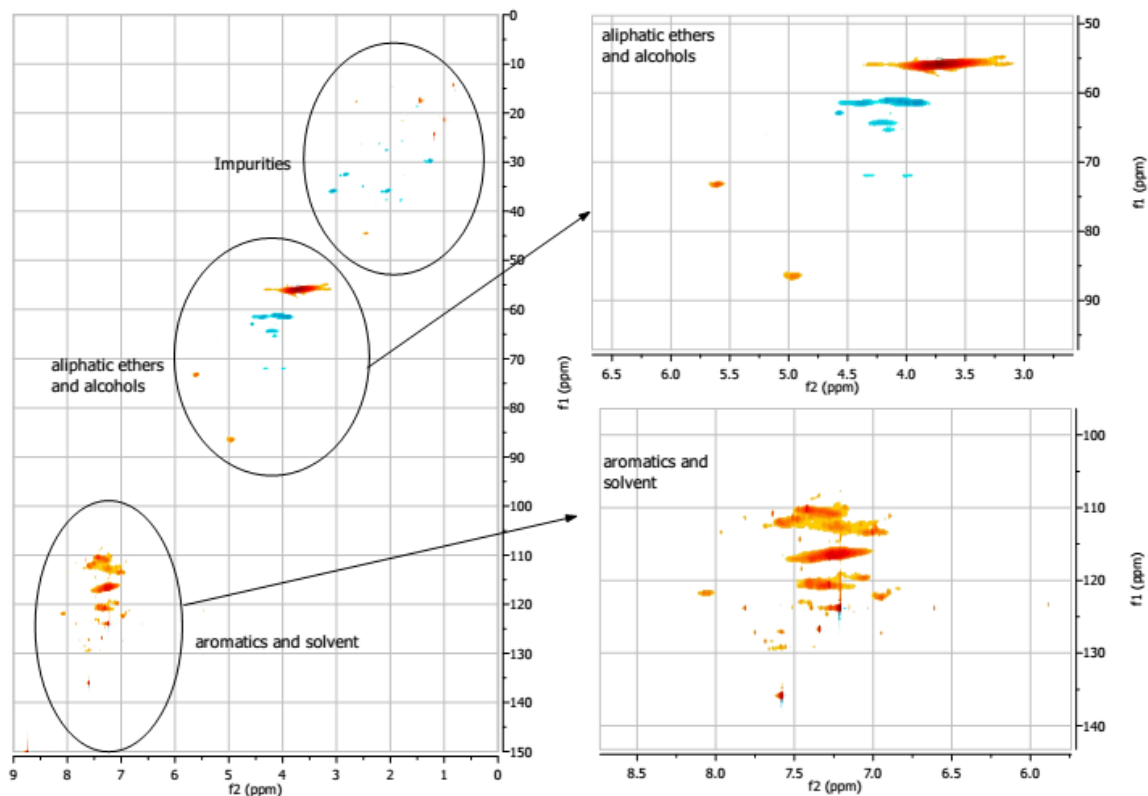
8. Spectroscopic data of lignin

8.1. HSQC spectra of lignin

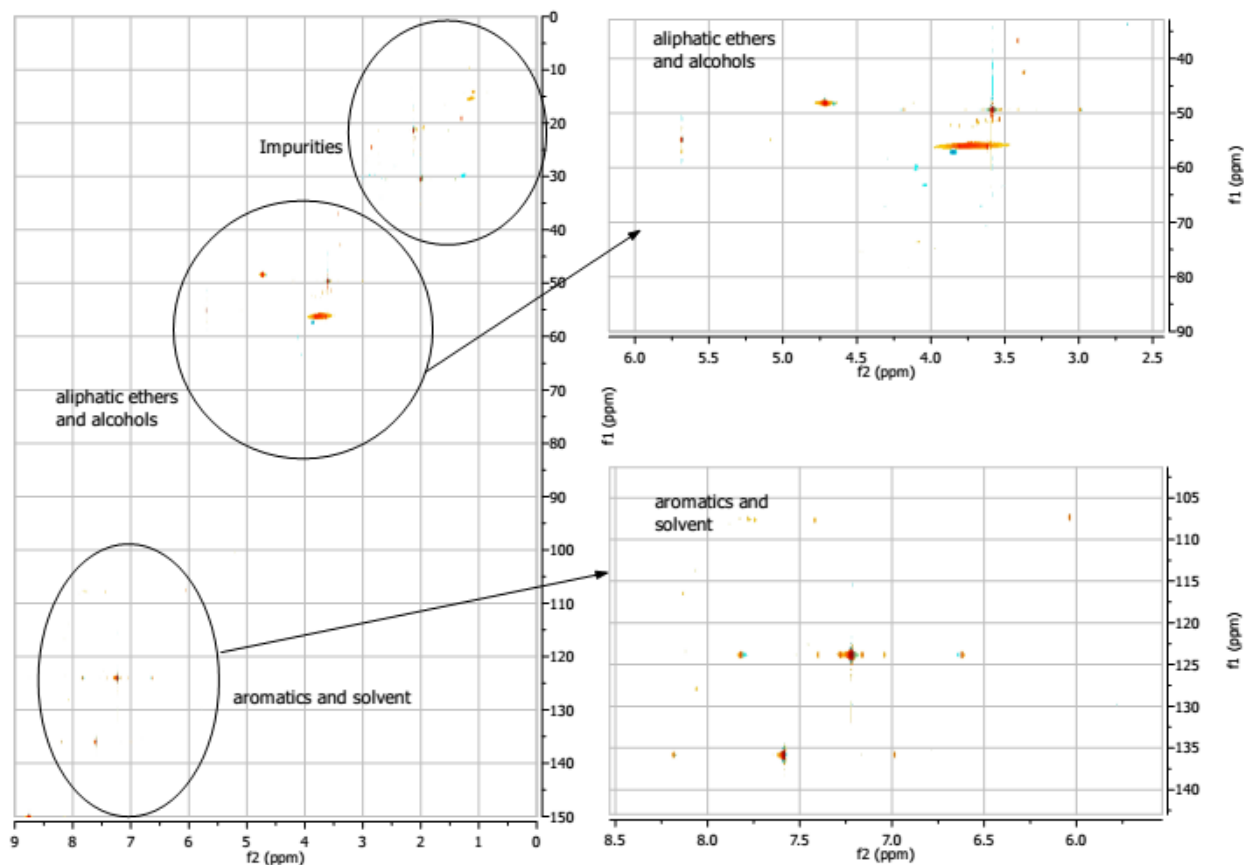
MPI organosolv beech lignin in DMSO- d_6



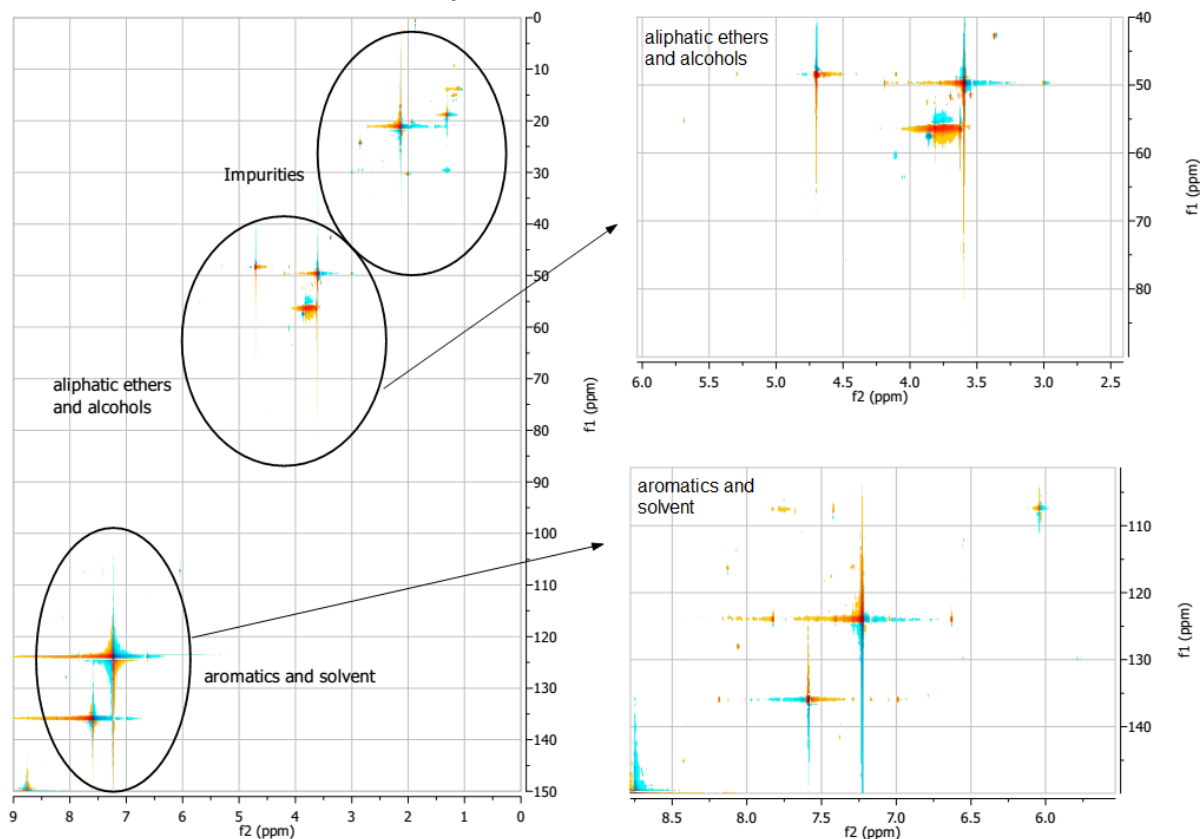
MPI organosolv beech lignin in pyridine- d_5

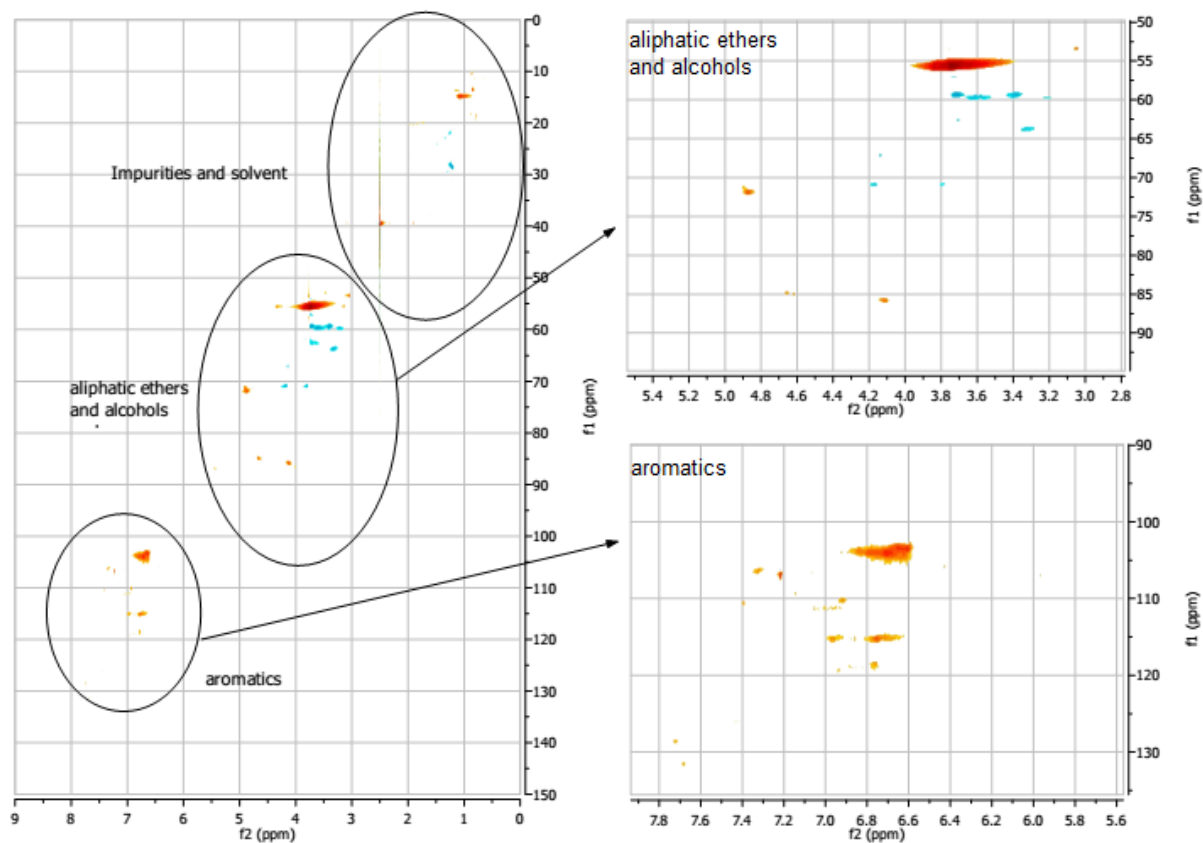
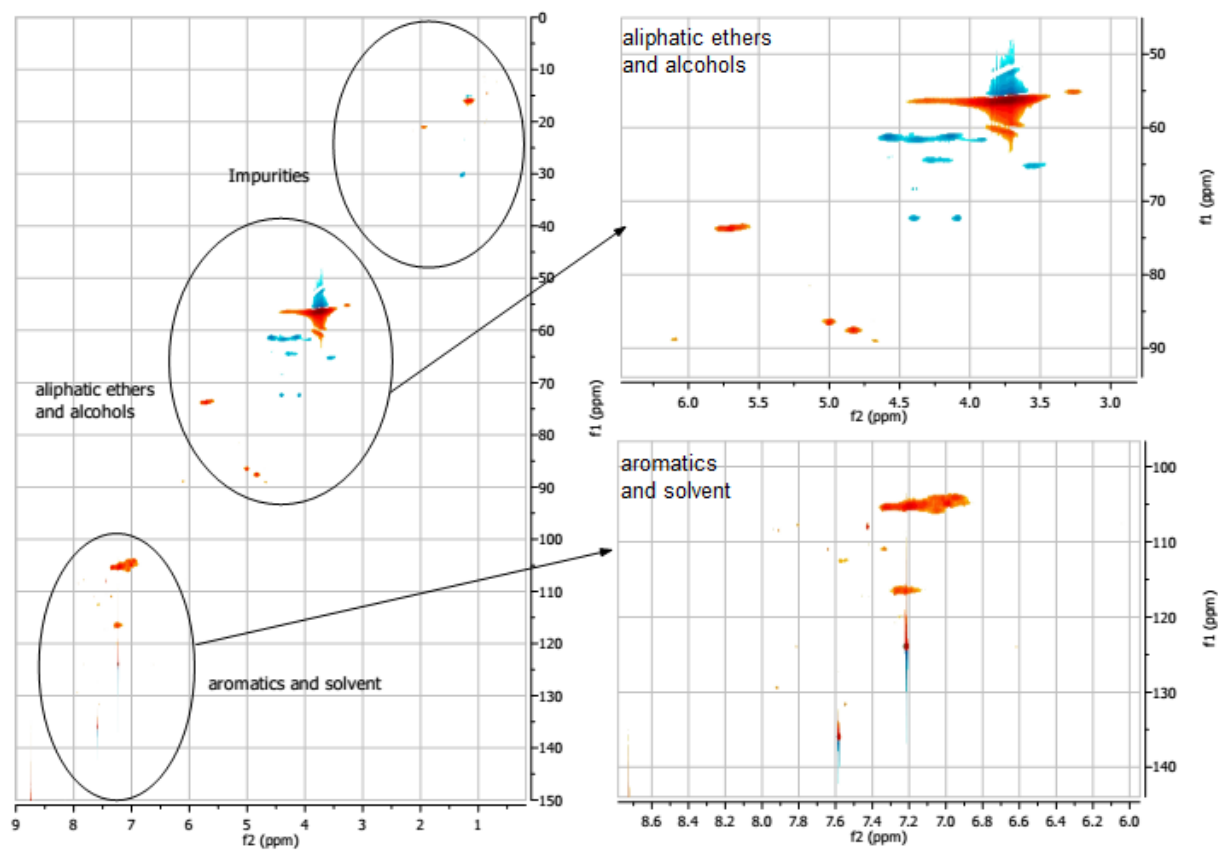


MPI organosolv beech lignin in pyridine- d_5 after the reaction with HTc-Cu-V as catalyst

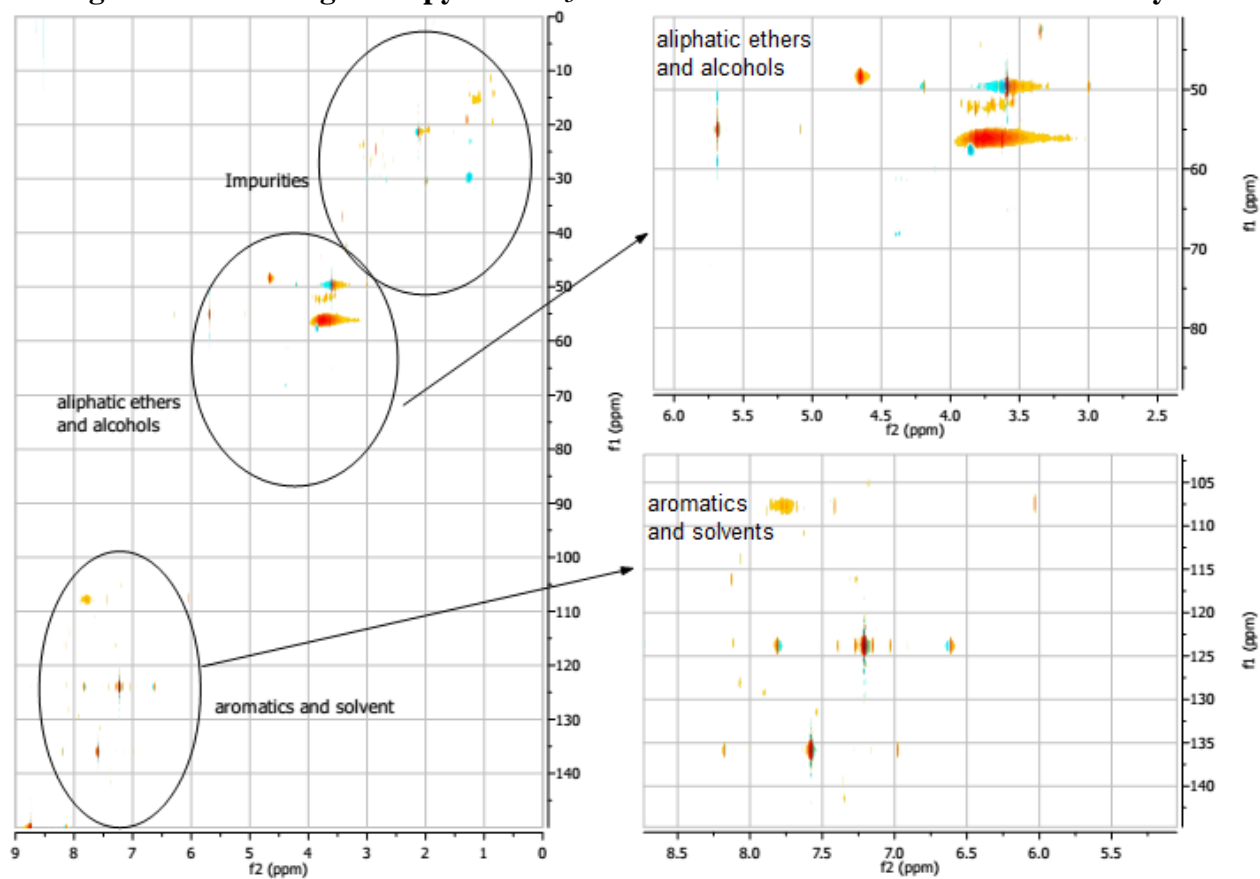


MPI organosolv beech lignin in pyridine- d_5 after the reaction with $V(acac)_3/Cu(NO_3)_2 \cdot 3H_2O$ as catalyst

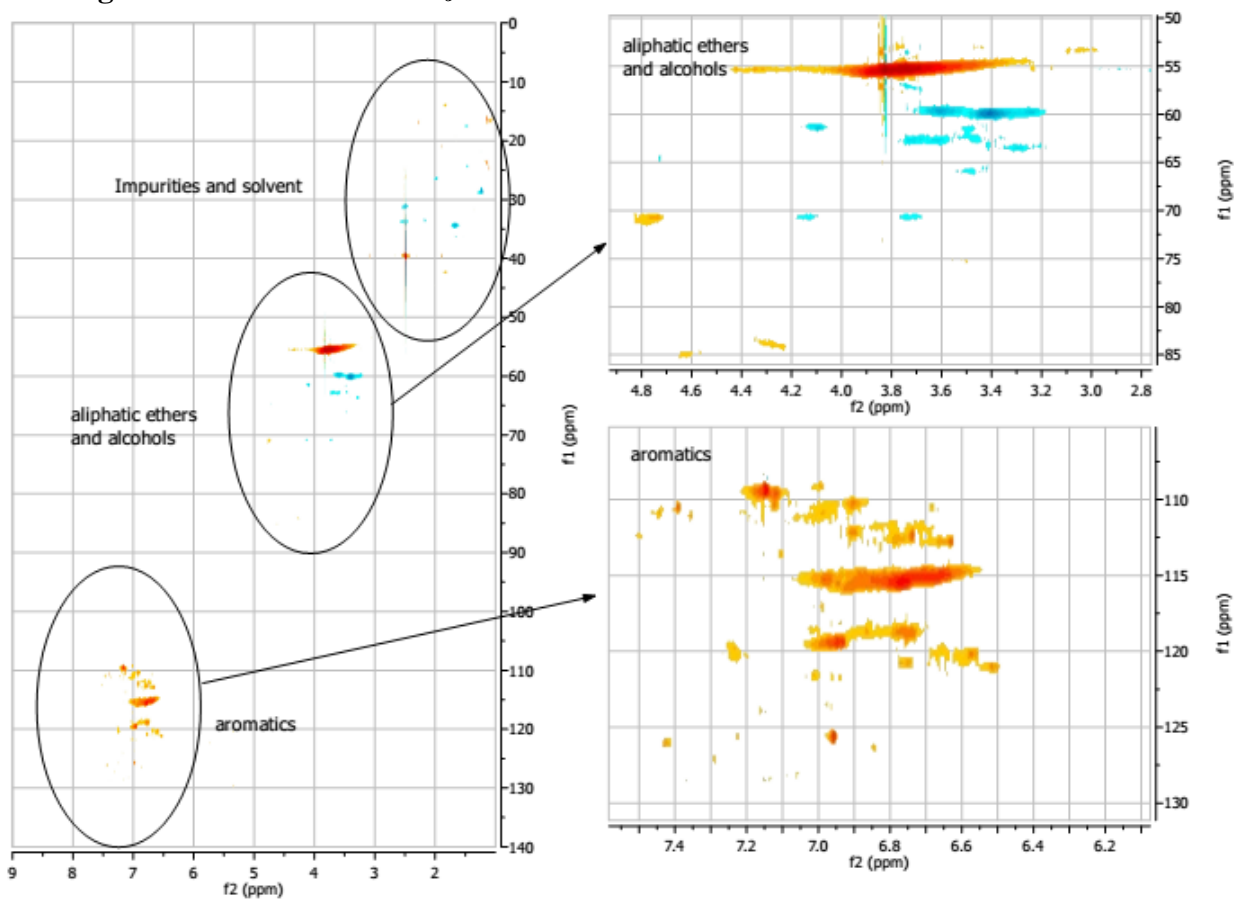


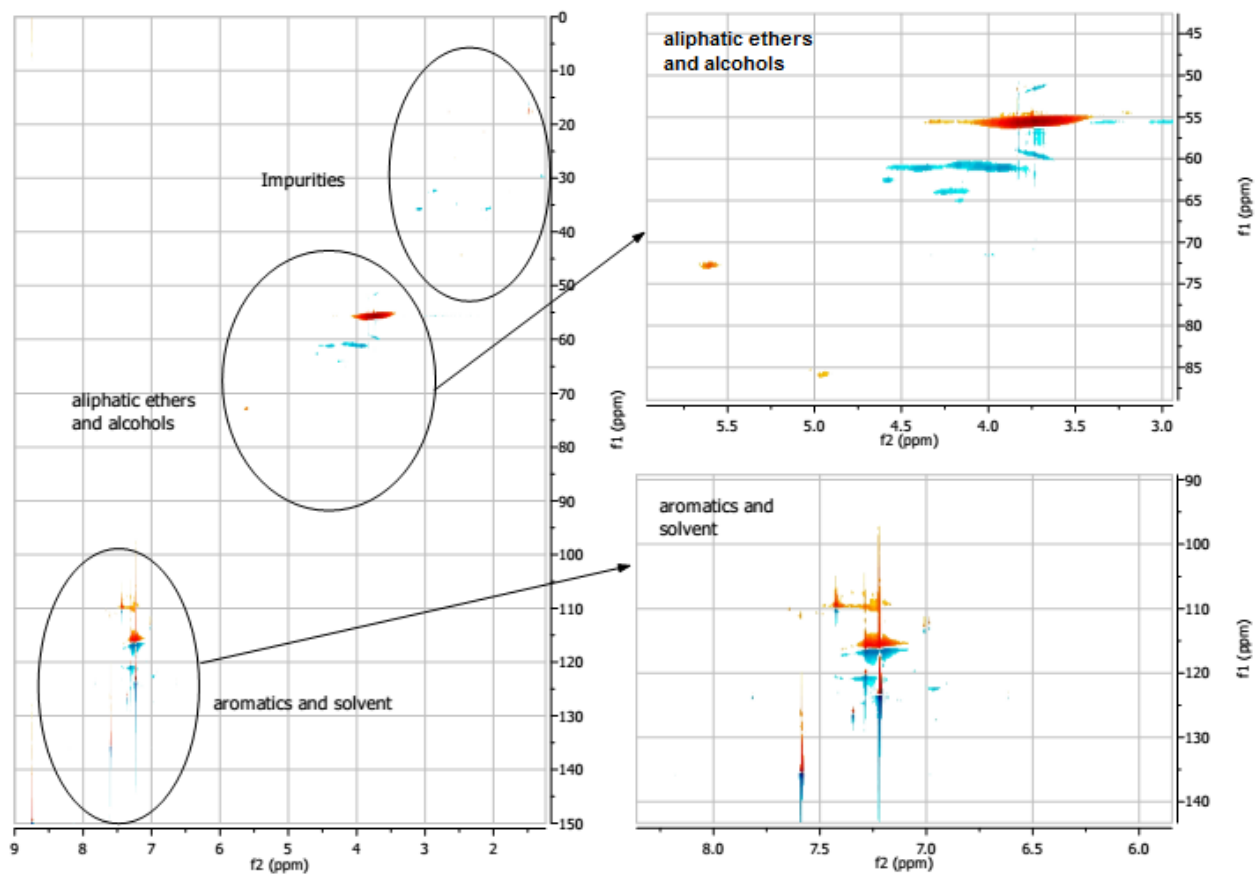
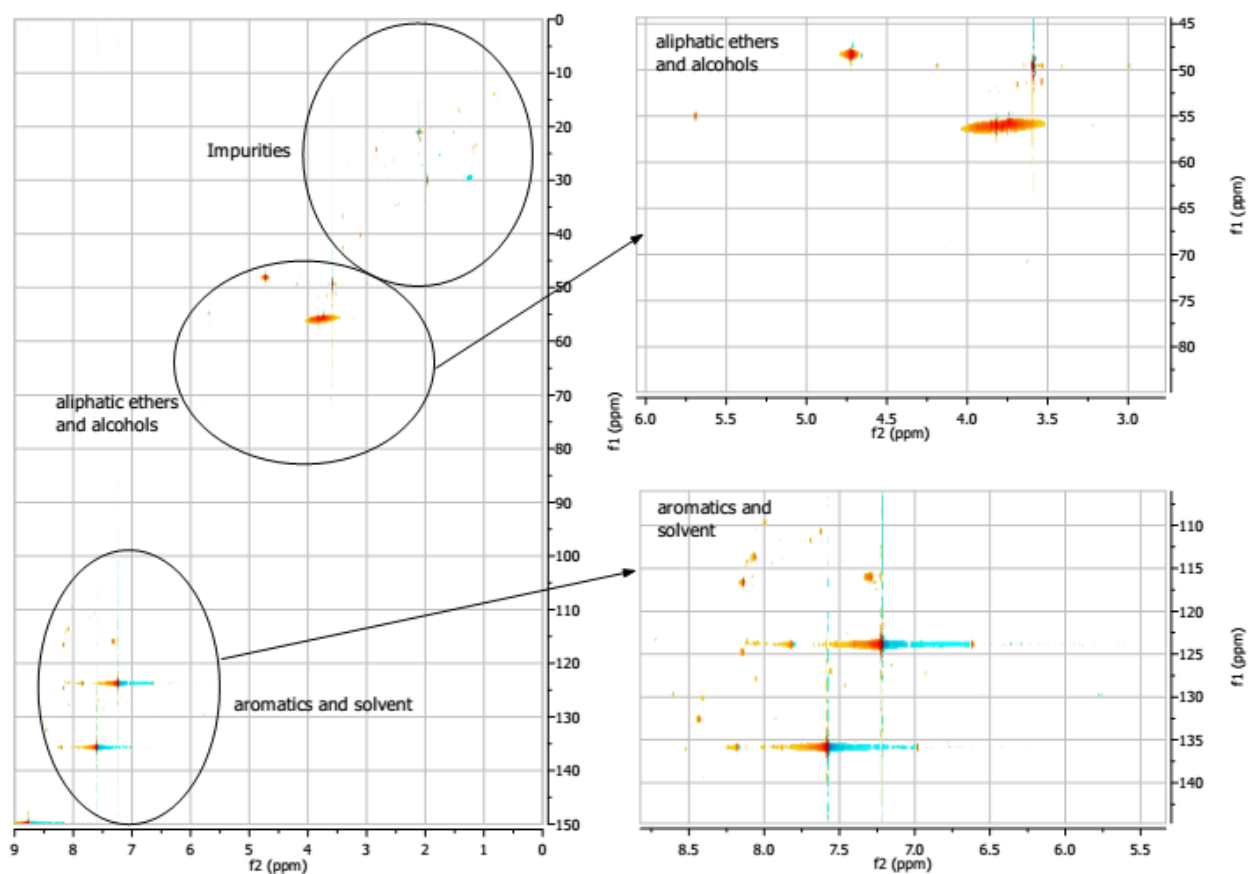
HH organosolv beech lignin in DMSO- d_6 **HH organosolv beech lignin in pyridine- d_5** 

HH organosolv beech lignin in pyridine- d_5 after the reaction with HTc-Cu-V as catalyst



Kraft lignin #370959 in DMSO- d_6

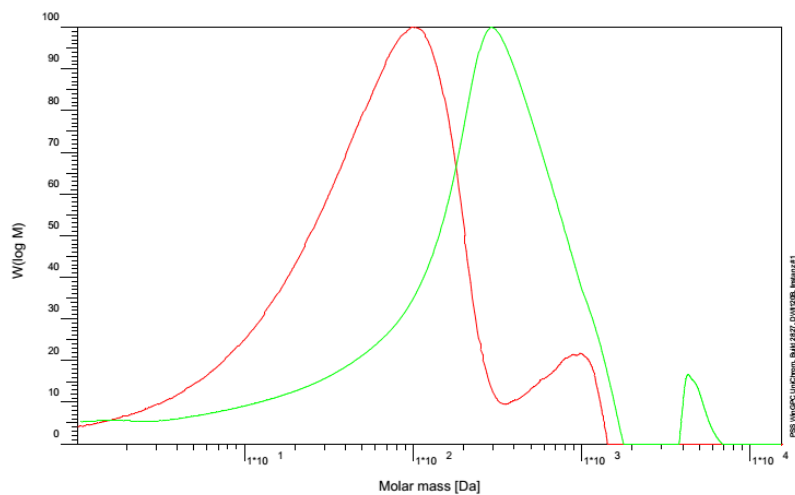


Kraft lignin #370959 in pyridine- d_5 **Kraft lignin #370959 after the reaction with HTc-Cu-V as catalyst**

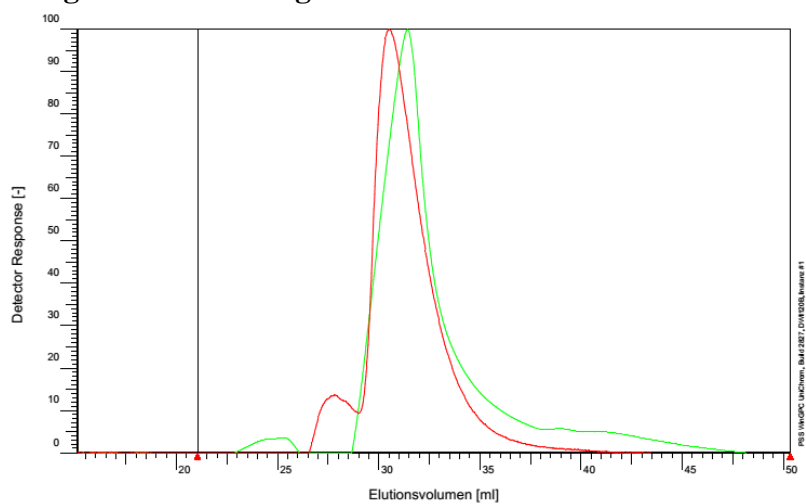
8.2. SEC of lignin

In red is the lignin source shown before the reaction and in green after the reaction.

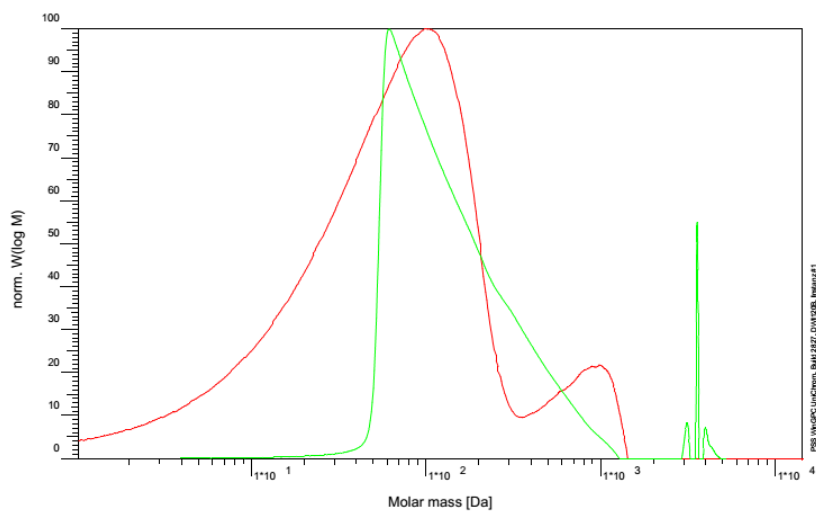
Mass distributions of MPI organosolv beech lignin with HTc-Cu-V after 48 h reaction time



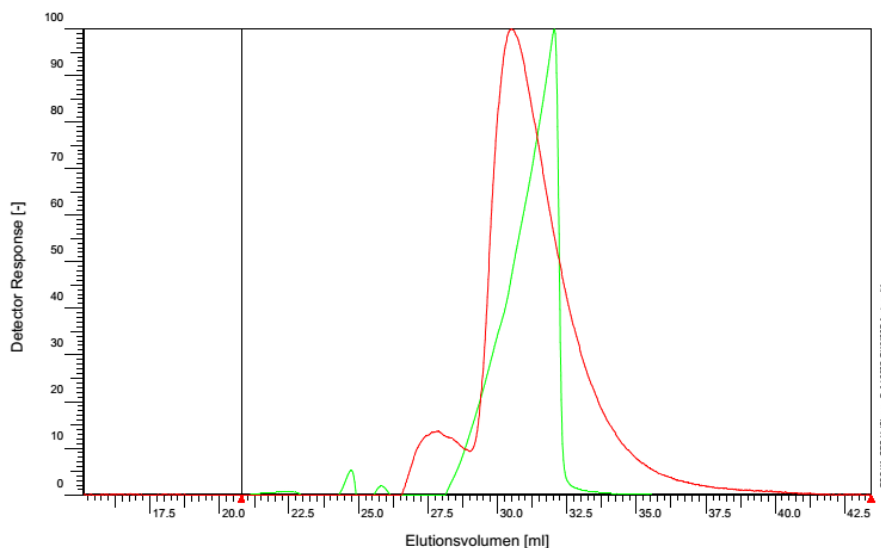
Elugram of MPI organosolv beech lignin with HTc-Cu-V after 48 h reaction time



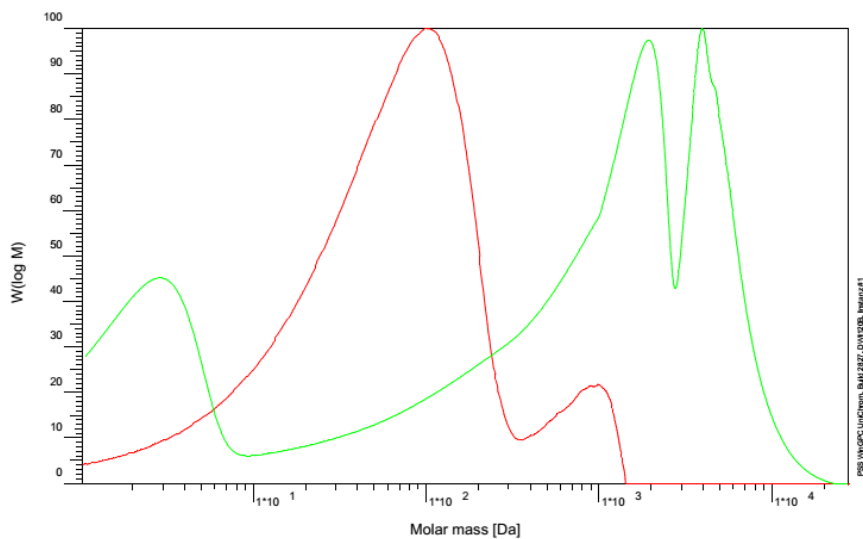
Mass distributions of MPI organosolv beech lignin with HTc-Cu-V after 40 h reaction time



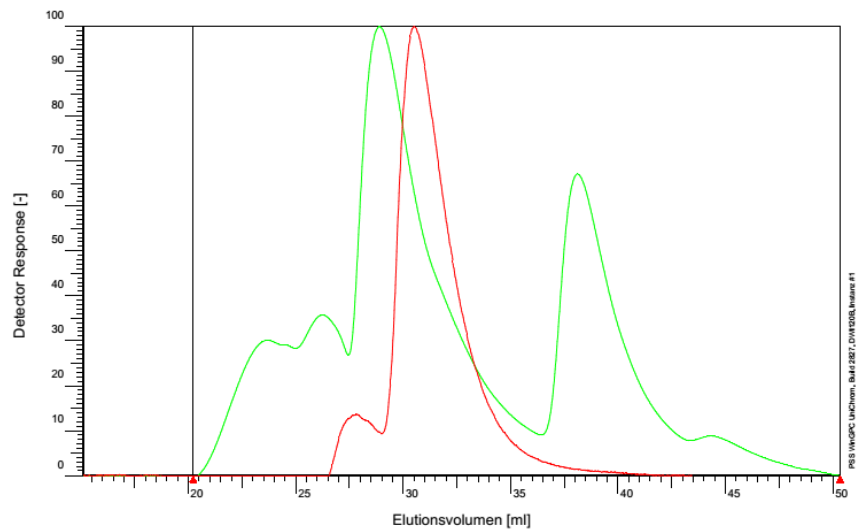
Elugram of MPI organosolv beech lignin with HTc-Cu-V after 40 h reaction time



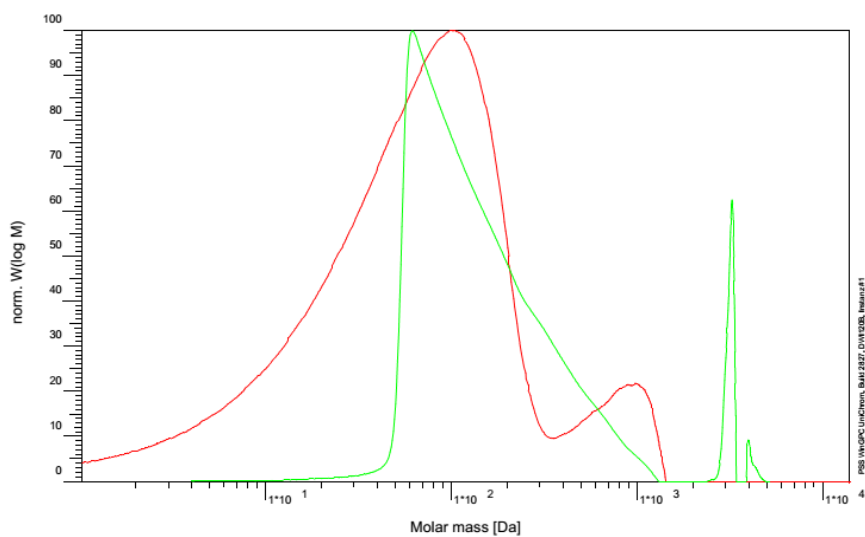
Mass distribution of MPI organosolv beech lignin after 40 h without catalyst



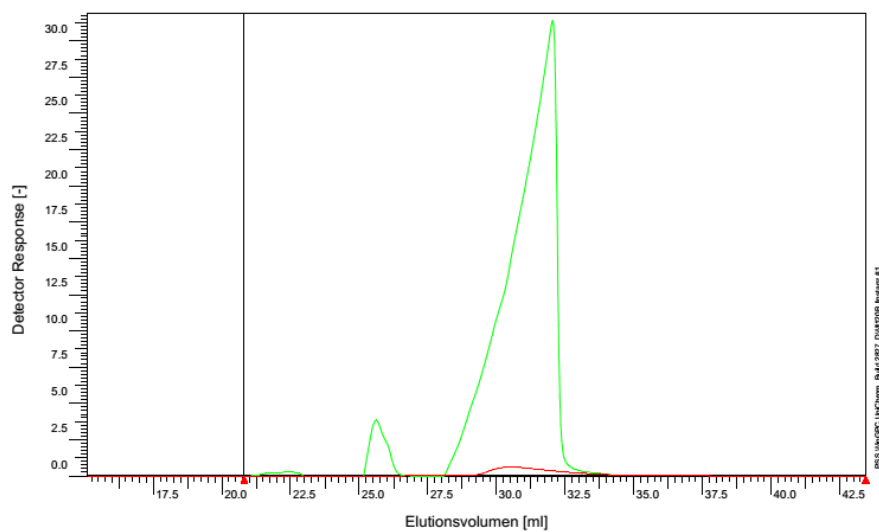
Elugram of MPI organosolv beech lignin after 40 h without catalyst

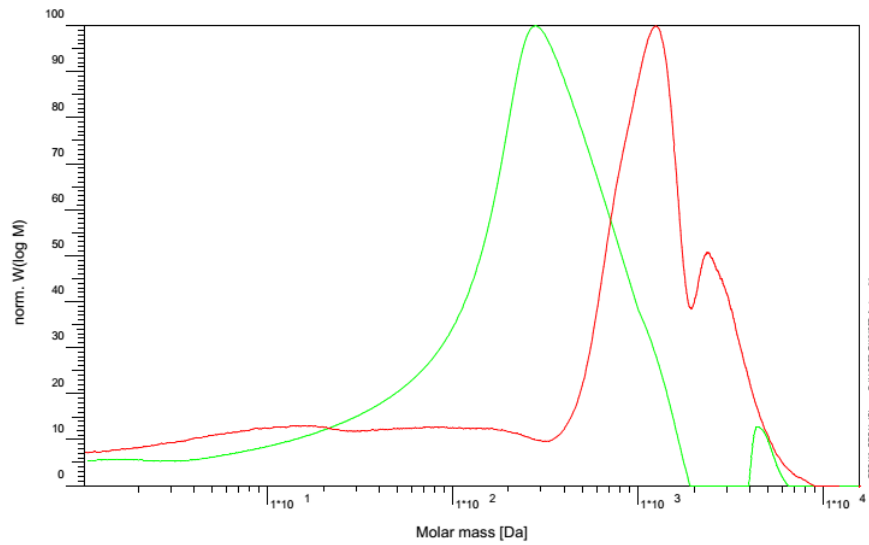
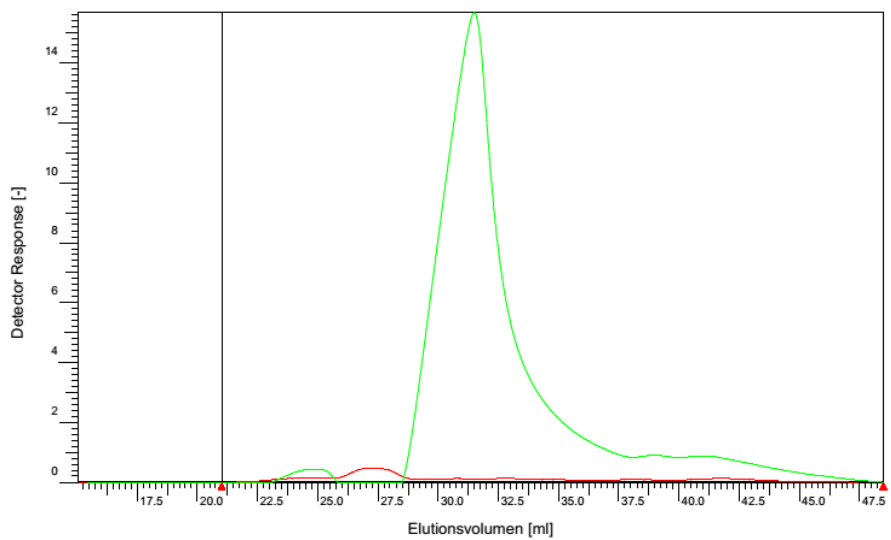
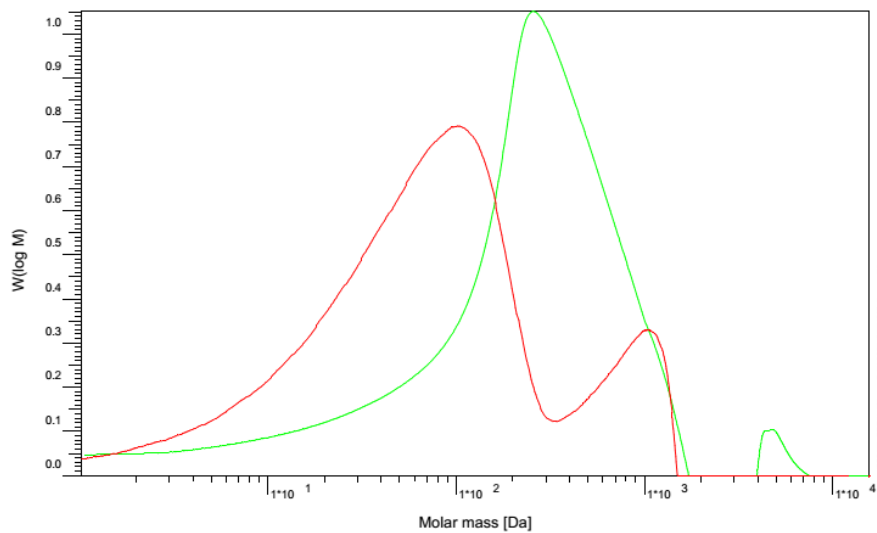


Mass distribution of MPI organosolv beech lignin with $V(acac)_3/Cu(NO_3)_2 \cdot 3H_2O$

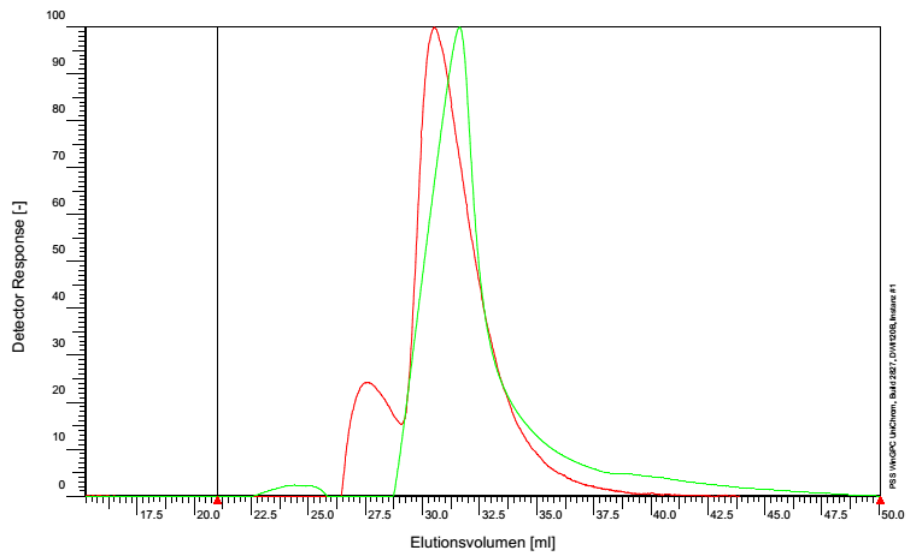


Elugram of MPI organosolv beech lignin with $V(acac)_3/Cu(NO_3)_2 \cdot 3H_2O$

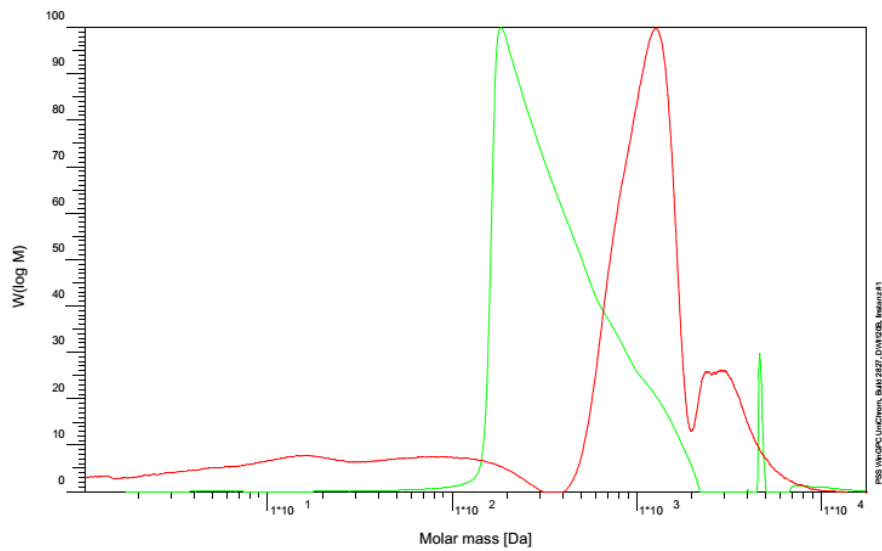


Mass distribution of HH organosolv beech lignin with HTc-Cu-V**Elugram of HH organosolv beech lignin with HTc-Cu-V****Mass distribution of kraft lignin #471003 with HTc-Cu-V**

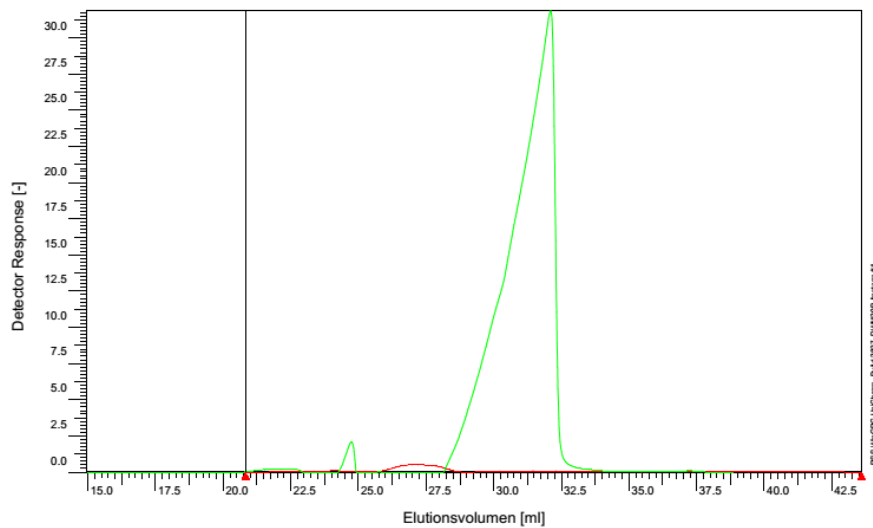
Elugram of kraft lignin #471003 with HTc-Cu-V



Mass distribution of kraft lignin #370959 with HTc-Cu-V

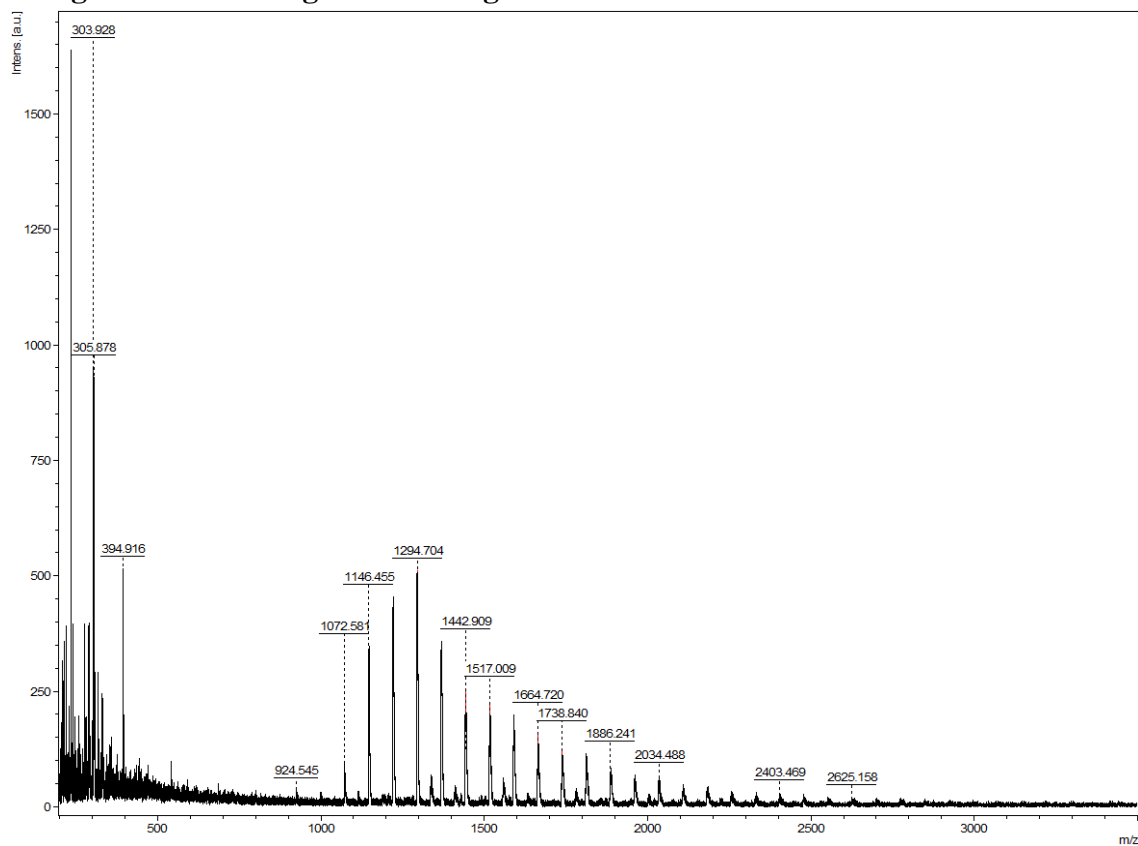


Elugram of kraft lignin #370959 with HTc-Cu-V

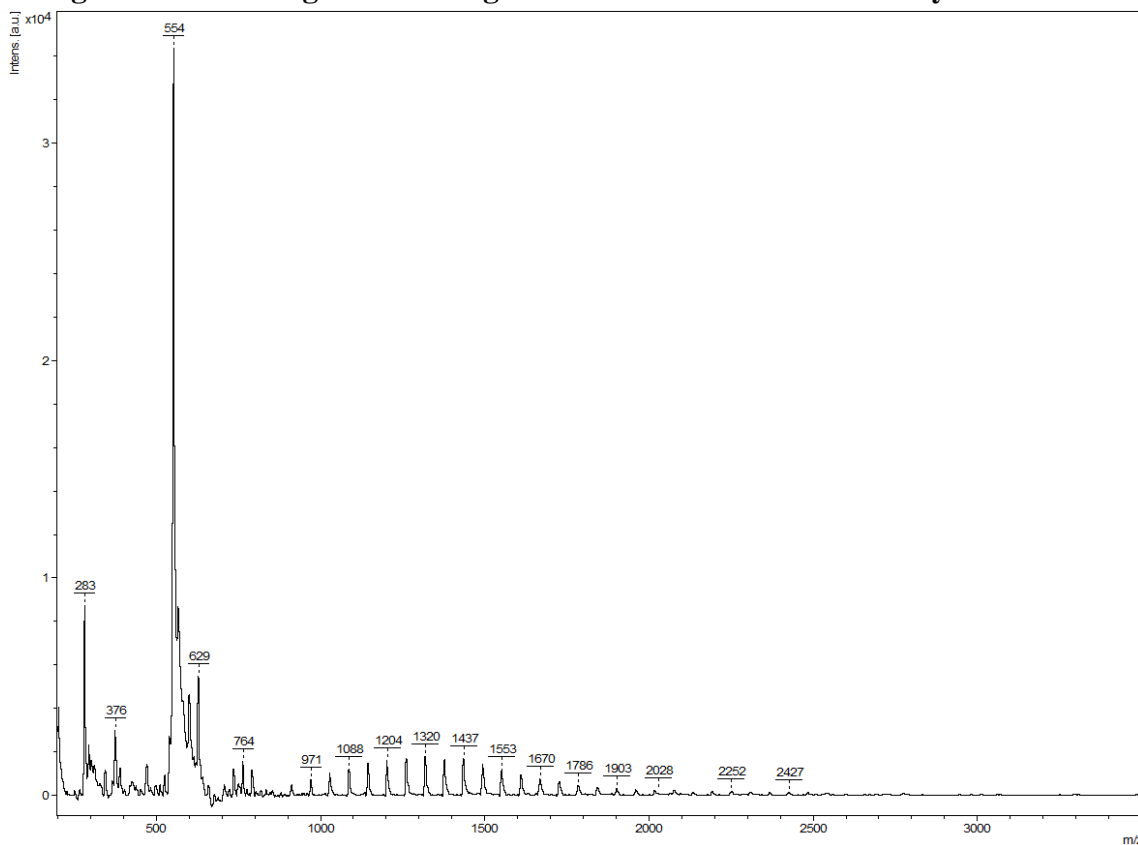


8.3. MALDI spectra of lignin

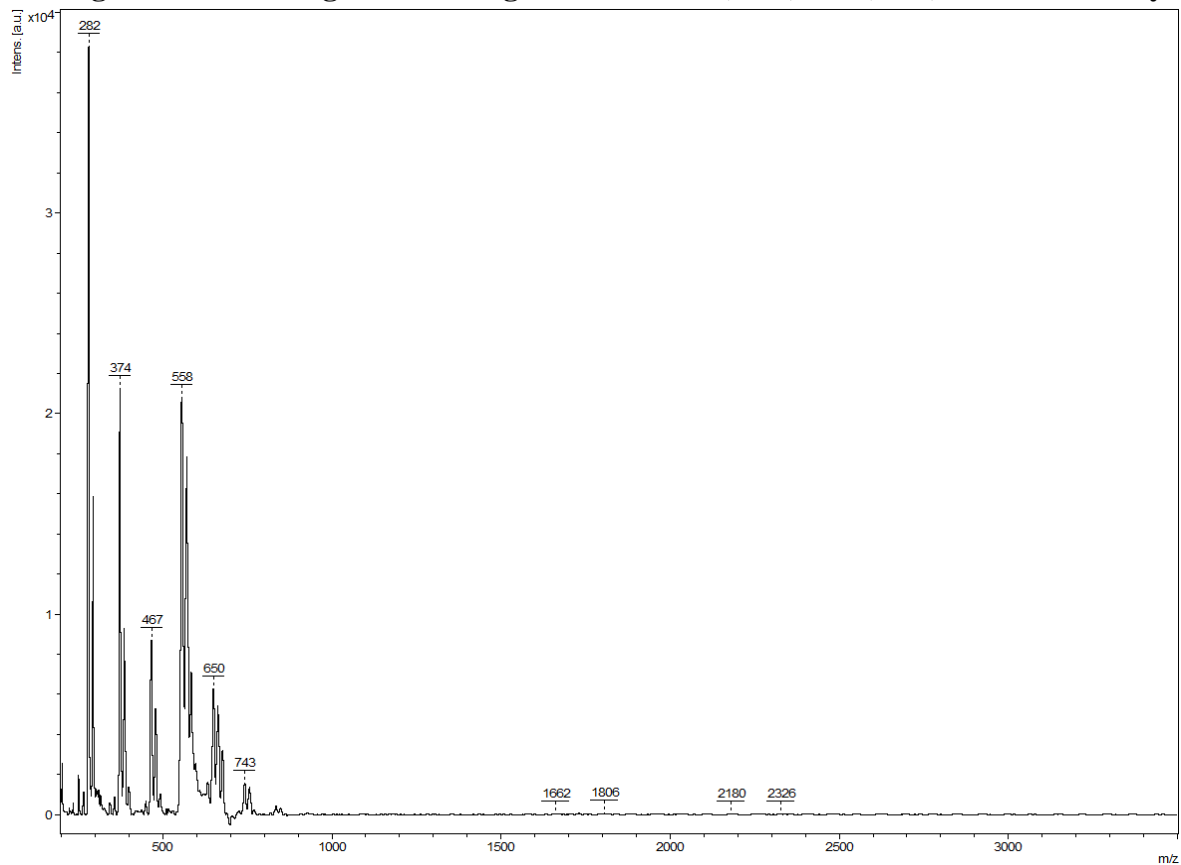
MPI organosolv beech lignin including matrix



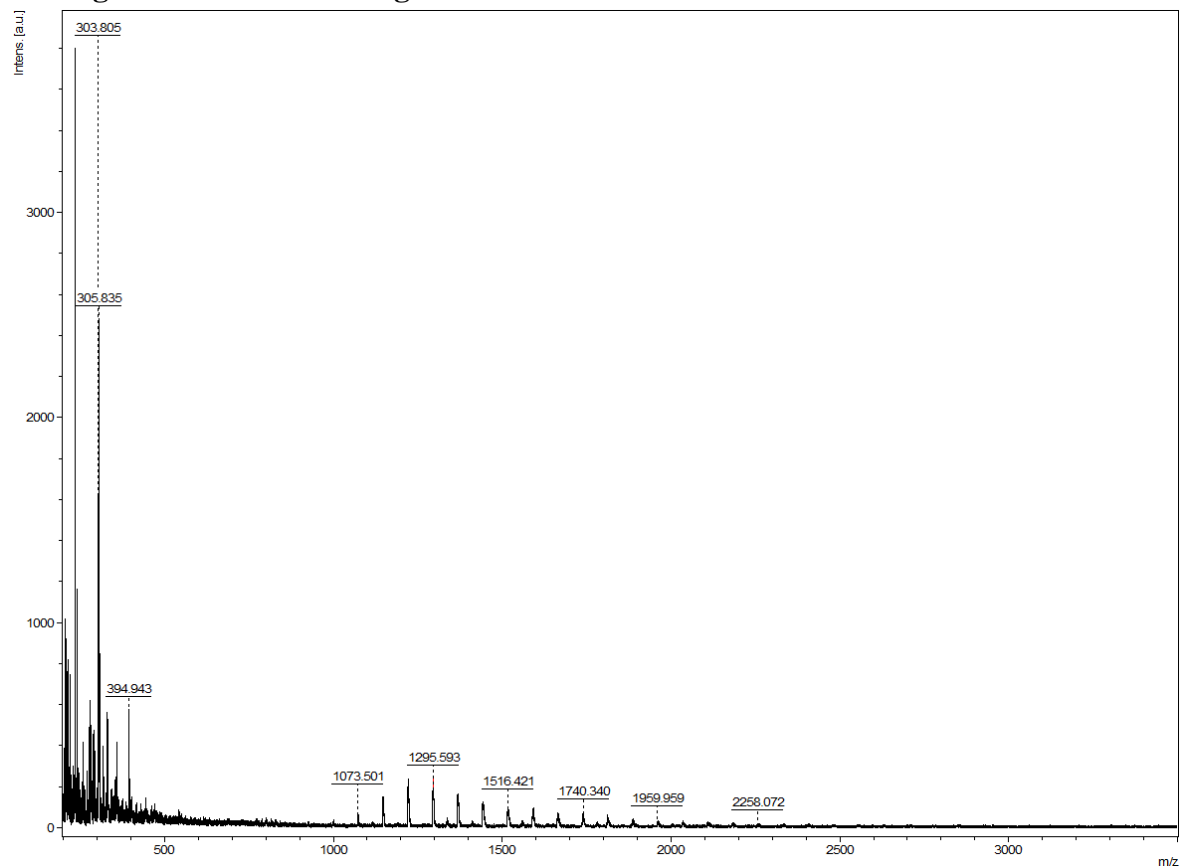
MPI organosolv beech lignin including matrix with HTc-Cu-V as catalyst

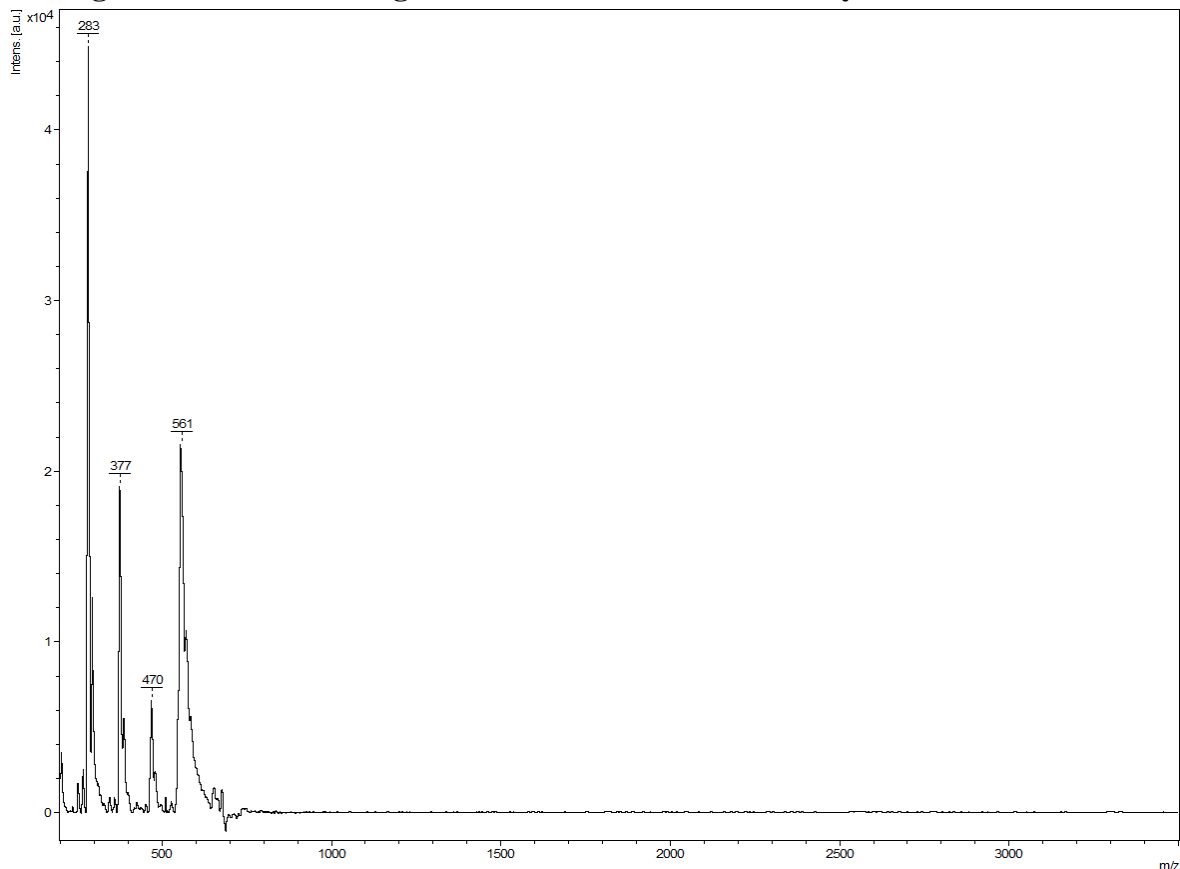


MPI organosolv beech lignin including matrix with $V(acac)_3/Cu(NO_3)_2 \cdot 3H_2O$ as catalyst



Kraft lignin #370959 including matrix



Kraft lignin #370959 including matrix with HTc-Cu-V as catalyst**8.4. Elemental analysis of lignin****8.4.1 Elemental analysis of lignin sources**

Elem. Anal. [MPI organosolv beech lignin]: Found C = 60.38%, H = 6.00%, N = 0.18%.

Elem. Anal. [HH organosolv beech lignin]: Found C = 61.68%, H = 5.81%, N = 0.11%.

Elem. Anal. [Kraft lignin #370959]: Found C = 62.61%, H = 5.85%, N = 0.47%.

8.4.2 Elemental analysis of lignin sources after the reaction with HTc-Cu-V

Elem. Anal. [MPI organosolv beech lignin]: Found C = 54.76%, H = 4.99%, N = 8.40%.

Elem. Anal. [HH organosolv beech lignin]: Found C = 57.12%, H = 4.97%, N = 8.30%.

Elem. Anal. [Kraft lignin #370959]: Found C = 51.24%, H = 4.64%, N = 6.94%.

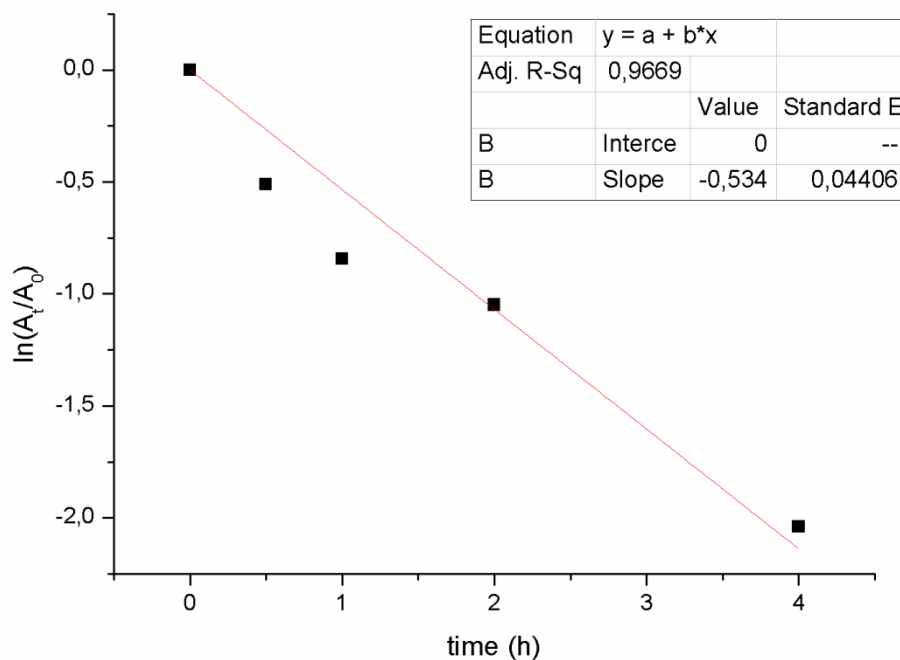
8.4.3 Elemental analysis of lignin source after the reaction with V(acac)₃/Cu(NO₃)₂·3H₂O

Elem. Anal. [MPI organosolv beech lignin]: Found C = 53.75%, H = 5.42%, N = 9.25%.

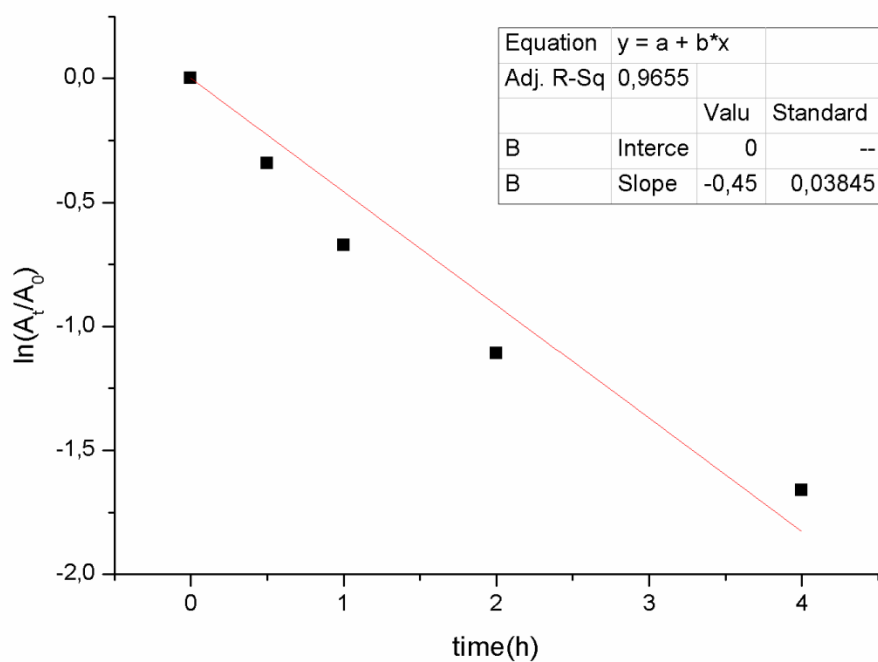
9. Rate constants k in kinetic experiments

9.1. Rate constants k for the cleavage of 3aE with $V(acac)_3$ and $Cu(NO_3)_2 \cdot 3H_2O$

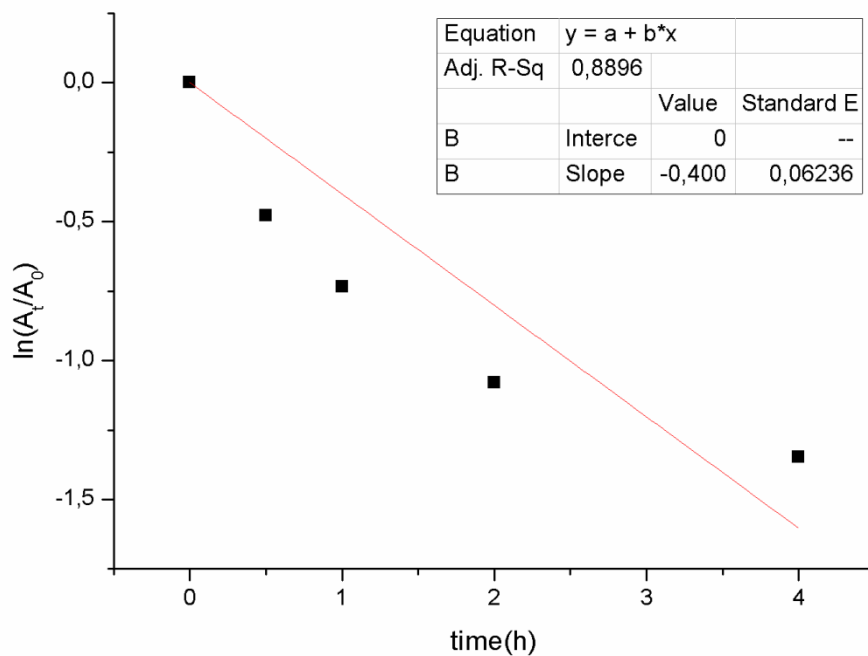
9.1.1 Rate constant $-k$ for the cleavage of 3aE with 5 mol% of $V(acac)_3/Cu(NO_3)_2 \cdot 3H_2O$



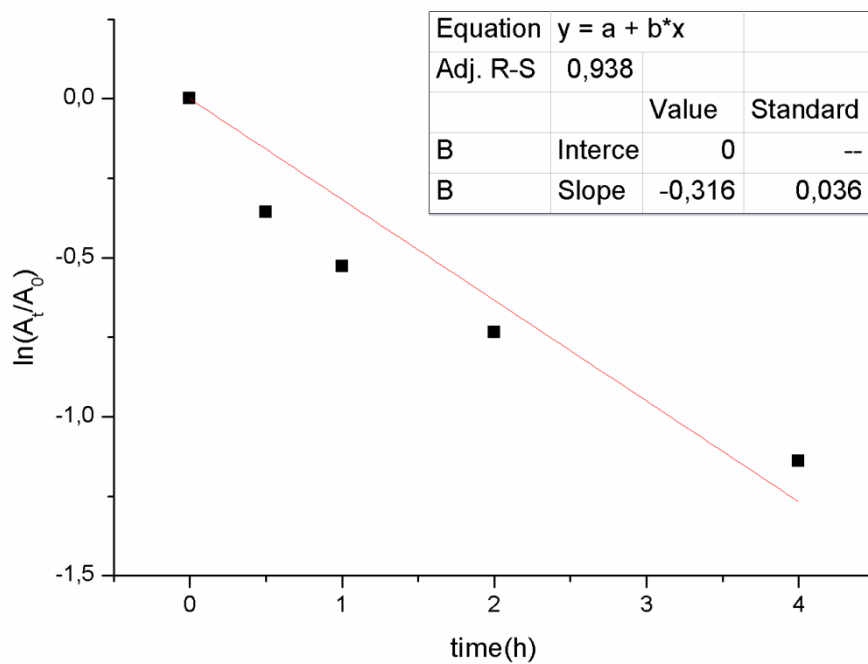
9.1.2 Rate constant $-k$ for the cleavage of 3aE with 2.5 mol% of $V(acac)_3/Cu(NO_3)_2 \cdot 3H_2O$

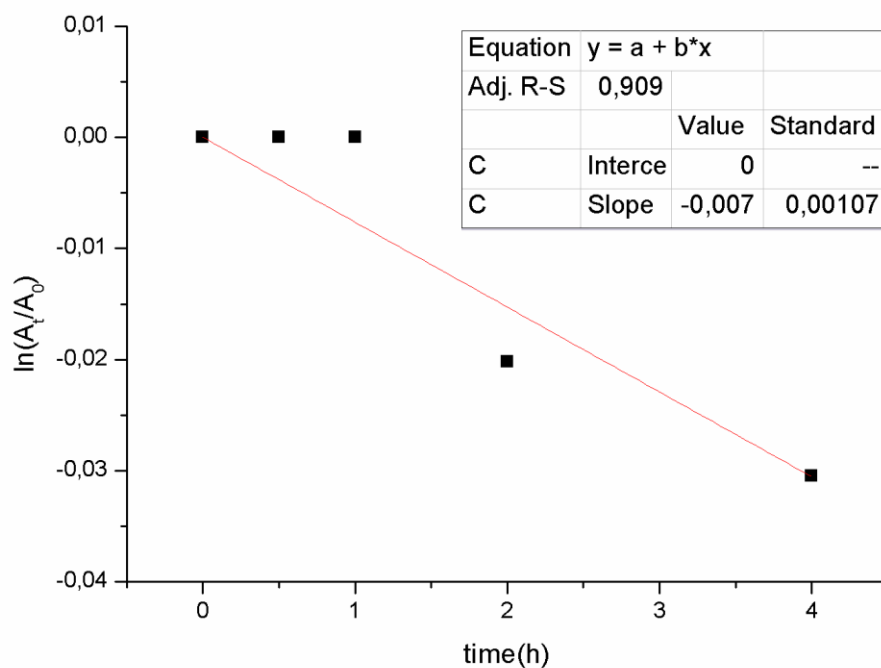
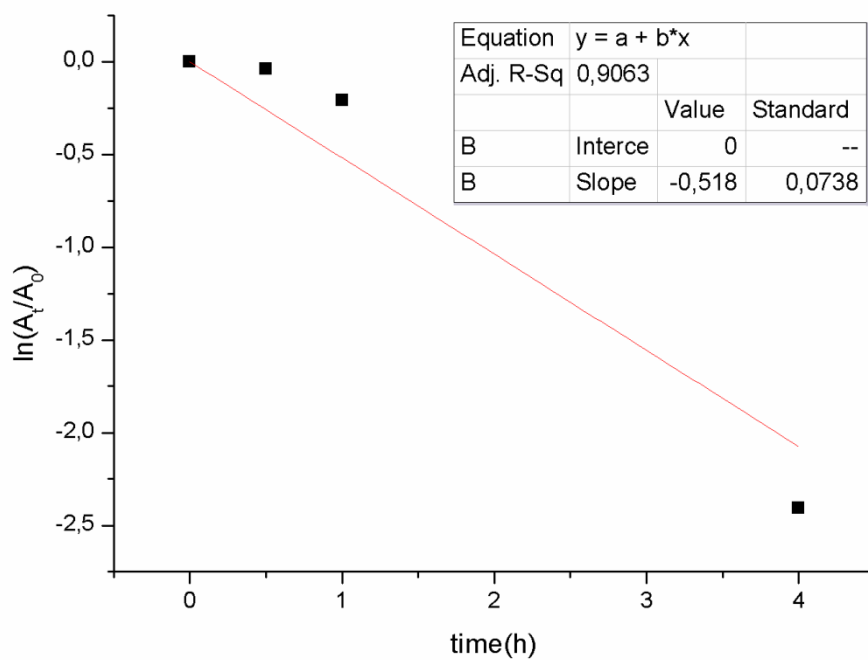


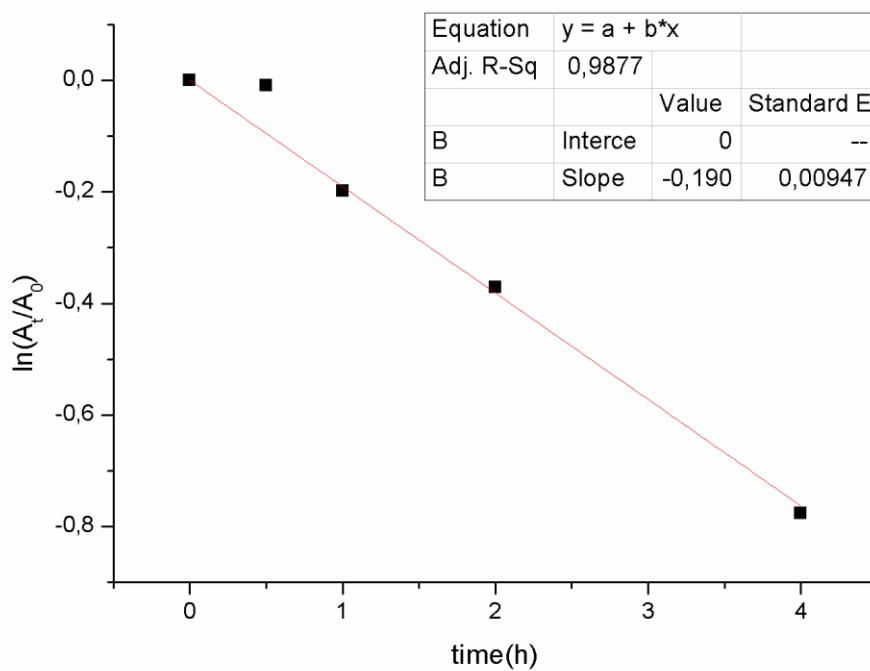
9.1.3 Rate constant $-k$ for the cleavage of 3aE with 5 mol% of $V(acac)_3$



9.1.4 Rate constant $-k$ for the cleavage of 3aE with 2.5 mol% of $V(acac)_3$

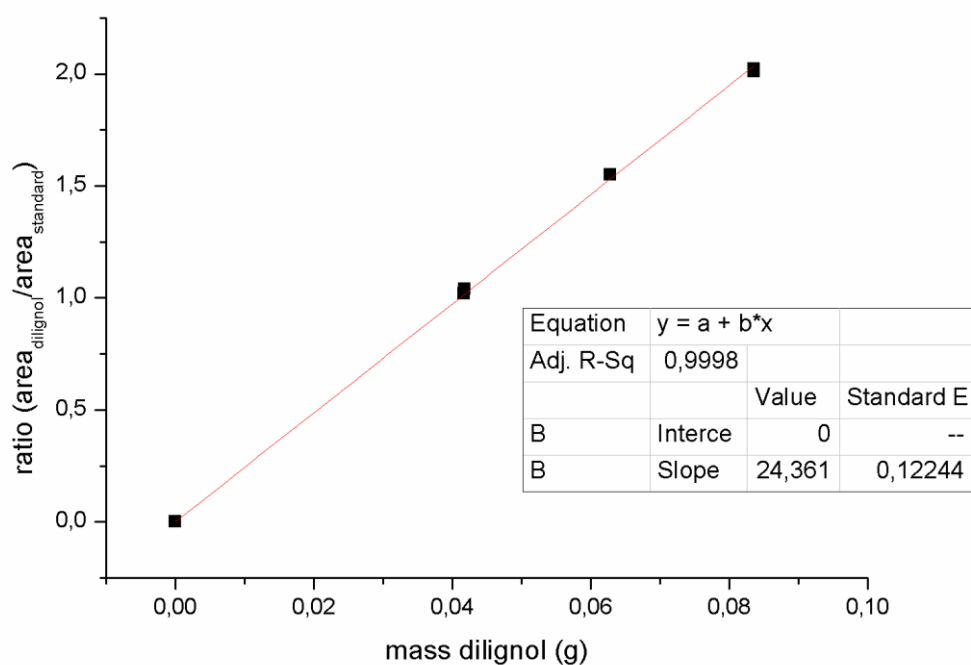


9.1.5 Rate constant $-k$ for the cleavage of 3aE with 5 mol% of $\text{Cu}(\text{NO}_3)_2 \cdot 3\text{H}_2\text{O}$ **9.2. Rate constants k for cleavage reactions with HTc-Cu-V****9.2.1 Rate constant $-k$ for the cleavage of 3aE with 20 wt% of HTc-Cu-V**

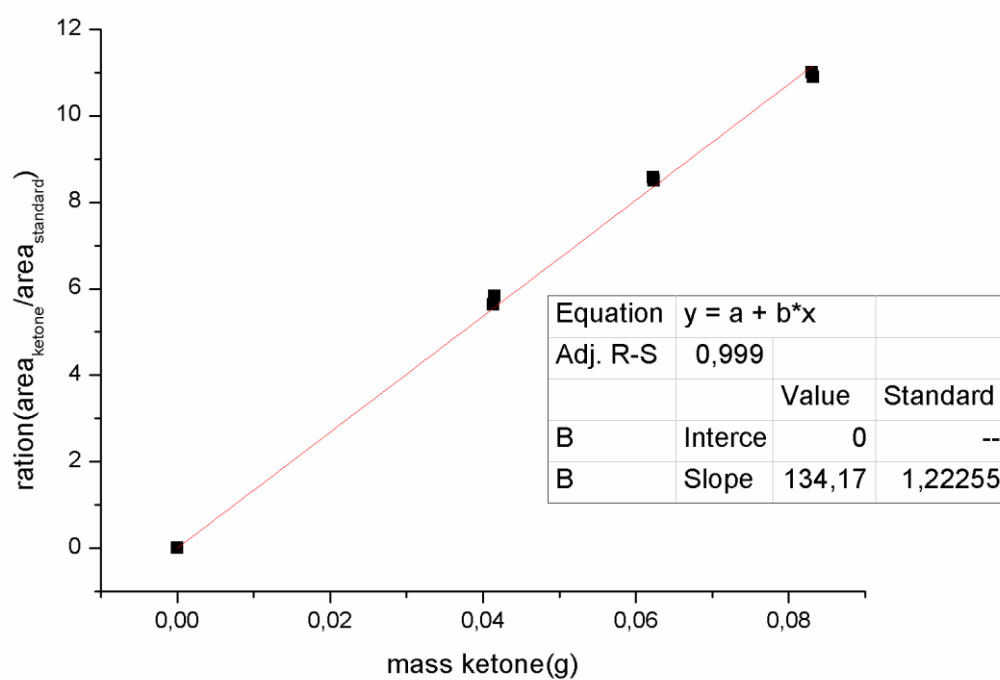
9.2.2 Rate constant $-k$ for the cleavage of 12a with 20 wt% of HTc-Cu-V

10. HPLC calibration

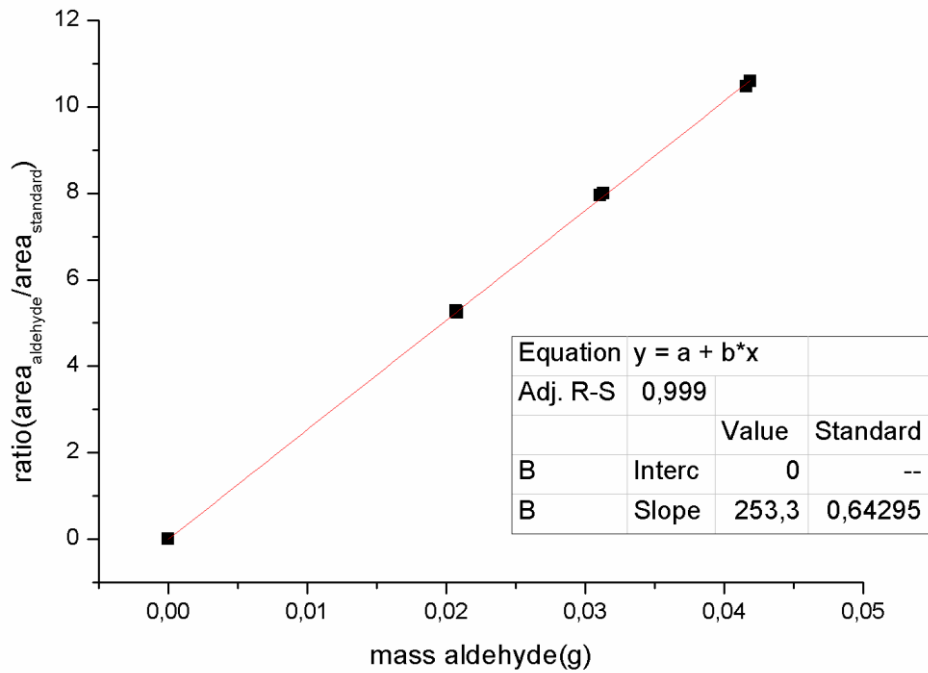
10.1. HPLC calibration for *erythro* 1-(3,4-Dimethoxyphenyl)-2-(2-methoxyphenoxy)-1,3-propanediol



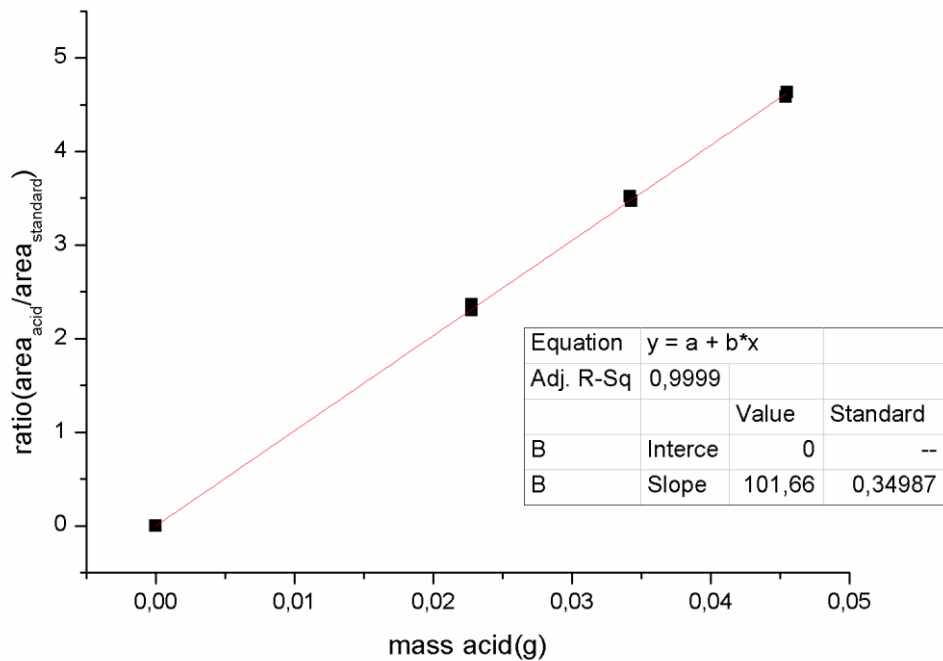
10.2. HPLC calibration for 1-(3,4-Dimethoxyphenyl)-3-hydroxy-2-(2-methoxyphenoxy)propan-1-one



10.3. HPLC calibration for 3,4-Dimethoxybenzaldehyde



10.4. HPLC calibration for 3,4-Dimethoxybenzoic acid



V. Abbreviations

Å	Angstrom
A	ampere
Ac	acetyl
AcOH	acetic acid
Bn	benzyl
b	broad (NMR signal)
Bu	butyl
<i>t</i> Bu	<i>tert</i> -butyl
calcd	calculated
C	celsius
CCD	charge coupled device
COD	1,5-cyclooctadiene
δ	chemical shift
d	doublet (NMR signal)
dd	doublet of doublets (NMR signal)
ddd	doublet of doublet of doublets (NMR signal)
Da	dalton
DAAD	Deutscher Akademischer Austausch Dienst
DABCO	1,4-diazabicyclo[2.2.2]octane
DAIB	(diacetoxyiodo)benzene
DCM	dichloromethane
DEAD	diethyl azodicarboxylate
Dip-Cl TM	diisopinocampheyl chloroborane
dipic	dipicolinate
DMC	dimethyl carbonate
DMEDA	<i>N,N'</i> -dimethylethylenediamine

DMF	<i>N,N</i> -dimethylformamide
DMSO	dimethylsulfoxide
Eds.	editors
EI	electronic impact
eq.	equivalent
EPR	electron paramagnetic resonance
ESI	electrospray ionization
Et	ethyl
Et ₃ N	triethylamine
EtOAc	ethyl acetate
eV	electron volt
G	gauss
GC	gas chromatography
GC-MS	gas chromatography-mass spectrometry
GPC	gel permeation chromatography
h	hour
HMTA	hexamethylenetetramine
HPLC	high-performance liquid chromatography
HRMS	high resolution mass spectroscopy
HSQC	heteronuclear single quantum coherence
HTc	hydrotalcite
Hz	hertz
ICP-OES	inductively coupled plasma optical emission spectrometry
ITQ	Instituto de Tecnología Química
J	joule
<i>J</i>	coupling constant (in NMR spectroscopy)
L	liter
LC-MS	liquid chromatography-mass spectrometry
LDA	lithium diisopropylamide

V. Abbreviations

m	multiplett (NMR signal)
M	molar
MALDI	matrix-assisted laser desorption/ionization
Me	methyl
mep	<i>N,N'</i> -dimethyl- <i>N,N'</i> -bis(2-pyridylmethyl)-ethane-1,2-diamine
min	minutes
mol	mole
m.p.	melting point
MPI	Max Planck Institut
MS	mass spectroscopy
MTO	methyltrioxorhenium
NBS	<i>N</i> -bromosuccinimide
NHC	<i>N</i> -heterocyclic carbene ligand
NMP	<i>N</i> -methyl-2-pyrrolidone
NMR	nuclear magnetic resonance
OAc	acetate
Pa	pascal
PEG	polyethylene glycol
phen	1,10-phenanthroline
PMDS	pentamethyldisiloxane
PMDTA	<i>N,N,N',N',N''</i> -pentamethyldiethylenetriamine
ppm	parts per million
<i>i</i> Pr	<i>iso</i> -propyl
q	quartet (NMR signal)
RI	refractive index
rt	room temperature
s	singlet (NMR signal)
SEC	size-exclusion chromatography
t	triplet (NMR signal)

TAML	tetraamido macrocyclic ligands
TBHP	<i>tert</i> -Butylhydroperoxide
td	triplet of doublets (NMR signal)
TEMPO	(2,2,6,6-tetramethylpiperidin-1-yl)-oxyl
<i>tert</i> -BuONa	sodium <i>tert</i> -butoxide
THF	tetrahydrofuran
TLC	thin layer chromatography
TMDS	tetramethyldisiloxane
TMEDA	<i>N,N,N',N'</i> -tetramethylethylenediamine
ToF	time of flight
TsOH·H ₂ O	<i>p</i> -toluenesulfonic acid monohydrate
V	volt
W	watt
XRD	X-ray diffraction

VI. References

- [1] A. Corma, S. Iborra, A. Velty, *Chem. Rev.* **2007**, *107*, 2411–2502.
- [2] R. C. Kuhad, A. Singh, *Crit. Rev. Biotechnol.* **1993**, *13*, 151–172.
- [3] G. W. Huber, S. Iborra, A. Corma, *Chem. Rev.* **2006**, *106*, 4044–4098.
- [4] P. Mäki-Arvela, P. Holmbom, T. Salmi, D. Y. Murzin, *Catal. Rev. - Sci. Eng.* **2007**, *49*, 197–340.
- [5] a) J. N. Chheda, G. W. Huber, J. A. Dumesic, *Angew. Chem.* **2007**, *119*, 7298–7318; *Angew. Chem. Int. Ed.* **2007**, *46*, 7164–7183; b) G. W. Huber, A. Corma, *Angew. Chem.* **2007**, *119*, 7320–7338; *Angew. Chem. Int. Ed.* **2007**, *46*, 7184–7201; c) C. Somerville, H. Youngs, C. Taylor, S. C. Davis, S. P. Long, *Science* **2010**, *329*, 790–792; d) F. Cherubini, A. H. Stroemman, *Energy Fuels* **2010**, *24*, 2657–2666.
- [6] European Parliament and the Council, Directive 2009/28/EC, **2009**.
- [7] R. D. Perlack, L. L. Wright, A. F. Turhollow, R. L. Graham, B. J. Stokes, D. C. Erbach, U.S. Department of Energy, Biomass as Feedstock for a bioenergy and bioproducts industry: the technical feasibility of a billion-ton annual supply, **2005**; DOI:10.2172/885984.
- [8] a) J. Zakzeski, P. C. A. Bruijninx, A. L. Jongerius, B. M. Weckhuysen, *Chem. Rev.* **2010**, *110*, 3552–3599; b) M. P. Pandey, C. S. Kim, *Chem. Eng. Technol.* **2011**, *34*, 29–41; c) C. Xu, R. A. D. Arancon, J. Labidi, R. Luque, *Chem. Soc. Rev.* **2014**, *43*, 7485–7500; d) R. Ma, Y. Xu, X. Zhang, *ChemSusChem* **2015**, *8*, 24–51.
- [9] a) Á. T. Martínez, J. Rencoret, G. Marques, A. Gutiérrez, D. Ibarra, J. Jiménez-Barbero, J. C. del Río, *Phytochemistry* **2008**, *69*, 2831–2843; b) R. Vanholme, B. Demedts, K. Morreel, J. Ralph, W. Boerjan, *Plant Physiol.* **2010**, *153*, 895–905; c) A. J. Ragauskas, G. T. Beckham, M. J. Biddy, R. Chandra, F. Chen, M. F. Davis, B. H. Davison, R. A. Dixon, P. Gilna, M. Keller, P. Langan, A. N. Naskar, J. N. Saddler, T. J. Tschaplinski, G. A. Tuskan, C. E. Wyman, *Science* **2014**, *344*, 1–10.
- [10] R. Parthasarathi, R. A. Romero, A. Redondo, S. Gnanakaran, *J. Phys. Chem. Lett.* **2011**, *2*, 2660–2666.
- [11] J. J. Bozell, J. E. Holladay, D. Johnson, J. F. White, *Top Value Added Candidates from Biomass, Volume II: Results of Screening for Potential Candidates from Biorefinery Lignin*; Pacific Northwest National Laboratory: Richland, WA, **2007**.
- [12] F. S. Chakar, A. J. Ragauskas, *Ind. Crops Prod.* **2004**, *20*, 131–141.
- [13] J. Gierer, *Wood Sci. Technol.* **1980**, *14*, 241–266.
- [14] E. Adler, B. O. Lindgren, U. Saedlén, *Svensk Papperstidning* **1952**, *55*, 245–254.
- [15] E. Adler, E. Eriksoo, *Acta Chem. Scand.* **1955**, *9*, 341–342.
- [16] S. Kawai, K. Okita, K. Sugishita, A. Tanaka, H. Ohashi, *J. Wood Sci.* **1999**, *45*, 440–443.
- [17] S. Ciofi-Baffoni, L. Banci, A. Brandi, *J. Chem. Soc. Perkin Trans. 1* **1998**, 3207–3217.
- [18] R. F. Helm, J. Ralph, *J. Wood Chem. Technol.* **1993**, *13*, 593–601.
- [19] R. F. Helm, K. Li, *Holzforschung* **1995**, *49*, 533–536.

- [20] a) K. Lundquist, S. Remmerth, *Acta Chem. Scand.* **1975**, *B29*, 276–278; b) I. Berndtsson, K. Lundquist, *Acta Chem. Scand.* **1977**, *B31*, 725–726; c) T. Ahvonen, G. Brouno, P. Kristersson, K. Lundquist, *Acta Chem. Scand.* **1983**, *B37*, 845–849.
- [21] F. Nakatsubo, K. Sato, T. Higuchi, *Holzforschung* **1975**, *29*, 165–168.
- [22] V. L. Pardini, C. Z. Smith, J. H. P. Utley, R. R. Vargas, H. Viertler, *J. Org. Chem.* **1991**, *56*, 7305–7313.
- [23] D. W. Cho, R. Parthasarathi, A. S. Pimentel, G. D. Maestas, H. J. Park, U. C. Yoon, D. Dunaway-Mariano, S. Gnanakaran, P. Langan, P. S. Mariano, *J. Org. Chem.* **2010**, *75*, 6549–6562.
- [24] a) M. M. Hepditch, R. W. Thring, *Can. J. Chem. Eng.* **2000**, *78*, 226–231; b) J. B. Binder, M. J. Gray, J. F. White, Z. C. Zhang, J. E. Holladay, *Biomass and Bioenergy* **2009**, *33*, 1122–1130; c) S. Jia, B. J. Cox, X. Guo, Z. C. Zhang, J. G. Ekerdt, *Ind. Eng. Chem. Res.* **2011**, *50*, 849–855; d) M. R. Sturgeon, S. Kim, K. Lawrence, R. S. Paton, S. C. Chmely, M. Nimlos, T. D. Foust, G. T. Beckham, *ACS Sustainable Chem. Eng.* **2014**, *2*, 472–485; e) A. Kaiho, M. Kogo, R. Sakai, K. Saito, T. Watanabe, *Green Chem.* **2015**, *17*, 2780–2783; f) P. J. Deuss, M. Scott, F. Tran, N. J. Westwood, J. G. de Vries, K. Barta, *J. Am. Chem. Soc.*, **2015**, *137*, 7456–7467.
- [25] a) R. W. Thring, *Biomass Bioenergy* **1994**, *7*, 125–130; b) J. E. Miller, L. Evans, A. Littlewolf, D. E. Trudell, *Fuel* **1999**, *78*, 1363–1366; c) S. Karagöz, T. Bhaskar, A. Muto, Y. Sakata, *Fuel* **2004**, *83*, 2293–2299; d) A. Vigneault, D. K. Johnson, E. Chornet, *Can. J. Chem. Eng.* **2007**, *85*, 906–916; e) S. Nenkova, T. Vasileva, K. Stanulov, *Chem. Nat. Compd.* **2008**, *44*, 182–185; f) J.-M. Lavoie, W. Baré, M. Bilodeau, *Bioresour. Technol.* **2011**, *102*, 4917–4920; g) V. M. Roberts, V. Stein, T. Reiner, A. Lemonidou, X. Li, J. A. Lercher, *Chem. Eur. J.* **2011**, *17*, 5939–5948; h) R. Beauchet, F. Monteil-Rivera, J. M. Lavoie, *Bioresour. Technol.* **2012**, *121*, 328–334; i) A. Toledano, L. Serrano, J. Labidi, *J. Chem. Technol. Biotechnol.* **2012**, *87*, 1593–1599; j) A. Toledano, L. Serrano, J. Labidi, *Fuel* **2014**, *116*, 617–624.
- [26] S. Dabral, J. Mottweiler, T. Rinesch, C. Bolm, *Green Chem.* **2015**, *17*, 4908–4912.
- [27] a) E. E. Harris, J. D’Ianni, H. Adkins, *J. Am. Chem. Soc.* **1938**, *60*, 1467–1470; b) C. P. Brewer, L. M. Cooke, H. Hibbert, *J. Am. Chem. Soc.* **1948**, *70*, 57–59; c) J. M. Pepper, W. Steck, *Can. J. Chem.* **1963**, *41*, 2867–2875.
- [28] a) J. M. Pepper, Y. W. Lee, *Can. J. Chem.* **1969**, *47*, 723–727; b) J. M. Pepper, Y. W. Lee, *Can. J. Chem.* **1970**, *48*, 477–479.
- [29] a) N. Yan, C. Zhao, P. J. Dyson, C. Wang, L. Liu, Y. Kou, *ChemSusChem* **2008**, *1*, 626–629; b) C. Zhao, Y. Kou, A. A. Lemonidou, X. B. Li, J. A. Lercher, *Angew. Chem. Int. Ed.* **2009**, *48*, 3987–3990; *Angew. Chem.* **2009**, *121*, 4047–4050; c) N. Yan, Y. A. Yuan, R. Dykeman, Y. A. Kou, P. J. Dyson, *Angew. Chem. Int. Ed.* **2010**, *49*, 5549–5553; *Angew. Chem.* **2010**, *122*, 5681–5685; d) C. Zhao, Y. Kou, A. A. Lemonidou, X. B. Li, J. A. Lercher, *Chem. Commun.* **2010**, *46*, 412–414; e) C. Zhao, J. Y. He, A. A. Lemonidou, X. B. Li, J. A. Lercher, *J. Catal.* **2011**, *280*, 8–16; f) A. L. Jongerius, R. Jastrzebski, P. C. A. Bruijninx, B. M. Weckhuysen, *J. Catal.* **2012**, *285*, 315–323; g) J. Zakzeski, A. L. Jongerius, P. C. A. Bruijninx, B. M. Weckhuysen, *ChemSusChem* **2012**, *5*, 1602–1609; h) A. G. Sergeev, J. D. Webb, J. F. Hartwig, *J. Am. Chem. Soc.* **2012**, *134*, 20226–20229; i) J. He, C. Zhao, J. A. Lercher, *J. Am. Chem. Soc.* **2012**, *134*, 20768–20775; j) Z. Strassberger, A. H. Alberts, M. J. Louwerse, S. Tanase, G. Rothenberg, *Green Chem.* **2013**, *15*, 768–774; k) T. H. Parsell, B. C. Owen, I. Klein, T. M. Jarrell, C. L. Marcum, L. J. Hauptert, L. M. Amundson, H. I. Kenttämä, F. Ribeiro, J. T. Miller, M. M. Abu-Omar, *Chem. Sci.* **2013**, *4*, 806–813.
- [30] a) W. Schweers, *Holzforschung* **1969**, *23*, 5–9; b) U. Schuchardt, O. A. Marangoni Borges, *Catal. Today* **1989**, *5*, 523–531.

- [31] a) T. Q. Hu, B. R. James, C.-L. Lee, *J. Pulp. Pap. Sci.* **1997**, *23*, J153–J156; b) M. Nagy, K. David, G. J. P. Britovsek, A. J. Ragauskas, *Holzforschung* **2009**, *63*, 513–520; c) A. G. Sergeev, J. F. Hartwig, *Science* **2011**, *332*, 439–443; d) Y. Ren, M. Yan, J. Wang, Z. C. Zhang, K. Yao, *Angew. Chem. Int. Ed.* **2013**, *52*, 12674–12678; *Angew. Chem.* **2013**, *125*, 12906–12910.
- [32] a) E. Feghali, T. Cantat, *Chem. Commun.* **2014**, *50*, 862–865; b) J. Zhang, Y. Chen, M. A. Brook, *ACS Sustainable Chem. Eng.* **2014**, *2*, 1983–1991.
- [33] a) J. M. Nichols, L. M. Bishop, R. G. Bergman, J. A. Ellman, *J. Am. Chem. Soc.* **2010**, *132*, 12554–12555; b) T. vom Stein, T. Weigand, C. Merckens, J. Klankermayer, W. Leitner, *ChemCatChem* **2013**, *5*, 439–441; c) D. Weickmann, B. Plietker, *ChemCatChem* **2013**, *5*, 2170–2173; d) J. D. Nguyen, B. S. Matsuura, C. R. J. Stephenson, *J. Am. Chem. Soc.* **2014**, *136*, 1218–1221; e) R. G. Harms, I. I. E. Markovits, M. Drees, W. A. Herrmann, M. Cokoja, F. E. Kühn, *ChemSusChem* **2014**, *7*, 429–434; e) T. v. Stein, T. d. Hartog, J. Buendia, S. Stoychev, J. Mottweiler, C. Bolm, J. Klankermayer, W. Leitner, *Angew. Chem. Int. Ed.* **2015**, *54*, 5859–5863; *Angew. Chem.* **2015**, *127*, 5957–5961.
- [34] J. Mottweiler, J. Buendia, E. Zuidema, C. Bolm, in M. Klaas, W. Schröder (Eds.), *Fuels from Biomass: An Interdisciplinary Approach*. Berlin Heidelberg: Springer-Verlag, **2015**, 105–116.
- [35] a) R. DiCosimo, H.-C. Szabo, *J. Org. Chem.* **1988**, *53*, 1673–1679; b) P. A. Watson, L. J. Wright, T. J. Fullerton, *J. Wood Chem. Tech.* **1993**, *13*, 371–389; c) C. Canevali, M. Orlandi, L. Pardi, B. Rindone, R. Scotti, J. Sipila, F. Morazzoni, *J. Chem. Soc., Dalton Trans.* **2002**, *15*, 3007–3014; d) W. Partenheimer, *Adv. Synth. Catal.* **2009**, *351*, 456–466; e) J. Zakzeski, P. C. A. Bruijninx, B. M. Weckhuysen, *Green Chem.* **2011**, *13*, 671–680; f) B. Biannic, J. J. Bozell, *Org. Lett.* **2013**, *15*, 2730–2733; g) C. Zhu, W. Ding, T. Shen, C. Tang, C. Sun, S. Xu, Y. Chen, J. Wu, H. Ying, *ChemSusChem* **2015**, *8*, 1768–1778.
- [36] a) P. A. Watson, L. J. Wright, T. J. Fullerton, *J. Wood Chem. Tech.* **1993**, *13*, 411–428; c) I. A. Weinstock, E. M. G. Barbuzzi, M. W. Wemple, J. J. Cowan, R. S. Reiner, D. M. Sonnen, R. A. Heintz, J. S. Bond, C. L. Hill, *Nature* **2001**, *414*, 191–195; d) C.-L. Chen, E. A. Capanema, H. S. Gracz, *J. Agric. Food Chem.* **2003**, *51*, 1932–1941; e) C.-L. Chen, E. A. Capanema, H. S. Gracz, *J. Agric. Food Chem.* **2003**, *51*, 6223–6232; f) C. Crestini, P. Pro, V. Nerib, R. Saladino, *Bioorg. Med. Chem.* **2005**, *13*, 2569–2578; g) A. Rahimi, A. Azarpira, H. Kim, J. Ralph, S. S. Stahl, *J. Am. Chem. Soc.* **2013**, *135*, 6415–6418; h) C. S. Lancefield, O. S. Ojo, F. Tran, N. J. Westwood, *Angew. Chem. Int. Ed.* **2015**, *54*, 258–262; *Angew. Chem.* **2015**, *127*, 260–264.
- [37] a) M. Shimada, T. Habe, T. Umezawa, T. Higuchi, T. Okamoto, *Biochem. Biophys. Res. Commun.* **1984**, *122*, 1247–1252; b) T. Habe, M. Shimada, T. Okamoto, B. Panijpan, T. Higuchia, *J. Chem. Soc., Chem. Commun.* **1985**, 1323–1324; c) P. A. Watson, L. J. Wright, T. J. Fullerton, *J. Wood Chem. Tech.* **1993**, *13*, 391–409; d) T. J. Collins, *Acc. Chem. Res.* **2002**, *35*, 782–790; e) F. Napoly, L. Jean-Gérard, C. Goux-Henry, M. Draye, B. Andrioletti, *Eur. J. Org. Chem.* **2014**, 781–787.
- [38] a) G. Wu, M. Heitz, *J. Wood Chem. Tech.* **1995**, *15*, 189–202; b) Q. Xiang, Y. Y. Lee, *Appl. Biochem. Biotechnol.* **2001**, *91*, 71–80; c) E. Araujo, A. J. Rodríguez-Malaver, A. M. González, O. J. Rojas, N. Peñaloza, J. Bullón, M. A. Lara, N. Dmitrieva, *Appl. Biochem. Biotechnol.* **2002**, *97*, 91–103; d) J. Zeng, C. G. Yoo, F. Wang, X. Pan, W. Vermerris, Z. Tong, *ChemSusChem* **2015**, *8*, 861–871.
- [39] a) C. Bolm, J. Legros, J. L. Paih, L. Zani, *Chem. Rev.* **2004**, *104*, 6217–6254; b) A. Correa, O. G. Mancheño, C. Bolm, *Chem. Soc. Rev.* **2008**, *37*, 1108–1117; c) C. Bolm, *Nat. Chem.* **2009**, *1*, 420; d) *Iron Catalysis in Organic Chemistry*, Ed. B. Plietker, Wiley, Weinheim, **2008**; e) A. A. O. Sarhan, C. Bolm, *Chem. Soc. Rev.* **2009**, *38*, 2730–2744; f) F. G. Gelalcha, *Adv. Synth. Catal.* **2014**, *356*, 261–299; g) F. Jia, Z. Li, *Org. Chem. Front.* **2014**, *1*, 194–214; h) P. P. Chandrachud, D. M. Jenkins, *Tetrahedron Lett.* **2015**, *56*, 2369–2376; i) I. Bauer, H.-J. Knölker, *Chem. Rev.* **2015**, *115*, 3170–3387; j) A. Fingerhut, O. V. Serdyuk and S. B. Tsogoeva, *Green Chem.* **2015**, *17*, 2042–2058.

- [40] a) N. Rahmawati, Y. Ohashi, Y. Honda, M. Kuwahara, K. Fackler, K. Messner, T. Watanabe, *Chem. Eng. J.* **2005**, *112*, 167–171; b) B. Sedai, C. Díaz-Urrutia, R. T. Baker, R. Wu, L. A. P. Silks, S. K. Hanson, *ACS Catal.* **2011**, *1*, 794–804; c) J. Zhang, Y. Liu, S. Chiba, T.-P. Loh, *Chem. Commun.* **2013**, *49*, 11439–11441; d) B. Sedai, C. Díaz-Urrutia, R. T. Baker, R. Wu, L. A. “Pete” Silks, S. K. Hanson *ACS Catal.* **2013**, *3*, 3111–3122 e) S. Nanayakkara, A. F. Patti, K. Saito, *Green Chem.* **2014**, *16*, 1897–1903; f) B. Sedai, T. Baker, *Adv. Synth. Cat.* **2014**, *356*, 3563–3574; g) S. Liu, C. Zhang, L. Li, S. Yu, C. Xie, F. Liu, Z. Song, *Ind. Eng. Chem. Res.* **2014**, *53*, 19370–19374; h) L. J. Mitchell, C. J. Moody, *J. Org. Chem.* **2014**, *79*, 11091–11100.
- [41] a) S. K. Hanson, R. T. Baker, J. C. Gordon, B. L. Scott, D. L. Thorn, *Inorg. Chem.* **2010**, *49*, 5611–5618; b) S. Son, F. D. Toste, *Angew. Chem.* **2010**, *122*, 3879–3882; *Angew. Chem. Int. Ed.* **2010**, *49*, 3791–3794; c) S. K. Hanson, R. Wu, L. A. “Pete” Silks, *Angew. Chem.* **2012**, *124*, 3466–3469; *Angew. Chem. Int. Ed.* **2012**, *51*, 3410–3413; d) J. M. W. Chan, S. Bauer, H. Sorek, S. Sreekumar, K. Wang, F. D. Toste, *ACS Catal.* **2013**, *3*, 1369–1377; e) S. K. Hanson, R. T. Baker, *Acc. Chem. Res.* **2015**, *48*, 2037–2048.
- [42] S. K. Hanson, R. T. Baker, J. C. Gordon, B. L. Scott, L. A. “Pete” Silks, D. L. Thorn, *J. Am. Chem. Soc.* **2010**, *132*, 17804–17816.
- [43] L. Das, P. Kolar, R. Sharma-Shivappa, *Biofuels* **2012**, *3*, 155–166.
- [44] a) D. B. Akolekar, S. K. Bhargava, I. Shirgoankar, J. Prasad, *Appl. Catal. A: Gen.* **2002**, *236*, 255–262; b) O. A. Makhotkina, S. V. Preis, E. V. Parkhomchuk, *Appl. Catal. B: Environ.* **2008**, *84*, 821–826; c) Y.-S. Ma, C.-N. Chang, Y.-P. Chiang, H.-F. Sung, A. C. Chao, *Chemosphere* **2008**, *71*, 998–1004.
- [45] a) C. Crestini, M. C. Caponi, D. S. Argyropoulos, R. Saladino, *Bioorg. Med. Chem.* **2006**, *14*, 5292–5302; b) Y. Zhao, Q. Xu, T. Pan, Y. Zuo, Y. Fu, Q.-X. Guo, *Appl. Catal. A: Gen.* **2013**, *467*, 504–508.
- [46] a) F. G. Sales, L. C. A. Maranhão, N. M. Lima-Filho, C. A. M. Abreu, *Chem. Eng. Sci.* **2007**, *62*, 5386–5391; b) H. Deng, L. Lin, Y. Sun, C. Pang, J. Zhuang, P. Ouyang, Z. Li, S. Liu, *Catal. Lett.* **2008**, *126*, 106–111; c) J. Zhang, H. Deng, L. Lin, *Molecules* **2009**, *14*, 2747–2757; d) H. Deng, L. Lin, Y. Sun, C. Pang, J. Zhuang, P. Ouyang, J. Li, S. Liu, *Energy Fuel* **2009**, *23*, 19–24; e) H. Deng, L. Lin, S. Liu, *Energy Fuel* **2010**, *24*, 4797–4802.
- [47] a) J. Gierer, F. Imsgard, I. Norén, *Acta Chem. Scand.* **1977**, *B31*, 561–572; b) C. Fargues, A. Mathais, A. Rodrigues, *Ind. Eng. Chem. Res.* **1996**, *35*, 28–36.
- [48] a) B. F. Sels, D. E. De Vos, P. A. Jacobs, *Catal. Rev. - Sci. Eng.* **2001**, *43*, 443–488; b) M. R. Othman, Z. Helwani, Martunus, W. J. N. Fernando, *Appl. Organometal. Chem.* **2009**, *23*, 335–346; c) D. P. Debecker, E. M. Gaigneaux, G. Busca, *Chem. Eur. J.* **2009**, *15*, 3920–3935; d) B. Zümreoglu-Karan, A. N. Ay, *Chemical Papers* **2012**, *66*, 1–10.
- [49] a) K. Zhu, C. Liu, X. Ye, Y. Wu, *Appl. Catal. A* **1998**, *168*, 365–372; b) L. Yumin, L. Shetian, Z. Kaizheng, Y. Xingkai, W. Yue, *Appl. Catal. A* **1998**, *169*, 127–135; c) K. Kaneda, T. Yamashita, T. Matsushita, K. Ebitani, *J. Org. Chem.* **1998**, *63*, 1750–1751; d) T. Matsushita, K. Ebitani, K. Kaneda, *Chem. Commun.* **1999**, 265–266; e) T. Nishimura, N. Kakiuchi, M. Inoue, S. Uemura, *Chem. Commun.* **2000**, 1245–1246.
- [50] J. Buendia, J. Mottweiler, C. Bolm, *Chem. Eur. J.* **2011**, *17*, 13877–13882.
- [51] D. W. Cho, J. A. Latham, H. J. Park, U. C. Yoon, P. Langan, D. Dunaway-Mariano, P. S. Mariano, *J. Org. Chem.* **2011**, *76*, 2840–2852.
- [52] T. Kishimoto, Y. Uraki, M. Ubukata, *Org. Biomol. Chem.* **2005**, *3*, 1067–1073.
- [53] J. C. Lee, Y. H. Bae, S.-K. Chang, *Bull. Korean Chem. Soc.* **2003**, *24*, 407–408.

- [54] M. C. White, A. G. Doyle, E. N. Jacobsen, *J. Am. Chem. Soc.* **2001**, *123*, 7194–7195.
- [55] M. S. Chen, M. C. White, *Science* **2007**, *318*, 783–787.
- [56] S. Navalon, M. Alvaro, H. Garcia, *Appl. Catal. B* **2010**, *99*, 1–26.
- [57] M. Nakanishi, C. Bolm, *Adv. Synth. Catal.* **2007**, *349*, 861–864.
- [58] G. Cahiez, V. Habiak, C. Duplais, A. Moyeux, *Angew. Chem.* **2007**, *119*, 4442–4444; *Angew. Chem. Int. Ed.* **2007**, *46*, 4364–4366.
- [59] T. Rinesch, *Master's Thesis*, Aachen, **2014**.
- [60] W. T. Dixon, R. O. C. Norman, A. L. Buley, *J. Chem. Soc.* **1964**, 3625–3634.
- [61] B. C. Gilbert, R. O. C. Norman, R. C. Sealy, *J. Chem. Soc., Perkin Trans. 2* **1975**, 303–308.
- [62] T. M. Santosusso, D. Swern, *J. Org. Chem.* **1976**, *41*, 2762–2768.
- [63] B.-M. Bertilsson, B. Gustafsson, I. Kühn, K. Torssell, *Acta Chem. Scand.* **1970**, *24*, 3590–3598.
- [64] M. S. Baker, J. M. Gebicki, *Arch. Biochem. Biophys.* **1986**, *246*, 581–588.
- [65] A. Rahimi, A. Ulbrich, J. J. Coon, S. S. Stahl, *Nature* **2014**, *515*, 249–252.
- [66] J. Mottweiler, T. Rinesch, C. Besson, J. Buendia, C. Bolm, *Green Chem.* **2015**, *17*, 5001–5008.
- [67] D. I. Enache, J. K. Edwards, P. Landon, B. Solsona-Espriu, A. F. Carley, A. A. Herzing, M. Watanabe, C. J. Kiely, D. W. Knight, G. J. Hutchings, *Science* **2006**, *311*, 362–365.
- [68] A. Abad, A. Corma, H. García, *Chem. Eur. J.* **2008**, *14*, 212–222.
- [69] A. Corma, H. García, *Chem. Soc. Rev.* **2008**, *37*, 2096–2126.
- [70] M. J. Climent, A. Corma, J. C. Hernández, A. B. Hungria, S. Iborra, S. Martínez-Silvestre, *J. Catal.* **2012**, *292*, 118–129.
- [71] T. Mallat, A. Baiker, *Chem. Rev.* **2004**, *104*, 3037–3058.
- [72] a) W.-C. Shieh, S. Dell, O. Repic, *Org. Lett.* **2001**, *3*, 4279–4281; b) P: Tundo, M. Selva, *Acc. Chem. Res.* **2002**, *35*, 706–716; c) Y. Ji, J. Sweeney, J. Zoglio, D. J. Gorin, *J. Org. Chem.* **2013**, *78*, 11606–11611.
- [73] A. Alejandre, F. Medina, X. Rodriguez, P. Salagre, J. E. Sueiras, *J. Catal.* **1999**, *188*, 311–324.
- [74] T.-Q. Yuan, S.-N. Sun, F. Xu, R.-C. Sun, *J. Agric. Food Chem.* **2011**, *59*, 10604–10614.
- [75] T. Kleine, J. Buendia, C. Bolm, *Green Chem.* **2013**, *15*, 160–166.
- [76] F. Tran, C. S. Lancefield, P. C. J. Kamer, T. Lebl, N. J. Westwood, *Green Chem.* **2015**, *17*, 244–249.
- [77] P. Picart, C. Müller, J. Mottweiler, L. Wiermans, C. Bolm, P. Domínguez de María, A. Schallmey, *ChemSusChem*, **2014** *7*, 3164–3171.
- [78] J. Mottweiler, M. Puche, C. Räuber, T. Schmidt, P. Concepción, A. Corma, C. Bolm, *ChemSusChem* **2015**, *8*, 2106–2113.
- [79] A. Wu, J. M. Lauzon, B. R. James, *Catal. Lett.* **2015**, *145*, 511–518.
- [80] Y. Yamamoto, *Adv. Synth. Catal.* **2010** *352*, 478–492.

- [81] A. Makriyannis, S. Fesik, *J. Am. Chem. Soc.* **1982**, *104*, 6463–6465.
- [82] R. V. Ottenbacher, D. G. Samsonenko, E. P. Talsi, K. P. Bryliakov, *Org. Lett.* **2012**, *14*, 4310–4313.

VII. Acknowledgements

First I would like to express my sincere gratitude to Prof. Dr. Carsten Bolm for showing faith and sustained interest in me joining his group. Over the last five years you have been my scientific mentor and your scientific curiosity has been an inspiration to me. I thank you for the great amount of freedom and trust you have given me during this entire research process. Through all my scientific endeavors and the realization of my interdoc in Spain I could always rely on your support.

Furthermore, I am deeply indebted to Prof. Dr. Avelino Corma for letting me conduct my interdoc under his supervision at the ITQ in Valencia. I thank you for introducing me to the world of heterogeneous catalysis and all the guidance you have given me during our collaboration. It has been a privilege to have both you and Prof. Dr. Carsten Bolm as my scientific mentors.

I am grateful to Dr. Patricia Concepción, Dr. Marcelo Domine and all the other staff members at the ITQ for all the help they have given me during my stays at the ITQ.

I thank Marta Puche Panadero, Dr. Raquel Juárez Marín, Aroa Alós Martí and Dr. Diego Fernando Cómbita Merchán for the synthesis gold and hydrotalcite-like catalysts.

I would also like to thank the following members of the cluster of excellence “TMFB” for research collaborations, help with the analytics, discussions and making interdisciplinary research an enjoyable experience: Dr. Thorsten vom Stein, Prof. Dr. Jürgen Klankermayer, Prof. Dr. Anett Schallmeyer, Dr. Pere Picart, Dr. Haifeng Liu, Simon Roth, Serafin Stiefel, Davide di Marino, Prof. Dr. Matthias Wessling, Prof. Dr. Regina Palkovits, Laurent Weisgerber, Heike Bergstein, Dr. Nico Anders, Dr. Camilla Lambertz, Dr. Leilei Zhu, Prof. Dr. Ulrich Schwaneberg, Manuel Dahmen, Juan Jose Wilhelm Victoria Villeda, Alena Sudholt, Barbara Graziano, Dr. Florian Kremer and all the others that I have inadvertently forgotten.

I thank Dr. Thomas Schmidt for the GPC and MALDI measurements and for all the discussions we have had on and off topic.

I thank Dr. Christoph Räuber for the NMR and lignin HSQC measurements and the fruitful discussions.

I thank Conny Vermeeren for the preparative HPLC measurements and for the advice on any HPLC related questions.

Desweiteren bedanke ich mich bei allen Angestellten des Instituts die zu dieser Arbeit beigetragen haben.

Mein Dank geht an Susi Grünebaum und Pierre Winandy für das Synthesieren vieler Substanzen und die schönen Karnevalsmomente.

Vielen Dank an Ingrid Voss für die Hilfe bei bürokratischen Problemen und den warmherzigen Umgang.

I would like to thank all former and current co-workers in the group of Prof. Dr. Carsten Bolm for the support and the nice working atmosphere. Special thanks go to Dr. Ankur Pandey, Dr. Julien Buendia, Dr. Seong Jun Park, Dr. Daniel Priebbenow, Dr. Manuel Jörres, Peter Becker and Frank Postleb.

The 3rd floor has been my home for the last five years and I thank all of current and former members for an awesome time especially Dr. Anne Nijs, Dr. Astrid Beyer, Dr. Isabelle Thomé, Dr. Stefanie Mersmann, Dr. Vincent Bizet, Dr. Ilga Mutule, Jens Reball, Dr. Christa Lehmann, Timon Ortloff and Dr. Ingo Schiffers.

During my stay at the ITQ Fran, Marta, Javi, Jose Miguel, Siris, Peter, Diego Fernando, Diego Armando, Victoria, Maike, Juan, Lina, Rubén, Marvin, Nacho, Raquel and Sara have made me feel right at home.

To my lab mates at the ITQ Sergio, Amparo and Nastia; it was awesome having you as my lab mates and I hope you can forgive me for breaking half of your glassware.

I feel privileged to have had Dr. Lianghua Zou and Carl Dannenberg as my lab mates. Both of you have helped me grow as a scientist and I enjoyed working with you.

I thank my former research students Thomas Lorenz, Josef Dib, Claudia Dähling, Christiane Schotten, Carl Dannenberg and Torsten Rinesch, my former Bachelor student Tai-Lam Nghiem, and TMFB HiWi Felix Krauskopf for their synthetic contributions and the fruitful discussions.

I thank Torsten Rinesch and Saumya Dabral for their patience and willingness to work with me. Supervising you has been a tremendous experience and I look forward to keep working with you.

I am grateful to Claudia Dähling, Carl Dannenberg, David Jefferson, Dr. Linus Reichenbach, Torsten Rinesch, Dr. Daniel Priebbenow and Dr. José Gregorio Hernández for proofreading parts of this dissertation.

Ich danke Dr. Linus Reichenbach für die willkommen Ablenkungen im Laboralltag und das gemeinsame Football gucken.

Ich danke allen meinen Freunden aus Aachen, allen ehemaligen Rheinländern und allen ehemaligen Leipzigern für die Unterstützung und die vielen schönen gemeinsamen Momente, nicht nur über die letzten fünf Jahre.

A special thanks goes to my former and current flat mates in Aachen and Valencia Björn, Rebekka, Deborah, Manu, Nico, Fritz, Jana and Sebastian. Living with you is and has been a wonderful experience and I am grateful for your friendship.

An meinen Patenonkel Jürgen Dobbers und an meine Patentante Ursel Dobbers richte ich meinen aufrichtigen Dank für ihre Liebe und Unterstützung während meiner Dissertation und darüber hinaus.

Last, but not least, möchte ich meinen Eltern Sage und Renke Mottweiler sowie meinen Geschwistern Liesel, Harald, Anneli, Lolli und Ella sowie deren Partner danken. Eure Liebe hat mich mein ganzes Leben lang getragen und ich freue mich mit euch und meinen Neffen und Nichten Lisa, Eleni, Jonas, Johan, Tobi, Justus und Mona meinen weiteren Lebensweg zu beschreiten.

VIII. Curriculum vitae

Personal Information

Name: Jakob Mottweiler
Nationality: German/American
Date of Birth: September 2nd, 1984
Place of Birth: Cologne, Germany

Education

08/1995 - 05/1996 Armond Bayou Elementary School Houston, TX
08/1996 - 05/1997 Space Center Intermediate School Houston, TX
09/1997 - 05/2004 Freiherr-vom-Stein-Gymnasium Leverkusen, Allgemeine Hochschulreife (cf. A levels)
10/2004 - 09/2007 University of Leipzig, Chemistry, Bachelor of Science
02/2008 - 08/2008 Universidad Complutense de Madrid, Erasmus exchange
10/2007 - 09/2009 University of Leipzig, Chemistry, Master of Science
11/2009 - 04/2010 Universidad Complutense de Madrid, Leonardo da Vinci Internship, Prof. Dr. Miguel Angel Sierra
06/2010 - 11/2015 RWTH Aachen University, Chemistry, Doctoral studies, Prof. Dr. Carsten Bolm

Research Experience

08/2007 - 09/2007 Bachelor's Thesis under the supervision of Prof. Dr. Rolf Breinbauer: "Synthesis of 2-disubstituted imidazolines and imidazolidines"
04/2009 - 09/2009 Master's Thesis under the supervision of Prof. Dr. Evamarie Hey-Hawkins: "Enantioselective synthesis of ferrocen-modified amino acids"
11/2009 - 04/2010 Leonardo da Vinci Internship under the supervision of Prof. Dr. Miguel Angel Sierra: "Oxidative coupling of amino acid anhydrides" and "Synthesis of chromium arentricarbonyl complexes for enantioselective desymmetrization of anhydrides"
3/2012 - 05/2012,
07/2012 - 08/2012,

04/2014 Interdoctoral research studies at the ITQ, Valencia, Spain under the supervision of Prof. Dr. Avelino Corma: “Oxidative cleavage of lignin β -O-4 model compounds with supported gold nanoparticles and hydrotalcite-like catalysts”

Scholarships

02/2008 - 08/2008 Erasmus scholarship

11/2009 - 04/2010 Leonardo da Vinci Mobility Scholarship, Program for lifelong learning

03/2012 - 05/2012 DAAD, Short-term doctoral scholarship

06/2010 - 05/2013 NRW Graduate School BrenaRo, Stipend for doctoral studies